SPATIAL AND TEMPORAL VARIATIONS IN LACUSTRINE DEPOSITIONAL CONTROLS FROM THE MIDDLE TO UPPER GREEN RIVER FORMATION, CENTRAL AND WESTERN UINTA BASIN, UTAH

by

Leah Catherine Toms

A thesis submitted to the faculty of
The University of Utah
in partial fulfillment of the requirements for the degree of

Master of Science

in

Geology

Department of Geology and Geophysics

The University of Utah

December 2014

The University of Utah Graduate School

STATEMENT OF THESIS APPROVAL

The thesis of **Leah Catherine Toms**

has been approved by the following supervisory committee members:

Lauren Birgenheier	, Chair	**8/27/14** Date Approved
Cari Johnson	, Member	**8/27/14** Date Approved
Michael Vanden Berg	, Member	**8/27/14** Date Approved

and by **John Bartley**, Chair/Dean of

the Department/College/School of **Geology and Geophysics**

and by David B. Kieda, Dean of The Graduate School.

ABSTRACT

The stratigraphy preserved in the Eocene Green River Formation provides key insights into the evolution of ancient Lake Uinta and the controls influencing sediment deposition and facies distribution. This study characterizes the stratigraphy of the middle to upper Green River Formation (transitional interval to the R8) in Gate Canyon, south-central Uinta Basin, and Willow Creek/Indian Canyon, western Uinta Basin. The examined sections were deposited during and after early Eocene hyperthermal events that followed the Paleocene-Eocene Thermal Maximum, allowing specific investigation of the transition between a pulsed, hyperthermal climate regime during the Early Eocene Climatic Optimum to a period of climatic stability.

Detailed outcrop and core descriptions along with paleocurrent data, thin sections, and X-ray fluorescence data reveal distinct suites of facies both spatially and temporally. Three evolutionary lake phases are suggested by the stratigraphy, from an overfilled basin (C1-Si.3), to a balanced-fill basin (C4-middle R8), to an underfilled basin (middle R8-saline facies). The facies of the first phase record a highly fluctuating lake with alternating carbonate and siliciclastic dominated packages that may be associated with Eocene hyperthermal events. The central portion of the basin contains a large proportion of coarser grained sandstone bodies, coarser grained carbonates, and microbialites whereas the western portion of the basin contains minor sandstone bodies, and abundant fine grained siliciclastic material and muddy carbonate units. The change in grain size

from east to west represents a transition off the main depositional axis of a major deltaic system in the central portion of the basin to a more low energy, shallow lake margin setting.

The stratigraphy of the second lake phase consists of organic-rich and poor carbonate mudstone, tuffs, and siltstone. These facies record a deep lacustrine environment, suggesting lake transgression as a result of the shift from a pulsed, hyperthermal climate regime to a period of climatic stability. The stratigraphy of the final lake phase consists of organic-rich and poor carbonate mudstone, tuffs, siltstone, minor sandstone, and saline deposits. These observations indicate lake regression and the eventual closing of Lake Uinta. Overall, this study seeks to link these regions to provide a more comprehensive understanding of the evolution of Lake Uinta.

“Man cannot discover new oceans unless he has the

courage to lose sight of the shore”

-André Gide

TABLE OF CONTENTS

ACKNOWLEDGEMENTS

I would first like to thank my advisor, Lauren Birgenheier, for her guidance and continued support with my research during the past two years. I will be forever grateful for the opportunity to have worked with her in the Green River Formation and for the graduate school experience I was offered at the University of Utah. I would also like to thank my committee members, Cari Johnson and Mike Vanden Berg, for taking time out of their busy schedules and providing useful insight towards my research. Mike was able to provide specific knowledge towards the Green River Formation, with which I was able to develop a well-rounded understanding of the lacustrine system. In addition, James Taylor greatly helped with this project by collecting and calibrating X-ray fluorescence data from both of the cores used in this study. This project would not have been possible without the financial support given from Total, as well as a fellowship given from ConocoPhillips.

I would like to extend thanks to my undergraduate advisor, Liz Hajek, who has been a role model for me throughout my academic career. I would not be in the position that I am today without her teachings and encouragement over the past couple of years. Many thanks also go to my other Penn State geology professors, who established my love of geology from the beginning and who inspired me to follow an academic course.

Thanks to my numerous field assistants, including Morgan Rosenberg, Andrew McCauley, Gavin Ferguson, Paul Thomas, Ellen Rosencrans, and Tom Etzel. My friends

both in and outside of the geology department have greatly added to my experience here in Utah, providing lasting friendships and unforgettable adventures. Finally, I would like to thank my family for their unwavering support of my interesting field of study, which happens to involve looking at a ton of rocks.

INTRODUCTION

Lacustrine systems contain economically significant stores of hydrocarbons (Carroll and Bohacs, 1999), and so an improved understanding of the controls on deposition and evolution within these systems is necessary for predicting the spatial distribution of organic-rich source facies and reservoir facies. Specifically, defining the relative importance of upstream and downstream controls is critical in lacustrine basins. Major controls include climate and tectonics, which promote sediment and water transport upstream and provide accommodation downstream (Figure 1).

Past and ongoing studies have focused on processes that control the stratigraphic architecture within marine basins in order to predict the location of hydrocarbons (e.g., Van Wagoner, 1995; Miall and Arush, 2001; Martin et al., 2009). Although marine and lacustrine systems have similar depositional controls, basin size, geometry, and variations in salinity in lake basins create unique sedimentologic characteristics that need to be considered. Meanwhile, modern lacustrine analogs are very diverse and record numerous controls such as hydrology, chemistry, and biology, which are far too complex to organize into a systematic study of lake basins (Johnson et al., 1987; Cohen, 1989; Bohacs et al., 2000). Ancient lacustrine deposits provide fairly uncomplicated information about lake conditions, and although data are somewhat difficult to interpret, can provide an important, long timescale perspective on lake evolution and the resulting stratigraphic architecture (Carroll and Bohacs, 2001). This study focuses on the Eocene

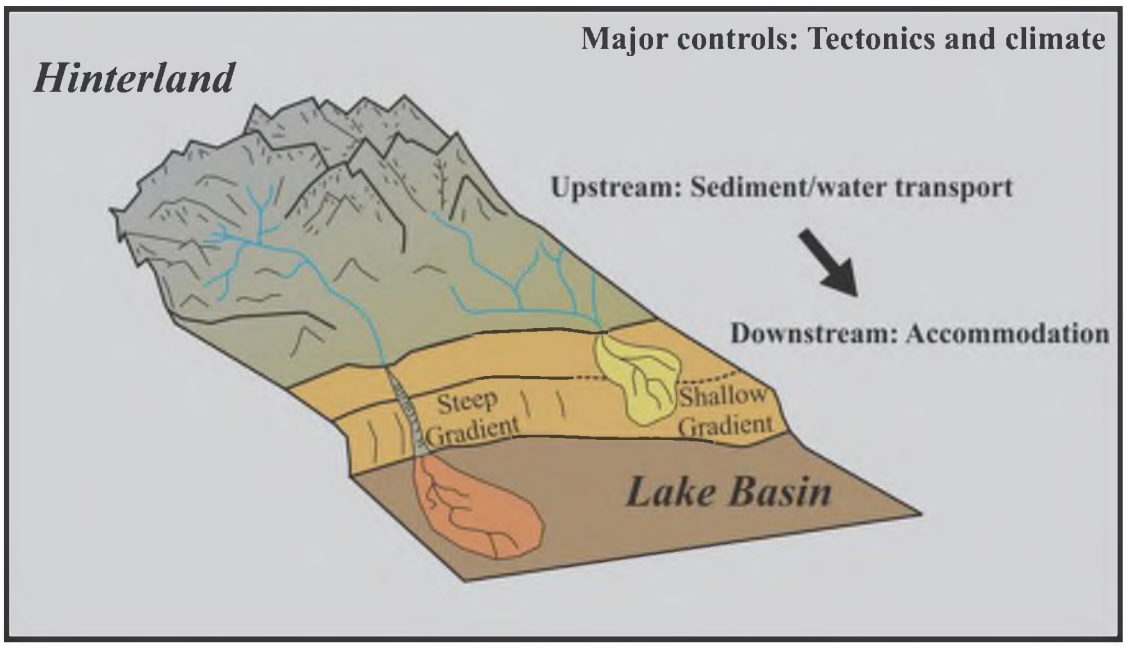

Figure 1 – Main depositional controls on lacustrine systems; modified from Sømme et al., 2009.

Green River Formation, which shows regional variations in depositional controls both spatially and temporally.

The Green River Formation is an Eocene lacustrine formation that was deposited in the Piceance Creek, Uinta, Greater Green River, and Washakie basins of the western United States (Figure 2). It represents a continental interior, terminal lake system known as Lake Uinta in the Piceance Creek and Uinta basins, and Lake Gosiute in the Greater Green River and Washakie basins (Johnson, 1985; Birgenheier and VandenBerg, 2011; Tanavsuu-Milkeviciene and Sarg, 2012). This study focuses on the Green River Formation deposited in the Uinta Basin of northeastern Utah via Lake Uinta. The long-term evolution of Lake Uinta, including occurrence, facies distribution, and stratigraphic architecture, was ultimately controlled by the balance between accommodation and sediment and water supply (Carroll and Bohacs, 1999; Carroll and Bohacs, 2001; Smith et al., 2008; Birgenheier and VandenBerg, 2011). This balance resulted in different lake phases, here referred to as overfilled, balanced-fill, or underfilled as termed by Carroll and Bohacs (1999), that reflect the relative levels of water and sediment as compared to surrounding basins.

Seminal models of the Green River Formation have been developed in numerous publications (e.g., Carroll and Bohacs, 1999); however, recent studies of other Eocene formations have illuminated global and regional records of major climatic events during this time period (e.g. Nicolo et al., 2007; Sexton et al., 2011; Abels et al., 2012; Aswasereelert et al., 2012). The formation was deposited during the hyperthermal events that followed the Paleocene-Eocene Thermal Maximum (PETM) (Wing and Greenwood, 1993; Wilf et al., 1998; Lourens et al., 2005; Bowen and Beitler Bowen, 2008; Sexton et

Figure 2 – Paleogeographic distribution of Lake Uinta and Lake Gosiute on modern basin margins in Utah, Colorado, and Wyoming; red outline highlights the Uinta Basin and red box highlights the field area for this study; modified from Birgenheier and VandenBerg (2011).

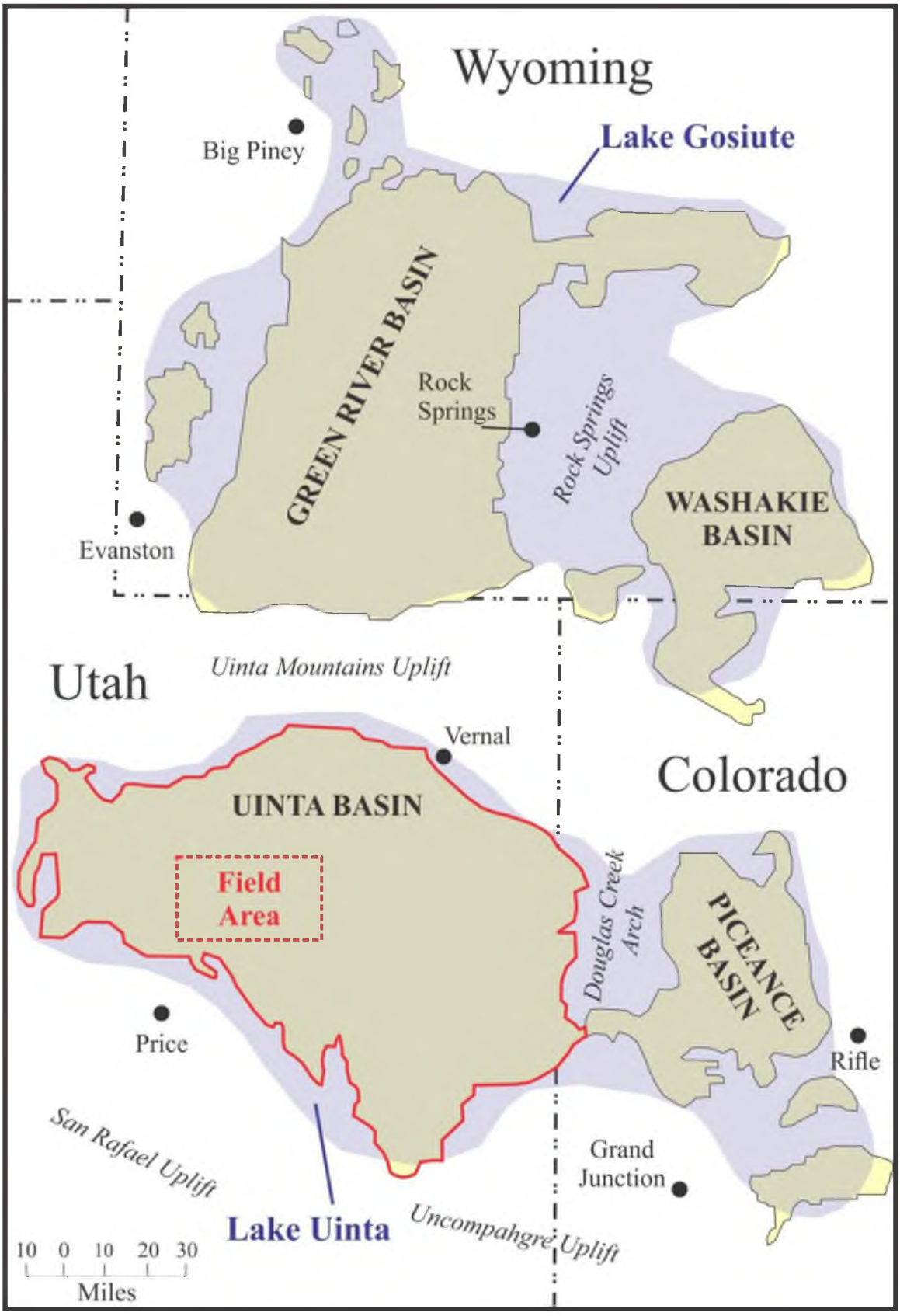
Wyoming
Big Piney
Lake Gosiute
GREEN RIVER BASIN
Rock Springs
Rock Springs Uplift
WASHAKIE BASIN
Evanston
Utah
Uinta Mountains Uplift
Vernal
Colorado
UINTA BASIN
Field Area
Douglas Creek Arch
PICEANCE BASIN
Price
Rifle
San Rafael Uplift
Grand Junction
Lake Uinta
Uncompahgre Uplift
10 0 10 20 30
Miles

al., 2011; Abels et al., 2012; Plink-Bjorklund and Birgenheier, in review), requiring the redevelopment of existing lacustrine models while incorporating these small-scale climate events. It is well documented that abrupt global warming events such as the PETM cause increased seasonality, at least regionally, or extreme periods of wetting and drying, and thus increased weathering and sedimentation rates (Tucker and Slingerland, 1997; Wilf et al., 1998; Kraus and Riggins, 2007; Birgenheier and VandenBerg, 2011; Foreman et al., 2012; Plink-Bjorklund and Birgenheier, in review). Although the hyperthermal events observed during the Eocene Climatic Optimum are much smaller in scale than the PETM, it is likely that the system would respond in a similar, yet more muted degree, with increased siliciclastic sedimentation occurring in response to these events.

The stratigraphy in the middle and upper members of the Green River Formation towards the south-central and western margins of the basin contain distinct carbonate dominated (C) and siliciclastic dominated (Si.) packages which may be a function of these hyperthermal events. During siliciclastic deposition, carbonate accumulation is limited as a result of the higher influx of siliciclastic sediment; in contrast, during carbonate deposition, siliciclastic input is limited. By closely examining the nature of the facies within these carbonate and siliciclastic dominated packages along with other major stratigraphic units, investigations can be made on specifically how climate change and/or tectonics both during and after these events may have influenced facies distribution, stratigraphic architecture, and overall lake evolution.

Although the Green River Formation is one of the most heavily cited ancient lacustrine successions, a detailed basin-wide stratigraphic framework that highlights

depositional controls and lake evolution is lacking from the Uinta Basin. The Green River Formation in the Uinta Basin contains a relative balance of siliciclastic, carbonate, and oil shale facies. In terms of economic interests, the formation hosts both conventional oil and gas reserves as well as a world-class oil shale resource in the upper Green River Formation (Vanden Berg, 2008) that is found in the alternating organic-rich and organic-lean zones in the basin. The oil shale deposits in the Uinta Basin hold an estimated total in-place oil of 1.32 trillion barrels (Johnson et al., 2010). This falls slightly under that of the Piceance Basin, which is estimated to have an in-place resource of 1.53 trillion barrels and is considered to be the largest oil shale deposit in the world (Johnson et al., 2010). A basin-wide model of the Green River Formation in the Uinta Basin is critical for predicting the spatial distribution of organic-rich source facies and reservoir facies in order to assist in future economic development of the basin.

This study focuses on a particularly understudied stratigraphic interval, the middle to upper Green River Formation (spanning the transitional interval to the R8), that is located in the south-central to western portions of the basin (Figures 2 and 3). Two field locations that are approximately 35 km apart, along with 2 cores located nearby, were used to provide a detailed sedimentologic and stratigraphic study that includes measured sections, stratigraphic architecture data, paleocurrent data, thin sections, and X-ray fluorescence data. This interval can be categorized both spatially and temporally, into the long-term lake phases described above (i.e., overfilled, balanced- fill, and underfilled). Furthermore, small-scale facies and architectural changes were interpreted in this interval to subdivide the lake phases, provide a detailed stratigraphic and sedimentologic interpretation, and compare it to ongoing and previous studies of the formation in other

Figure 3 – Generalized stratigraphy in the central and western portions of the Uinta Basin; red box highlights the stratigraphic intervals of interest for this study, from the transitional interval to the R8; GR = Green River Formation, R = organic-rich zones; volcanic ages from Smith, 2010.

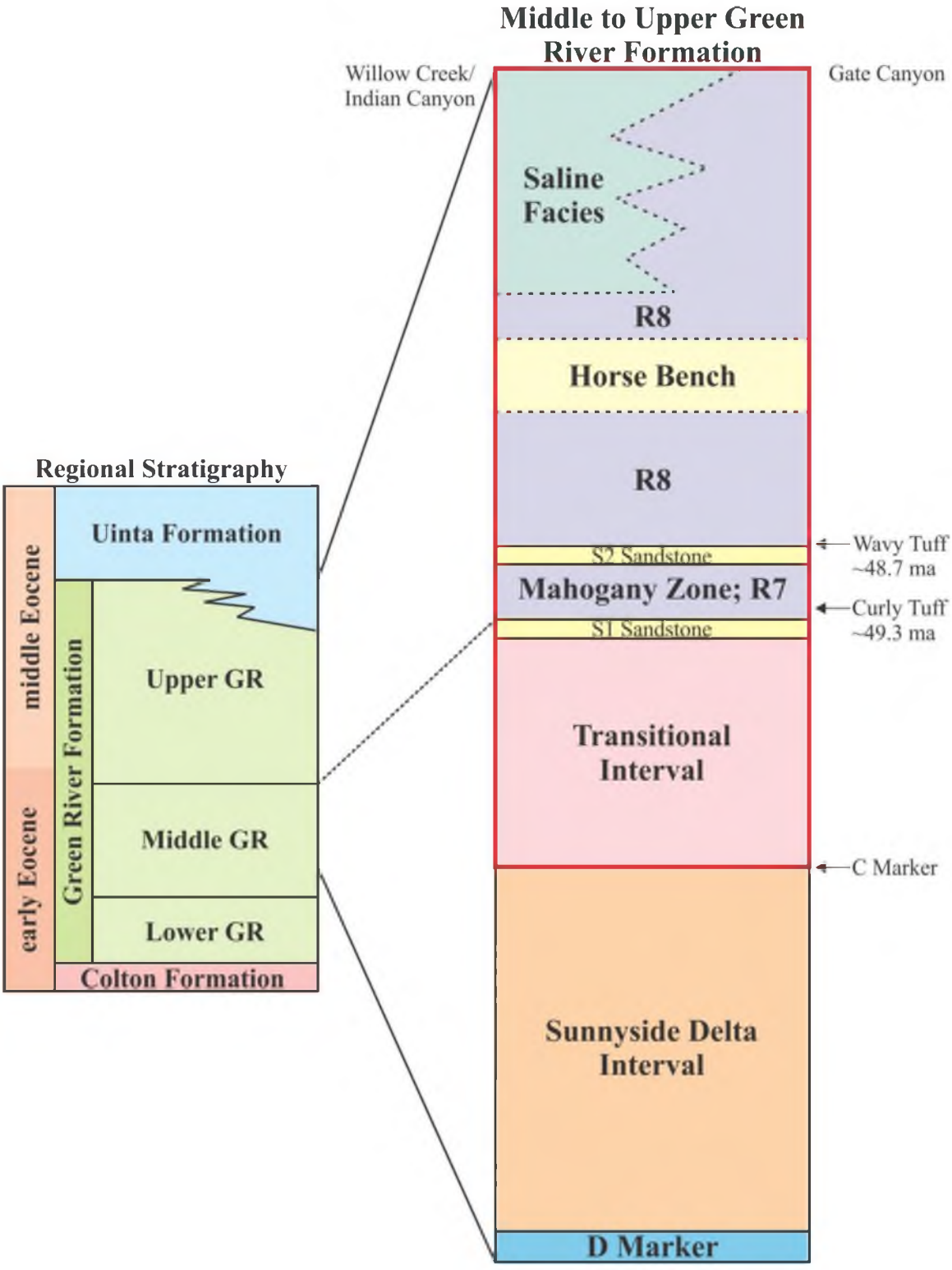
Middle to Upper Green River Formation
Willow Creek/ Indian Canyon
Gate Canyon
Saline Facies
R8
Horse Bench
R8
S2 Sandstone
Wavy Tuff ~48.7 ma
Mahogany Zone; R7
Curly Tuff ~49.3 ma
S1 Sandstone
Transitional Interval
C Marker
Sunnyside Delta Interval
D Marker
Regional Stratigraphy
middle Eocene
early Eocene
Uinta Formation
Green River Formation
Upper GR
Middle GR
Lower GR
Colton Formation

portions of the basin. Finally, comparisons between the lake phases observed in the stratigraphy and modern analogs were established in order to develop a complete understanding of lake evolution.

GENERAL SETTING AND STRATIGRAPHY

The Uinta Basin and other continental basins scattered around the central Rocky Mountain Region were formed by Laramide block uplifts that were variably active during the Cretaceous through the Eocene (Dickinson et al., 1988). These basins occupy the broken Sevier fold and thrust belt and record the evolution from large fluvial systems of the Sevier to long-lived lake systems with shifting hydrologic patterns (Franczyk and Pitman, 1991; Davis et al., 2008). Open lacustrine deposition related to the Green River Formation occurred throughout the early to middle Eocene (~53-43 Ma) (Davis et al., 2008; Tanavsuu-Milkeviciene and Sarg, 2012) (Figure 2). Various events influenced accommodation and hydrology and inevitably led to the connection or isolation of the lakes in the different basins through time (Smith et al., 2008).

The Uinta Basin in eastern Utah is bounded by Laramide uplifts, including the Uinta Uplift to the north and the San Rafael Swell and Uncompaghre Uplift to the south (Johnson, 1985; Moore et al., 2012). To the west, the Uinta Basin is bounded by the younger, more recently uplifted Wasatch Range and Wasatch Plateau (Cashion, 1995; Johnson et al., 2010). To the east, the Uinta Basin is separated from the Piceance by a north-south trending, Laramide-age anticline known as the Douglas Creek Arch (Johnson, 1985; Bader, 2009; Johnson et al., 2010). While subsidence of the basins on either side continued, the Douglas Creek Arch persisted as a positive topographic feature that acted as a sill occasionally separating the two lake systems (Osmond, 1965;

Rosenberg, 2013; Rosenberg et al., in press).

Underlying the Green River Formation is the Wasatch/Colton Formation that was deposited across the Paleocene-Eocene boundary (Fouch, 1975, 1976; Ryder et al., 1976) (Figure 3). These formations represent the fluvial and small lacustrine systems that were deposited prior to the large-scale, basin-wide lacustrine systems. Overlying and interfingering with the top of the Green River Formation is the fluvial Uinta Formation (Cashion, 1995) (Figure 3).

Stratigraphic nomenclature in the Green River Formation is only locally applicable and changes based on lithology and author (Ryder et al., 1976; Keighley et al., 2003; Birgenheier and VandenBerg, 2011). It can be divided into the lower, middle, and upper members (Remy, 1992; Morgan, 2003; Birgenheier and VandenBerg, 2011) (Figure 3). Towards the south central and western region of the basin, the lower member is composed of dominantly lacustrine facies that interfinger with the fluvial Wasatch/Colton Formation whereas the middle member is composed of fluvial-deltaic and carbonate facies. In stratigraphic order, the middle member contains the Sunnyside delta interval and the transitional interval. The C marker, a regional unit that consists of a series of carbonate beds ~2-8 m thick, marks the boundary between these two intervals within the middle member (Remy 1992) (Figure 3).

This study focuses on the stratigraphy from the transitional interval up through the R8 (Figure 3). The transitional interval, which was informally named by Remy (1992), consists of the alternating lithologic units here referred to as carbonate packages (C) and siliciclastic packages (Si.). These packages are roughly correlative to the organic-rich and organic-lean zones identified in other studies of the middle and upper Green River

Formation, including outcrop (e.g., Rosenberg, 2013) and subsurface log studies (e.g., Johnson et al., 2010). However, in Gate Canyon and Willow Creek/Indian Canyon, these organic-rich and lean zones are difficult to recognize due to the proximity and influence of the lake margin and the absence of profundal oil shale in the transitional interval. Therefore, separate terminology is used in this study (C and Si.) in order to distinguish these packages from the aforementioned rich and lean zones. Above the transitional interval is the S1 sandstone, which marks the top of the middle Green River Formation (Weiss et al., 1990; Remy, 1992) (Figure 3).

The base of the upper member is found at the base of the Mahogany zone (R7), which is the richest oil shale unit in the Green River Formation (Vanden Berg, 2008) (Figure 3). Following R7 deposition is another siliciclastic unit referred to as the S2 sandstone that is overlain by the regionally extensive R8 zone. For this study, the S1 sandstone, Mahogany zone, and S2 sandstone are referred to as the Mahogany interval. The upper R8 zone consists of the Horse Bench Sandstone, which is a regional sandstone body that prograded into the basin from the west. In the central portion of the basin, the R8 is considered the top of the Green River Formation. In the west, the R8 transitions into the saline facies which is considered the top of the Green River Formation in this area of the basin (Dyni et al., 1985) (Figure 3). The upper units are together informally referred to as the R8 interval.

METHODS

A detailed field and core-based sedimentologic and stratigraphic study was performed to highlight key vertical and lateral facies changes along with bed geometries and architectural features. Two composite cm- to m-scale sections were measured from high-quality outcrop exposures in Gate Canyon and Willow Creek/Indian Canyon along with two cores that were described near these field areas (Figure 4). The two composite sections, each approximately 400 m thick, are located about 35 km apart and stratigraphically span the transitional interval through the Horse Bench Sandstone (Appendices A and B). Key stratigraphic units were identified in the field using Morgan (2003) and Remy (1992), for Indian Canyon and Gate Canyon, respectively. Both measured sections were followed laterally and translated up canyon as outcrop exposure dictates. Key features such as lithology, organic richness, grain size, color variations, sedimentary structures, and bed thicknesses, geometry, and contacts were documented. Paleocurrent orientation data were also recorded from trough cross beds, current ripples, and accretion sets to determine directional accretion of sandstone body deposits (Appendix B). Furthermore, photopans of each outcrop were compiled in order to document architectural features and highlight different stratigraphic units.

Detailed sedimentologic, stratigraphic, and geochemical analysis of two cores, the Henderson 3 core (110 m, 361 ft.) and the Half Moon Canyon core (426 m, 1398 ft.), was performed. The Henderson 3 core, which is located 10.5 km north of the Gate Canyon

Figure 4 – Paleogeographic map and field area map; A) Paleogeographic map of Utah, Colorado, and Wyoming during the Eocene illustrating the extent of the Green River Formation in the 3 major basins; the field area for this study is highlighted by the red box; modified from Blakey and Ranney (2008). B) DEM showing the locations of the 2 measured outcrop sections and the 2 cores.

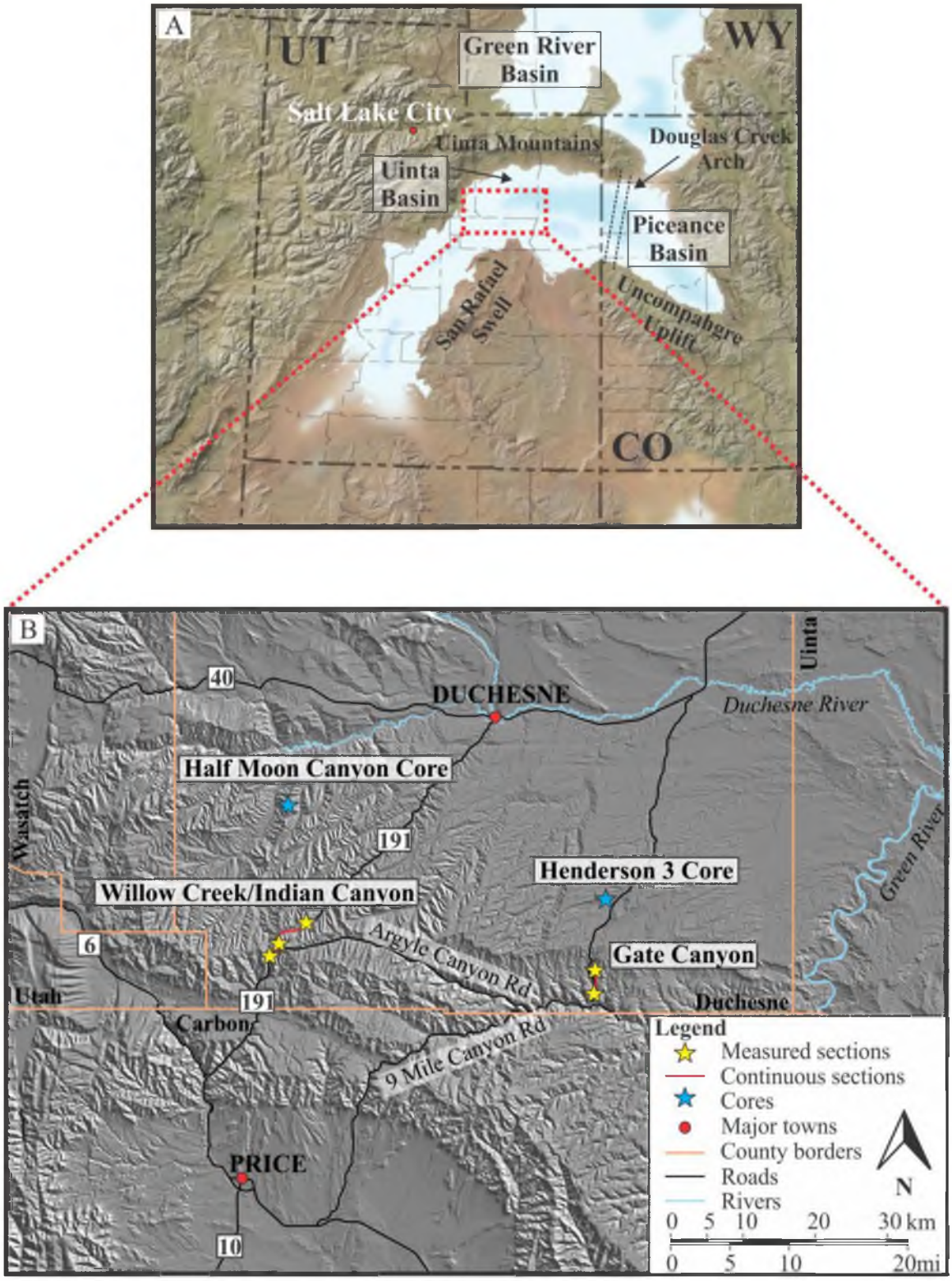
A
UT
WY
CO
Green River Basin
Salt Lake City
Uinta Mountains
Douglas Creek Arch
Uinta Basin
Piceance Basin
San Rafael Swell
Uncompahgre Uplift
B
40
DUCHESNE
Duchesne River
Uinta
Half Moon Canyon Core
Wasatch
191
Henderson 3 Core
Willow Creek/Indian Canyon
Green River
Argyle Canyon Rd
6
Gate Canyon
Utah
191
Duchesne
Carbon
9 Mile Canyon Rd
Legend
Measured sections
Continuous sections
Cores
Major towns
County borders
Roads
Rivers
N
0 5 10 20 30 km
0 5 10 20mi
PRICE
10

outcrop, stratigraphically spans the upper transitional interval to the S2 sandstone (Figure 3, Appendix B). Examination of this cored interval allowed detailed visual investigation of the Mahogany interval along with thin sections and X-Ray fluorescence (XRF) that outcrop does not afford. The Half Moon Canyon core is located 19 km north of the Willow Creek/Indian Canyon outcrop and stratigraphically spans the Mahogany zone at the base through the saline facies above the Horse Bench Sandstone at the top (Figure 3, Appendix B).

Sixteen thin sections of the Henderson 3 core were petrographically described to better define the key facies observed (Appendix C). Thin sections of predominantly mudstone were stained for calcite and iron and were impregnated with red fluorescent epoxy in order to maintain the quality of the thin sections. Features systematically noted include grain size, sedimentary structures, sorting, rounding, matrix type and percentages, as well as the abundance of certain grains, such as quartz, skeletal carbonate grains, non-skeletal carbonate grains, dolomite, marcasite, saline crystals, and organics (Williamson, 1972; Williamson and Picard, 1974; Freytet and Verrecchia, 2002; Scholle and Ulmer-Scholle, 2003; Bereskin et al., 2004). Multiple photomicrographs of each thin section were taken in order to highlight significant features.

Nondestructive XRF analysis in both cores was performed to better understand the observed stratigraphic units (Appendix D). Using a Brüker AXS TRACER III-V energy dispersive handheld XRF unit, major and trace elemental abundance measurements were recorded at roughly 3 m intervals, with increased measurements taken in highly variable sections of the core. Raw data were collected as a spectrogram and converted to weight percent. A matrix specific calibration was required (Rowe et al.,

2012). To ensure accuracy, a standard pressed pellet was run periodically throughout testing. Detailed XRF analysis allows for more detailed lithologic descriptions, especially within fine grained material that might be difficult to describe through visual inspection alone.

RESULTS

Facies Associations and Related Facies

Thirteen facies are defined in the middle to upper Green River Formation based on lithology or composition, sedimentary structures, organic richness, and overall geometry (Table 1). The thirteen facies are grouped into the following six main facies associations (F): F1) steep gradient, littoral to sublittoral siliciclastic deposits; F2) shallow gradient, littoral to sublittoral siliciclastic deposits; F3) low siliciclastic sediment supply, littoral to sublittoral carbonate deposits; F4) siliciclastic sediment-starved, profundal lake deposits; F5) saline deposits; and F6) volcanic deposits. These six facies associations reflect dominant lithologies, basin geometry, relative siliciclastic sediment supply, and lake zonation based on energy level and water depth (Figures 5 and 6). Measured sections, core descriptions, and thin section descriptions along with their respective facies association designations are documented in Appendices B and C.

Facies Association 1: Steep gradient, littoral to sublittoral siliciclastic deposits

Facies Association 1 (F1) occurs in the transitional interval and the R8 interval of the basin and consists of very fine to medium grained sandstone with interbeds of siltstone and very fine sandstone (Figures 6 and 7). This facies association is laterally related to Facies Association 2 (F2).

Table 1 – Facies and facies associations observed in outcrop and core; GC - Gate Canyon, WC/IC - Willow Creek/Indian Canyon, H3 - Henderson 3 core, HMC - Half Moon Canyon core.

Facies		Description	Geometry	Stratigraphic Occurence	Depositional Environment
Facies Association 1: Steep gradient, littoral to sublittoral siliciclastic deposits					
F1.1	Strongly channelized sandstone	Fine to medium grained sandstone, lateral accretion sets, trough cross stratification (TCS), current ripples, planar parallel laminations (PPL), soft sediment deformation (SSD), rip-up clasts, minor fish debris	1-5 m thick, erosionally based	Horse Bench (WC/IC), transitional interval (GC)	Terminal distributary channels
F1.2	Interbedded calcareous siltstone and sandstone	Siltstone and very fine sandstone, PPL, current ripples and wave ripples, climbing ripples, low angle laminations (LAL), SSD, minor burrows	1-5 m, tabular or gradational	Transitional interval (GC), thin sections 1, 2, 10, 11	Mouthbar deposits
F1.3	Tabular sandstone	Very fine to medium grained sandstone, wave ripples, PPL, LAL, minor burrows, ostracod debris, carbonate grains	1-3 m, tabular to wavy bedding, flaggy weathering	R8, Horse Bench (GC)	Shoreface deposits
Facies Association 2: Shallow gradient, littoral to sublittoral siliciclastic deposits					
F2.1	Weakly channelized sandstone	Very fine to fine grained sandstone, downstream accretion sets, low angle laminations (LAL), current ripples, minor TCS, PPL, wavy laminations, SSD	1-3 m, slightly erosionally based, sheet-like	Transitional interval (WC/IC)	Terminal distributary channels
F2.2	Heterolithic channel	Interbedded muddy siltstone and very fine grained sandstone, current ripples, LAL, minor wave ripples	1-2 m, slightly erosionally based	Transitional interval (WC/IC)	Lake flat channels
F2.3	Calcareous siltstone	Green siltstone with calcareous matrix, massive, minor PPL, minor burrows, mottled, interbedded with green mudstones	1-8 m, tabular, flaggy weathering	Transitional interval (WC/IC)	Lake flat deposits
F2.4	Paleosol	Green/purple mudstone and minor siltstone, mottled, pedogenic, slicks, current ripples in siltstone	10-50 cm, tabular to lenticular	Transitional interval (WC/IC)	Floodplain/lake flat

Table 1 – Continued

Facies		Description	Geometry	Stratigraphic Occurence	Depositional Environment
Facies Association 3: Low siliciclastic sediment supply, littoral to sublittoral carbonate deposits					
F3.1	Microbialite	Stromatolite and thrombolite, minor fish debris	10-50 cm, wavy to tabular	Transitional interval (GC,WC/IC)	Carbonate ramp (high energy)
F3.2	Coarse grained carbonate	Wackestone and grainstone, massive to PPL to wavy laminations, minor current and wave ripples, minor burrows, fish and ostracod debris, carbonate rip ups, minor LAL	10 cm - 2 m, tabular to wavy	Transitional interval (GC, WC/IC, H3), thin sections 13, 16	Carbonate ramp (high energy)
F3.3	Organic-poor carbonate mudstone	Micrite, massive to PPL to wavy laminations, rhythmites, occasional rip ups, SSD, siltstone interbeds, disseminated dolomite, algal pellets	20 cm - 2 m, tabular to wavy, flaggy weathering	Transitional interval, Mahogany zone, R8 (GC, WC/IC, H3), thin sections 3, 4, 5, 8, 12, 14, 15	Carbonate ramp and lake flat, littoral and sublittoral (low energy)
Facies Association 4: Siliciclastic sediment starved, profundal lake deposits					
F4.1	Organic-rich carbonate mudstone	Oil shale, massive to PPL to wavy laminations, SSD, minor salines and marcasite, precipitated carbonate nodules, disseminated dolomite, organic lenses	20 cm - 2 m, tabular to wavy	Mahogany zone and R8 (GC, WC/IC, H3), thin sections 6, 7, 9	Deep open water deposits
Facies Association 5: Saline deposits					
F5.1	Saline deposits	Nahcolite and shortite, small and large voids (mm to cm), crystals, PPL, fracture fill (from core)	–	Mahogany zone (H3), saline facies (HMC), thin section 9	Associated with organic-rich carbonate mudstone
Facies Association 6: Volcanic deposits					
F6.1	Volcanic deposits	Tuff, rhyolitic texture, diagenetic red iron bands, SSD	5 - 30 cm, wavy to tabular	WC/IC, HMC, GC, H3	–

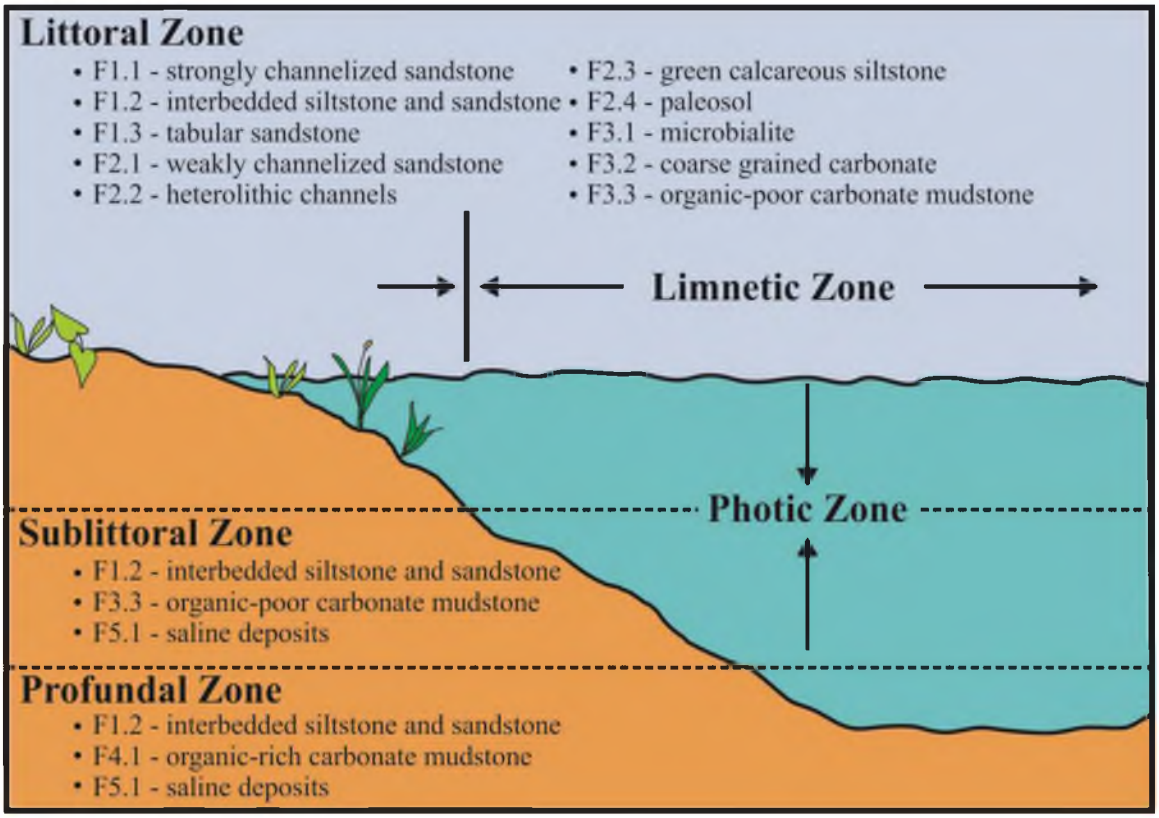

Figure 5 – Lake zonations with defined facies from Table 1.

Figure 6 – Depositional model of facies from Table 1. Note the transition from a steep gradient (left) to a shallow gradient (right) and the resulting facies and facies distributions. The steep gradient is representative of Gate Canyon (central region) and the shallow gradient is representative of Willow Creek/Indian Canyon (western region).

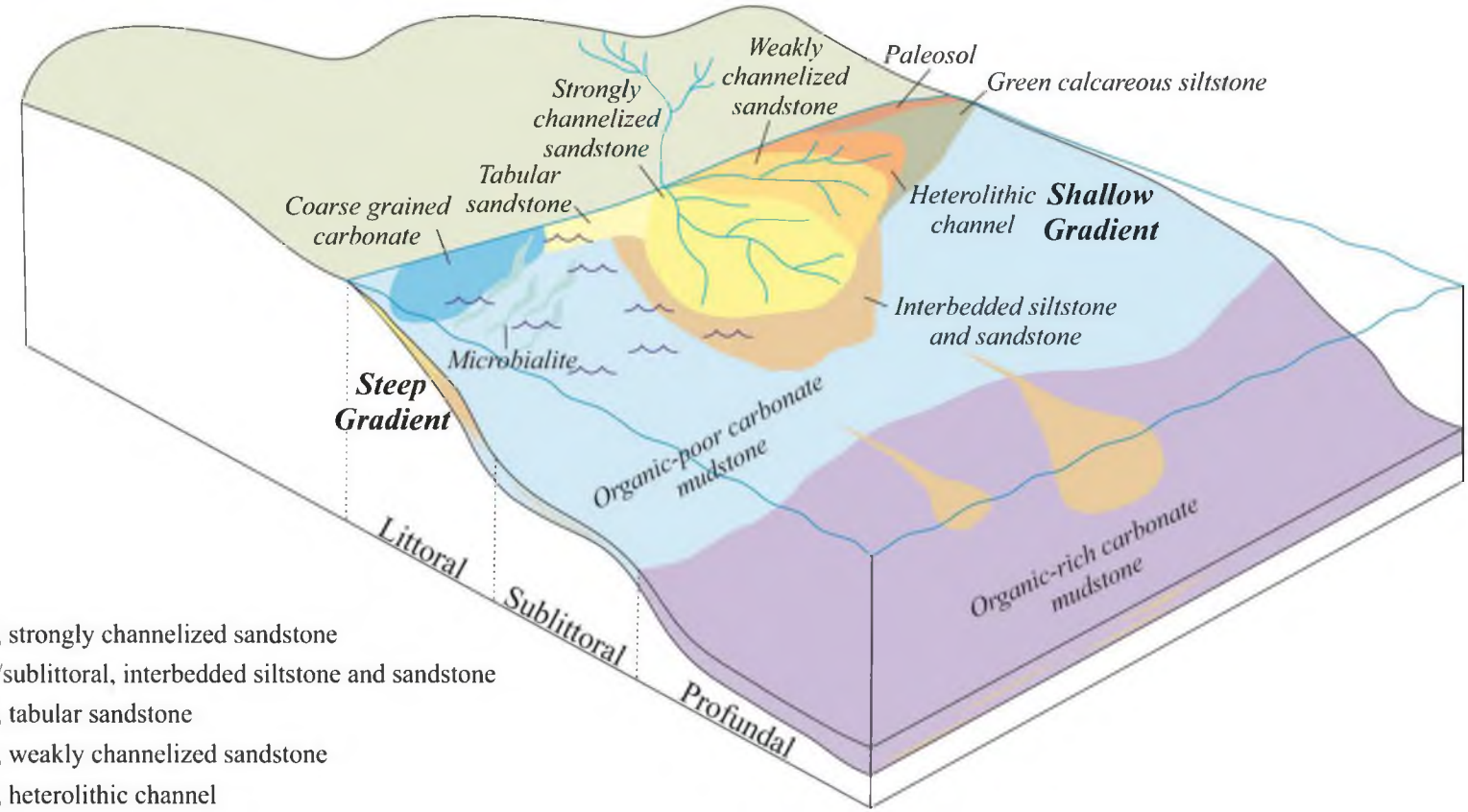

- F1.1: Littoral, strongly channelized sandstone
- F1.2: Littoral/sublittoral, interbedded siltstone and sandstone
- F1.3: Littoral, tabular sandstone
- F2.1: Littoral, weakly channelized sandstone
- F2.2: Littoral, heterolithic channel
- F2.3: Littoral, calcareous siltstone
- F2.4: Littoral, paleosol
- F3.1: Littoral, microbialite
- F3.2: Littoral, coarse grained carbonate
- F3.3: Littoral/sublittoral, organic-poor carbonate mudstone
- F4.1: Profundal, organic-rich carbonate mudstone

Figure 7 - Facies Association 1: Steep gradient, littoral to sublittoral siliciclastic deposits. A) Facies 1.1 from Indian Canyon Horse Bench; strongly channelized littoral sandstone body. B) Facies 1.1 from Gate Canyon transitional interval; base of channel rip-up clasts composed of carbonate clasts and stromatolites heads. C) Facies 1.1 from Gate Canyon transitional interval; current ripple sets. D) Facies 1.1 from Gate Canyon S1 sandstone; trough cross stratification. E) Facies 1.2 from Gate Canyon transitional interval; very fine sandstone bed encased in siltstone, current ripples, tabular. F) Facies 1.2 from Gate Canyon R8; syneresis cracks at the base of a thin siltstone bed. G) Facies 1.2 from Gate Canyon transitional interval; tannish grey calcareous siltstone. H) Facies 1.3 from Gate Canyon Horse Bench; tabular sandstone bodies representative of shoreface deposits. I) Facies 1.3 from Gate Canyon Horse Bench; wave ripple dominated, tabular sandstone body. J) Facies 1.3 from Gate Canyon Horse Bench; burrowed sandstone.

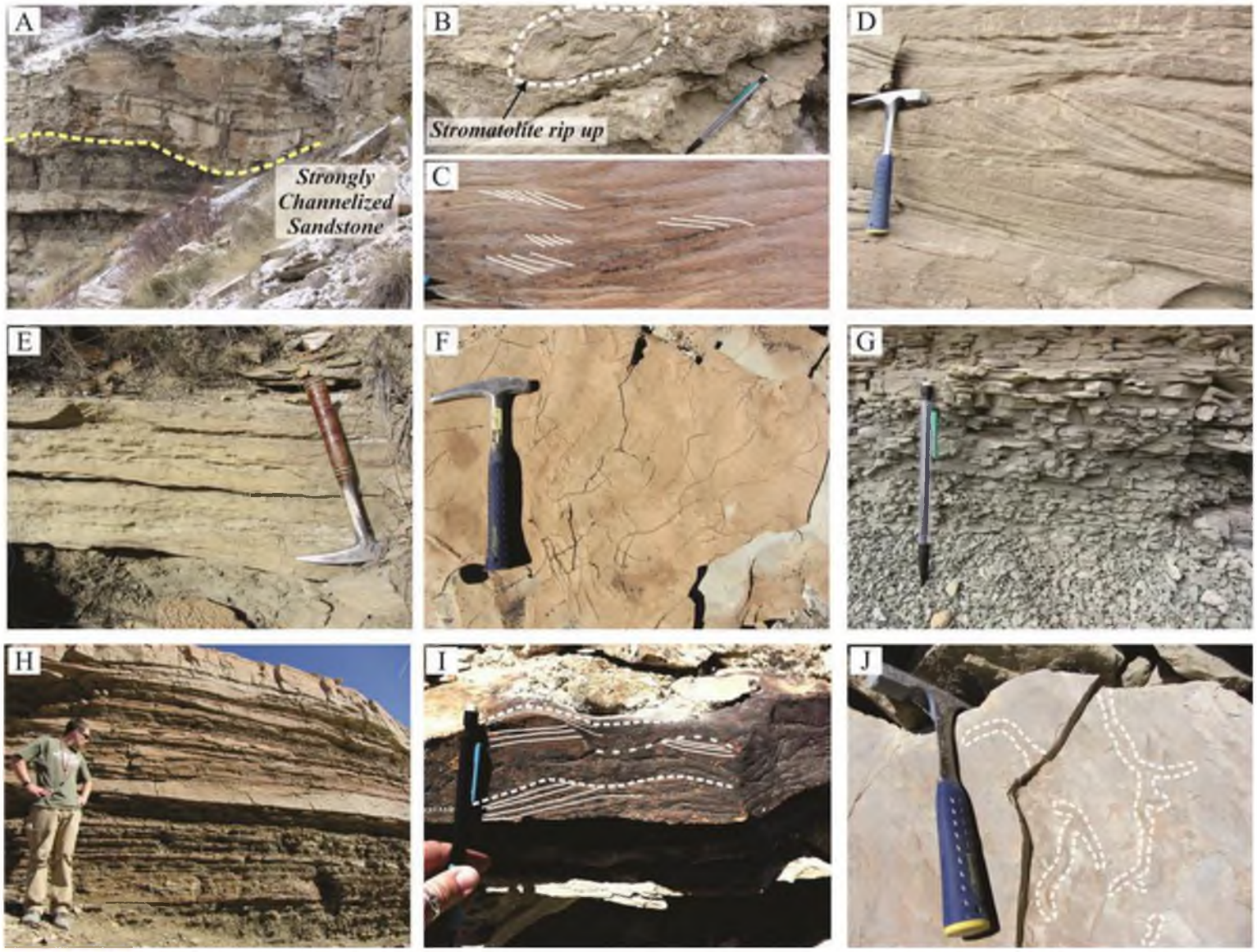
A
Strongly Channelized Sandstone
B
Stromatolite rip up
C
D
E
F
G
H
I
J

Facies 1.1 (F1.1)

Facies 1.1 consists of fine to medium grained, strongly channelized sandstone bodies that are laterally discontinuous (Table 1, Figure 7a-d). Lateral accretion sets, trough cross stratification, rip-up clasts, and fish debris are common towards the base of these channel bodies and generally grade into current ripples and climbing ripples towards the top of the channel bodies. Soft sediment deformation and planar parallel laminations can be found throughout. Channel bodies range from 1 to 5 m thick and are typically multistoried, with lateral amalgamation and some vertical amalgamation. The channel bodies are erosionally based and can be found to erode into one another, with story thicknesses ranging from 5 to 10 m. The multistoried channel bodies are overlain by interbedded current and wave rippled sandstone and siltstone.

Facies 1.1 is interpreted as terminal distributary channels with subaqueous erosion, as evidenced by the lack of floodplain paleosols and desiccation features above or below these channel bodies (Olariu and Bhattacharya, 2006; Tanavsuu-Milkeviciene and Sarg, 2012). Climbing ripples and soft sediment deformation indicate high sediment supply and rapid deposition, respectively, whereas basal channel rip-up clasts indicate rapid flow. The erosional and narrow characteristics of these terminal distributary channels suggest that they were being deposited along a steep gradient, where flow into the lake was rapid enough to allow for continued channelization (Wright, 1977; Olariu and Bhattacharya, 2006). These channel bodies are interpreted to have formed in the proximal delta front area, based on the coarse grain sizes relative to other sandstone facies within the succession. The laterally extensive, current and wave ripple dominated siltstone and sandstone beds encasing these channelized sandstone bodies are

characteristic of fluvial mouthbar deposits (F1.2) (Edmonds and Slingerland, 2007; Schomacker et al., 2010; Moore et al., 2012; Rosenberg, 2013; Rosenberg et al., in press) (Figure 8). The presence of fish scales indicates fresh to brackish waters, where fish were able to thrive. This facies is typically found in the transitional interval of the central portion of the basin and paleocurrent measurements from the channels indicate dominant flow direction to the north-northwest with sediment derived from the south. This facies is also found in the R8 interval in the western portion of the basin, where paleocurrents are towards the north-northeast.

Facies 1.2 (F1.2)

Facies 1.2 is composed of laterally extensive, interbedded greenish grey, calcareous siltstone and claystone and very fine sandstone deposits (Table 1, Figure 7e-g). The major sedimentary structures include planar parallel laminations, current ripples with occasional wave modification, climbing ripples, low angle laminations, soft sediment deformation, minor burrows, and syneresis cracks. These packages tend to be tabular or vertically gradational and range from 1 to 5 m thick, with sandstone beds ranging in thickness from a few centimeters to 2 m. This facies is also represented in the Henderson 3 core and thin sections, which show normal grading, erosional contacts, well to moderate sorting, and ostracod debris that are not observed in outcrop alone (Figure 9).

This facies is interpreted as deposited in the lower littoral to sublittoral realm and represents classic fluvial mouthbar packages that were deposited basinward from F1.1 (Figure 6). The thicker, sharp-based sandstone packages represent proximal fluvial mouthbars deposited in the lower littoral realm (Wright, 1977; Edmonds and Slingerland,

Figure 8 – Relationship between terminal distributary channels (F1.1) and fluvial mouthbar deposits (F1.2); A) Close up of a terminal distributary channel scouring into the lower mouthbar deposits; B) Large-scale relationship between terminal distributary channels and the surrounding mouthbar deposits (example from L5 zone).

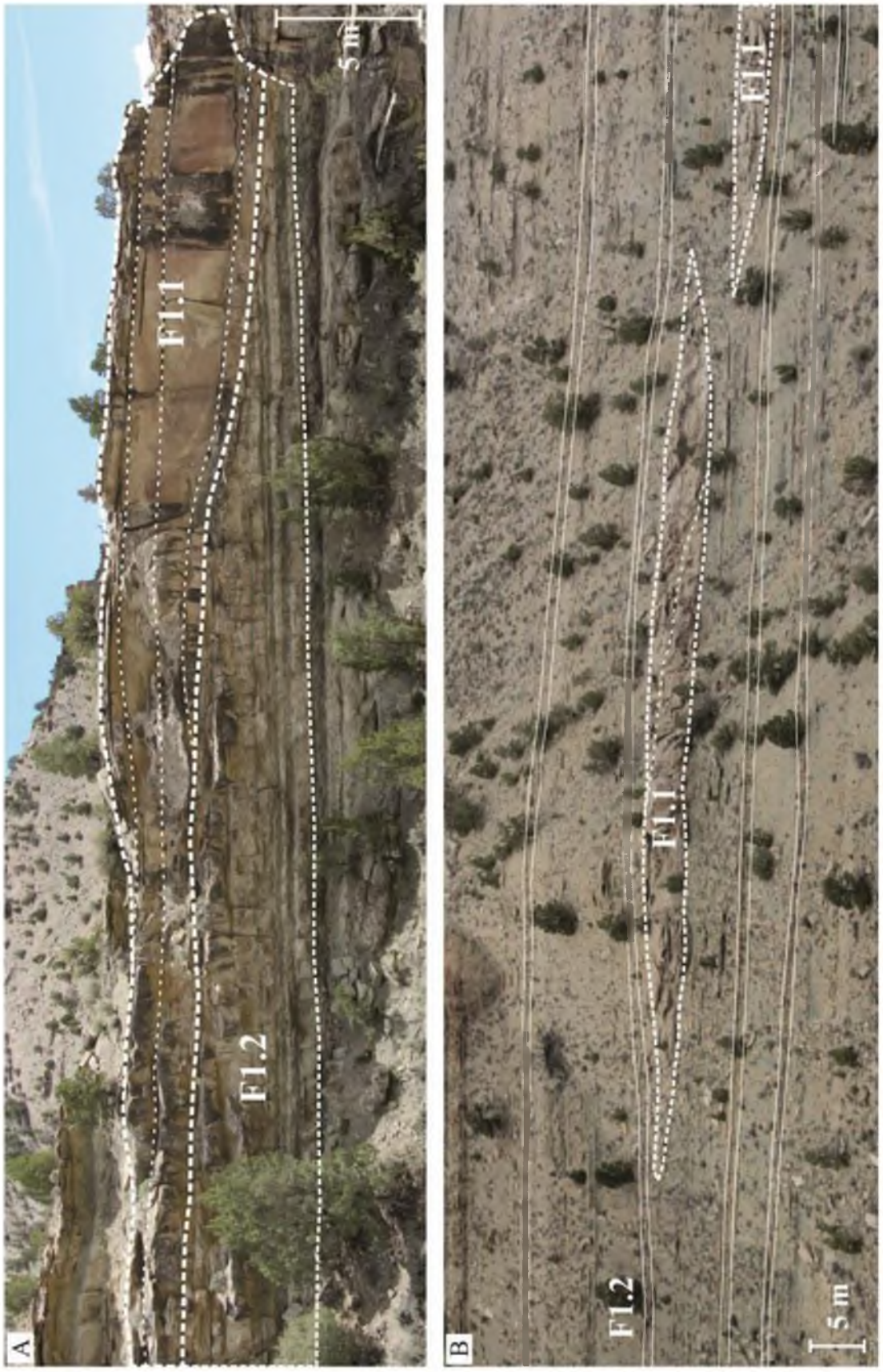
A
F1.1
F1.2
5 m
B
F1.1
F1.1
F1.2
5 m

Figure 9 – Core photo and thin sections of F1.2 from the Henderson 3 core. A) Core photo of the S2 sandstone showing a normally graded turbidite sequence that contains characteristic parallel laminated (PPL), fine sandstone that transitions upwards to ripple laminated, very fine sandstone overlain by parallel laminated siltstone. B) Very fine sandstone to siltstone from the S2 sandstone (cross polarized light, thin section 1). C) Sharp, erosional boundary between mudstone and siltstone from the S2 sandstone (cross polarized light, thin section 2); representative of boundary between two turbidite packages. D) Fine sandstone with ostracod debris from the S1 sandstone (cross polarized light, thin section 10).

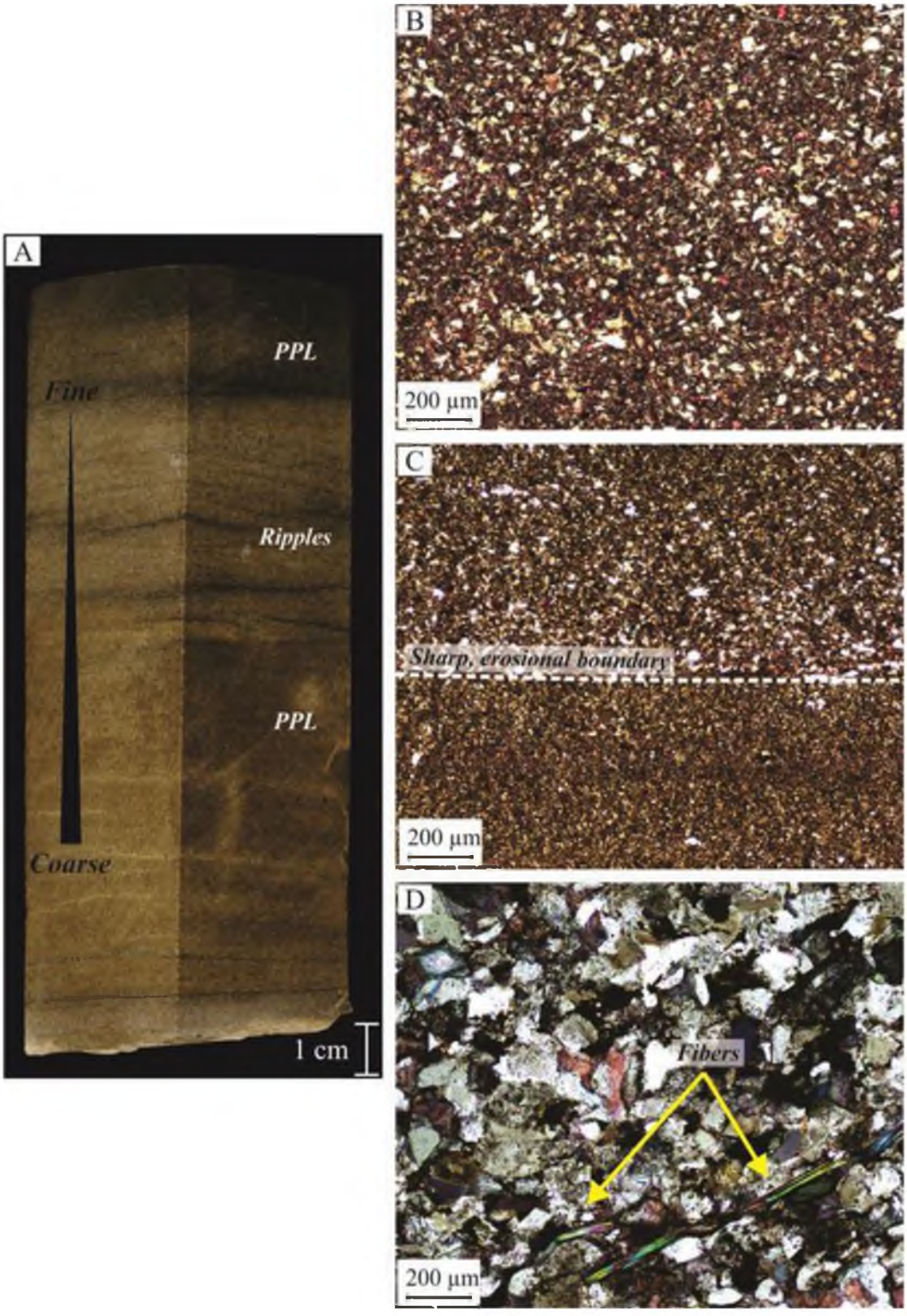
A
PPL
Fine
Ripples
PPL
Coarse
1 cm
B
200 µm
C
Sharp, erosional boundary
200 µm
D
Fibers
200 µm

2007; Schomacker et al., 2010; Moore et al., 2012). These low angle laminated sandstone packages range from 1-2 m and are interpreted as proximal delta front packages that are deposited when a flow with a high sediment load meets a large standing body of water. They display soft sediment deformation and climbing ripples, indicative of fast deposition and high sediment supply. The sharp base and lack of subaerial exposure represents subaqueous erosion from the channelized flow entering the lake (Tanavsuu-Milkeviciene and Sarg, 2012).

The finer grained, gradational packages represent turbidite packages deposited basinward from the mouthbar packages, in the sublittoral realm (Rosenberg, 2013; Rosenberg et al., in press) (Figure 6). The turbidites were deposited via hyperpycnal flows, which hug the bottom when a high density, sediment laden flow enters a low density standing body of water. Evidence for turbidites is illustrated in the Henderson 3 core, where thin deposits of siltstones and very fine sandstones with normal grading and sharp, erosional contacts are observed (Osleger et al., 2009) (Figure 9a, c). These sandstones and siltstones are vertically associated with thinly laminated siltstones and carbonate mudstones, which are thought to be derived from sediment fallout (Moore et al., 2012). The presence of syneresis cracks in these sublittoral gradational packages indicates rapid salinity fluctuations during deposition of the fine grained deposits (Pratt, 1998) (Figure 7f). During deposition, swelling clays contract in response to salinity changes, producing cracks that are then filled with siltstone (Plummer and Gostin, 1981). Facies 1.2 is mainly documented in the transitional interval and the R8 interval of the central portion of the basin and the R8 interval of the western portion of the basin. It is also observed in S1 and S2 sandstones in the Henderson 3 core, where the units were

deposited basinward from the outcrops.

Facies 1.3 (F1.3)

Facies 1.3 consists of laterally continuous, very fine to medium grained, tabular sandstone bodies with planar parallel laminations, low angle laminations, wave ripples, and minor burrowing throughout (Table 1, Figure 7h-j). Shell debris and carbonate grains are found within these sandstone bodies. The sandstone bodies range in thickness from 50 cm to 3 m and are tabular and wavy bedded with flaggy weathering. Sandstone beds are sharp based and interbedded with planar parallel laminated siltstone beds. Internally, packages coarsen upwards. Paleocurrent measurements indicate flow direction to the north-northeast with sediment derived from the south.

Facies 1.3 records wave ripple dominated, siliciclastic shoreface deposits along the lake margin. Wavy laminations and symmetrical ripples are indicative of wave action (Allen, 1981; Pietras and Carroll, 2006) (Figure 7i). The lack of hummocky cross stratification suggests that the lake level was too shallow along the margin to allow hummocks to form (Eyles and Clark, 1986). Shell debris and carbonate grains represent deposition in a high energy environment and the coarsening upwards trends indicate overall shallowing (Renaut and Gierlowski-Kordesch, 2010). These shoreface deposits are significantly different than those of typical marine shoreface sequences. The sandstone beds are poorly developed and are interbedded with mudstones and siltstones, which indicate shallow waters and low relief typical along a lake margin (Bohacs et al., 2000) (Figure 7h). The primary transport method is thought to be long shore drift, but could also be interpreted as a wave dominated delta. However, this distinction is difficult

to make in the rock record (Keighley, 2008; Tanavsuu-Milkeviciene and Sarg, 2012). The lack of asymmetrical ripples and channel deposits in lateral association with this facies suggests a shoreface rather than a wave dominated delta deposit. Again, the lack of fish debris in this area could suggest that there is no fresh water input, thus confirming that this area is dominated by long shore drift. This facies is found in the R8 interval in the central portion of the basin.

F1 Interpretation

Facies Association 1 is composed of siliciclastic dominated packages deposited in a littoral to sublittoral environment via fluvial (F1.1 and F1.2) and shoreface (F1.3) processes. The characteristics of these deposits, including strong channelization, subaqueous erosion, sandy mouthbar deposits, and turbidite packages, support the interpretation of a lake margin with a relatively steep depositional gradient (Figure 6). These facies are predominantly found in the central portion of the basin, but can also be found in the western R8 interval.

Facies Association 2: Shallow gradient, littoral to sublittoral siliciclastic deposits

Facies Association 2 (F2) is found in the transitional interval of the western portion of the basin and consists of weakly channelized sandstone bodies, heterolithic channels, green calcareous siltstone, and paleosol deposits (Figures 6 and 10). Facies Association 2 is laterally related to F1.

Figure 10 – Facies Association 2: Shallow gradient, littoral to sublittoral siliciclastic deposits. A) Facies 2.1 from Willow Creek/Indian Canyon transitional interval; weakly channelized sandstone body overlying red/green paleosol deposits. B) Facies 2.1 from Willow Creek/Indian Canyon transitional interval; low angle laminations with fish debris. C) Facies 2.1 from Willow Creek/Indian Canyon transitional interval; soft sediment deformation (SSD). D) Facies 2.2 from Willow Creek/Indian Canyon transitional interval; heterolithic channel deposits with internal accretion sets highlighted in yellow. E) Facies 2.2 from Willow Creek/Indian Canyon transitional interval; heterolithic channel fill deposit with basal channel scour highlighted in yellow. F) Facies 2.3 from Willow Creek/Indian Canyon transitional interval; green calcareous siltstone with purple mottling. G) Facies 2.3 from Willow Creek/Indian Canyon transitional interval; calcareous siltstone with vertical burrows. H) Facies 2.4 from Willow Creek/Indian Canyon transitional interval; paleosol deposits underlying a channel body.

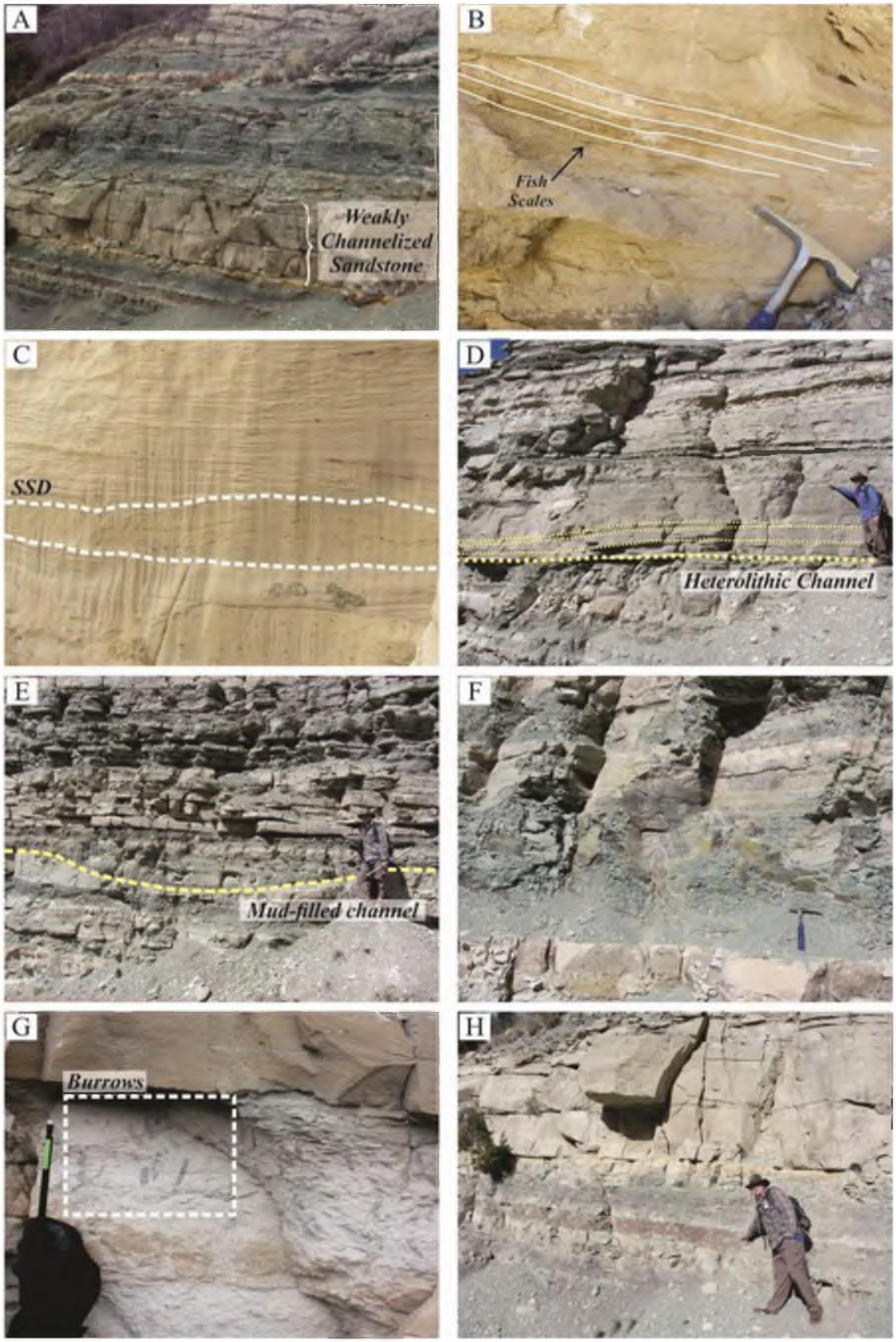
A
Weakly Channelized Sandstone
B
Fish Scales
C
SSD
D
Heterolithic Channel
E
Mud-filled channel
F
G
Burrows
H

Facies 2.1 (F2.1)

Facies 2.1 is composed of laterally discontinuous, very fine to fine grained, weakly channelized sandstone bodies (Table 1, Figure 10a-c). These channel bodies are dominated by low angle laminations, minor downstream accretion sets, and minor trough cross stratification towards the base with plant debris, some rip-up clasts, and very minor fish debris. Current ripples, climbing ripples, planar parallel laminations, and wavy laminations can be observed towards the top of these channel bodies. Channel bodies range from 1 to 3 m and are typically single-storied. These channel bodies can be lenticular or tabular and are more sheet-like than F1.1. Paleocurrent data suggest a dominant north-northeast flow direction. The channels are overlain by greenish mudstones and siltstones that commonly display evidence of subaerial exposure.

Facies 2.1 is interpreted as fluvial distributary channel packages that are deposited along a very shallow gradient. The shallow gradient discouraged rapid flow across the substrate, limiting erosion into the substrate, and encouraged more sheet-like deposition with poorly-confined flows (Edmonds and Slingerland, 2007; Maestro, 2008). Climbing ripples and soft sediment deformation are indicative of high sediment supply and rapid deposition, similar to F1.1. The interbedded mudstones and siltstones with some evidence of subaerial exposure (F2.3) suggest that these packages were deposited along a shallow lake margin where surrounding deposits include lake flat and lagoonal type mudstones (Keighley et al., 2002; Keighley et al., 2003). The scarce amount of fish scales related to this facies may possibly indicate high salinities due to low freshwater input. Paleocurrent data suggest a sediment source from the south and flow to the north, similar to F1.1. This facies is found in the transitional interval of the western portion of

the basin.

F1.1 and F2.1 are both considered terminal distributary channels and yet they represent two depositional styles that are controlled by lake margin slope (gradient) and lake depth. These two facies are not only different in terms of their internal structures and characteristics, but also in terms of their surrounding deposits. F1.1 is typically overlain by current dominated siltstones and mudstones (F1.2) whereas F2.1 is overlain by mottled, green, calcareous siltstone and mudstone (F2.3) with some evidence of subaerial exposure. F1.1 is considered to be deposited in an open lake margin setting where subaerial exposure is not evident. The lake margin slope, or gradient, was relatively steep, which allowed for erosion into the underlying substrate and confined flow, resulting in distinct, channelized sandstone body lenses (Figure 11a). F2.1 is interpreted as deposited along a lake margin with a shallow gradient, based on the lack of erosion into the underlying sediments, hence discouraging confined flow and depositing sheet-like sandstone bodies (Figure 11b).

Facies 2.2 (F2.2)

Facies 2.2 consists of laterally discontinuous, channelized interbedded muddy siltstone and very fine sandstone deposits (Table 1, Figure 10d, e). Sedimentary structures are scarce in the sandstone beds but where present include current ripples, low angle laminations, and soft sediment deformation. The channelized heterolithic bodies range from 1 to 2 m thick and are single-storied with minor basal erosion. Interbed thicknesses within the heterolithic channel fills range from 5 to 20 cm. Some channel forms are filled with dominantly sandstone or dominantly mudstone (Figure 10d, e). Fine

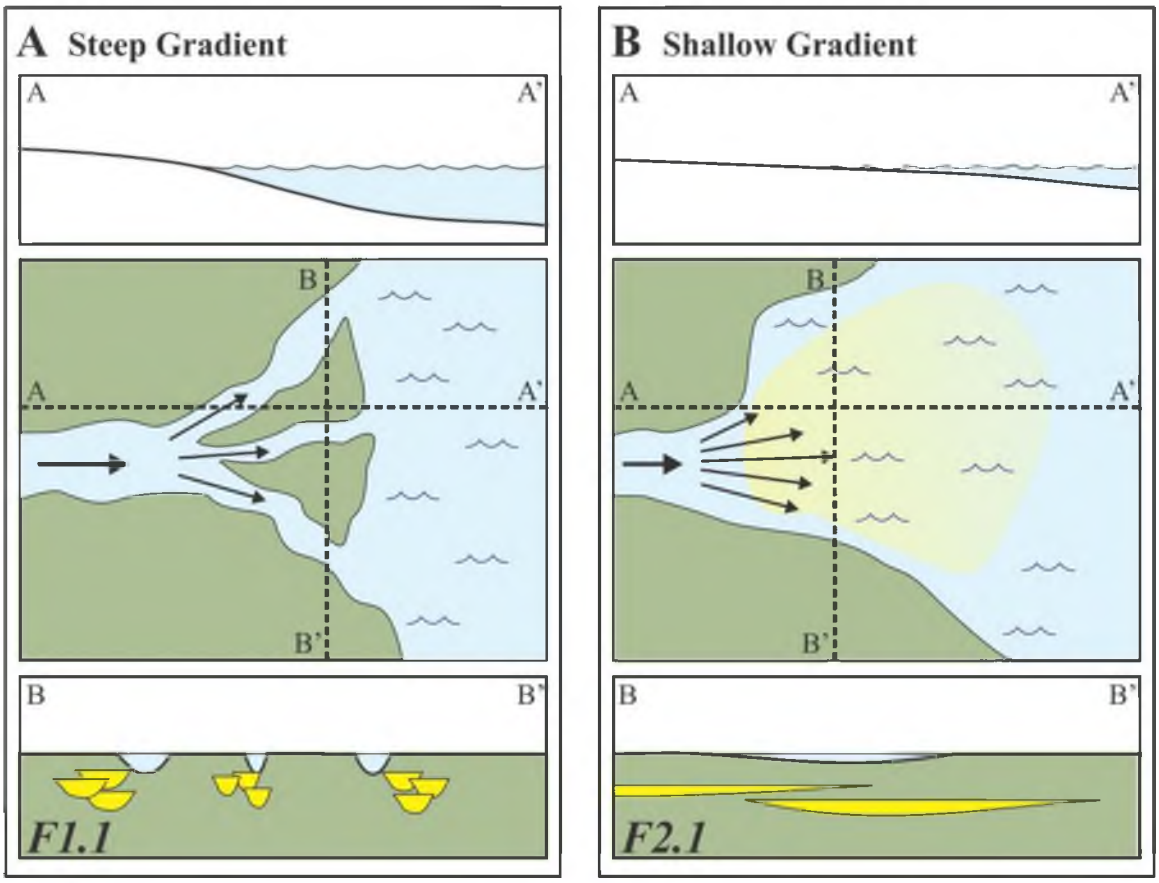

Figure 11 – Paleodepositional model comparing the two distributary channel styles in the transitional interval; A) The steep gradient encourages rapid flow and erosion/confinement into the substrate, producing channelized sandstone lenses of F1.1; B) The shallow gradient discourages rapid flow and erosion, therefore producing weakly channelized sandstone bodies of F2.1.

grained deposits overlying and underlying these channelized bodies tend to display subaerial exposure. Dominant paleocurrent data indicate flow was to the north-northeast.

Facies 2.2 records heterolithic channels that are interpreted as littoral lake flat channels. These channels are typically laterally related to the weakly channelized distributary channels of F2.1 as well as the paleosols of F2.4 (Figure 6). These isolated, heterolithic channels represent deposition away from the main channel belt of F2.1. The sandstone dominated lenses represent higher energy channels with major sediment deposition within the channel body (Ryder et al., 1976). The mudstone dominated lenses represent abandonment and fill with lake flat mudstones (Figure 10d, e). These channels are primarily found in the transitional interval of the western portion of the basin.

Facies 2.3 (F2.3)

Facies 2.3 consists of green calcareous siltstone that is commonly interbedded with greenish purple mudstone (Table 1, Figure 10f, g). These deposits are dominantly massive and mottled but can also have planar parallel laminations, current ripples, and minor burrowing. Bed thicknesses range from 1 to 8 m and are tabular with flaggy weathering.

Facies 2.3 is interpreted as lake flat deposits that are found along the lake margin and lagoonal environments. The green color, as opposed to a grey or brown color indicative of organic matter, is interpreted to result from a shallow lake level which allowed for the destruction of primary organic matter by bacteria and bottom feeders (Picard, 1955). The mottled texture is a result of periodic subaerial exposure and pedogenic modification (Eugster and Hardie, 1975; Keighley et al., 2002). This facies is

found only in the transitional interval in the western portion of the basin. This facies is laterally associated with F2.1, F2.2, and F2.4 (Figure 12).

Facies 2.4 (F2.4)

Facies 2.4 is composed of green and purple mudstone with minor siltstone beds. Beds are mottled and contain slicks, both of which are evidence of pedogenesis. In some cases, blocky peds are evident. Current ripples are present within the siltstone beds (Table 1, Figure 10h).

Facies 2.4 is interpreted as poorly developed floodplain paleosols, similar to those observed in the study by Keighley et al. (2003). These paleosols contain current rippled siltstones that are indicative of overbank deposits from the related distributary channels of F2.1. This facies is laterally and vertically related to F2.1, F2.2, and F3.3, and is found in the transitional interval of the western portion of the basin.

F2 Interpretation

The four facies that comprise F2 were deposited in the littoral to sublittoral zone along fluvial and shallow lake flat environments. The abundance of fine grained material and weak channelization support the interpretation of a low siliciclastic sediment supply, shallow depositional gradient environment. Coarse, weakly channelized sediment occasionally reached this part of the system, but it is mainly dominated by mudstones and siltstones representative of lake margin mudflats. The weakly channelized sandstones could be related to a much larger system and could possibly represent distal, crevasse splay deposits. Major flooding events, similar to those seen in the Burdekin River in

Figure 12 – Relationship of sheet-like terminal distributary channels (F2.1) and green, calcareous lake flat deposits (F2.3).

Australia during flashy, monsoonal events, could trigger fluvial discharge events that carry large volumes of sediment to the more distal part of the deltaic system (Fielding et al., 2005).

Facies Association 3 (F3): Low siliciclastic sediment supply, littoral to sublittoral carbonate deposits

Facies Association 3 (F3) includes microbialites, coarse grained carbonates, and organic-poor carbonate mudstones, all of which are associated with littoral and sublittoral lake environments (Figures 6 and 13). This facies association can be found throughout the middle to upper Green River Formation.

Facies 3.1 (F3.1)

Facies 3.1 is characterized by microbialite beds that display either stromatolitic or stromatolitic-thrombolitic textures (Table 1, Figure 13a-c). Microbialite beds typically overlie carbonate mudstone, grainstone, and wackestone beds and may contain fish debris. Bed thicknesses range from 10 to 50 cm with wavy to tabular bedding. As compared to the microbialite beds observed elsewhere in the Uinta Basin (e.g., east of this field area), those present in the study area are thin. Many of the stromatolites have well-defined domes (or heads) that indicate formation within the photic zone (Williamson and Picard, 1974). Dome size ranges from a few cm to 10 cm. The thrombolites observed are typically thin and underlie the stromatolite packages. Microbialites are largely found in the central portion of the basin at Gate Canyon in the Transition Interval and are mostly absent from the same interval at Willow Creek/Indian Canyon in the west.

Facies 3.1 is interpreted as being deposited in a high energy, littoral setting

Figure 13 – Facies Association 3: low siliciclastic sediment supply, littoral to sublittoral carbonate deposits. A) F3.1 from Gate Canyon transitional interval; thrombolitic to stromatolitic texture. B) F3.1 from Gate Canyon transitional interval; stromatolite head overlying carbonate mudstone. C) F3.1 from Willow Creek/Indian Canyon transitional interval; thin carbonate bed with a fine-scale stromatolitic texture characteristic of the microbialites in the western region. D) F3.2 from Gate Canyon transitional interval; amalgamated, massive ostracodal grainstone beds. E) F3.2 from Gate Canyon transitional interval; thin, tabular ostracodal (small brownish red round grains) grainstone beds with interbedded organic-poor carbonate mudstone. F) F3.2 from Gate Canyon transitional interval; thin ostracodal grainstone bed overlying organic-poor carbonate mudstone; burrows present at the base of the bed. G) F3.3 from Willow Creek/Indian Canyon transitional interval; massive organic-poor carbonate mudstone bed overlain and underlain by calcareous green siltstone of F2.2. H) F3.3 from Willow Creek/Indian Canyon transitional interval; close up of amalgamated, massive, white, organic-poor carbonate mudstone beds.

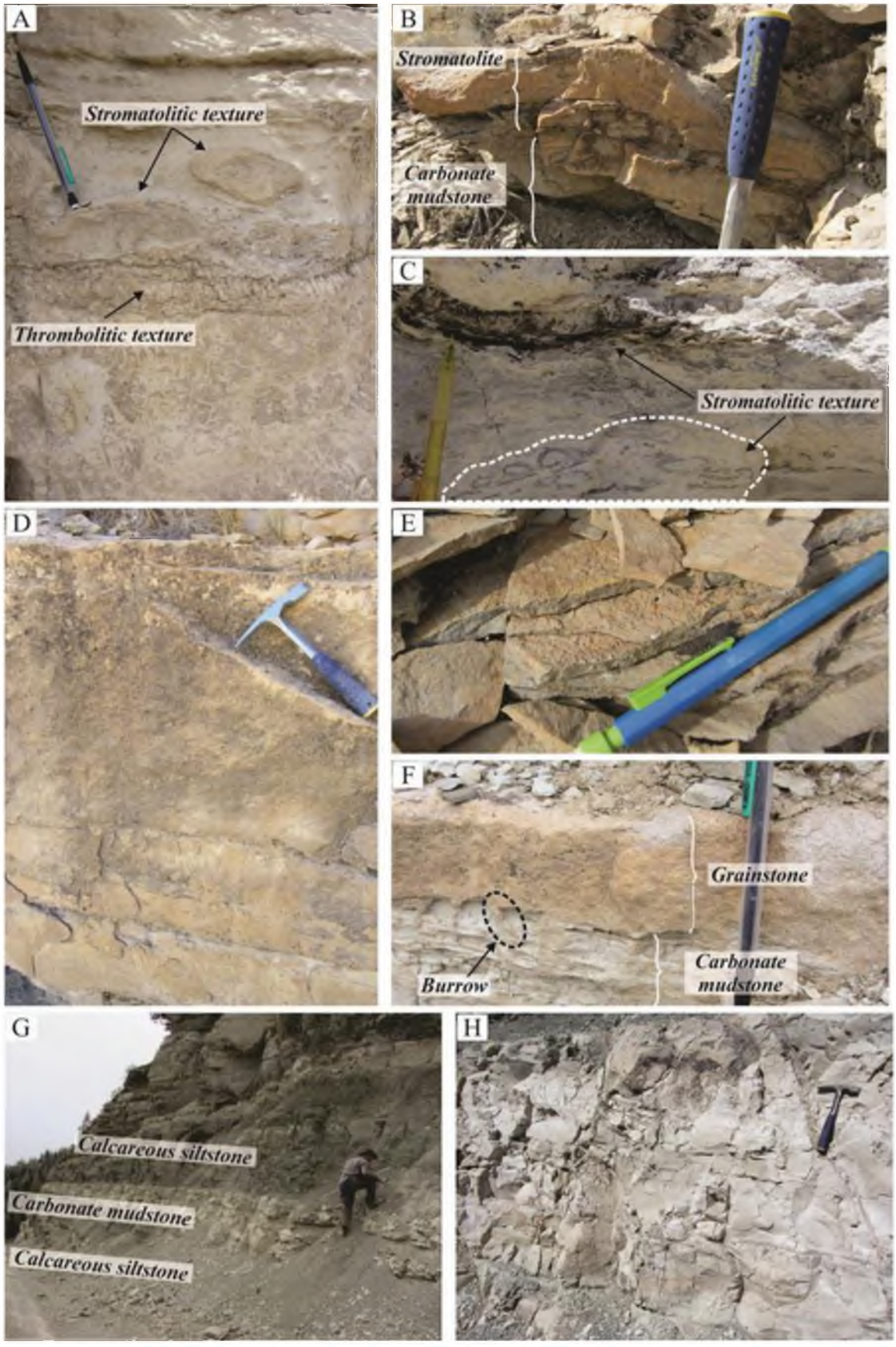
A
Stromatolitic texture
Thrombolitic texture
B
Stromatolite
Carbonate mudstone
C
Stromatolitic texture
D
E
F
Grainstone
Burrow
Carbonate mudstone
G
Calcareous siltstone
Carbonate mudstone
Calcareous siltstone
H

dominated by carbonate deposition (Feldmann and McKenzie, 1998). This facies is indicative of a carbonate ramp environment, where algal mat construction and sediment trapping was promoted. Towards the central part of the basin, stromatolite and thrombolite complexes are well defined and relatively thick (20 to 50 cm), with thrombolites representing slightly deeper water and the overlying stromatolites representing slight shallowing events (Feldmann and McKenzie, 1998). Because this area has a scarce amount of microbialites as compared to other parts of this lacustrine system, it may suggest the gradient on the front of the axis of the delta system was too high, resulting in unstable substrates and discouraging abundant microbialite buildup (Renaut and Gierlowski- Kordesch, 2010; Rosenberg, 2013; Rosenberg et al., in press). Towards the west, microbialite sequences are very thin (10 to 20 cm) and are less abundant. The lack of thrombolitic textures in this area suggests very shallow water. In both areas, the microbialites are not laterally extensive. Modern microbialite formation and preservation has been demonstrated to be salinity and energy sensitive (Dupraz and Visscher, 2005). A modern study of the Great Salt Lake shows that in the south arm of the lake, where salinity is roughly 16%, there is limited competition and stromatolites are able to form (Baskin et al., 2012). In the north arm of the lake, the salinity is near saturation (~26%) and stromatolites are not able to survive (Baskin et al., 2012). Similarly, the western portion of the Uinta Basin could possibly have a higher salinity because of lower fresh water input. However, the salinity of Lake Uinta during Green River deposition is not known, therefore further investigation is required to fully understand the implications of the lack of microbialites towards the west.

Facies F3.2

Facies 3.2 is composed of grainstone and wackestone that are massive or planar parallel to wavy laminated. Beds also display minor current and wave ripples, minor burrows, and minor low angle laminations. These coarse grained carbonates are composed of a variety of grains that include carbonate mudstone rip-up clasts, ostracod debris, and fish debris. Bed thicknesses range from 10 cm to 2 m and are typically tabular to wavy. The ostracodal grainstones are easily observed in outcrop (Table 1, Figure 13d, e, f) whereas the wackestone are more accurately described in thin sections from the Henderson 3 core (Figure 14). Wackestone grains found in thin sections that were not observed in outcrop include ooids, stromatolite debris, marcasite, and algal pellets. Thin sections also display siliciclastic lenses, some organic material, small dewatering structures, erosional contacts, moderate sorting, and subangular to subrounded grains.

This facies is interpreted as deposited in a littoral to lower littoral zone along high energy carbonate ramp settings (Renaut and Gierlowski-Kordesch, 2010). The ostracodal grainstones are more littoral and represent shoaling environments, where ostracods are reworked along an open lake margin ramp by energetic wave action (Picard and High, 1972; Tucker and Wright, 2009). The wackestones are lower energy deposits that contain abundant transported grains, such as the ostracod and stromatolite debris (Tucker and Wright, 2009). The presence of siliciclastics suggests a nearby fluvial-deltaic influence. Facies 3.2 is found primarily in the transitional interval in the central region of the basin. Thin but rare beds of facies 3.2 are found in the western region of the basin, suggesting that this area of the lake was very low energy where wave energy was dissipated.

Figure 14 – Core photos and thin sections of F3.2 from the Henderson 3 core. A) Core photo from the upper R6; wackestone; transported carbonate mudstone clasts encased in organic-poor carbonate mudstone. B) Core photo from the upper R6; wackestone; carbonate mudstone rip-up clasts displaying erosion into the underlying organic-rich mudstone. C) Intraclastic wackestone from the upper R6 (plain light, thin section 16); stromatolite debris and ostracod debris in a carbonate mudstone matrix. D) Wackestone from the upper R6 (plain light, thin section 13); ostracod debris in a carbonate mudstone matrix with algal pellets throughout. E) Wackestone from the upper R6 (plain light, thin section 13); carbonate mudstone intraclasts. F) Intraclastic wackestone from the upper R6 (plain light, thin section 16); radial ooid encased in carbonate mudstone.

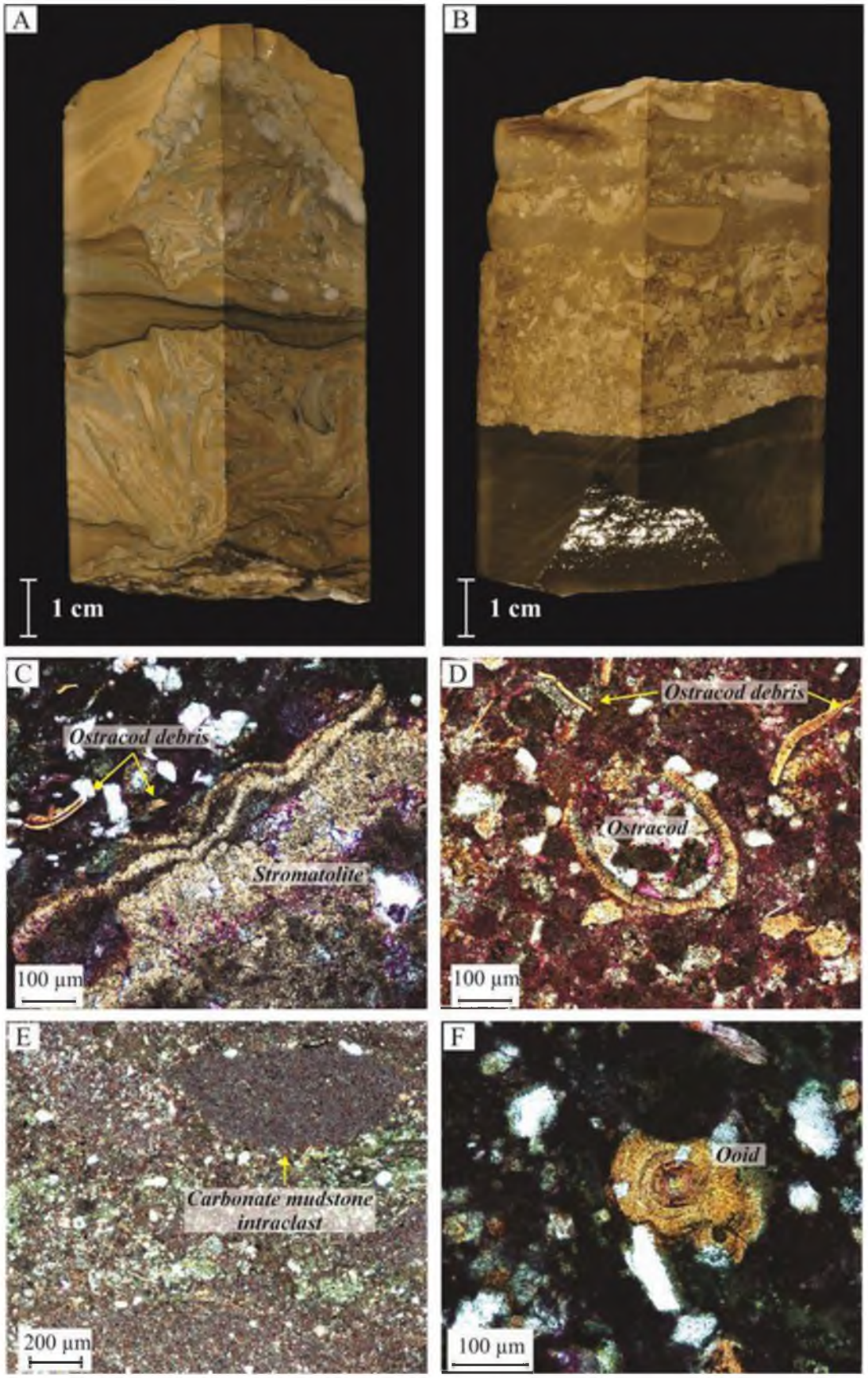
A
1 cm
B
1 cm
C
Ostracod debris
Stromatolite
100 µm
D
Ostracod debris
Ostracod
100 µm
E
Carbonate mudstone intraclast
200 µm
F
Ooid
100 µm

Facies F3.3

Facies 3.3 consists of organic-poor carbonate mudstone that is massive or planar and wavy laminated (Table 1, Figure 13g, h). Rhythmites are common. Other notable characteristics include carbonate rip-up clasts or intraclasts, dewatering structures, siltstone interbeds, disseminated dolomite, marcasite, and algal pellets, all of which are best observed in core and thin sections (Figure 15). Bed thicknesses range from 20 cm to 2 m and can be tabular or wavy, with flaggy weathering in outcrop. This facies is observed throughout the stratigraphy of the study interval and in both the central and western areas of the basin. However, this facies occurs as a result of a variety of drastically different conditions and so context using surrounding deposits is necessary in order to better understand the depositional environments of this facies. F3.3 is observed in the transitional interval in Gate Canyon and is typically associated with overlying microbialites (F3.1) and coarse grained carbonate (F3.2) beds. Conversely, in the transitional interval in Willow Creek/Indian Canyon, F3.3 is typically associated with overlying and underlying calcareous green siltstone (F2.3).

F3.3 is interpreted as deposited in a sublittoral carbonate ramp setting in the central portion of the basin (Gate Canyon) and littoral lake flat settings in the western portion of the basin (Willow Creek/ Indian Canyon). In the carbonate ramp setting, the carbonate mudstone is deposited in a low energy setting where organic matter is lacking due to low productivity, dilution, or low preservation (Renaut and Gierlowski-Kordesch, 2010; Rosenberg, 2013; Rosenberg et al., in press). In the lake flat setting, slight rises in lake level allowed for deposition of organic-poor carbonate mudstone beds whereas low energy discouraged deposition of coarse grained carbonates (F3.2) and microbialites

Figure 15 – Core photos and thin sections of F3.3 from the Henderson 3 core. A) Core photo from the upper R6; organic-poor carbonate mudstone with carbonate intraclasts and small dewatering structures; planar to wavy laminations. B) Core photo from the upper R6; organic-poor carbonate mudstone with black marcasite (black specks) throughout; planar parallel laminations. C) Core photo from the upper R6; organic-poor carbonate mudstone interbedded with organic-rich carbonate mudstone (F?); example of rhythmites. D) Organic-poor carbonate mudstone from the upper R6 (plain light, thin section 12); mottled green and black with some minor quartz grains. E) Organic-poor carbonate mudstone with marcasite crystals (black radial crystals) from the upper R6 (plain light, thin section 15). F) Green, dolomitized (multicolored crystals throughout thin section), organic-poor carbonate mudstone from Mahogany zone (cross polarized light, thin section 4). G) Organic-poor carbonate mudstone with wavy laminations and dewatering structures from Mahogany zone (plain light, thin section 8); thin section shows green algal pellets that display a mottled internal texture.


A
Carbonate intraclasts
Dewatering structures
1 cm
B
46
1 cm
C
1 cm
D
200 µm
E
200 µm
F
100 µm
G
Algal pellets
100 µm

(F3.1). This organic-poor carbonate mudstone is recognized in multiple studies that define it as palustrine carbonates that are typically deposited along lakes with low gradients and low energy margins (Brand, 2002; Alonso-Zarza, 2003; Tucker and Wright, 2009). The presence of siltstone throughout this facies in the western region indicates proximity to source, supporting the interpretation that F3.3 was deposited fairly close to the lake margin (Picard and High, 1972). Marginal carbonate mudstone units lack any organic matter, suggesting they were deposited in an arid environment (Alonso-Zarza, 2003). In both the sublittoral carbonate ramp and the littoral lake flat settings, energy is very low and siliciclastic sediment supply is limited.

F3 Interpretation

Facies Association 3 contains three facies that are carbonate dominated and considered to be deposited in the littoral and sublittoral realm. These facies are observed throughout the Green River Formation and indicate periods when carbonate deposition outpaced siliciclastic deposition rates (Figure 6). Carbonate deposition occurs when the lake waters become super saturated with calcium carbonate and precipitation occurs (Tucker and Wright, 2009; Renaut and Gierlowski-Kordesch, 2010). A hinterland source of carbonates for weathering and fluvial transport of ions into the lake is a prerequisite for lake carbonate precipitation (Gierlowski-Kordesch, 1998; Alonso-Zarza, 2003; Renaut and Gierlowski-Kordesch, 2010). In Lake Uinta, carbonate deposition was ongoing. Older limestone units were likely abundant in surrounding uplifts (e.g., late Paleozoic limestones, Triassic Sinbad Limestone, and Jurassic Twin Creek Limestone). Alluvial systems provided a sustained calcium carbonate ion supply to the lake. At times,

siliciclastic sediment supply overwhelmed the rate of carbonate deposition. Therefore, carbonate deposition represents either regional or local hiatuses in siliciclastic sediment deposition.

Facies Association 4 (F4): Siliciclastic sediment starved, profundal lake deposits

Facies Association 4 consists of one facies, the organic-rich carbonate mudstone (F4.1), colloquially referred to as "oil shale" (Table 1, Figures 6 and 16). Characteristics of this facies include massive to planar or wavy laminations, soft sediment deformation, minor saline mineral precipitation, marcasite mineralization, precipitated carbonate nodules, disseminated dolomite, and lenses of organic matter. Most of these detailed characteristics are only observable in thin section and core. Outcrop units typically weather white and form ledges, with thicknesses ranging from 20 cm to 2 m. F4.1 is found in the Mahogany zone and R8 intervals in both the central and western portions of the basin.

Facies 4.1 is interpreted as deposited along a carbonate ramp setting in the profundal lake zone basinward from F1, F2, and F3 (Ryder et al., 1976; Kelts, 1988; Tanavsuu-Milkeviciene and Sarg, 2012). Lack of siliciclastics within this facies suggests that it was deposited away from the lake margin in a relatively deep, open lake environment. The organic richness of the carbonate mudstone is indicative of an anoxic environment, enhanced by density stratification of the lake, where bacteria and other organisms that degrade the organic matter were not able to survive and thus allowed for the preservation of organic matter. The presence of limited occurrences of saline crystals (Figure 16d) within the profundal facies but not within the adjacent sublittoral and littoral

Figure 16 – Facies Association 4: siliciclastic sediment starved, profundal lake deposits. A) F4.1 from Willow Creek/Indian Canyon Mahogany zone; outcrop exposure showing dark beds of organic-rich carbonate mudstone (oil shale). B) F4.1 from Gate Canyon Mahogany zone; outcrop photo showing organic-rich carbonate mudstone weathered to white; flakey. C) Core photo from the Mahogany zone in Henderson 3 core; organic-rich carbonate mudstone with small rhythmic interbeds of organic-poor carbonate mudstone. D) Core photo from the Mahogany zone in Henderson 3 core; organic-rich carbonate mudstone with saline crystals (white small disseminated blebs). E) Organic-rich carbonate mudstone with precipitated carbonate grains from the Mahogany zone (cross polarized light, thin section 6). F) Organic-rich carbonate mudstone with disseminated dolomite crystals from the Mahogany zone (cross polarized light, thin section 7). G) Organic-rich carbonate mudstone with marcasite from Mahogany zone (cross polarized light, thin section 9). H) Organic-rich carbonate mudstone with possible saline crystals throughout from Mahogany zone (cross polarized light, thin section 9).

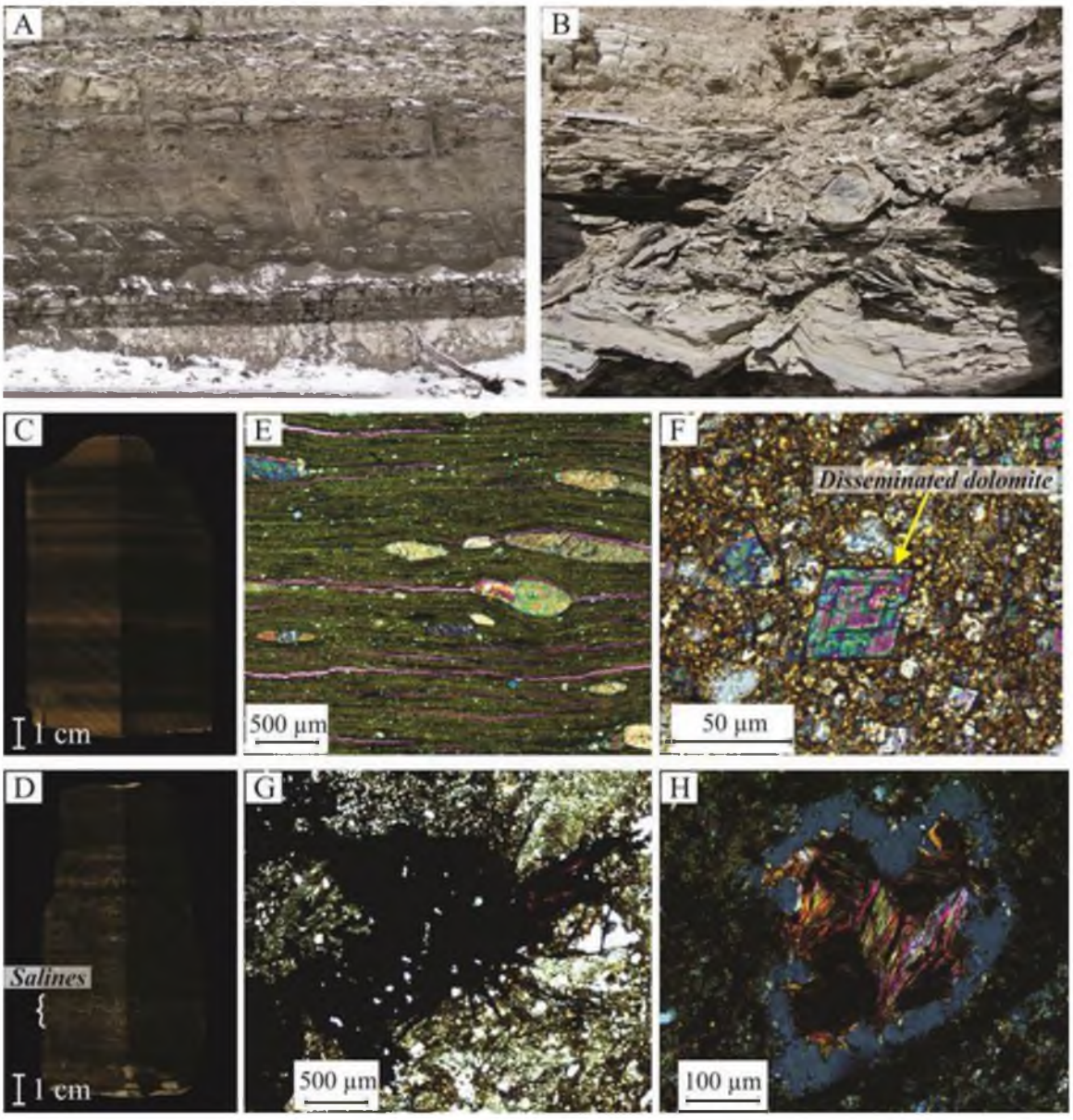
A
B
C
1 cm
E
500 µm
F
Disseminated dolomite
50 µm
D
Salines
1 cm
G
500 µm
H
100 µm

facies further indicates density stratification of the lake waters and oversaturation of salines, allowing for precipitation to occur at the sediment-water interface or in deeper stratified lake waters (Tanavsuu-Milkeviciene and Sarg, 2012). The stratigraphic and geographic distribution of saline crystals provides insight to the duration (episodic versus long-lived) and extent (geographically limited or basin-wide) of water column density stratification.

Facies Association 5 (F5): Saline deposits

Facies Association 5 includes the saline deposits (F5.1) found in the Mahogany zone in the Henderson 3 core, as well as in the saline facies within the Half Moon Canyon core. These salines are observed in a variety of forms, including voids (mm to cm sized), crystals (mm sized), laminated layers or beds (mm to cm thick), and vertical to subvertical fracture fills (Table 1, Figure 17). They are thought to be composed of nahcolite and shortite, which are the characteristic saline crystals found in the Green River Formation, and are only observed in core and thin section.

Facies 5.1 is commonly associated with organic-rich carbonate mudstone, and by association is interpreted as also deposited in the profundal lake zone, where the lake waters can be supersaturated with ions as a result of density water column stratification (Schubel and Lowenstein, 1997; Tanavsuu-Milkeviciene and Sarg, 2012).

Facies Association 6 (F6): Volcanic deposits

Facies Association 6 contains the volcanic deposits (F6.1) that are observed throughout the Green River Formation, most commonly in the R8 Interval. Facies 6.1

Figure 17 – Facies Association 5: Saline deposits; core photos from the saline facies in the Half Moon Canyon Core. A) Small voids with saline crystals within; encased in organic-poor carbonate mudstone. B) Large voids with saline crystals within; encased in moderately organic-rich carbonate mudstone. C) Randomly dispersed saline crystals in moderately organic-rich carbonate mudstone. D) Large, dispersed saline crystals in moderately organic-rich carbonate mudstone. E) Planar parallel laminated saline deposits in organic-poor carbonate mudstone. F) Fractures filled with saline crystals in organic-rich carbonate mudstone.

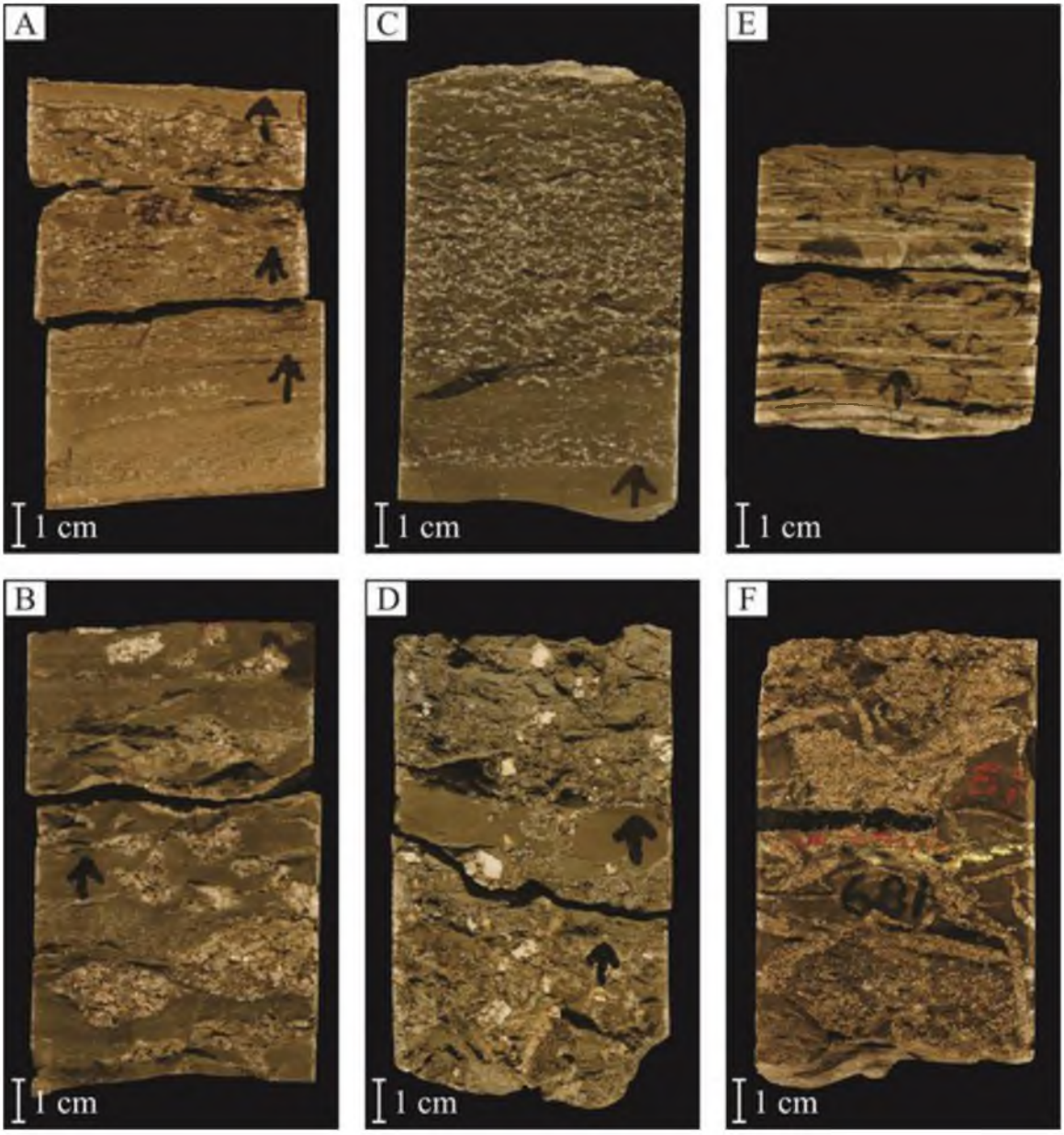
A
1 cm
C
1 cm
E
1 cm
B
1 cm
D
1 cm
F
1 cm

consists of volcanic ash with soft sediment deformation (tuff) (Table 1, Figure 18). Colors are typically grey, orange, and red with thicknesses ranging from 5 to 30 cm. Bed geometries are wavy to tabular.

The tuffs present in the Green River Formation most likely originate from the Absaroka Volcanic province (Smith et al., 2008). Where the tuffs are massive, they are thought to be ash fall deposits. Commonly, tuffs have internal features, such as wavy laminations and soft sediment deformation, and so they may be somewhat reworked by lake processes. Two significant tuffs in the Green River Formation are the Curly and the Wavy tuffs, which can be confidently identified throughout the eastern Uinta Basin. The Curly Tuff lies towards the base of the Mahogany zone and the Wavy Tuff lies in the lower R8 zone above the S2 sandstone (Desborough, 1978; Cashion, 1995) (Appendix B). Samples of these volcanic beds from Nine Mile Canyon have been dated using $^{40}Ar/^{39}Ar$ methods and constrain the ages at 49.3 Ma and 48.7 Ma, respectively (Smith et al., 2008; Smith et al., 2010).

Stratigraphic Units and Associated Facies Architecture

Three major stratigraphic intervals occur in the study area and are informally referred to as the transitional interval, the Mahogany interval, and the R8 interval. Thirteen stratigraphic units were identified and correlated within these intervals that record a variety of lake conditions, both laterally and vertically (Figure 19 and 20). These units are described in numerous other studies, and the specific nomenclature used for this work is based on Remy (1992) for the transitional interval through the Horse Bench (assigned in 9 Mile Canyon) and Weiss et al. (1990) for the saline facies. The

Figure 18 – Facies Association 6: Volcanic deposits. A) Outcrop photo from the R8 in Gate Canyon; thin, tabular, grey tuff. B) Outcrop photo from the R8 in Willow Creek/Indian Canyon; tabular, wavy tuff with diagenetic red iron band in center. C) Core photo from the Mahogany interval of the Henderson 3 core; thin, tabular, grey tuff. D) Core photo from the Mahogany interval of the Henderson 3 core; reworked tuff overlying and underlying organic-rich carbonate mudstone. E) Core photo from the Mahogany interval of the Henderson 3 core; reworked tuff. F) Core photo of the saline facies from the Half Moon Canyon Core; coarse grained rhyolitic tuff deposit.

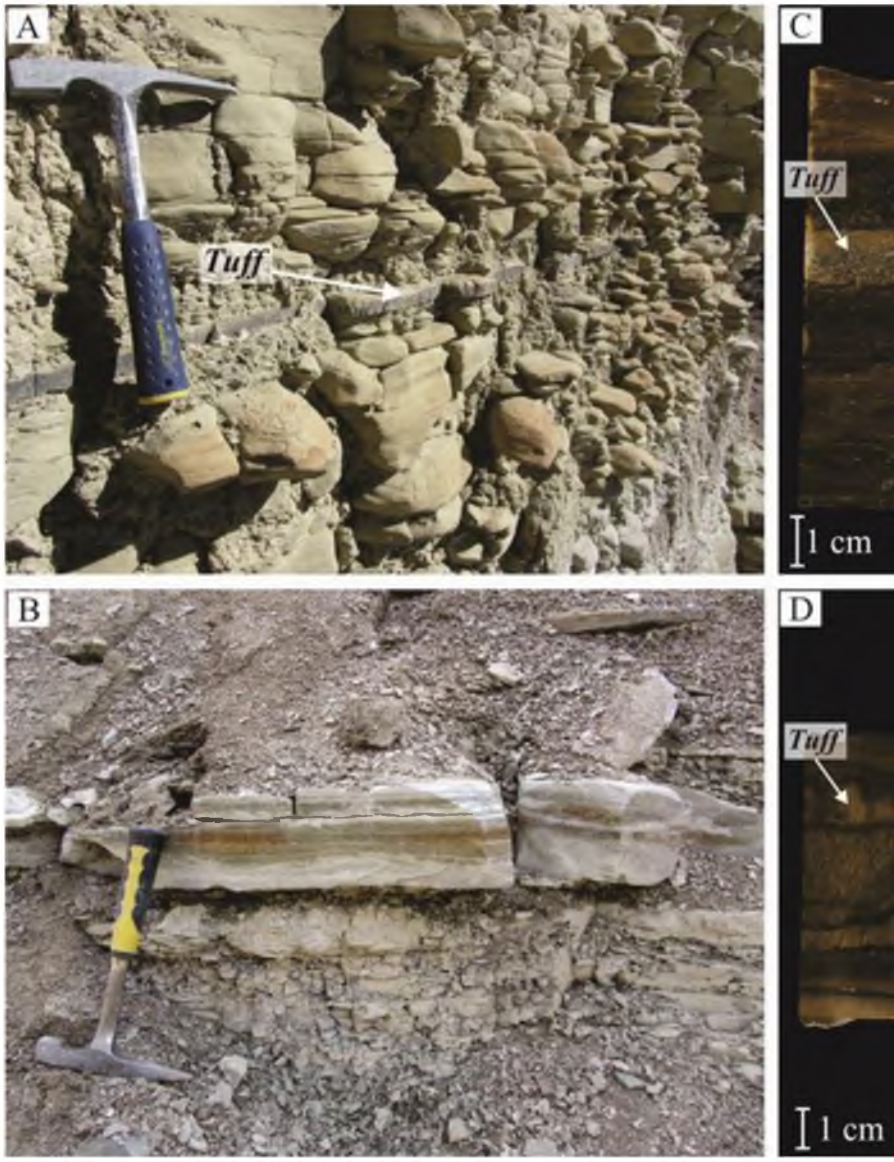
A
Tuff
C
Tuff
1 cm
B
1
D
Tuff
1 cm

E
Tuff
1 cm
F
704
1 cm

Figure 19 – Cross section of identified stratigraphic units present in the Willow Creek/Indian Canyon and Gate Canyon outcrops.

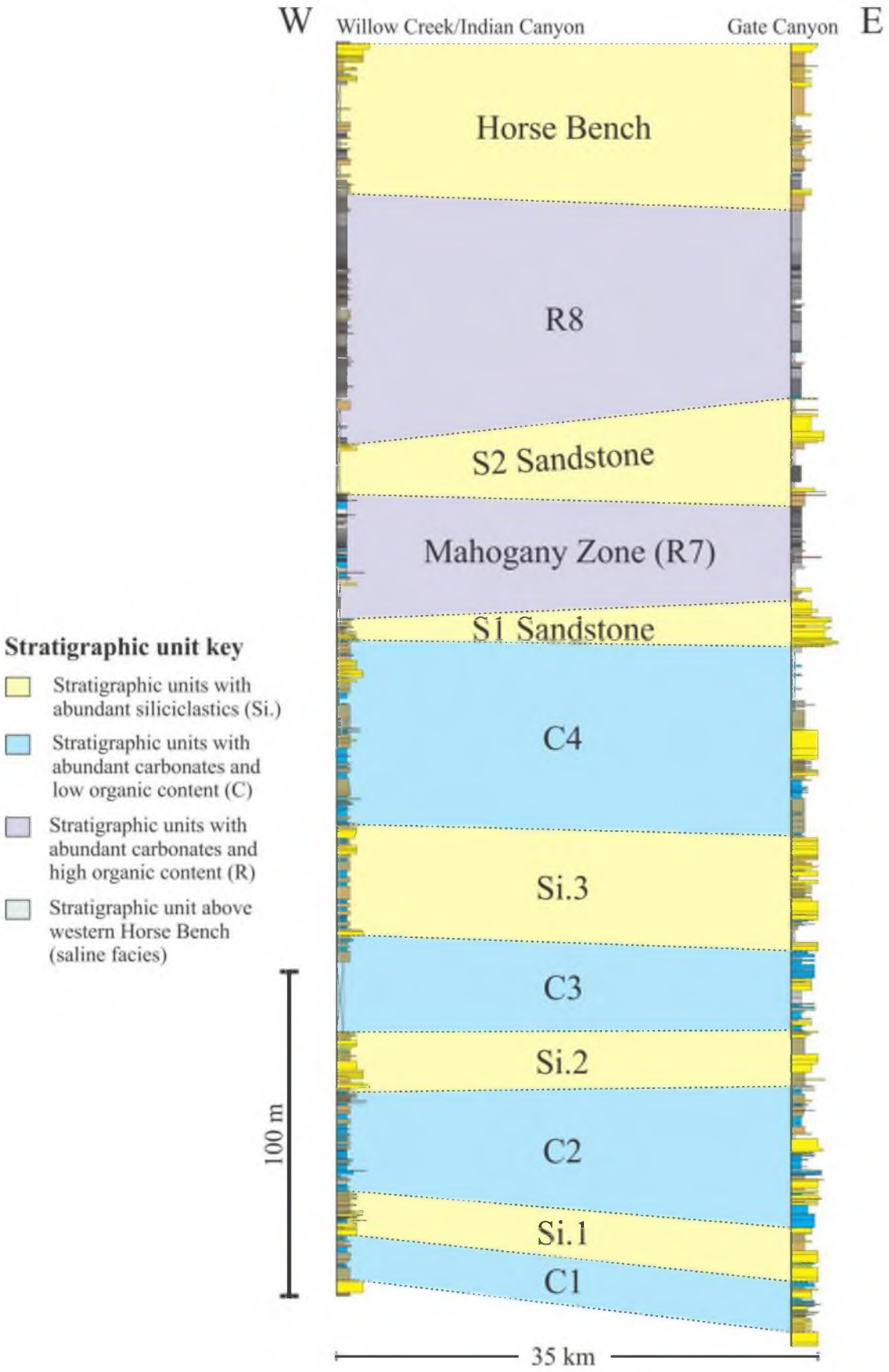
W
Willow Creek/Indian Canyon
Gate Canyon
E
Horse Bench
R8
S2 Sandstone
Mahogany Zone (R7)
S1 Sandstone
C4
Si.3
C3
Si.2
C2
Si.1
C1
100 m
35 km
Stratigraphic unit key
Stratigraphic units with abundant siliciclastics (Si.)
Stratigraphic units with abundant carbonates and low organic content (C)
Stratigraphic units with abundant carbonates and high organic content (R)
Stratigraphic unit above western Horse Bench (saline facies)

Figure 20 – Cross section of identified stratigraphic units present in the Willow Creek/Indian Canyon and Gate Canyon outcrops and the Half Moon Canyon (HMC) and Henderson 3 (H3) cores.

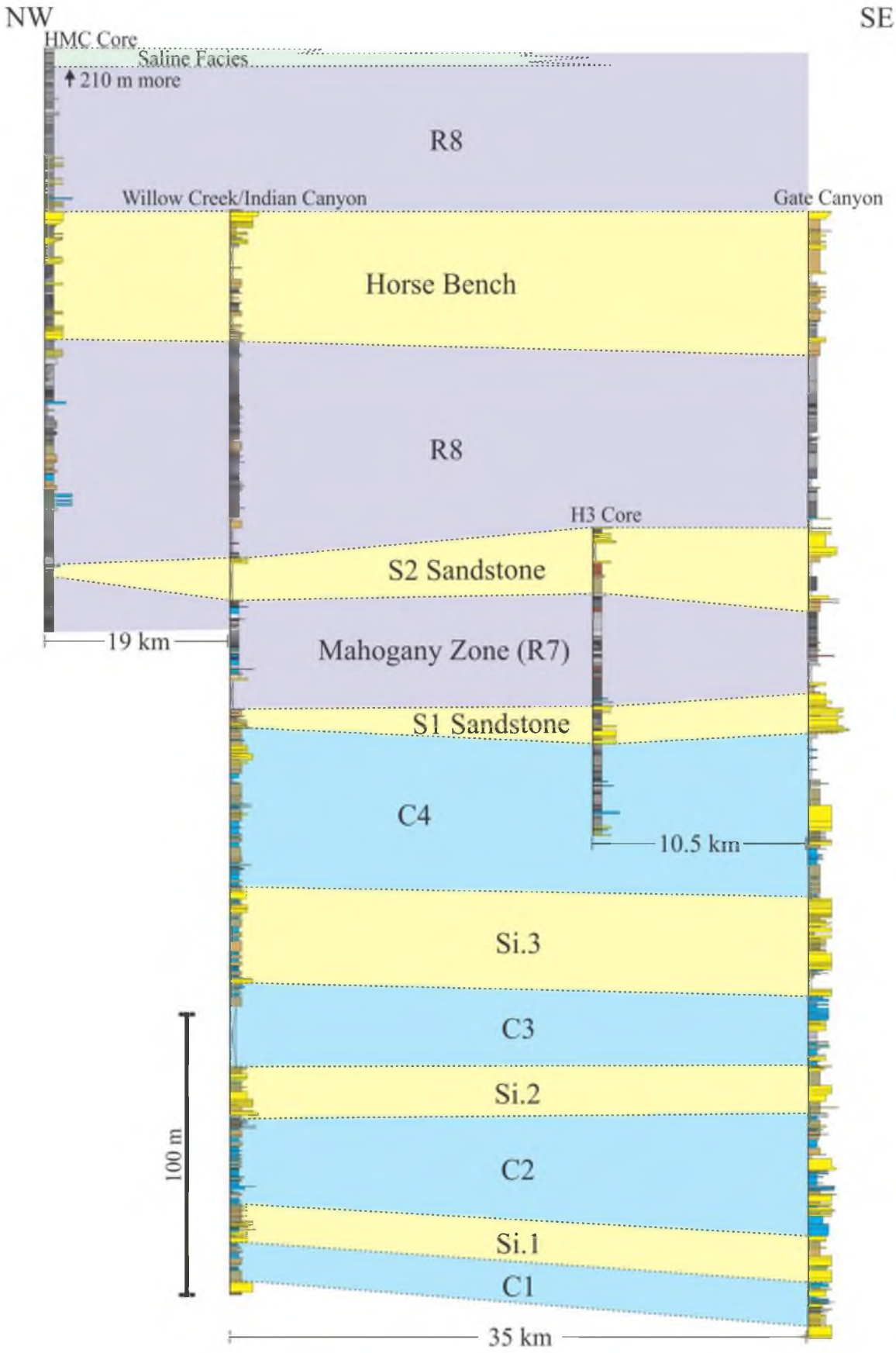
NW
SE
HMC Core
Saline Facies
210 m more
R8
Willow Creek/Indian Canyon
Gate Canyon
Horse Bench
R8
H3 Core
S2 Sandstone
19 km
Mahogany Zone (R7)
S1 Sandstone
C4
10.5 km
Si.3
C3
Si.2
C2
Si.1
C1
100 m
35 km

stratigraphic units identified vary in terms of the siliciclastic versus carbonate ratio and the abundance of organic content within the carbonate dominated units. Further outcrop correlations were made using the facies defined in the previous section in order to observe spatial and temporal changes across the study area (Figures 21, 22, 23, and 24). By interpreting the distinct changes in facies architecture within each of the major intervals (transitional, Mahogany, and R8), observations can be made about the depositional settings and overall lake evolution. Table 2 further compares the thicknesses and facies observed within each stratigraphic unit in the outcrop sections.

The transitional interval of the Green River Formation is by far the most heterogeneous interval and contains the most diverse facies observed throughout the study (Figure 21, Table 2). The interval consists of alternating successions of carbonate packages (C) and siliciclastic packages (Si.), from C1 to C4 (Figure 19). The overall stratigraphic thickness of the transitional interval is relatively constant; 215 m thick in the central region and the 200 m thick in the western region. Internal thicknesses of the 7 carbonate (C) and siliciclastic (Si.) packages within the transitional interval are also fairly consistent, with minor thinning towards the west within the carbonate packages (C). The most important observation is the transition from abundant coarse grained sandstone and coarse grained carbonate deposits in the central study area to fine grained sandstone and carbonate deposits in the western study area.

The Mahogany interval overlies the transitional interval and contains the S1 through the S2 sandstones which encompass the Mahogany zone (R7) (Figures 19 and 20). Traditionally, the S1 sandstone is grouped into the lower transitional interval (Remy, 1992) but for the purposes of this study, it was placed in the Mahogany interval due to its

Figure 21 – Lithostratigraphic cross section of the Willow Creek/Indian Canyon and Gate Canyon outcrops spanning the C1-C4.

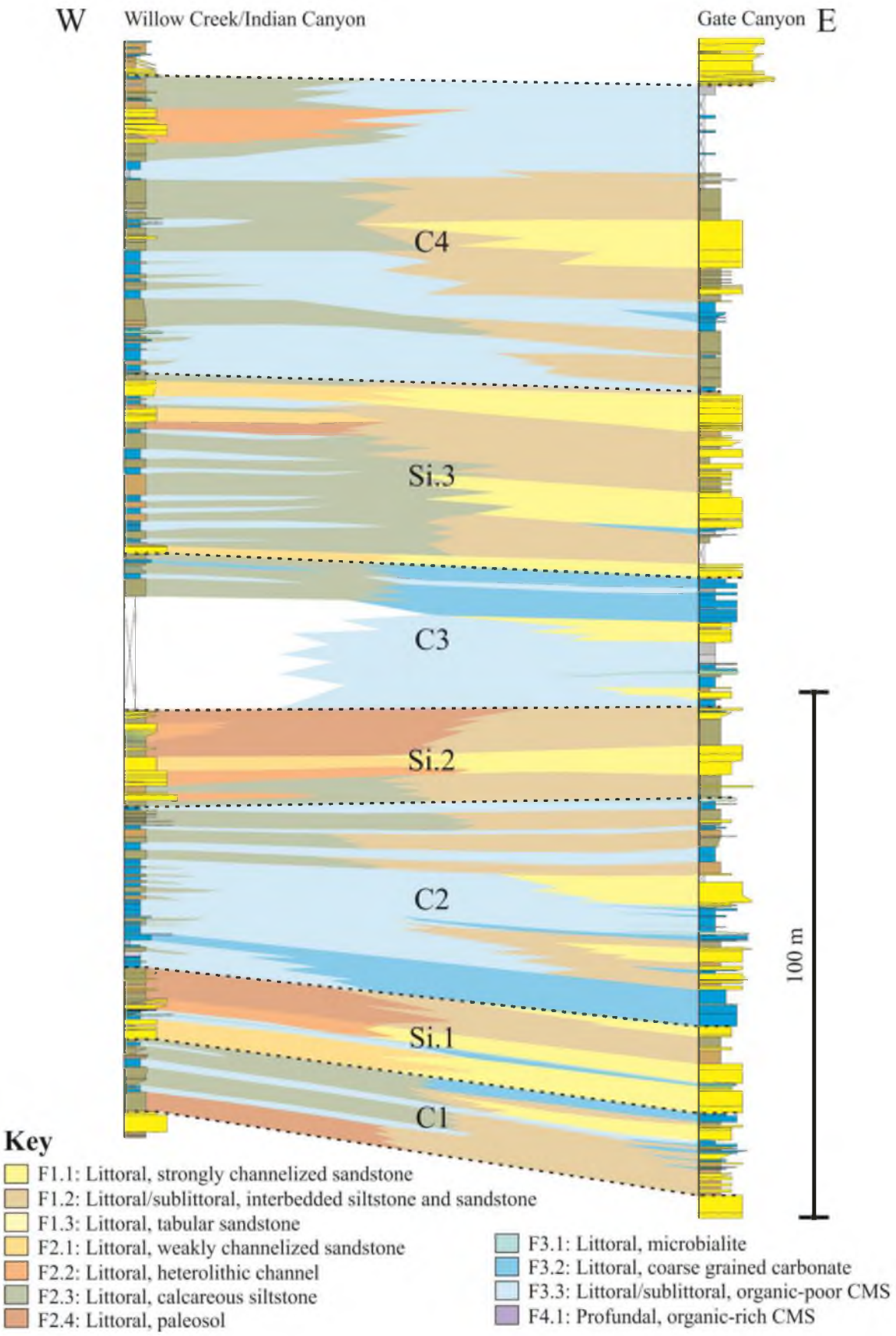
W
Willow Creek/Indian Canyon
Gate Canyon
E
C4
Si.3
C3
Si.2
C2
Si.1
C1
100 m
Key
F1.1: Littoral, strongly channelized sandstone
F1.2: Littoral/sublittoral, interbedded siltstone and sandstone
F1.3: Littoral, tabular sandstone
F2.1: Littoral, weakly channelized sandstone
F2.2: Littoral, heterolithic channel
F2.3: Littoral, calcareous siltstone
F2.4: Littoral, paleosol
F3.1: Littoral, microbialite
F3.2: Littoral, coarse grained carbonate
F3.3: Littoral/sublittoral, organic-poor CMS
F4.1: Profundal, organic-rich CMS

Figure 22 – Lithostratigraphic cross section of the Willow Creek/Indian Canyon and Gate Canyon outcrops spanning the S1 sandstone to Horse Bench sandstone.

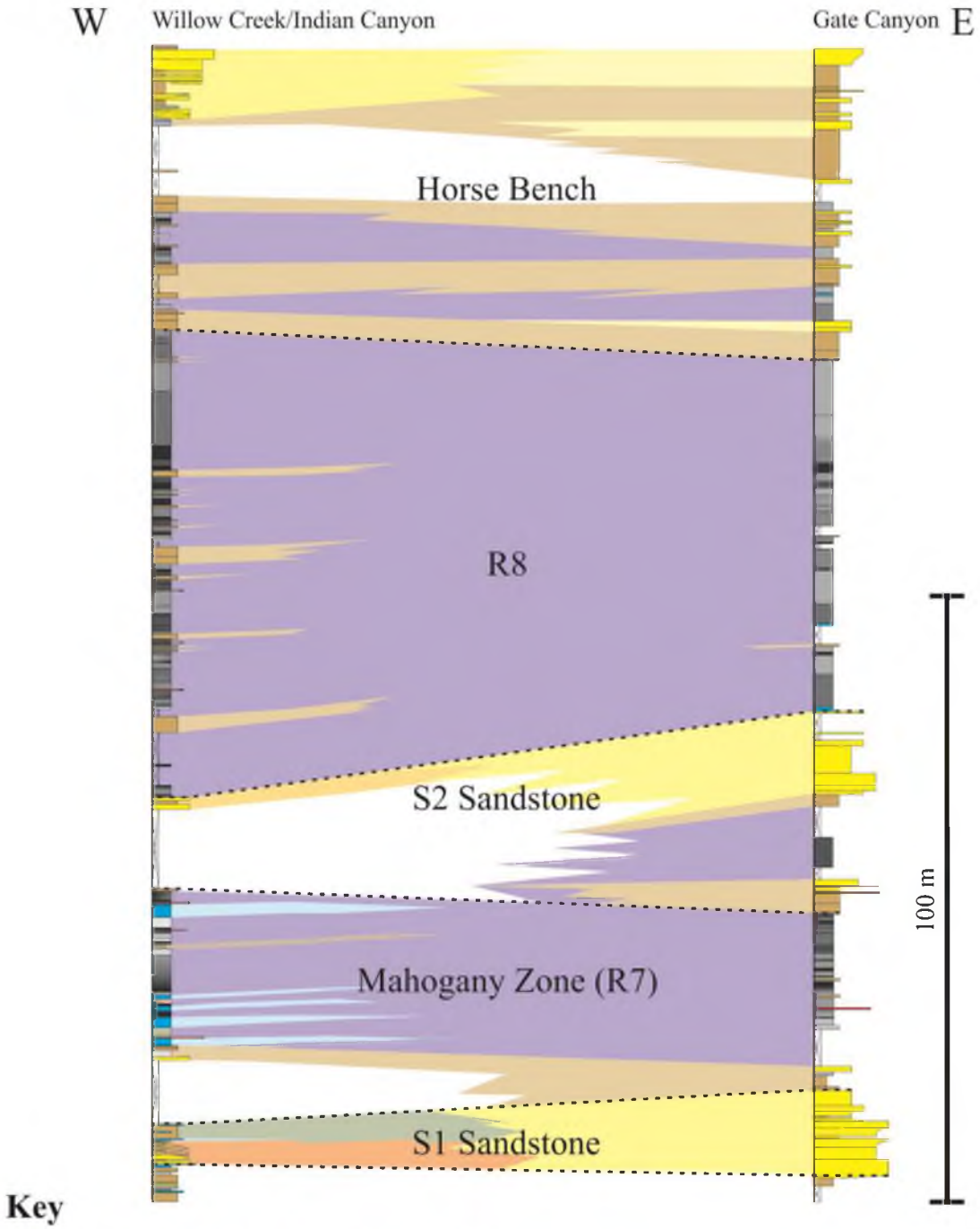

Key

- F1.1: Littoral, strongly channelized sandstone
- F1.2: Littoral/sublittoral, interbedded siltstone and sandstone
- F1.3: Littoral, tabular sandstone
- F2.1: Littoral, weakly channelized sandstone
- F2.2: Littoral, heterolithic channel
- F2.3: Littoral, calcareous siltstone
- F2.4: Littoral, paleosol
- F3.1: Littoral, microbialite
- F3.2: Littoral, coarse grained carbonate
- F3.3: Littoral/sublittoral, organic-poor carbonate mudstone
- F4.1: Profundal, organic-rich carbonate mudstone

Figure 23 – Gate Canyon outcrop photopans; A) Gate Canyon transitional interval (note highlighted channel bodies); B) upper Gate Canyon R8 interval; C) lower Gate Canyon Mahogany interval.

A Gate Canyon Transitional Interval

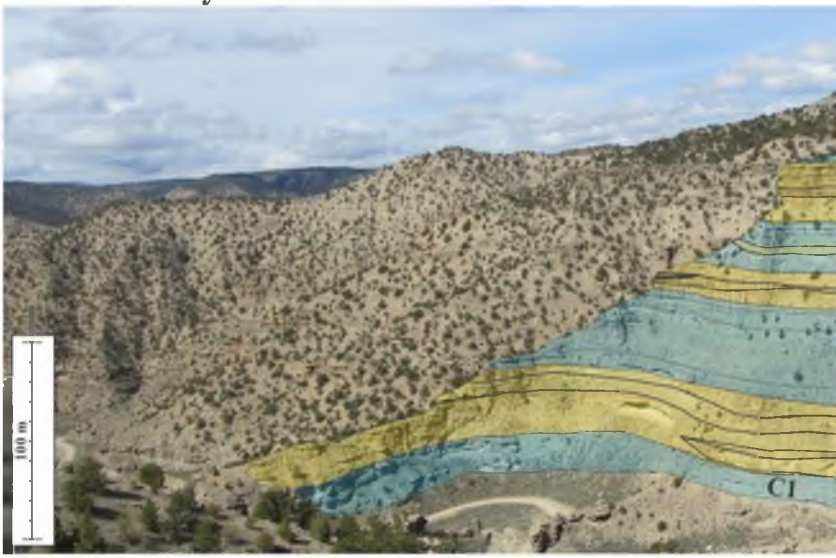

Stratigraphic unit key

- Stratigraphic units with abundant siliciclastics (Si.)
- Stratigraphic units with abundant carbonates and low organic content (C)

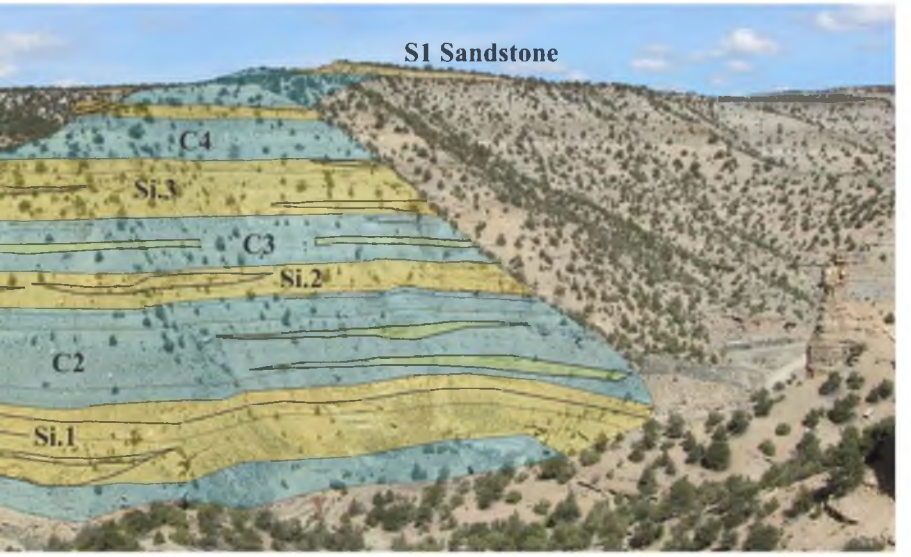
S1 Sandstone
C4
Si.3
C3
Si.2
C2
Si.1

B Gate Canyon R8 Interval

C Gate Canyon Mahogany Interval

Stratigraphic unit key

- Stratigraphic units with abundant siliciclastics
- Stratigraphic units with abundant carbonates and high organic content (R)

Figure 23 – Continued

Figure 24 – Willow Creek/Indian Canyon outcrop photopans; A) Road Outcrop 1 - transitional interval from C1-Si.2; B) Road Outcrop 2 - transitional interval from C3 to C4; C) Road Outcrop 3 – C4-S1 Sandstone; D) Road Outcrop 4 - Mahogany zone; E) Road Outcrop 5 - R8; F) Outcrop 6 - R8 interval.

A Willow Creek/Indian Canyon Transitional Interval (Road Outcrop 1)

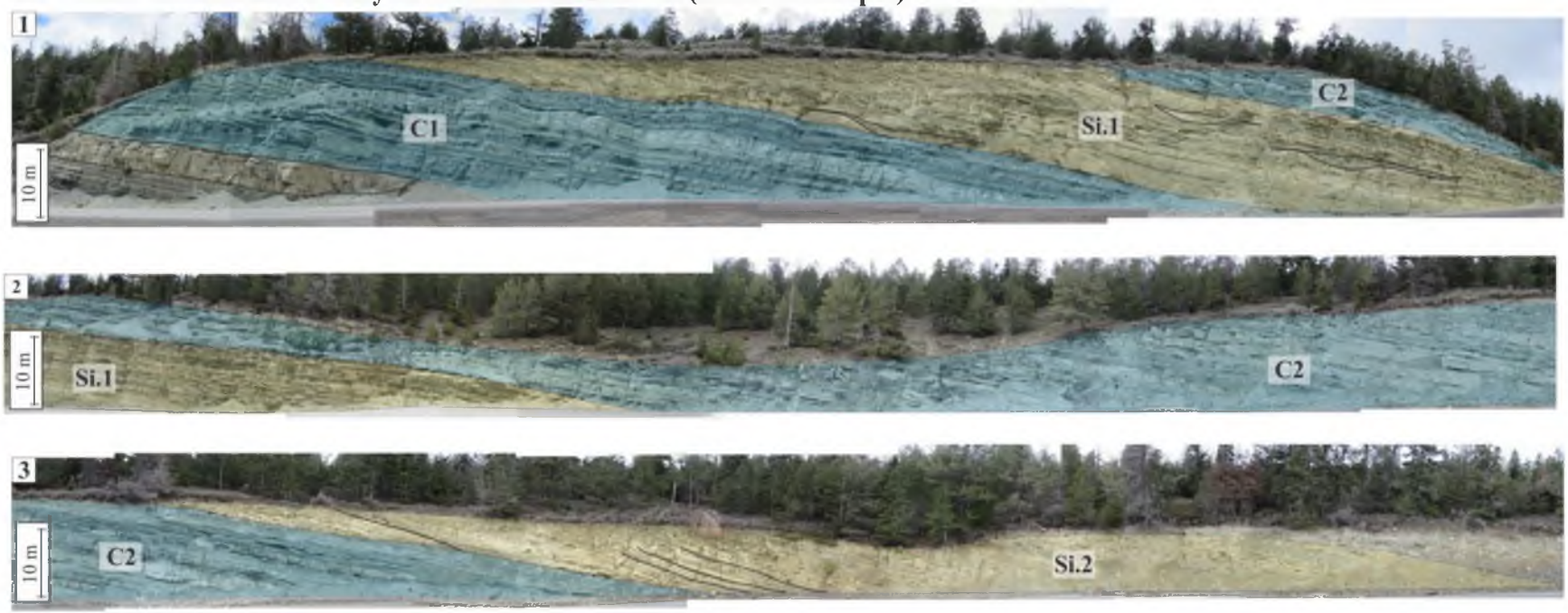

Stratigraphic unit key

- Stratigraphic units with abundant siliciclastics (Si.)
- Stratigraphic units with abundant carbonates and low organic content (C)

B **Willow Creek/Indian Canyon Transitional Interval (Road Outcrop 2)**

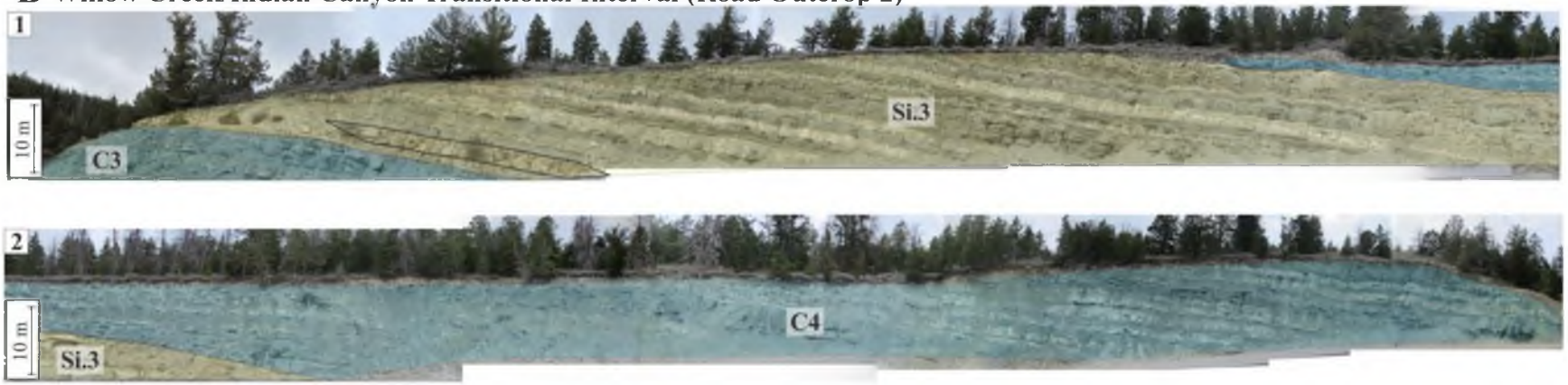

C **Willow Creek/Indian Canyon Transitional to Mahogany Interval (Road Outcrop 3)**

Stratigraphic unit key

- Stratigraphic units with abundant siliciclastics (Si.)
- Stratigraphic units with abundant carbonates and low organic content (C)

Figure 24 – Continued

D Willow Creek/Indian Canyon Mahogany Interval (Road Outcrop 4)

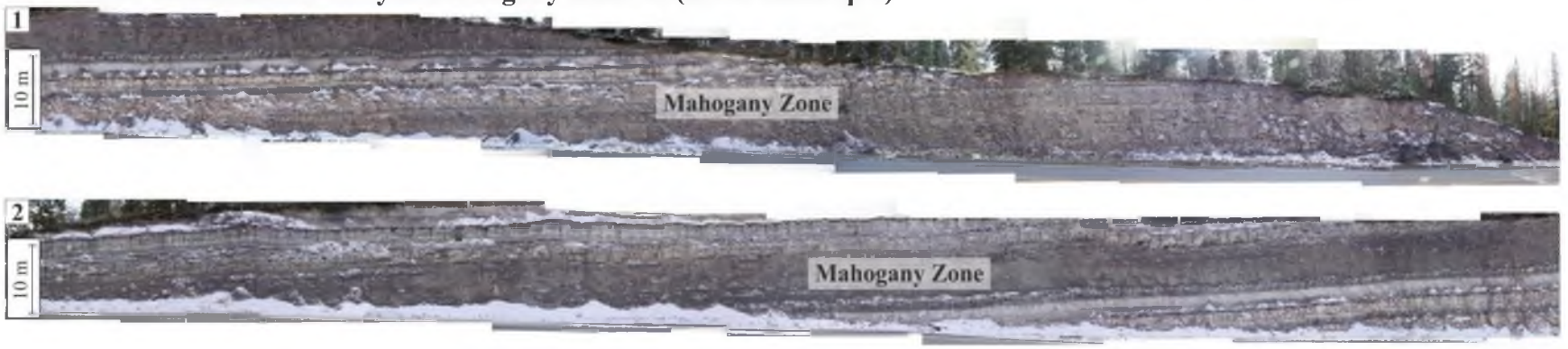

E Willow Creek/Indian Canyon R8 Interval (Road Outcrop 5)

Stratigraphic units
with abundant carbonates and
high organic content (R)

Figure 24 – Continued

E **Willow Creek/Indian Canyon R8 Interval (Road Outcrop 6)**

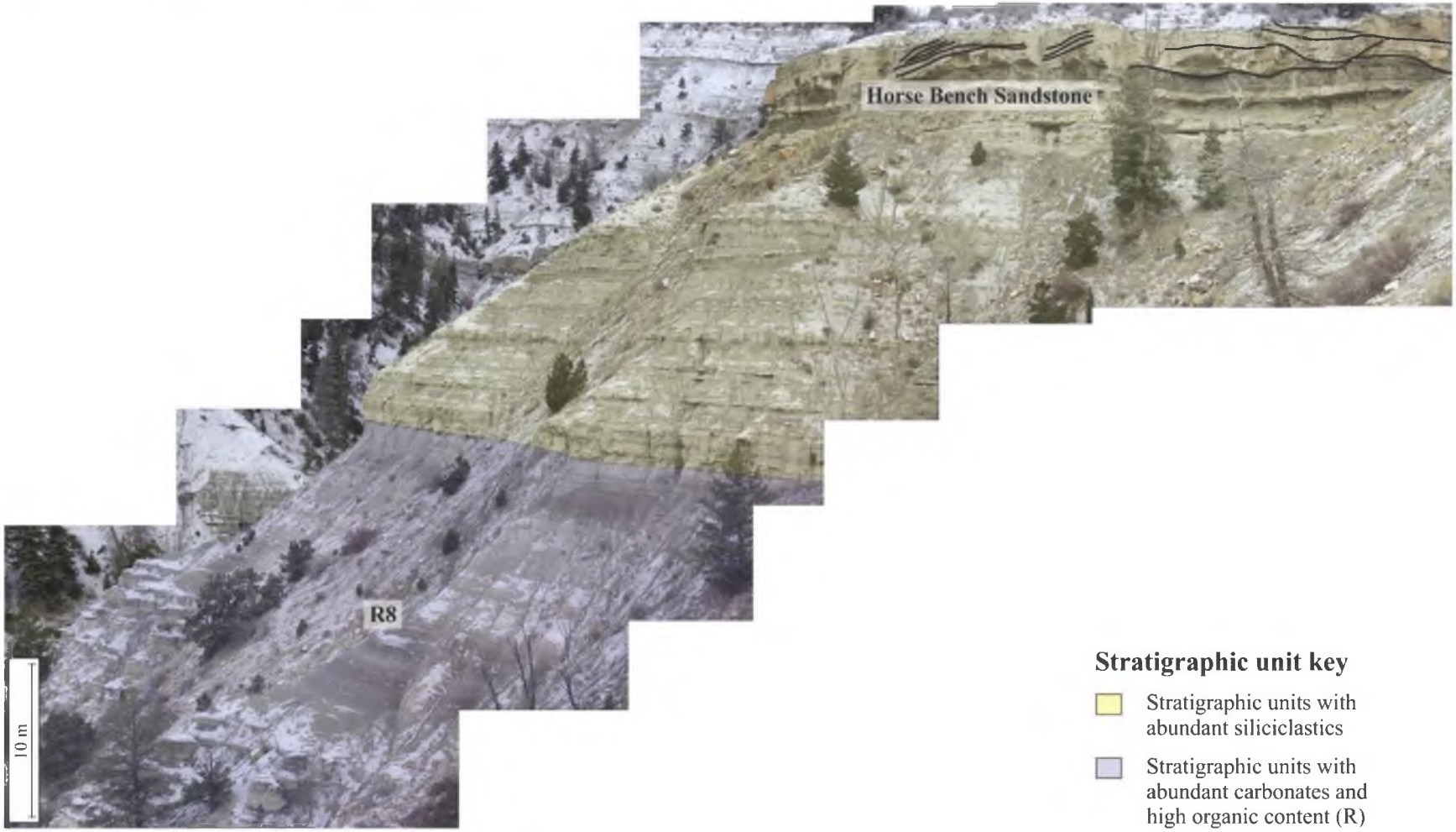

Figure 24 – Continued

Table 2 – Summary of stratigraphic units and associated facies.

Interval	Stratigraphic Unit	Willow Creek/Indian Canyon		Gate Canyon		Key Observations
		Thickness	Facies	Thickness	Facies	
Transitional Interval (C1-C4)	C4	58 m	F2.2, F2.3, F3.3, F3.1	59 m	F1.1, F1.2, F3.3	Western region contains mainly carbonate mudstone and calcareous siltstone; central region contains channelized sandstone bodies with interbedded siltstone and sandstone and carbonate mudstone
	Si.3	33 m	F2.1, F2.2, F2.3, F2.4	35 m	F1.1, F1.2, F3.1, F3.2	Minor siliciclastic input in west, dominantly calcareous siltstone and carbonate mudstone, minor channel bodies; abundant siliciclastic input in central region with strongly channelized sandstone bodies
	C3	30 m (?)	F2.3, F3.3, F3.1	25 m	F3.1, F3.2, F3.3, F1.1	Largely covered in west, exposures suggest mainly calcareous siltstone and organic-poor carbonate mudstone; central region dominated by carbonate mudstone and coarse grained carbonate with minor channelized sandstone bodies
	Si.2	17 m	F2.1, F2.2, F2.3, F2.4	17 m	F1.1, F1.2	Relatively muddy compared to other lean zones; west contains paleosols with heterolithic and weakly channelized sandstone bodies; central region contains mainly siltstone and interbedded sandstone
	C2	32 m	F3.3, F3.1, F2.3	44 m	F3.1, F3.2, F3.3, F1.1, F1.2	Thins towards west; west dominated by carbonate mudstone with some calcareous siltstone; two large channel bodies in central region underlain by coarse grained carbonate bodies
	Si.1	13 m	F2.1, F2.2, F2.4, F3.1	16 m	F1.1, F1.2, F3.1	First lean zone in the transitional interval; paleosols and heterolithic channels in western region; strongly channelized sandstone bodies in the central region
	C1	14 m	F2.3, F2.4, F3.3	16 m	F1.1, F1.2, F3.2	Lowermost rich zone in the transitional interval; contains the C marker bed; calcareous siltstone and carbonate mudstone in western region; strongly channelized sandstone bodies in central region

Table 2 - Continued

Interval	Stratigraphic Unit	**Willow Creek/Indian Canyon** Thickness	Facies
R8 Interval	Horse Bench	47 m	F1.1, F1.2, F4.1
	R8	78 m	F4.1, F3.3, F1.2, F6.1
	S2 Sandstone	17 m (?)	F2.1
Mahogany Interval (S1-S2 Sandstone)	R7; Mahogany Interval	39 m	F3.3, F4.1, F6.1
	S1 Sandstone	6 m	F2.2, F2.3, F3.2

Gate Canyon		Key Observations
Thickness	Facies	
45 m	F1.3, F1.2, F3.3	Both regions coarsen upwards from turbidite deposits to sandstone bodies; sandstone in the western region is strongly channelized; sandstone in central portion is shoreface
64 m	F3.3, F4.1, F1.2, F6.1	Thick unit with thinning towards the east; both regions contain abundant organic-rich carbonate mudstone deposits; organic-richness higher in the west
22 m	F1.1, F1.2	Largely covered in west, exposures show weakly channelized sandstone body; in the central portion, sandstone is strongly channelized, similar to S1
29 m	F3.3, F4.1, F1.2, F6.1	Both intervals contain organic-rich carbonate mudstones, slightly richer towards the central portion of the basin; more organic-poor carbonate mudstone in west
14 m	F1.1, F1.2	Thins to west; channelized sandstone bodies transition from heterolithic with large accretion sets in the west to strongly channelized with large accretion sets in the central region

unique characteristics as compared to the other siliciclastic packages. The Mahogany interval thins slightly to the west from 65 m to 60 m. Internally, the S1 sandstone and the S2 sandstone thin towards the west and the Mahogany zone thins towards the east. The lithologies in both regions are somewhat similar, but the Mahogany interval in the central region contains a higher occurrence of profundal oil shale beds as compared to the western region (Figure 22, Table 2).

The Henderson 3 core, located basinward from Gate Canyon, spans the S1 through the S2 sandstone (Figure 20). Fischer Assay and XRF data show a unique geochemical signature surrounding the interval known as the Mahogany oil shale bed, which is considered the richest oil shale bed within the Mahogany zone (Cashion, 1967; Rosenberg, 2013; Rosenberg et al., in press) (Figure 25). The Fischer Assay data shows a notably higher oil yield within this interval as compared to the rest of the stratigraphy. There is also an increase in heavy metals (e.g. titanium, iron, nickel, zinc, zirconium, manganese) which may be related to the anoxia interpreted during deposition of this bed (Birgenheier and VandenBerg, 2011). Crossplots of the XRF data show unique differences between the lean S1 and S2 sandstone bodies and the carbonate rich Mahogany zone (Figure 26), with the siliciclastic packages containing a higher abundance of quartz and clay and the carbonate packages containing a higher abundance of carbonate. The ternary plot diagram comparing variations in CaO, Al_2O_3, and SiO_2 further supports these major mineralogical differences (Rowe et al., 2012) (Figure 26).

The R8 interval spans the R8 through the Horse Bench Sandstone and thickens to the west from 110 m in the central region to 125 m in the western region (Figures 19 and 20). Most of this westward thickening occurs in the R8 zone, which also contains more

Figure 25 – Fischer Assay data and XRF data from the Henderson 3 core highlighting the Mahogany oil shale bed.

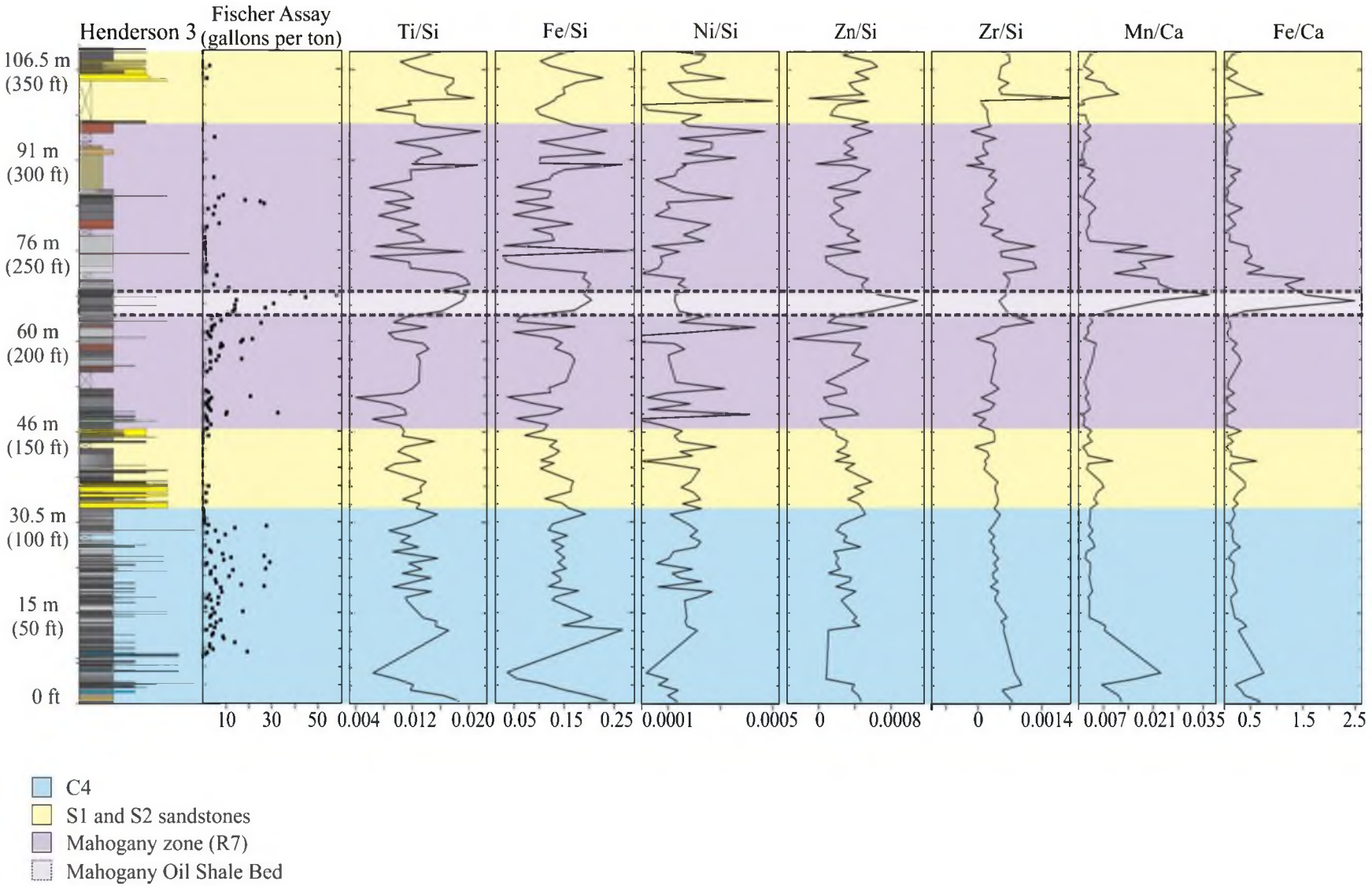
Henderson 3
Fischer Assay (gallons per ton)
Ti/Si
Fe/Si
Ni/Si
Zn/Si
Zr/Si
Mn/Ca
Fe/Ca
106.5 m (350 ft)
91 m (300 ft)
76 m (250 ft)
60 m (200 ft)
46 m (150 ft)
30.5 m (100 ft)
15 m (50 ft)
0 ft
10 30 50
0.004 0.012 0.020
0.05 0.15 0.25
0.0001 0.0005
0 0.0008
0 0.0014
0.007 0.021 0.035
0.5 1.5 2.5
C4
S1 and S2 sandstones
Mahogany zone (R7)
Mahogany Oil Shale Bed

Figure 26 – Scatter plots of XRF data from the Henderson 3 core; A-H) Scatter plots of XRF data from Henderson 3 core showing geochemical relationships between the carbonate packages (C4 and Mahogany) and siliciclastic packages (S1 and S2 sandstones); I) Ternary plot diagram showing relative variations in CaO, Al_2O_3, and SiO_2 that reflect mineralogical variations in the major stratigraphic units.

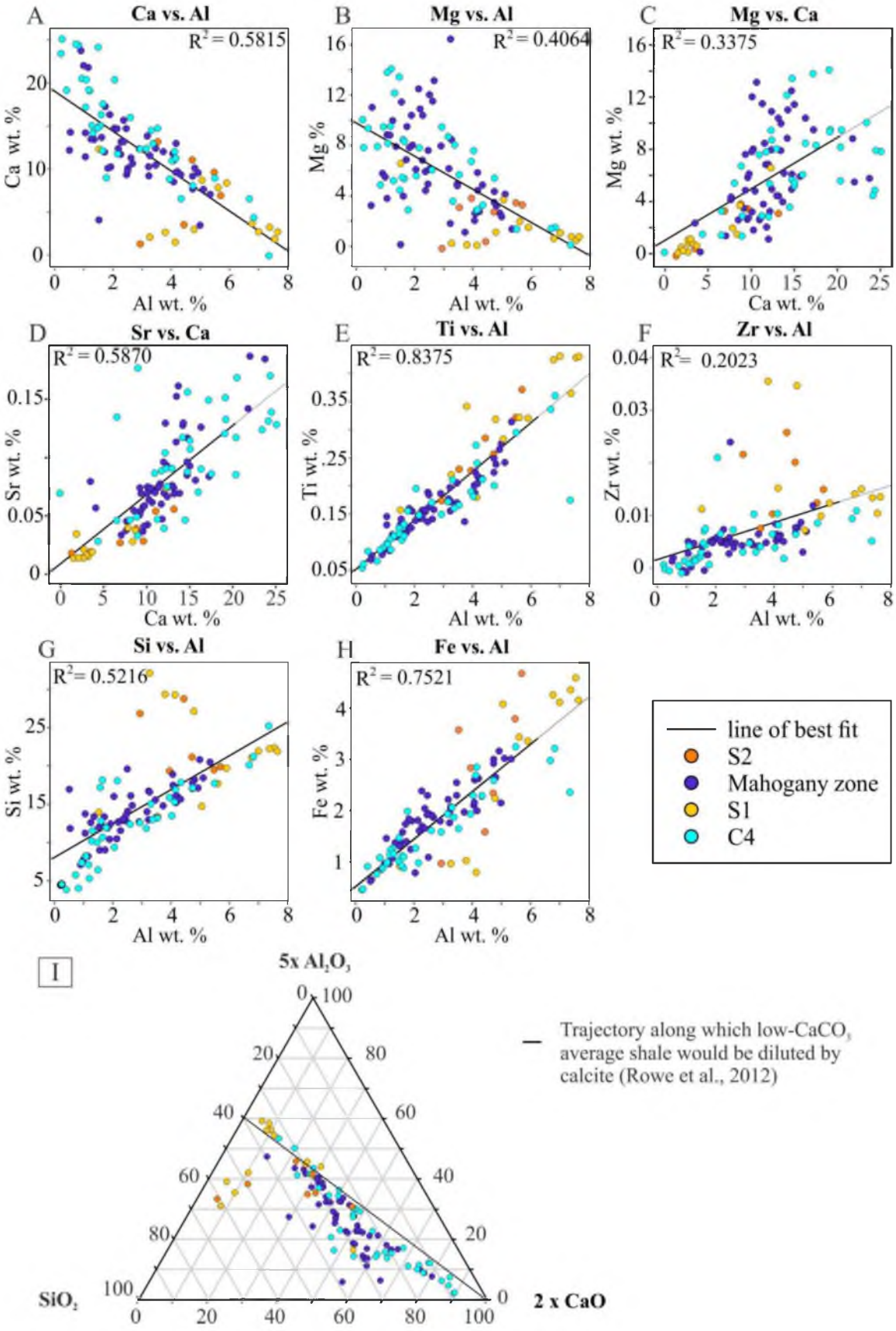
A
Ca vs. Al
R² = 0.5815
Ca wt. %
Al wt. %
B
Mg vs. Al
R² = 0.4064
Mg %
Al wt. %
C
Mg vs. Ca
R² = 0.3375
Mg wt. %
Ca wt. %
D
Sr vs. Ca
R² = 0.5870
Sr wt. %
Ca wt. %
E
Ti vs. Al
R² = 0.8375
Ti wt. %
Al wt. %
F
Zr vs. Al
R² = 0.2023
Zr wt. %
Al wt. %
G
Si vs. Al
R² = 0.5216
Si wt. %
Al wt. %
H
Fe vs. Al
R² = 0.7521
Fe wt. %
Al wt. %
line of best fit
S2
Mahogany zone
S1
C4
I
5x Al2O3
SiO2
2 x CaO
Trajectory along which low-CaCO3 average shale would be diluted by calcite (Rowe et al., 2012)

profundal oil shale units in the west (Figure 22, Table 2). The Horse Bench Sandstone is roughly of equivalent thickness in both regions, but reflects significantly different depositional styles. In Gate Canyon, this sandstone is interpreted as a shoreface succession (F1.3). In Willow Creek/Indian Canyon, the sandstone is dominated by large distributary channels and mouthbar deposits, with paleocurrents towards the northeast (F1.1) (Figure 22, Table 2). Traditionally, the Horse Bench sandstone only refers to the sandstone body and not the lower siltstone beds, but for the purposes of this study the siltstone beds are included because of their genetic relationship with the overlying sandstone body

The Half Moon Canyon core, which is located to the northwest and basinward from Willow Creek/Indian Canyon, spans the R8 through the lower saline facies. XRF crossplots from this core highlight major differences between the saline facies and the lower R8 interval (Figure 27). The saline facies is geochemically similar to the rich R8 zone, except for a higher concentration of strontium, sulfur, and sodium. Surprisingly, the Horse Bench Interval, although mostly sand and silt, behaves similarly to the carbonate rich R8 zone. Unlike the S1 and S2 sandstones, which were noticeably sandy, it appears that the siliciclastic input in this area of the basin did not heavily influence the geochemical signature.

Figure 27 – Scatter plots of XRF data from the Half Moon Canyon core; A-E) Scatter plots of XRF data from Half Moon Canyon core showing geochemical relationships between R8, Horse Bench, and saline facies; F) Ternary plot diagram showing relative variations in CaO, Al_2O_3, and SiO_2 that reflect mineralogical variations in the major stratigraphic units.

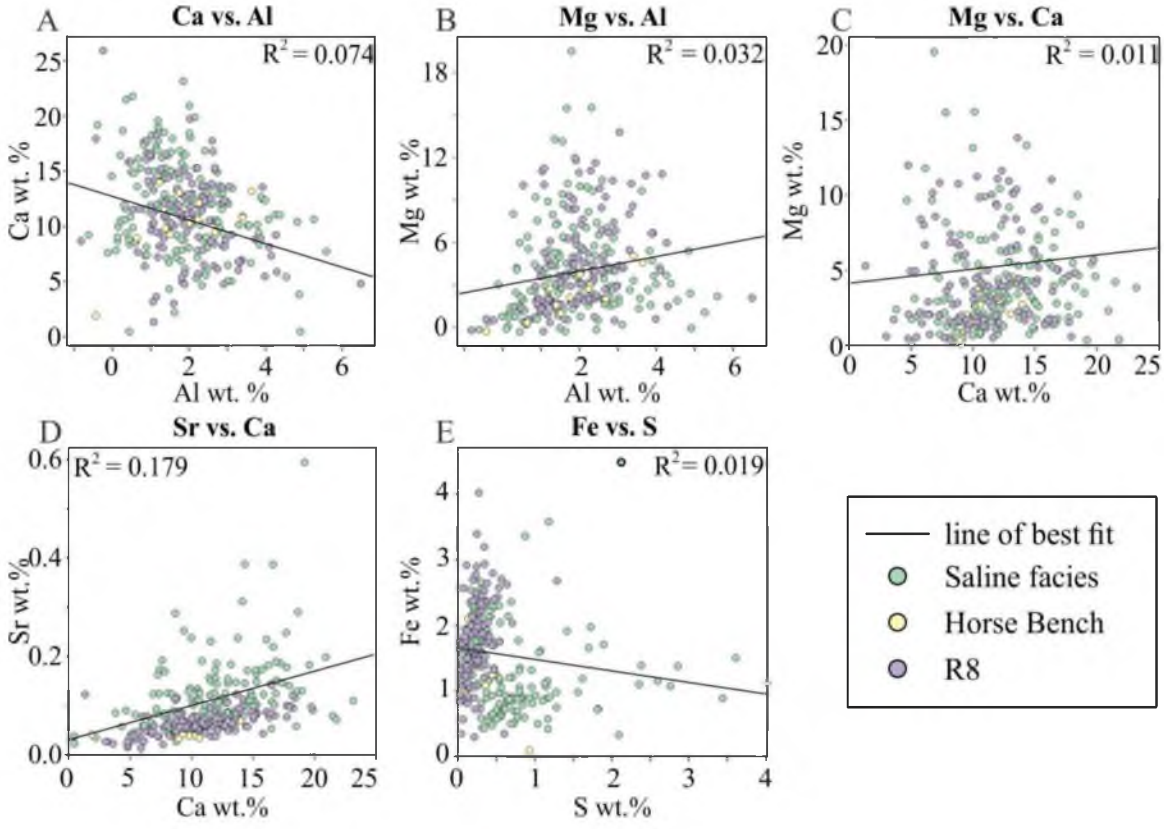
A
Ca vs. Al
$R^2 = 0.074$
Ca wt. %
Al wt. %
B
Mg vs. Al
$R^2 = 0.032$
Mg wt. %
Al wt. %
C
Mg vs. Ca
$R^2 = 0.011$
Mg wt.%
Ca wt.%
D
Sr vs. Ca
$R^2 = 0.179$
Sr wt.%
Ca wt.%
E
Fe vs. S
$R^2 = 0.019$
Fe wt.%
S wt.%
line of best fit
Saline facies
Horse Bench
R8

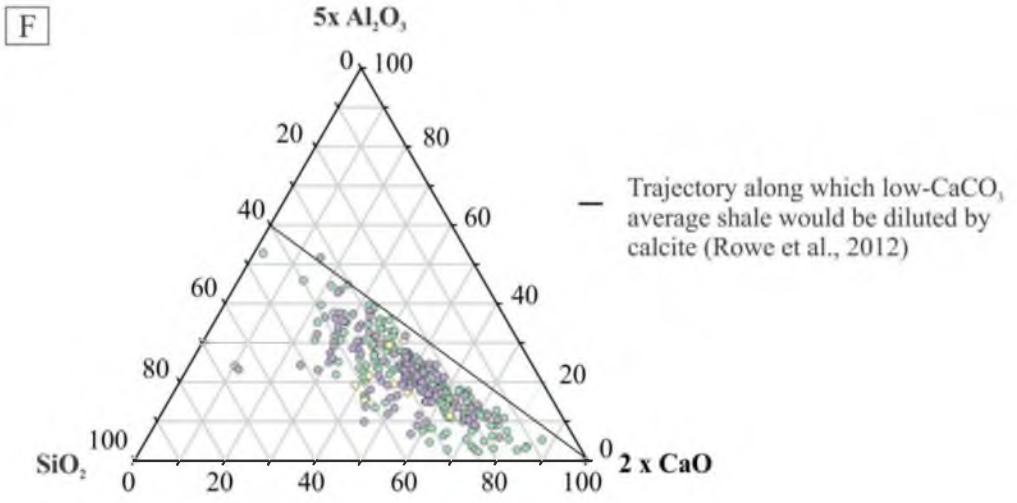
F
5x Al_2O_3
SiO_2
2 x CaO
Trajectory along which low-$CaCO_3$ average shale would be diluted by calcite (Rowe et al., 2012)

DISCUSSION

The three main stratigraphic intervals of the middle and upper Green River Formation defined herein exhibit significant spatial and temporal changes across the central and western portions of the Uinta Basin that are controlled by the interplay of climate and tectonics. An understanding of these controls allows for the development of a model expressing long-term lake evolution using the major lake stages as defined by Carroll and Bohacs (1999) overlain with short-term climatic changes. Finally, the major stratigraphic intervals and facies are compared with modern lacustrine analogs.

The Transitional Interval

Spatial Controls

The diverse facies present throughout the carbonate and siliciclastic packages in the transitional interval in both regions of the basin indicate depositional environments that were continuously exposed to different levels of energy (Figures 19 and 21, Tables 1 and 2). The succession of facies found in the central portion of the basin support the idea of a steep, carbonate ramp environment with high energy, including erosional distributary channels and some wave action. Conversely, the western portion of the basin contains more sheet-like distributary channels and lake flat deposits that are evidence of a shallow ramp environment with low energy (Picard, 1957; Keighley et al., 2002). The different gradients and thus energy levels in the central and western portions of the basin is

interpreted as a result of the formation of a siliciclastic wedge along the depositional axis, which created a topographic high in the south-central region of the basin (Bereskin et al., 2004).

The main source of siliciclastic sediment that contributed to the formation of the siliciclastic wedge, specifically during Sunnyside delta deposition, is thought to have originated from the southeast, where basement cored uplifts formed during the Laramide Orogeny (Dickinson et al., 1986; Dickinson et al., 1988). Paleocurrent data collected throughout the transitional interval in both regions of the study area indicate dominant flow direction towards the north with sediment derived from the south. Major uplifts that could have supplied the siliciclastic sediment and created this wedge include the Uncompaghre, San Rafael, and San Luis uplifts (Dickinson et al., 1988; Pusca, 2003; Davis et al., 2008) (Figure 28).

More recent provenance studies of the underlying Wasatch/Colton Formation show that sediment may also be derived from the California paleoriver, a large drainage system sourced from the Cordilleran magmatic arc in California (Davis et al., 2010; Dickinson et al., 2012) (Figure 28). The Sunnyside delta interval, though temporally and stratigraphically distinct from the Colton Formation, is also thought to have been sourced from this paleoriver and was deposited via a large deltaic system that prograded into the Uinta Basin from the south (Schomacker et al., 2010; Dickinson et al., 2012; Moore et al., 2012). The small deltaic systems observed in the transitional interval of this study may also be sourced from the California paleoriver, similar to the Sunnyside delta.

The amount of siliciclastic sediment input from this system was highest during the deposition of the Sunnyside delta interval. Sediment supply decreased during deposition

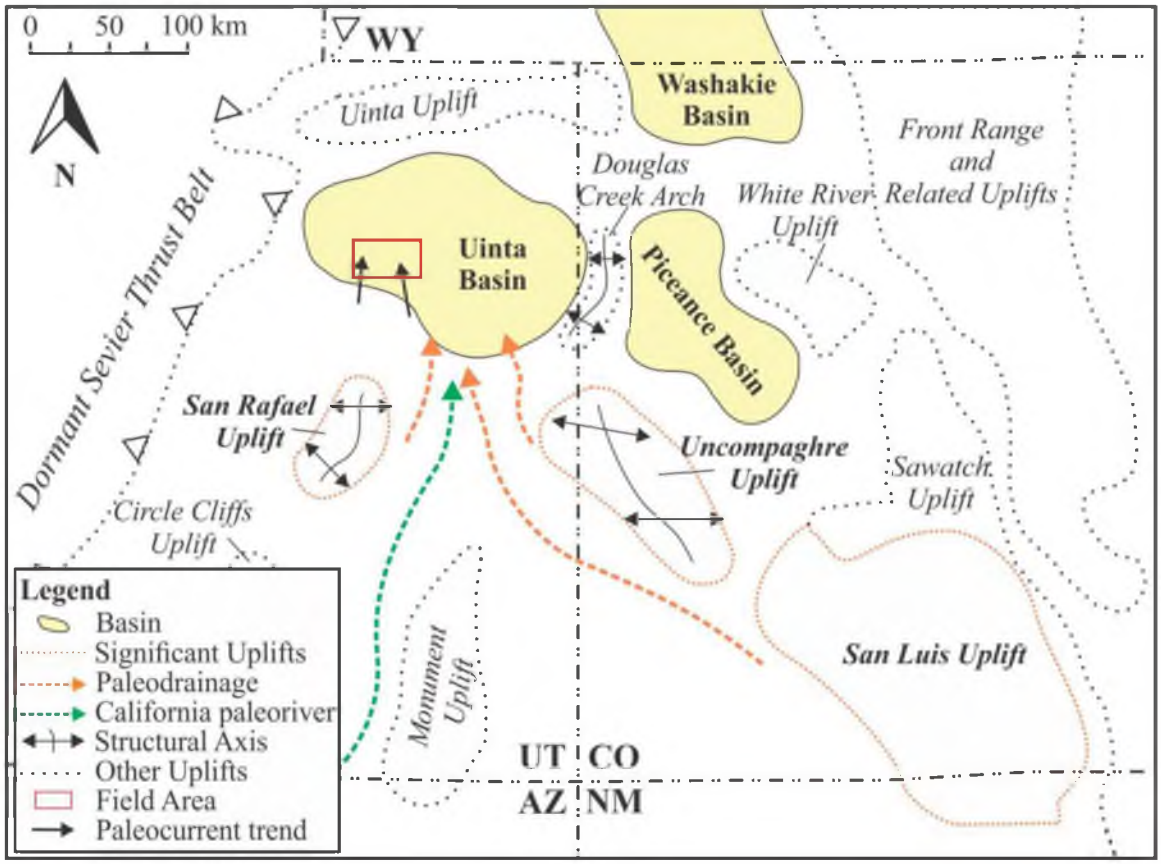

Figure 28 – Interpreted paleodrainage of siliciclastic sediment from surrounding Laramide uplifts and the California paleoriver into the Uinta Basin (using Dickinson et al., 1986 and Dickinson et al., 2012) with structural axes of uplifts from Cashion (1995).

of the transitional interval, which allowed for periods of carbonate deposition (Remy, 1992). The Sunnyside delta interval, like the transitional interval, is known for its high proportions of large sandstone bodies towards the central portion of the basin, supporting the interpretation that this was on the main depositional axis (Remy, 1992; Schomacker et al., 2010; Moore et al., 2012). However, towards the west in Willow Creek/Indian Canyon, stratigraphically equivalent intervals, including the transitional interval of this study and the underlying delta facies, are lacking in abundant sandstone deposits and so are interpreted as deposited on the fringes of the siliciclastic wedge (Morgan, 2003) (Figure 29a).

Temporal Controls

The development of the carbonate and siliciclastic packages during the deposition of the transitional interval is a function of sediment supply and accommodation, which allowed for the accumulation of siliciclastic facies versus carbonate facies (Figure 29). Examination of key surfaces across the study area provides insight into the main controls on deposition. First, surfaces of erosion at the base of distributary channels and mouthbar deposits in this study typically mark the base of the siliciclastic packages (Si.) and the onset of siliciclastic deposition. Basal surfaces of erosion are found at the base of the Si.1, Si.2, and the Si.3 packages and can be correlated across the field area. Basal erosional surfaces are more apparent in Gate Canyon, where coarse grained sandstone bodies (F1) are found immediately above coarse grained carbonate deposits (F3). These are similar to those interpreted by Keighley et al. (2003) which examined the Sunnyside delta interval below the transitional interval in Gate Canyon and placed surfaces of

Figure 29 – Paleodepositional models from the C1 through Si.3; a) Model showing lean zone deposition from the base of the C1 through the Si.3 in an overfilled basin; lean zone deposition occurs during the hyperthermal events, which cause pulses of sediment to enter the lake basin; b) Model showing rich zone deposition from the base of the C1 through the Si.3 in an overfilled basin; rich zone deposition occurs between the hyperthermal events.

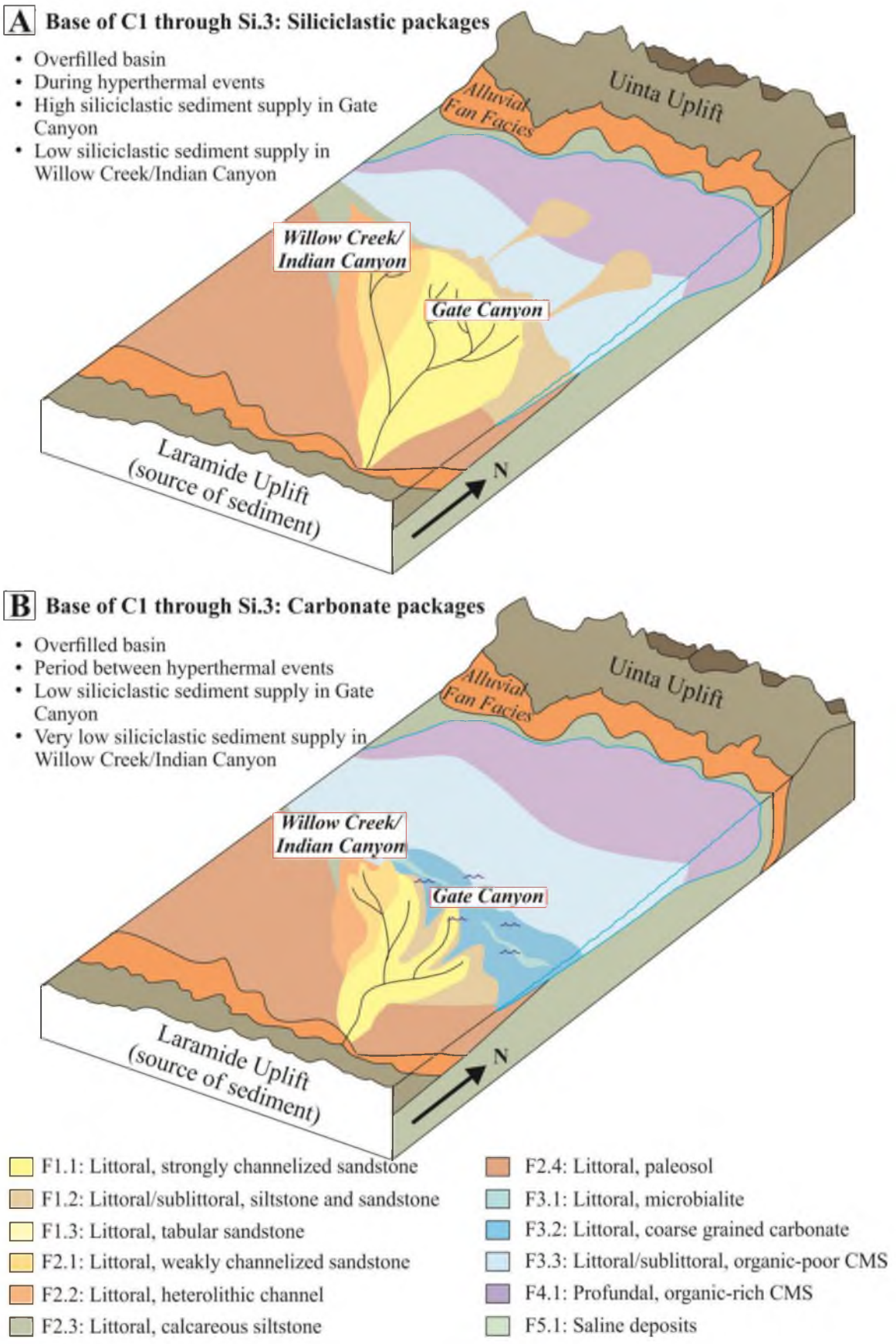
A Base of C1 through Si.3: Siliciclastic packages
• Overfilled basin
• During hyperthermal events
• High siliciclastic sediment supply in Gate Canyon
• Low siliciclastic sediment supply in Willow Creek/Indian Canyon
Alluvial Fan Facies
Uinta Uplift
Willow Creek/ Indian Canyon
Gate Canyon
Laramide Uplift (source of sediment)
N
B Base of C1 through Si.3: Carbonate packages
• Overfilled basin
• Period between hyperthermal events
• Low siliciclastic sediment supply in Gate Canyon
• Very low siliciclastic sediment supply in Willow Creek/Indian Canyon
Alluvial Fan Facies
Uinta Uplift
Willow Creek/ Indian Canyon
Gate Canyon
Laramide Uplift (source of sediment)
N
F1.1: Littoral, strongly channelized sandstone
F1.2: Littoral/sublittoral, siltstone and sandstone
F1.3: Littoral, tabular sandstone
F2.1: Littoral, weakly channelized sandstone
F2.2: Littoral, heterolithic channel
F2.3: Littoral, calcareous siltstone
F2.4: Littoral, paleosol
F3.1: Littoral, microbialite
F3.2: Littoral, coarse grained carbonate
F3.3: Littoral/sublittoral, organic-poor CMS
F4.1: Profundal, organic-rich CMS
F5.1: Saline deposits

erosion at the base of channel and floodplain dominated packages. In Willow Creek/Indian Canyon, the lack of large sandstone bodies and coarse grained carbonate deposits make the identification of these surfaces more difficult. Therefore, the surfaces are interpreted at the base of the more siliciclastic dominated zones, which are identified as a shift from abundant organic-poor carbonate mudstone beds (F3.3) to abundant paleosols (F2.4) and calcareous green siltstone deposits (F2.3).

The siliciclastic packages that overlie the erosional surfaces in Gate Canyon contain laterally discontinuous sandstone bodies that display no stratigraphic pattern (i.e., randomly spaced) (F1.1). The random dispersal of sandstone bodies within these packages suggests an autocyclic control on deposition. However, because the packages themselves are correlative across this study area, it is reasonable to infer that the deposition is controlled by allocyclic processes, such as climate or tectonics, which resulted in a large pulsed input of siliciclastic sediment into the system (Figure 29a).

In sequence stratigraphy, it is often assumed that a basinward shift in facies represents a drop in base level. However, the appearance of these siliciclastic packages does not represent a basinward shift in facies or a drop in lake level. The coarse grained carbonates that typically underlie the sandstone bodies in Gate Canyon are interpreted as littoral to sublittoral deposits, similar to the sandstone bodies, and so there is no substantial evidence of a significant change in lake level (Rosenberg, 2013; Rosenberg et al., in press). Outcrop evidence suggests channels cut less than 1 m into the underlying substrate, a relatively small degree of erosion. If lake level fell drastically, highly incised and vertically amalgamated channels and possibly incised valleys would be expected (Bohacs et al., 2000). The presence of channelized sandstone bodies and their associated

mouthbar deposits are the result of an increase in siliciclastic sediment input into the lake (Figure 29a). Similar to what is observed in studies by Keighley et al. (2003) in the Sunnyside delta interval in Nine Mile Canyon (specifically their 'Type B sequence boundaries') and Rosenberg et al. (in press) in the Douglas Creek and Parachute Creek members of the Green River Formation to the east, the laterally extensive surfaces of erosion are considered to represent a decrease in accommodation associated with the progradation of siliciclastic sediment.

In Willow Creek/Indian Canyon, because the gradient in the western portion of the basin was shallow, the facies change in short, meter-scaled stratigraphic succession from littoral, subaerial exposed siltstone and mudstone deposits (F2.3) to littoral, subaqueous, organic-poor carbonate mudstone deposits (F3.3) in both the siliciclastic and carbonate packages. The rapid changes in lithology are often associated with shallow ramp environments, where even minor increases in lake level result in significant lateral facies changes as a result of lake flat inundation (Remy, 1989; Alonso-Zarza and Wright, 2010; Rosenberg, 2013; Rosenberg et al., in press). The siliciclastic packages do however contain a higher ratio of siliciclastic sediment which indicates that whereas the central portion of the region was receiving the bulk of sediment, it was also influencing the siliciclastic packages in the west.

The second major surface recognized in this study is laterally extensive flooding surfaces, which mark the onset of carbonate deposition (Figure 29b). These surfaces are found at the base of the C1, C2, C3, and C4 packages, where carbonate deposition abruptly overlies siliciclastic deposition. The top of some siliciclastic packages in the study area contain wave ripple modified sandstones and burrows, indicating a relative

rise in lake level.

The carbonate packages overlying the flooding surfaces are dominated by coarse grained carbonates (F3.2) in the central portion of the basin, and organic-poor carbonate mudstone in the western portion of the basin (F3.3) (Figure 21). Sparse isolated channelized sandstone bodies can be found throughout these carbonate packages, predominantly in the central portion of the basin. These channelized sandstone bodies are expected in this region because deposition is occurring along the axis of a large deltaic system. Although the amount of siliciclastics entering the lake margin decreased significantly during deposition of the carbonate packages, fluvial sediment transport and deposition did not cease completely and autogenic controls likely caused these channels to form as a result of upstream processes, such as avulsion.

The siliciclastic packages and the carbonate packages are controlled by the presence or absence of siliciclastic sediment input, which ultimately is controlled by tectonics or climate (Figure 29). Past studies of the Green River Formation equate these lithologic changes to lake level changes with siliciclastic packages representing lower lake level and carbonate packages representing higher lake level (Keighley et al., 2003; Johnson et al., 2010), but according to the facies observed in this study and more recent studies, carbonates and siliciclastics can be deposited at various depths and occur along one shoreline profile concurrently (Birgenheier and VandenBerg, 2011; Aswasereelert et al., 2012; Tanavsuu-Milkeviciene and Sarg, 2012; Rosenberg et al., in press). Their occurrence can be based on environmental factors rather than lake level fluctuations.

Recent studies have established a relationship between siliciclastic input and climate change during the Paleocene to early Eocene (Tucker and Slingerland, 1997;

Foreman et al., 2012; Abels et al., 2013). Early Eocene hyperthermal events, or abrupt global warming events, were first observed in marine isotope records (Nicolo et al., 2007). Some limited terrestrial isotope records of early Eocene hyperthermal events have been developed, thus allowing direct investigation of the response of terrestrial systems to climate change (Abels et al., 2012; Abels et al., 2013). Hyperthermal events are associated with increased precipitation and seasonality that cause increased weathering and fluvial siliciclastic sedimentation (Aswasereelert et al., 2012; Foreman et al., 2012; Abels et al., 2013). The most complete and well-studied terrestrial record is that of the PETM, a short-lived yet severe hyperthermal event that occurred at the Paleocene-Eocene boundary (~56 Ma) (Koch et al., 2003; Smith et al., 2009). In a recent study by Foreman et al. (2012), there is direct evidence of increased sedimentation within fluvial systems of the underlying Wasatch Formation in the Piceance Basin across the PETM.

Although the PETM occurred prior to the deposition of the Green River Formation, smaller, early Eocene hyperthermal events occurred during the deposition of the lacustrine system and it is likely that this terrestrial system responded similarly (Lourens et al., 2005; Sexton et al., 2011). Marine records indicate increases in temperature of about 2-4° C and events occurring every 100-400 kyr with a duration of about 40 kyr (Sexton et al., 2011). These small events have been interpreted as being orbitally induced and are documented isotopically in the terrestrial Willwood Formation of the Bighorn Basin (Abels et al., 2012; Aswasereelert et al., 2012). Terrestrial systems, such as the Willwood Formation and the Green River Formation of the Greater Green River Basin, show increased siliciclastic sediment deposition that have been related to these events via isotope records and volcanic tuff dating (Smith et al., 2010; Abels et al.,

2012; Aswasereelert et al., 2012). Within the Green River Formation, the events are associated with the previously mentioned organic-lean zones that are found throughout this lacustrine formation (Smith et al., 2010; Aswasereelert et al., 2012). The siliciclastic and carbonate packages observed in this study are most likely similarly related to these hyperthermal events, yet direct isotopic evidence of the relationship has yet to be formally established.

Multiple climate studies in the Laramide foreland suggest that the early-middle Eocene was increasingly warm and wet, with abundant precipitation (Wilf et al., 1998; Sewall and Sloan, 2006). However, during deposition of the Green River Formation in the region of the Uinta Basin, it is thought that the climate was fairly arid with less precipitation than the surrounding basins, including the Piceance Basin (Wilf et al., 1998; Sewall and Sloan, 2006; Tanavsuu-Milkeviciene and Sarg, 2012). Arid environments are thought to promote longer periods of landscape stability, and so the lack of abundant siliciclastics within the carbonate packages may be a result of stable landscape conditions, possibly resulting in the accumulation of the carbonate packages (C1-C4) (Smith et al., 2009) (Figure 29b). Conversely, increases in seasonality during the hyperthermal events, which are considered to be even more arid yet more monsoonal, resulted in large pulses of sediment due to unstable seasonal flooding conditions and hence may possibly be associated with the siliciclastic packages that consist of large distributary channels and mouthbar deposits (Si.1-Si.3) (Figure 29a).

The Mahogany Interval

The Mahogany interval in this study, which overlies the transitional interval, consists of the S1 sandstone, Mahogany zone, and S2 sandstone (Figures 19 and 22). These units are fairly similar in both study areas, and so controls on deposition are thought to be similar across the region. The S1 sandstone is a regional, laterally continuous, cliff forming sandstone body that consists of large-scale accretion sets and amalgamated channel bodies (F1.1) with paleocurrent flow towards the north and east (Figure 22, Table 2). According to Remy (1992), it is finer grained and less prominent both east and west of Gate Canyon, and so the sediment source is most likely from the same deltaic system that sourced the siliciclastic packages in the transitional interval. The S1 sandstone represents an abrupt, progradation of siliciclastic sediment (Rosenberg, 2013; Rosenberg et al., in press). Facies within the underlying C4 package suggest a slow but steady lake transgression occurring in the lacustrine system during this time, as evidenced by the appearance of organic-poor mudstones and lack of coarse grained carbonates and paleosols. The S1 sandstone is similar to the siliciclastic packages in the transitional interval, and represents a minor regression associated with the progradation of siliciclastic sediment during this overall lake transgression.

The Mahogany zone, deposited after the S1 sandstone, is a basin-wide unit that consists of sublittoral siltstones (F1.2), organic-poor carbonate mudstones (F3.3), and profundal oil shale deposits (F4.1) (Figure 22, Table 2). This zone represents a regional transgression of the lake following deposition of the S1 sandstone. Although the Gate Canyon section contains more profundal oil shale beds than the Willow Creek/Indian Canyon section, both regions represent deep, open lake deposits (Figure 30a). In the

Figure 30 – Paleodepositional models from the Mahogany zone and the R8 through saline facies; a) Model showing the extent of profundal carbonate mudstone during Mahogany zone deposition in a balanced-fill basin; regional profundal oil shale deposition occurred during an increase in humidity and precipitation, resulting in the link between the Uinta and Piceance basins; b) Model showing evaporative facies deposition in the distal part of the basin, mouthbar deposition towards the western region of the basin, and shoreface deposition towards the central portion of the basin during the middle R8 interval.

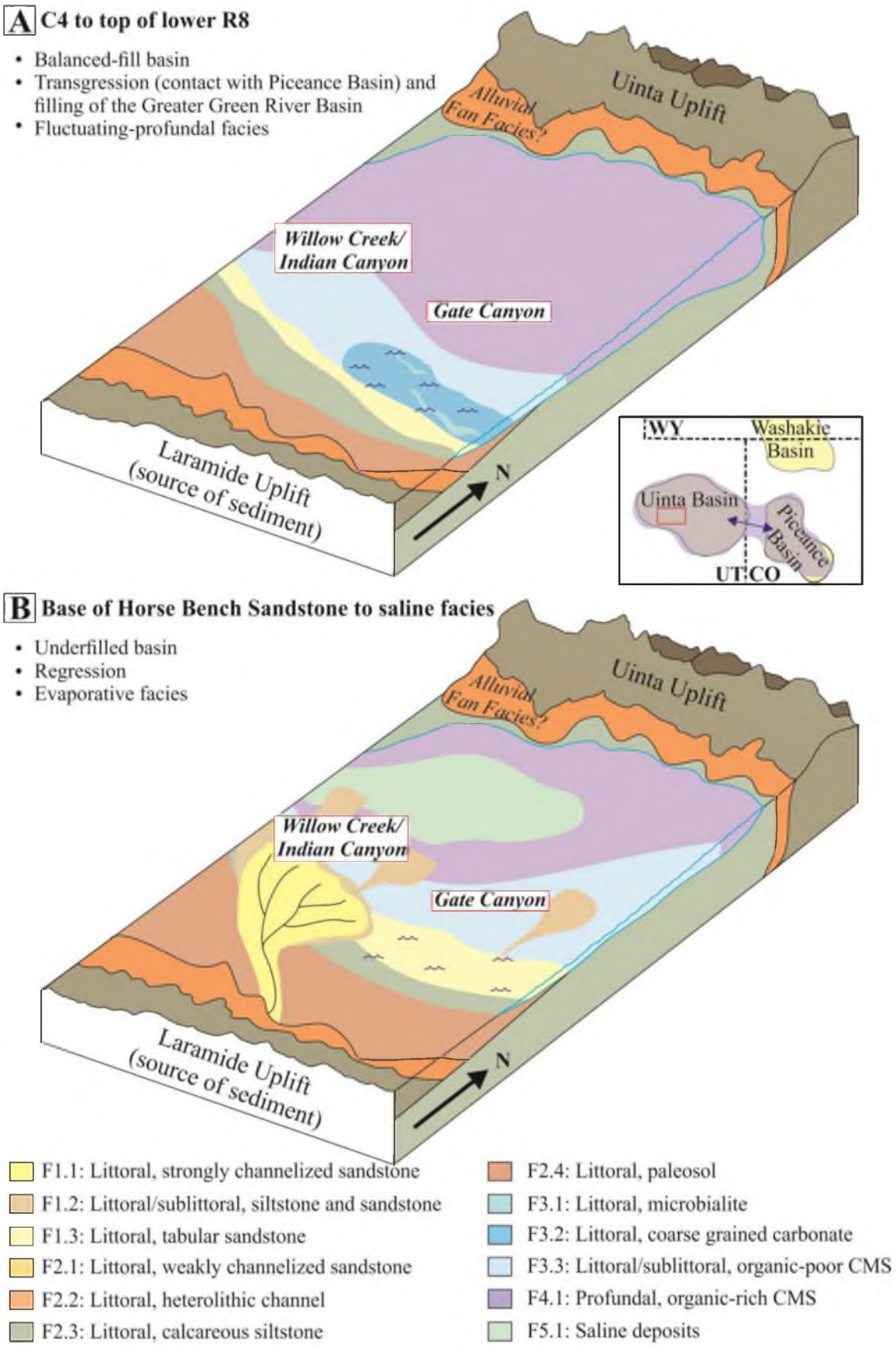
A C4 to top of lower R8
• Balanced-fill basin
• Transgression (contact with Piceance Basin) and filling of the Greater Green River Basin
• Fluctuating-profundal facies
Uinta Uplift
Alluvial Fan Facies?
Willow Creek/ Indian Canyon
Gate Canyon
Laramide Uplift (source of sediment)
N
WY
Washakie Basin
Uinta Basin
Piceance Basin
UT
CO
B Base of Horse Bench Sandstone to saline facies
• Underfilled basin
• Regression
• Evaporative facies
Uinta Uplift
Alluvial Fan Facies?
Willow Creek/ Indian Canyon
Gate Canyon
Laramide Uplift (source of sediment)
N
F1.1: Littoral, strongly channelized sandstone
F1.2: Littoral/sublittoral, siltstone and sandstone
F1.3: Littoral, tabular sandstone
F2.1: Littoral, weakly channelized sandstone
F2.2: Littoral, heterolithic channel
F2.3: Littoral, calcareous siltstone
F2.4: Littoral, paleosol
F3.1: Littoral, microbialite
F3.2: Littoral, coarse grained carbonate
F3.3: Littoral/sublittoral, organic-poor CMS
F4.1: Profundal, organic-rich CMS
F5.1: Saline deposits

Henderson 3 core, which spans the Mahogany zone and is located to the north or basinward of Gate Canyon, facies are dominantly profundal oil shale deposits. Saline crystals, disseminated dolomite, and precipitated carbonate deposits found within the Mahogany zone of the core are representative of a stratified lake (Schubel and Lowenstein, 1997; Tanavsuu-Milkeviciene and Sarg, 2012). Stratification is also indicated by the XRF data, which displays an increase in heavy metals during oil shale deposition (Figure 25). The overlying S2 sandstone represents another progradation of siliciclastic sediment, and consists of wave-ripple dominated sandstone bodies in Gate Canyon and current ripple dominated siltstones in Willow Creek/Indian Canyon (Figure 22, Table 2). According to Remy (1992) the highest sediment input occurred east of Gate Canyon (eastern Nine Mile Canyon), with facies that resemble those of the S1 sandstone. The relocation of the main sediment input towards the east may be due to reworking of the deltaic system following higher lake level during Mahogany deposition.

The progradation of siliciclastic sediment during S1 and S2 sandstone deposition and the overall lake transgression during Mahogany deposition are interpreted to be related to both climate and tectonics. The lake began transgressing during the upper transitional interval and into the Mahogany zone, as is also observed in the neighboring Piceance Basin (Tanavsuu-Milkeviciene and Sarg, 2012). Lake transgression is associated with continued tectonic subsidence of the basin combined with an increasingly wet climate following the cessation of the Eocene hyperthermal events. Also contributing to lake transgression was the filling of Lake Gosiute, which caused major lake water displacement into the Piceance and Uinta basins (Wilf et al., 1998; Keighley et al., 2003). Following the end of these hyperthermal events, overall fluvial siliciclastic sediment

supply decreased. As a result of increased precipitation and the rearrangement of drainage patterns, a deep, open lacustrine system formed in both the Uinta and Piceance basins (Keighley et al., 2003; Davis et al., 2008; Tanavsuu-Milkeviciene and Sarg, 2012). The minor regressions observed in the stratigraphy at the S1 and S2 sandstones represent slight regressions. These events may be associated with small-scale, weaker hyperthermal events that are not well documented in the terrestrial record but would continue through the Eocene if orbitally induced (Sexton et al., 2011; Aswasereelert et al., 2012).

The R8 Interval

The R8 interval overlies the Mahogany interval and consists of profundal oil shales, carbonate mudstones, and siltstones that are capped by the Horse Bench Sandstone (Figures 19 and 22). The lower R8 zone is a thick, rich zone that overlies the S2 sandstone and consists of profundal oil shales (F4.1) that transition into organic-poor carbonate mudstones (F3.3) towards the top (Figure 22, Table 2). Throughout this zone, abundant volcanic tuff beds are found. The shift back to the deep, open lacustrine facies towards the bottom of this zone signifies another lake transgression following the regression during S2 deposition. At this point in time, Lake Uinta in the Piceance Basin had begun filling with sediment (Tanavsuu-Milkeviciene and Sarg, 2012). The Willow Creek/Indian Canyon R8 section contains more profundal oil shale deposits than in Gate Canyon because it is located slightly more basinward (Figure 30b).

A gradual shift from lake transgression to lake regression occurs towards the top of the lower R8 zone. From the top of the lower R8 zone to the Horse Bench Sandstone, there is an increase in siltstone deposition (F1.2), interpreted as turbidites, in both regions

of the basin (Figure 22). These siltstones, considered to be part of the Horse Bench Sandstone, indicate closer proximity to the lake margin and lake contraction.

The Horse Bench Sandstone is a regional unit within the R8 zone that changes in character and depositional processes from east to west. In Gate Canyon, the tabular heterolithic sandstone at the top of the unit is dominated by wave ripples and interpreted as a shoreface sequence (F1.3); in Willow Creek/Indian Canyon, the sandstone body consists of large, channelized deposits (F1.1) representative of a large distributary channel network (Table 2). The distributary channels are sourced from the southwest with paleocurrents towards the northeast. The Horse Bench Sandstone in both portions of the basin are considered to be depositionally related along a shoreline profile. The channels in the west prograded towards the eastern part of the basin and likely sourced the shoreface deposits in Gate Canyon via long-shore drift. Further evidence that this sandstone body prograded from the west is supported by the stratigraphy in the east (Evacuation Creek), where the Horse Bench Sandstone is missing within the R8 zone.

The saline facies lies above the Horse Bench Sandstone in the western portion of the basin. This thick unit was only observed in the Half Moon Canyon core, and consists of profundal oil shale deposits (F4.1) and organic-poor carbonate mudstones (F3.3) with increasingly abundant saline crystals (F5.1). The deposition of the saline facies represents initial closure of Lake Uinta, with the main outflow mechanism being evaporation (Carroll and Bohacs, 1999). XRF data indicate an increase in strontium concentrations towards the top of the Half Moon Canyon core and provide further evidence supporting evaporation (Appendix D). Strontium in carbonate lake systems is precipitated with an increase in salinity, and so it is likely that the lake system became heavily concentrated in

saline crystals which resulted in an increase in strontium precipitation within the carbonate deposits (Witherow and Lyons, 2011). Following the rapid regression associated with the Horse Bench Sandstone, the lake regressed slowly and eventually closed from the east to the west (Vanden Berg and Birgenheier, 2014).

The consistent lake regression from the base of the Horse Bench Sandstone to the top of the saline facies can be attributed to both tectonics and climate. Tectonic activity of the Uinta Uplift resulted is re-isolation of the lake systems and rearrangement of drainage patterns in the Uinta and Greater Green River basins (Davis et al., 2008; Tanavsuu-Milkeviciene and Sarg, 2012). Furthermore, climatic cooling after the Eocene Climatic Optimum contributed to increased precipitation as well as increased sedimentation, which resulted in the closing of the Piceance Basin (Tanavsuu-Milkeviciene and Sarg, 2012). With the Uinta Basin isolated from the other continental basins, accommodation remained high, but water influx decreased, leading to extreme evaporation of the lacustrine system.

Lake Phases

The studied intervals from the middle and upper Green River Formation reflect spatial and temporal changes as a result of both climatic and tectonic controls. These controls illustrate basin-wide lake evolution that can be associated with the different lake-basin types defined by Carroll and Bohacs (1999). The lake-basin types, which reflect a balance between the influx of water and sediment and rates of potential accommodation, are termed overfilled, balanced-fill, and underfilled. Overfilled basins occur when the influx of water and sediment exceeds potential accommodation and so inflow is equal to

outflow. In overfilled basins, fluvial-lacustrine facies dominate (Bohacs et al., 2000). Balanced-fill basins are established when the influx of water and sediment equals potential accommodation, and lake level fluctuates above and below sill level. Fluctuating-profundal facies are common in this type of lacustrine basin (Bohacs et al., 2000). Underfilled basins occur when accommodation exceeds water and sediment influx, and so lake levels do not reach sill level. In this case, evaporation is the only outflow mechanism and evaporative facies dominate (Bohacs et al., 2000).

From the base of the C1 to the top of the Si.3, Lake Uinta is interpreted as overfilled with very low accommodation (Figure 29). This type of lacustrine system is closely related to marginal fluvial systems that act to carry siliciclastic sediment into the basin, and fluvial-lacustrine facies dominate. Lake hydrology is open and lake level fluctuations from climate change are negligible (Bohacs et al., 2000). Throughout this interval, climate change was the main control for the input of siliciclastic sediment (Figure 29).

From the base of the C4 to the top of the lower R8, the lake is interpreted as a balanced-fill basin with fluctuating-profundal facies (Figure 30a). In balanced-fill basins, inflow is periodically sufficient enough to fill potential accommodation but does not necessarily match outflow. Lake level rise from climate change can occur as a result of this imbalance (Bohacs et al., 2000). Climate is considered to be increasingly wet with high precipitation, thus resulting in lake level rise above the Douglas Creek Arch and linkage to the lacustrine system in the Piceance Basin, as suggested by the facies observed in these sections (Davis et al., 2008; Gierlowski-Kordesch et al., 2008). Throughout this interval, siliciclastic input was very low and accommodation was very

high, as evidenced from the abundance of deep, open lake facies (Figure 30a).

From the base of the Horse Bench Sandstone to the top of the Green River Formation, the lake basin was underfilled and contained evaporative facies (Figure 30b). Following the balanced-fill basin, climate began cooling and lake drainages were rearranged, resulting in re-isolation of the lacustrine systems (Tanavsuu-Milkeviciene and Sarg, 2012). Tectonic activity caused further isolation (Davis et al., 2008). The rearrangement of drainages resulted in low water influx throughout the basin and infilling with sediment from the east to the west, eventually leading to severe evaporation and the termination of Lake Uinta.

The lake phases defined here match several other studies of the middle and upper Green River Formation. Rosenberg et al. (in press) examined the middle and upper Green River Formation on the eastern side of the Uinta Basin and defined lake phases from the same stratigraphic intervals. Rosenberg et al. (in press) was able to identify detail in the lake stages based on stratigraphic stacking patterns that are not discernible in this study area. However, the long-term evolution from overfilled to balanced-fill to underfilled are equivalent and correspond to the same stratigraphic units. Another model by Tanavsuu-Milkeviciene and Sarg (2012) within the Piceance Basin shows similar lake evolution in the neighboring lacustrine system.

Modern Analogs

Modern lakes record numerous controls that are not directly observable in the ancient, including climate, hydrology, chemistry, and biology (Bohacs et al., 2000). The complexity of these controls makes it difficult to compare modern lake systems to ancient

lake systems, where only three key end-member facies associations are typically used to characterize the ancient stratigraphy (i.e., fluvial-lacustrine, fluctuating profundal, and evaporative facies) (Carroll and Bohacs, 1999). Whereas the Green River Formation records a long-lived perennial lake system that deposited thick and laterally extensive sequences, most modern lakes with similar deposits are very short-lived and smaller (Anadon et al., 2009). For this reason, multiple modern analogs must be used to explain the different intervals of the Green River Formation, which were subject to significantly different spatial and temporal controls (Table 3).

Facies throughout the base of the C1 to the top of the Si.3 are placed into the broad category of fluvial-lacustrine facies, where the margin of the lake and the lacustrine system are closely related. Modern analogs for the siliciclastic packages in this interval include the margin of Lake Baikal and Lake Bogoria, which are located in southern Siberia and the central Kenya Rift, respectively (Renaut, 1994; Flower et al., 1995; Back et al., 1999; Bohacs et al., 2000; Renaut et al., 2000) (Figure 31a, b). Lake Baikal, a freshwater rift lake, is asymmetrical with marginal deposits similar to those observed along the margins of Lake Uinta. The western flank of the lake is characterized by base-of-slope alluvial fans that are comparable to those observed on the northern flank of Lake Uinta (Back et al., 1999). The northern part of the lake is dominated by a large fluvial-deltaic system that is analogous to the fluvial-deltaic system interpreted along the southern margin of Lake Uinta (Back and Strecker, 1998). This deltaic system transitions from a large deltaic plain with meandering channels and floodplain swamps to a delta front with axial channel and mouthbar deposits with multiple lobes expressing upstream avulsion (Back and Strecker, 1998; Back et al., 1999) (Figure 31a). The delta plain is

Table 3 – Modern analogs of Lake Uinta

Lake Type	Modern Analog	Description
Overfilled Basin (C1-Si.3)	**<u>Lean Zones</u>**	
	Lake Baikal, southern Siberia	Freshwater rift lake
	Lake Bogoria, Kenya Rift	Stratified saline rift lake
	<u>Rich Zones</u>	
	Lake Tanganyika, central Africa	Mildy alkaline, carbonate lake
	Las Tablas de Daimiel, central Spain	Carbonate wetlands
Balanced-fill Basin (C4-middle R8)	Lake Malawi, central Africa	Stratified saline rift lake
	Lake Bogoria, Kenya Rift	Stratified saline rift lake
Underfilled Basin (middle R8-Saline Facies)	Dabusun Lake, western China	Shallow saline lake
	Lake Magadi, Kenya Rift	Saline rift lake

Key Similarities	Literature
Large, fluvial deltaic system to the north, similar to south-central Lake Uinta	Back et al., 1999 Back and Strecker, 1998
Small deltaic systems (Loburu and Sandai) similar to south-central Lake Uinta	Ashley et al., 2004 Driese et al., 2004 Renaut, 1994
Carbonate deposits (calcareous siltstone, wackestone, grainstone, stromatolites and thrombolites)	Cohen and Thouin, 1987
Lake flat carbonate deposits (organic-poor carbonate mudstone)	Alonso-Zarza and Wright, 2010 Alonso-Zarza, 2003
Laminated, organic-rich carbonate mudstone and siltstone	Scholz, 1995 Pilskaln and Johnson, 1991
Organic-rich carbonate mudstone with precipitated nahcolite and calcite	Renaut, 1994
Extreme evaporation, abundant saline deposits	Schubel and Lowenstein, 1997 Yang et al., 1995
Shallow saline lake with abundant saline precipitation	Eugster, 1986 Jones et al., 1977 Surdam and Eugster, 1976

Figure 31 – Modern analogs of Lake Uinta; A) Lake Baikal, representative of overfilled basin with distributary channel/mouthbar deposition in the transitional interval; B) Lake Bogoria, representative of overfilled basin with distributary channel/mouthbar deposition in the transitional interval and balanced-fill basin with profundal mudstone deposition in the Mahogany interval; C) Lake Tanganyika, representative of overfilled basin with coarse grained carbonate deposition in the transitional interval; D) Las Tablas de Daimiel, representative of overfilled basin with littoral carbonate mudstone deposition in the transitional interval; E) Lake Malawi, representative of balanced-fill basin with profundal mudstone deposition in the Mahogany interval; F) Dabusun Lake, representative of underfilled basin with evaporite deposition after the Horse Bench Sandstone; G) Lake Magadi, representative of underfilled basin with evaporite deposition after the Horse Bench Sandstone.

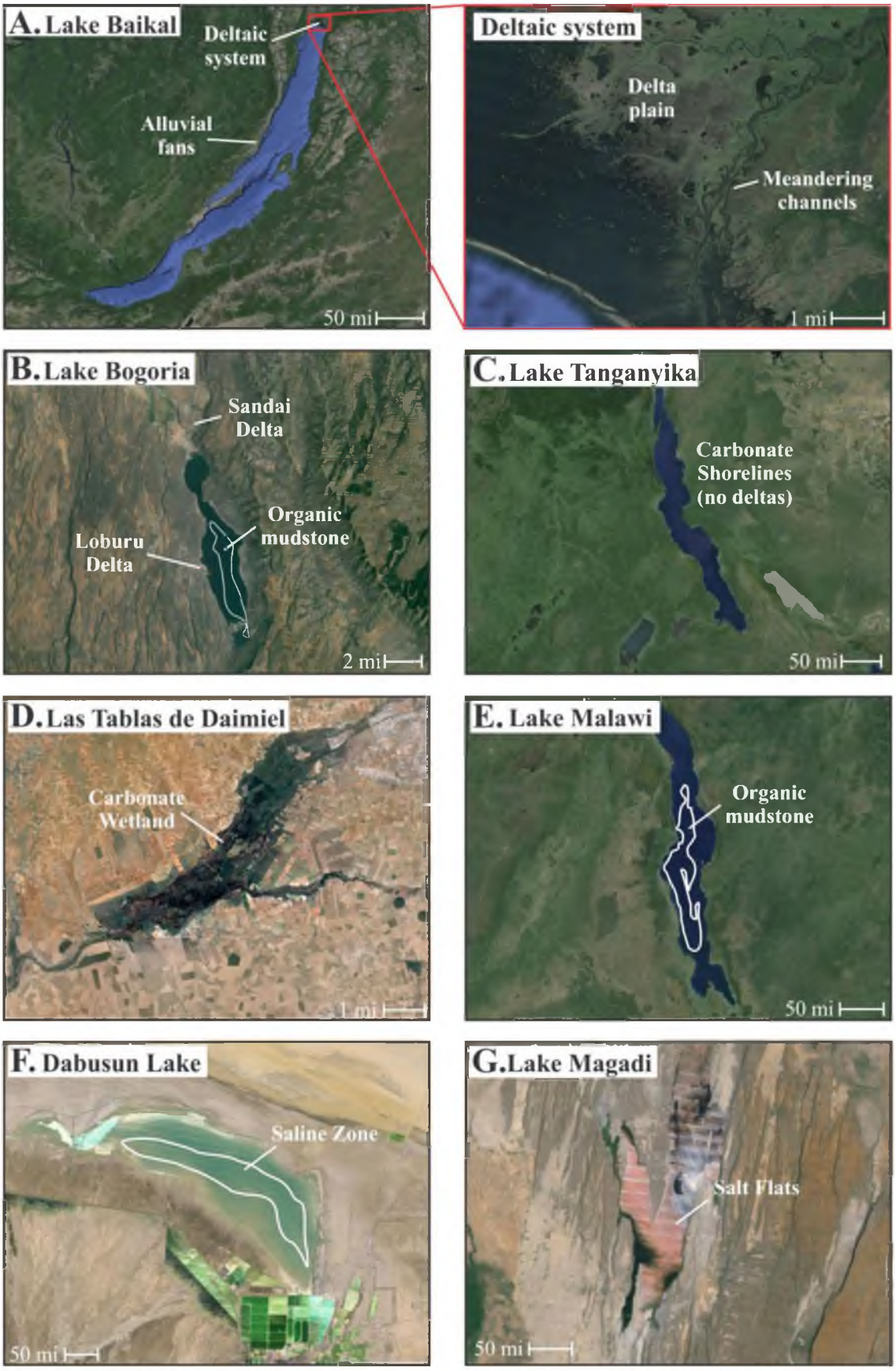
A. Lake Baikal
Deltaic system
Alluvial fans
50 mi
Deltaic system
Delta plain
Meandering channels
1 mi
B. Lake Bogoria
Sandai Delta
Organic mudstone
Loburu Delta
2 mi
C. Lake Tanganyika
Carbonate Shorelines (no deltas)
50 mi
D. Las Tablas de Daimiel
Carbonate Wetland
1 mi
E. Lake Malawi
Organic mudstone
50 mi
F. Dabusun Lake
Saline Zone
50 mi
G. Lake Magadi
Salt Flats
50 mi

comparable to the lake flat interpretations in Willow Creek/Indian Canyon whereas the delta front and pro-delta is similar to the observations in Gate Canyon (Figure 31a).

Lake Bogoria is a stratified, saline lake with less dense waters lying above deeper anoxic waters, similar to the conditions interpreted for Lake Uinta (Desborough, 1978) (Figure 31b). Deltas of Lake Bogoria, specifically the Loburu Delta, produce facies that are similar to those observed along the south-central margin of Lake Uinta (Renaut, 1994). Although modern deltas of Lake Bogoria are smaller with coarser siliciclastic sediment compared to those found along the south-central margin of Lake Uinta, similar incision and channel organization across the lake flat and into the lake occurs, with mouthbar and turbidite deposition occurring basinward. The Sandai Delta, another smaller deltaic system along this lake, deposits facies comparable to those found on the western margin of Lake Uinta. This low gradient delta consists of mainly mudstones and siltstones with local ephemeral washes and sheetwash floods like those found in Willow Creek/Indian Canyon (Renaut, 1994). Loboi Swamp, a siliciclastic dominated wetland separating Lake Bogoria from its northern, freshwater counterpart, can also be used as a modern analog for the lake flat deposits found in Willow Creek/Indian Canyon, including the calcareous green siltstones and paleosols (Ashley et al., 2004; Driese et al., 2004).

During deposition of the carbonate packages in the Green River Formation, siliciclastic input was diminished and resulted in the accumulation of carbonates. Modern analogs for these carbonate lakes include Lake Tanganyika and the Las Tablas de Daimiel wetlands, which are associated with coarse grained carbonates and marginal carbonate mudstones, respectively (Cohen and Thouin, 1987; Alonso-Zarza, 2003; Alonso-Zarza and Wright, 2010) (Figure 31c, d). Lake Tanganyika, located in central

Africa, is a mildly alkaline, carbonate lake that formed under similar though slightly more tropical climate conditions as Lake Uinta (Cohen and Thouin, 1987) (Figure 31c). The littoral and sublittoral carbonate facies observed in this modern lake include carbonate cemented sands, calcareous siltstones, skeletal carbonate shoals (ostracodal grainstone), and small stromatolites and thrombolites (Cohen and Thouin, 1987). All of these facies are similar to those seen in the carbonate packages of the Green River Formation towards the south-central portion of the basin.

The Las Tablas de Daimiel wetlands in Spain are used as a recent analog for the lake flat organic-poor carbonate mudstones, or palustrine carbonates, observed on the western margin of Lake Uinta (Alonso-Zarza and Wright, 2010) (Figure 31d). Palustrine carbonates form in a variety of environments, including low gradient lake margins with low energy (Alonso-Zarza and Wright, 2010). Carbonate wetlands are commonly used as modern analogs for palustrine carbonate deposition because their lithological and chemical characteristics are most closely related to ancient palustrine carbonate deposits (Alonso-Zarza and Wright, 2010). Cores of the Las Tablas de Daimiel wetlands suggest high sedimentation rates with facies ranging from massive chalky carbonates to wackestones and packstones with evidence of subaerial exposure (Alonso-Zarza and Tanner, 2006). Although the Willow Creek/Indian Canyon section lacks wackestones and packstones, there are organic-poor carbonate mudstones that are both massive and mottled from subaerial exposure.

The C4 to the top of the lower R8 consists of fluctuating-profundal facies. Deep lake facies dominate this system, including oil shales, organic-poor mudstone, and turbidites. Modern analogs include Lake Malawi and Lake Bogoria (Pilskaln and

Johnson, 1991; Renaut, 1994; Scholz, 1995; Bohacs et al., 2000) (Figure 31b, e). Lake Malawi, a rift valley lake located in east Africa, is permanently stratified and anoxic in the deepest parts of the lake (Scholz, 1995). Thick sequences of undisturbed, laminated organic-rich mudstones and siltstones can be found basinward of the marginal deltaic sequences (Pilskaln and Johnson, 1991). The organic richness and extent of these deep water sequences are similar to those observed throughout the Mahogany interval of the Green River Formation. Similarly, in the deep parts of Lake Bogoria where siliciclastic sediments are unable to reach, sediments are characterized by organic-rich carbonate mudstones and chemically precipitated sediments (Renaut, 1994). Precipitated sediments include nahcolite and calcite, both of which are observed in the thin sections of the Mahogany zone in the Henderson 3 core.

From the base of the Horse Bench Sandstone to the top of the Green River Formation, the facies can be categorized into the evaporative facies sequence. Dabusun Lake, located in the Qaidam Basin of western China, can be used as a modern analog for the evaporative stage of Lake Uinta (Yang et al., 1995) (Figure 31f). This shallow lake records a number of stages, from dilute to saline to desiccated, which deposit various sedimentary and saline structures (Schubel and Lowenstein, 1997). The saline lake stage occurs when the rate of evaporation is higher than the rate of inflow, similar to what is interpreted during the closing of Lake Uinta (Schubel and Lowenstein, 1997; Bohacs et al., 2000). Another modern analog for the evaporative lake stage is Lake Magadi, located in the lower part of the Kenyan Rift system (Surdam and Eugster, 1976; Eugster, 1986) (Figure 31g). Similar to the evaporative stage of Lake Uinta, Lake Magadi was once part of a larger, freshwater lake system. The lake water is presently concentrated with sodium-

carbonate, similar to that expected in Lake Uinta, and seasonal runoff and evaporation are the main inputs and outputs, respectively (Jones et al., 1977). Residual brines show a complex history of precipitation and resolution (Jones et al., 1977). This process could explain the strange sedimentary structures observed in the core of the saline facies, such as the saline fractures and voids.

CONCLUSIONS

A detailed study involving stratigraphy, sedimentology, and geochemistry of the middle and upper Green River Formation in the western and south-central Uinta Basin allows for a thorough analysis of lake evolution both spatially and temporally. Thirteen facies were identified in outcrop and core that were deposited in six different facies associations: F1) steep gradient, littoral to sublittoral siliciclastic deposits; F2) shallow gradient, littoral to sublittoral siliciclastic deposits; F3) low siliciclastic sediment supply, littoral to sublittoral carbonate deposits; F4) siliciclastic sediment-starved, profundal lake deposits; F5) saline deposits; and F6) volcanic deposits. The facies reflect depositional changes across the lake margin as well as short-term climatic changes and long-term tectonic controls through time. Stratigraphy from the transitional interval through the R8 shows that Lake Uinta evolved in three phases: 1) an overfilled lake characterized by siliciclastic and carbonate packages and overall lake transgression from the C1 through the Si.3, 2) a balanced-fill lake characterized by deep, open lake deposits from the C4 through the lower R8, and 3) an underfilled lake characterized by evaporative facies and lake regression from the base of the Horse Bench Sandstone through the R8.

The siliciclastic and carbonate packages of the first phase are associated with small hyperthermal events that occurred during the early Eocene. These hyperthermal events, which are characterized by increased seasonality or monsoonal episodes, resulted in increased weathering and siliciclastic deposition. In contrast, the carbonate packages

document periods between these hyperthermal events which allowed for uninterrupted accumulation of carbonate deposits. From the base of the C1 through the Si.3, there is a shift from littoral to sublittoral deposition, which reflects a slight lake transgression during lake evolution. In the central Gate Canyon area and the western Willow Creek/Indian Canyon area, there is a significant shift in depositional environments. Deposits in the south-central region of the basin are dominantly coarse grained siliciclastics and coarse grained carbonates whereas towards the west, the deposits are dominantly mudstones and siltstones with minor coarser grained siliciclastic deposition. This shift suggests that the primary sediment source was from the south towards the central region of the basin, creating a topographic high that resulted in a steeper gradient, ramp environment. The western region lies off of this depositional trend and was deposited along a shallower gradient, marginal ramp environment.

The second phase is characterized by major lake transgression as a result of the shift from a pulsed climate regime during the Eocene hyperthermal events to a period of relative stability during the Eocene Climatic Optimum. This climate shift is associated with increased precipitation which caused lake level to rise. Facies suggest that the lacustrine system in the Uinta Basin was linked with the lacustrine system in the Piceance Basin. The south-central Gate Canyon section and the Henderson 3 core contain more profundal oil shale facies as compared to the west, suggesting that the depocenter of Lake Uinta persisted in the eastern part of the basin at this time. Following this deep, open lake system was the third phase, which is associated with major lake regression. The closing of Lake Uinta began during this phase as a result of the rearrangement of lake drainages and tectonic activity that isolated the large Eocene lacustrine systems.

Through observations of facies variations in the Green River Formation and interpretations of overall controls on these spatial and temporal changes, both small- and large-scale climatic and tectonic events can be determined that shaped the lake system through time. Furthermore, increased understanding of climatic and tectonic events in these highly sensitive lacustrine systems helps elucidate the impact these events have on similar depositional systems in the region.

APPENDIX A

ROAD LOGS

GATE CANYON ROAD LOG

- Follow U.S. Highway 6/191 past Price, heading towards Wellington, UT
- **Turn left** onto Soldier Creek Road (the turn is immediately after the Chevron)
- Starting at Chevron gas station: 0.0 miles (Soldier Creek becomes 9 Mile Canyon)
- ine Mile Ranch sign (wooden sign): 24 miles
- Argyle Canyon Junction (keep right): 31.9 miles
- Gate Canyon Junction: **turn left**, 39.0 miles

First Outcrop: Transitional Interval

- 40.3 miles on the left side of the road; park on the right side road (Figure 32a, b)

Second Outcrop: Mahogany Interval

- S1 sandstone meets road: 42.5 miles
- 42.6 miles on the right side of the road (cross over stream) (Figure 32c, d)

Third Outcrop: R8

- Turn off for R8 on the right side of the road: 42.9 miles
- 43.7 miles to well pad, where we park to get to R8 section (left)
- Walk past creepy trailer (Figure 32e, f)
- S2 sandstone meets road: 43.0 miles

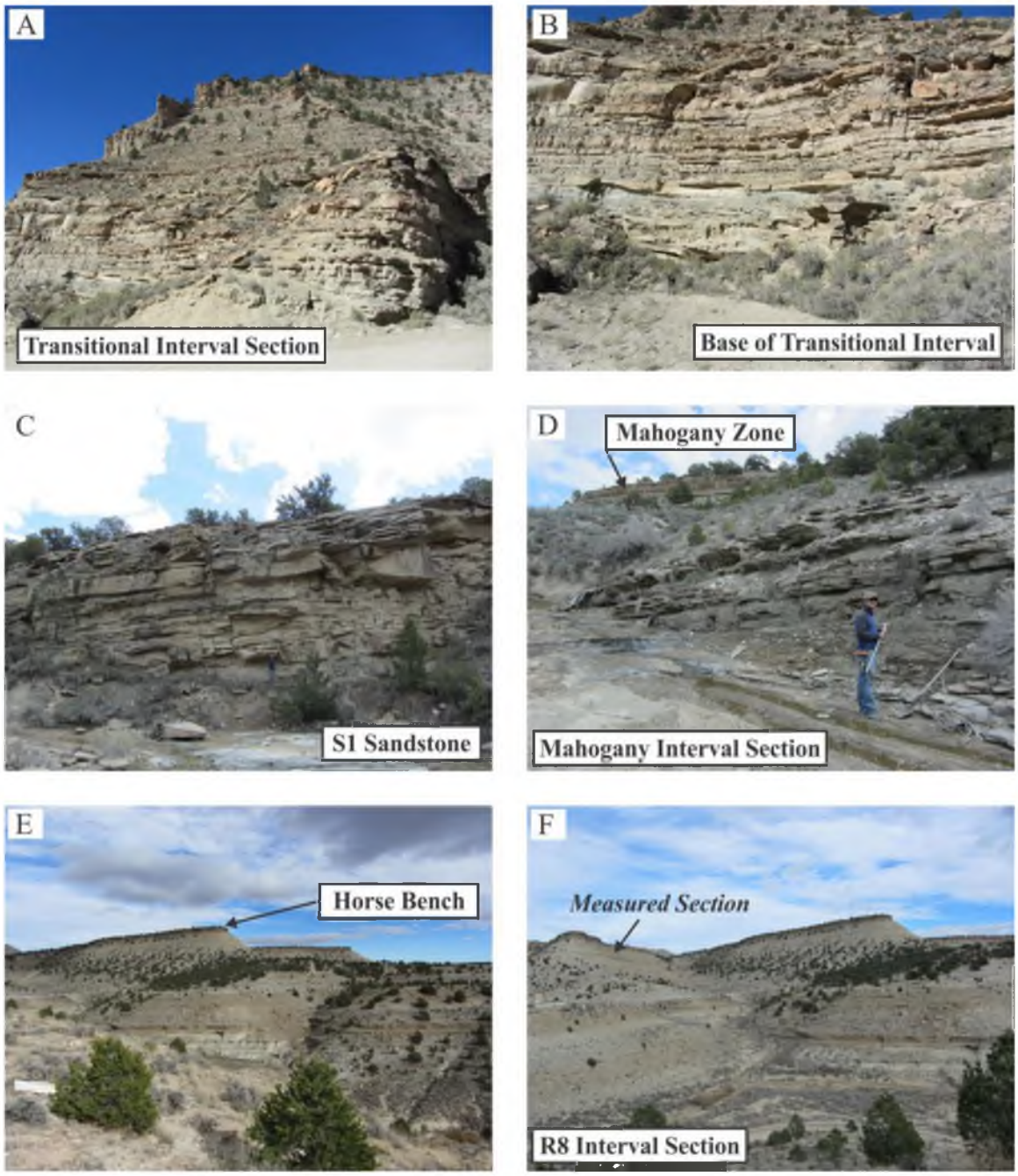

Figure 32 – Gate Canyon field area photos.

WILLOW CREEK/INDIAN CANYON ROAD LOG

- Turn off of U.S. Highway 6 onto U.S. Highway 191 to Duchesne
- Starting at bridge crossing over Willow Creek: 0.0 miles

Transitional Interval

- **Road Outcrop 1 (section above delta facies)**
  - 5.2 miles from where road crosses over Willow Creek (4.9 miles from the county line) (Figure 33a)
- **Road Outcrop 2**
  - 5.5 miles from Willow Creek (5.2 miles from county line) (Figure 33b)

Mahogany Interval

- **Road Outcrop 3 (S1 sandstone)**
  - 5.9 miles from Willow Creek (5.6 miles from county line) (Figure 33c)
- **Road Outcrop 4 (Mahogany zone)**
  - 6.2 miles from Willow Creek (5.9 miles from county line) (Figure 33d)

R8 Interval

- **Road Outcrop 5 (summit)**
  - Wavy Tuff: 7.3 miles from Willow Creek (7 miles from county line)
  - S2 sandstone: 7.6 miles from Willow Creek (7.3 miles from county line) (Figure 33e)
  - Summit: 7.8 miles from Willow Creek (7.5 miles from county line) (Figure 33f)
- **Road Outcrop 6 (Horse Bench)**
  - 10.6 miles from Willow Creek (10.3 miles from county line)
  - Outcrop right past mile marker 270 near sign that says "Icy road next 9 mi" (on left when driving down road)
  - Park: N 39°54'36.8" W 110°42'09.5" (Figure 34a, b)
  - Follow gully into trees, stay to the right, outcrop starts along stream bed (Figure 34c)
  - Outcrop: N 39°54'43.6" W 110°42'16.1"
  - Topped by Horse Bench Sandstone (Figure 34d)

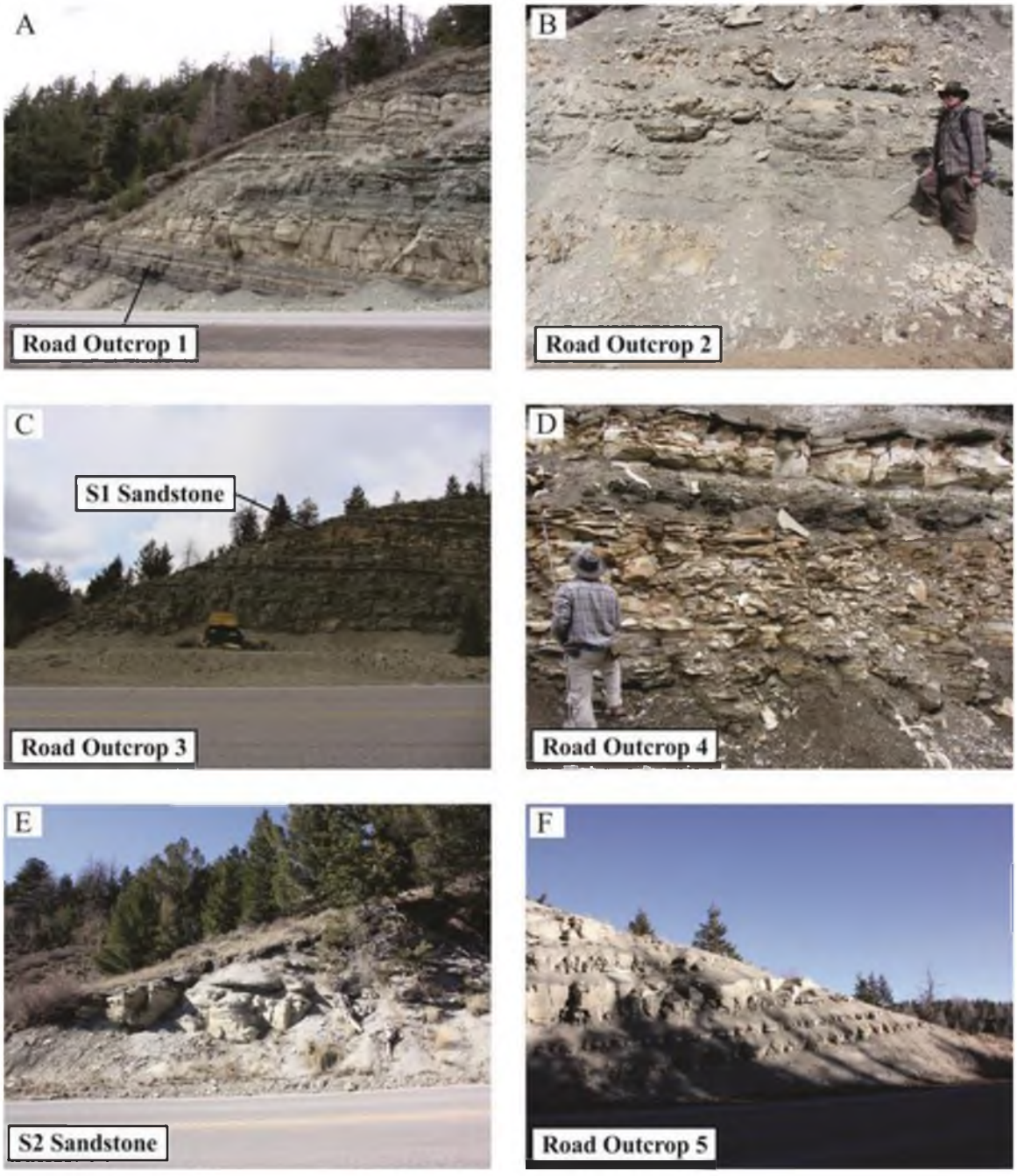

Figure 33 – Willow Creek road outcrop photos.

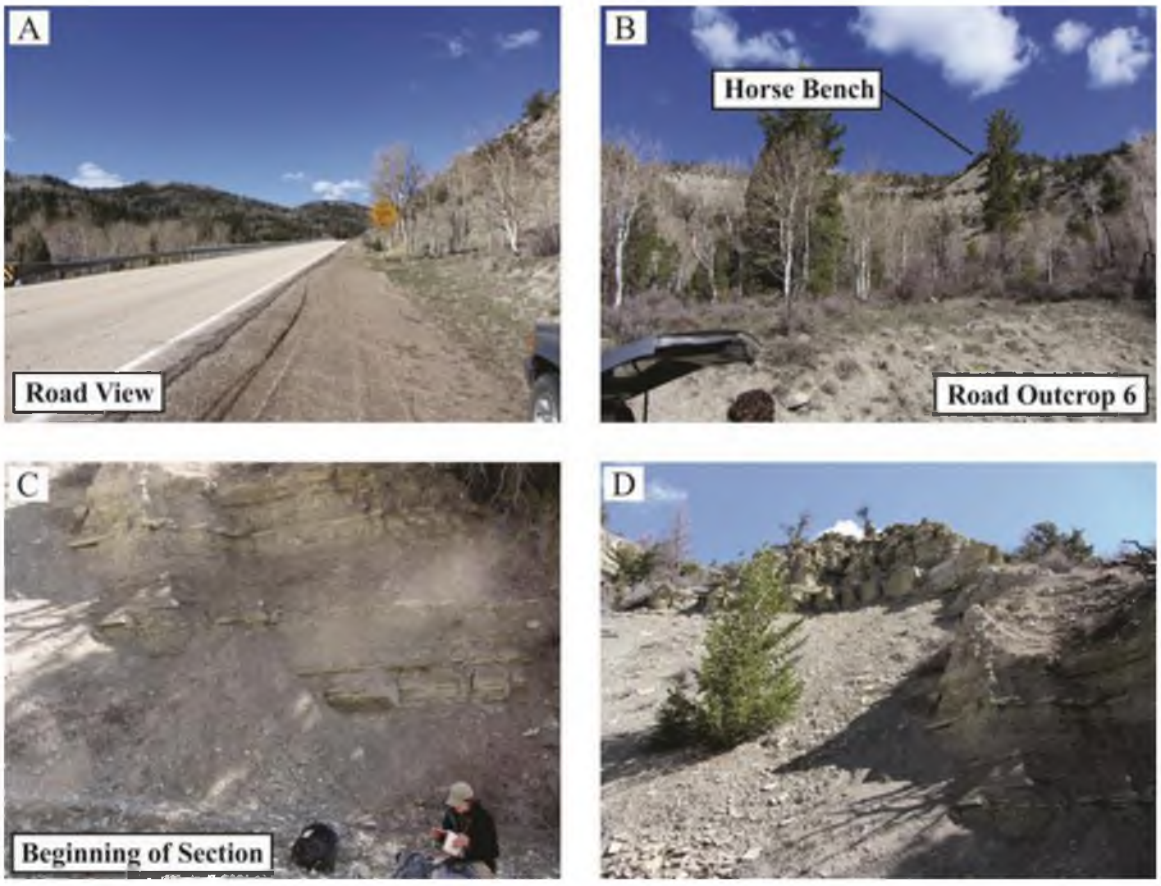

Figure 34 – Willow Creek Horse Bench Outcrop 6 photos.

APPENDIX B

MEASURED STRATIGRAPHIC SECTIONS

Appendix A contains 11 measured sections from the 2 outcrop areas (Gate Canyon and Willow Creek/Indian Canyon) and the 2 measured cores (Henderson 3 and Half Moon Canyon). A legend of symbols is provided.

Explanation

Acronyms

SS = Sandstone
CMS = Carbonate mudstone
OC = Organic content
VF = Very fine
F = Fine
M = Medium
LAL = Low angle laminations
PPL = Planar parallel laminations
TCS = Trough cross stratification
SSD = Soft sediment deformation

Paleocurrents

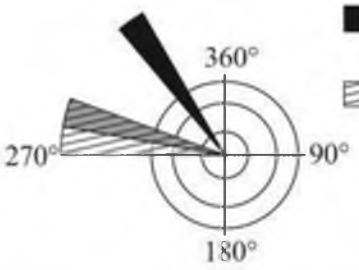

Internal sedimentary structures (ss)
Accretion sets (as)

n_{type} = sample #, v.m. = vector mean

Lithology

Sandstone
Siltstone, clastic mudstone
Paleosols
Carbonate mudstone (o.c. increasing to left)
Carbonates (including carbonate mudstone with no o.c.)
Microbiolites
Volcanics

Symbols

Planar lamination
Low angle
Wavy lamination
Current ripples
Wave ripples
Trough cross stratification
Convolute bedding
Mottling
Slicks
Bioturbation
Syneresis
Thin sections

Plant debris
Shell material
Ostracods
Stromatolite
Thrombolite
Fish
Carbonate grains
Siliciclastic grains
Lenses
Bot flies

Salines
Voids
Fracture fill
Planar parallel laminations

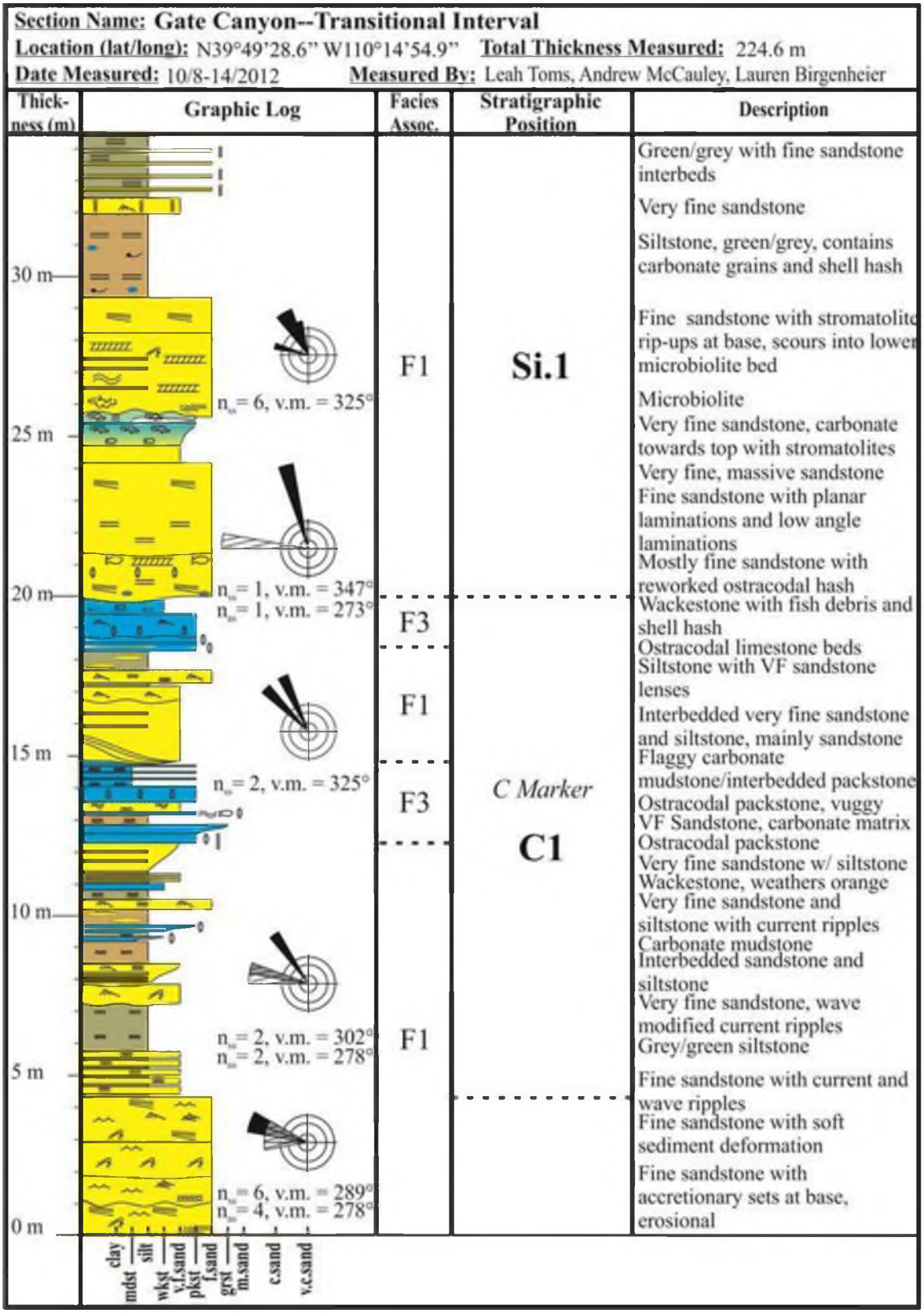
Section Name: Gate Canyon--Transitional Interval
Location (lat/long): N39°49'28.6" W110°14'54.9"
Total Thickness Measured: 224.6 m
Date Measured: 10/8-14/2012
Measured By: Leah Toms, Andrew McCauley, Lauren Birgenheier
Thick-ness (m)
Graphic Log
Facies Assoc.
Stratigraphic Position
Description
30 m
25 m
20 m
15 m
10 m
5 m
0 m
n = 6, v.m. = 325°
n = 1, v.m. = 347°
n = 1, v.m. = 273°
n = 2, v.m. = 325°
n = 2, v.m. = 302°
n = 2, v.m. = 278°
n = 6, v.m. = 289°
n = 4, v.m. = 278°
F1
F3
F1
F3
F1
Si.1
C Marker
C1
Green/grey with fine sandstone interbeds
Very fine sandstone
Siltstone, green/grey, contains carbonate grains and shell hash
Fine sandstone with stromatolite rip-ups at base, scours into lower microbiolite bed
Microbiolite
Very fine sandstone, carbonate towards top with stromatolites
Very fine, massive sandstone
Fine sandstone with planar laminations and low angle laminations
Mostly fine sandstone with reworked ostracodal hash
Wackestone with fish debris and shell hash
Ostracodal limestone beds
Siltstone with VF sandstone lenses
Interbedded very fine sandstone and siltstone, mainly sandstone
Flaggy carbonate mudstone/interbedded packstone
Ostracodal packstone, vuggy
VF Sandstone, carbonate matrix
Ostracodal packstone
Very fine sandstone w/ siltstone
Wackestone, weathers orange
Very fine sandstone and siltstone with current ripples
Carbonate mudstone
Interbedded sandstone and siltstone
Very fine sandstone, wave modified current ripples
Grey/green siltstone
Fine sandstone with current and wave ripples
Fine sandstone with soft sediment deformation
Fine sandstone with accretionary sets at base, erosional
clay
silt
mdst
wkst
v.f.sand
pkst
f.sand
grst
m.sand
c.sand
v.c.sand

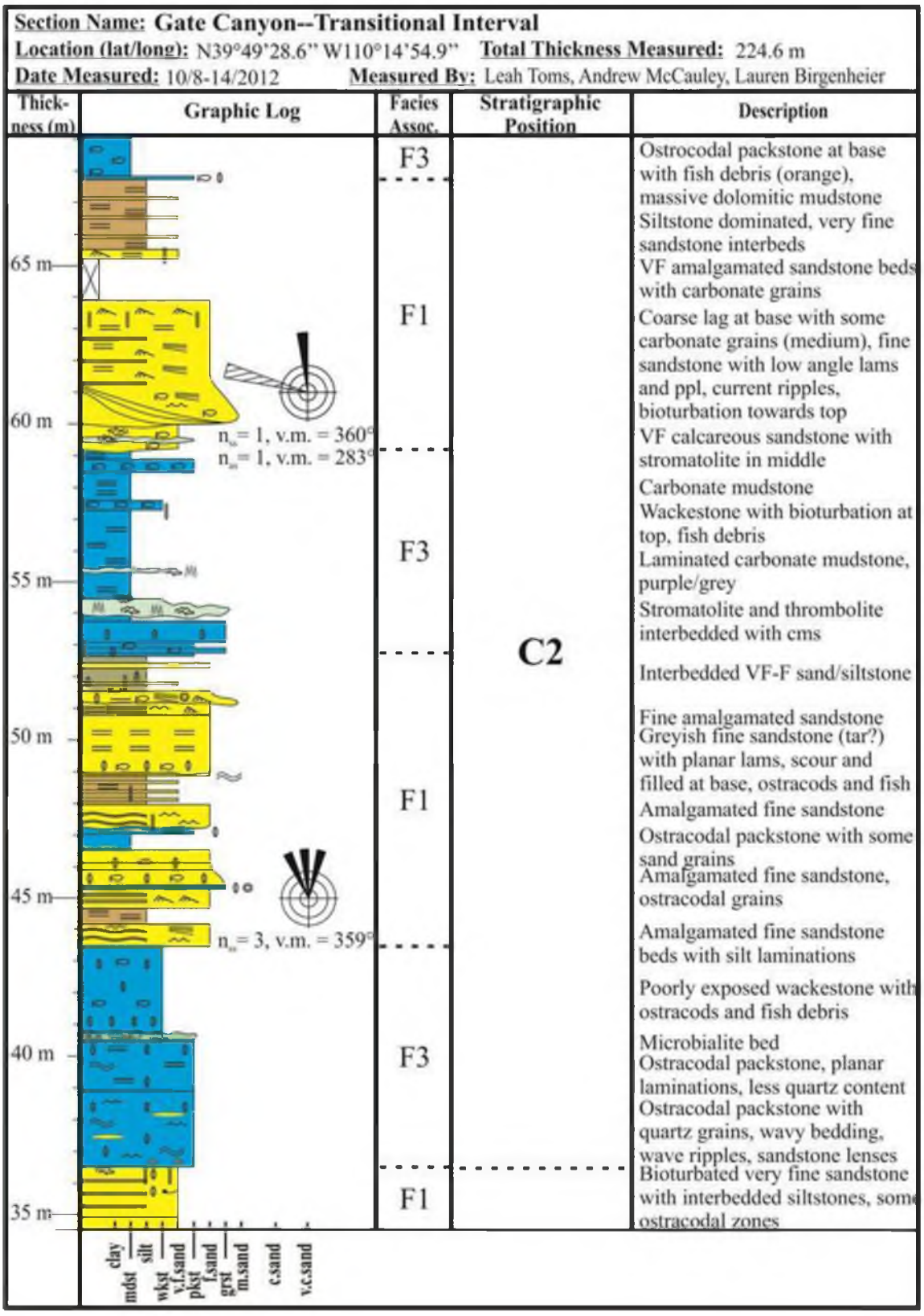
Section Name: Gate Canyon--Transitional Interval
Location (lat/long): N39°49'28.6" W110°14'54.9"
Total Thickness Measured: 224.6 m
Date Measured: 10/8-14/2012
Measured By: Leah Toms, Andrew McCauley, Lauren Birgenheier
Thick-ness (m)
Graphic Log
Facies Assoc.
Stratigraphic Position
Description
65 m
60 m
55 m
50 m
45 m
40 m
35 m
F3
F1
F3
F1
F3
F1
C2
n = 1, v.m. = 360°
n = 1, v.m. = 283°
n = 3, v.m. = 359°
Ostrocodal packstone at base with fish debris (orange), massive dolomitic mudstone
Siltstone dominated, very fine sandstone interbeds
VF amalgamated sandstone beds with carbonate grains
Coarse lag at base with some carbonate grains (medium), fine sandstone with low angle lams and ppl, current ripples, bioturbation towards top
VF calcareous sandstone with stromatolite in middle
Carbonate mudstone
Wackestone with bioturbation at top, fish debris
Laminated carbonate mudstone, purple/grey
Stromatolite and thrombolite interbedded with cms
Interbedded VF-F sand/siltstone
Fine amalgamated sandstone
Greyish fine sandstone (tar?) with planar lams, scour and filled at base, ostracods and fish
Amalgamated fine sandstone
Ostracodal packstone with some sand grains
Amalgamated fine sandstone, ostracodal grains
Amalgamated fine sandstone beds with silt laminations
Poorly exposed wackestone with ostracods and fish debris
Microbialite bed
Ostracodal packstone, planar laminations, less quartz content
Ostracodal packstone with quartz grains, wavy bedding, wave ripples, sandstone lenses
Bioturbated very fine sandstone with interbedded siltstones, some ostracodal zones
clay
silt
mdst
wkst
v.f.sand
pkst
f.sand
grst
m.sand
c.sand
v.c.sand

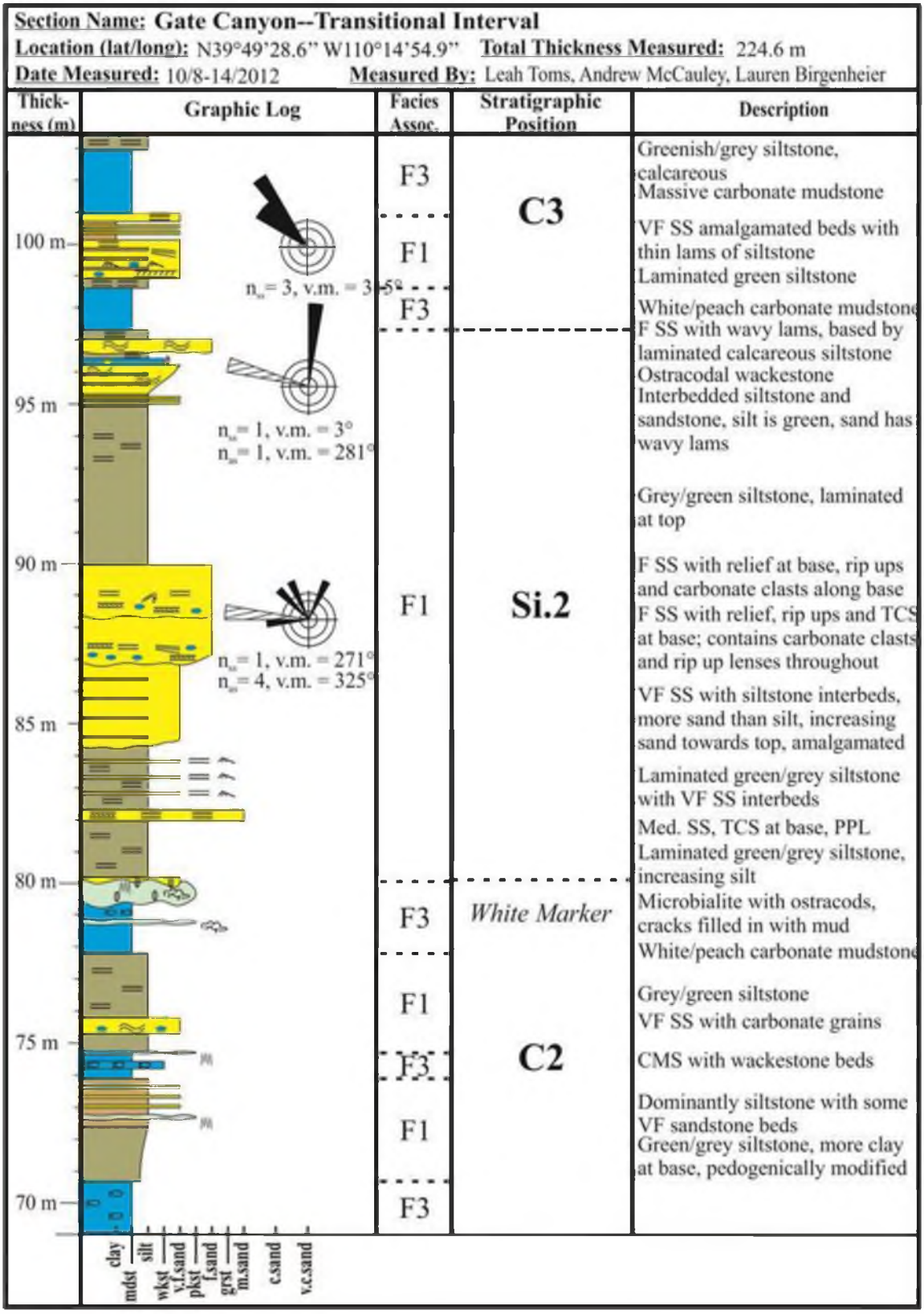
Section Name: Gate Canyon--Transitional Interval
Location (lat/long): N39°49'28.6" W110°14'54.9"
Total Thickness Measured: 224.6 m
Date Measured: 10/8-14/2012
Measured By: Leah Toms, Andrew McCauley, Lauren Birgenheier
Thick-ness (m)
Graphic Log
Facies Assoc.
Stratigraphic Position
Description
100 m
95 m
90 m
85 m
80 m
75 m
70 m
n = 3, v.m. = 3°
n = 1, v.m. = 3°
n = 1, v.m. = 281°
n = 1, v.m. = 271°
n = 4, v.m. = 325°
F3
F1
F3
F1
F3
F1
F3
F1
F3
C3
Si.2
White Marker
C2
Greenish/grey siltstone, calcareous
Massive carbonate mudstone
VF SS amalgamated beds with thin lams of siltstone
Laminated green siltstone
White/peach carbonate mudstone
F SS with wavy lams, based by laminated calcareous siltstone
Ostracodal wackestone
Interbedded siltstone and sandstone, silt is green, sand has wavy lams
Grey/green siltstone, laminated at top
F SS with relief at base, rip ups and carbonate clasts along base
F SS with relief, rip ups and TCS at base; contains carbonate clasts and rip up lenses throughout
VF SS with siltstone interbeds, more sand than silt, increasing sand towards top, amalgamated
Laminated green/grey siltstone with VF SS interbeds
Med. SS, TCS at base, PPL
Laminated green/grey siltstone, increasing silt
Microbialite with ostracods, cracks filled in with mud
White/peach carbonate mudstone
Grey/green siltstone
VF SS with carbonate grains
CMS with wackestone beds
Dominantly siltstone with some VF sandstone beds
Green/grey siltstone, more clay at base, pedogenically modified
clay
silt
mdst
wkst
v.f.sand
pkst
f.sand
grst
m.sand
c.sand
v.c.sand

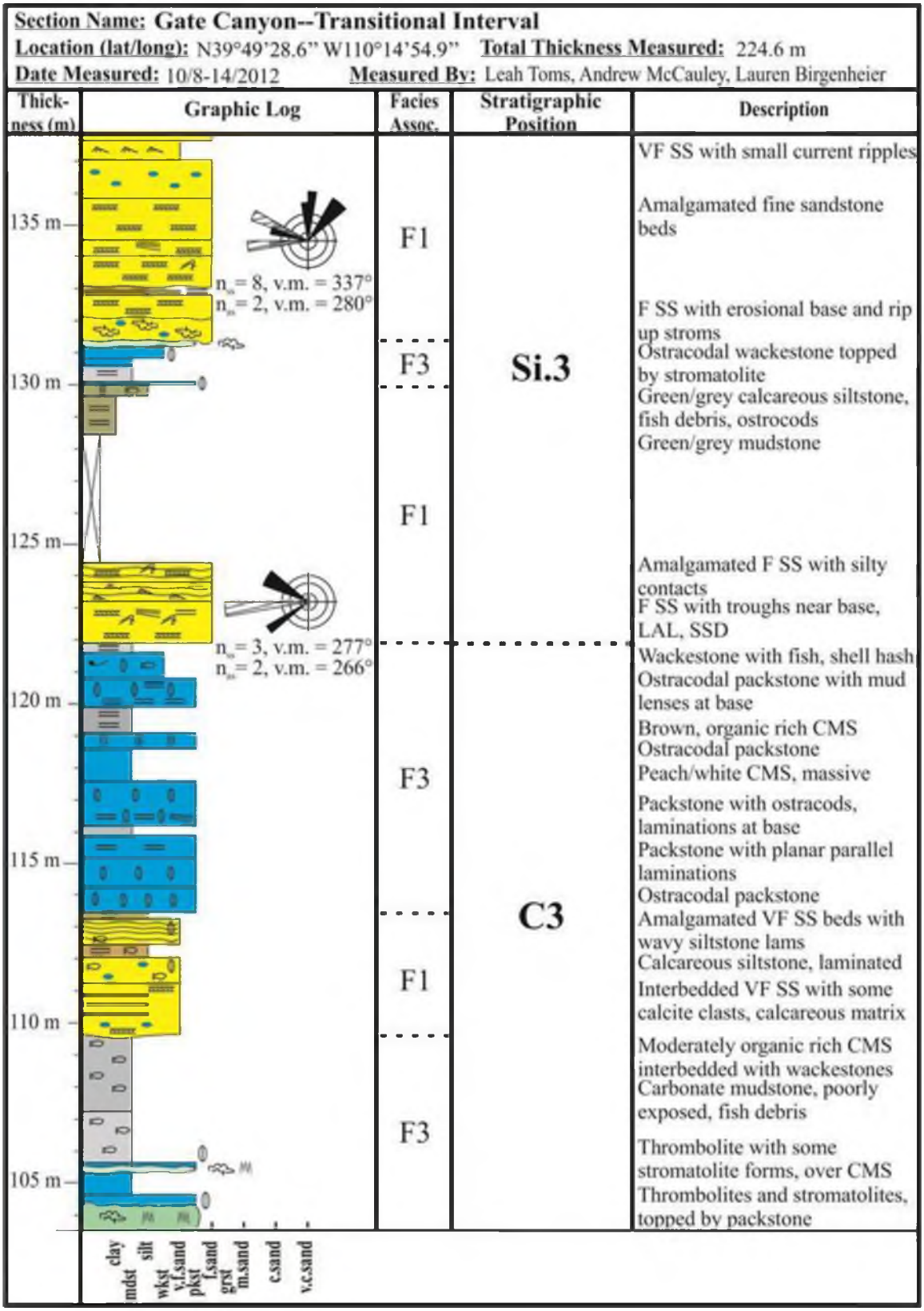
Section Name: Gate Canyon--Transitional Interval
Location (lat/long): N39°49'28.6" W110°14'54.9"
Total Thickness Measured: 224.6 m
Date Measured: 10/8-14/2012
Measured By: Leah Toms, Andrew McCauley, Lauren Birgenheier
Thick-ness (m)
Graphic Log
Facies Assoc.
Stratigraphic Position
Description
135 m
130 m
125 m
120 m
115 m
110 m
105 m
n = 8, v.m. = 337°
n = 2, v.m. = 280°
n = 3, v.m. = 277°
n = 2, v.m. = 266°
F1
F3
F1
F3
F1
F3
Si.3
C3
VF SS with small current ripples
Amalgamated fine sandstone beds
F SS with erosional base and rip up stroms
Ostracodal wackestone topped by stromatolite
Green/grey calcareous siltstone, fish debris, ostrocods
Green/grey mudstone
Amalgamated F SS with silty contacts
F SS with troughs near base, LAL, SSD
Wackestone with fish, shell hash
Ostracodal packstone with mud lenses at base
Brown, organic rich CMS
Ostracodal packstone
Peach/white CMS, massive
Packstone with ostracods, laminations at base
Packstone with planar parallel laminations
Ostracodal packstone
Amalgamated VF SS beds with wavy siltstone lams
Calcareous siltstone, laminated
Interbedded VF SS with some calcite clasts, calcareous matrix
Moderately organic rich CMS interbedded with wackestones
Carbonate mudstone, poorly exposed, fish debris
Thrombolite with some stromatolite forms, over CMS
Thrombolites and stromatolites, topped by packstone
clay
mdst
silt
wkst
v.f.sand
pkst
f.sand
grst
m.sand
c.sand
v.c.sand

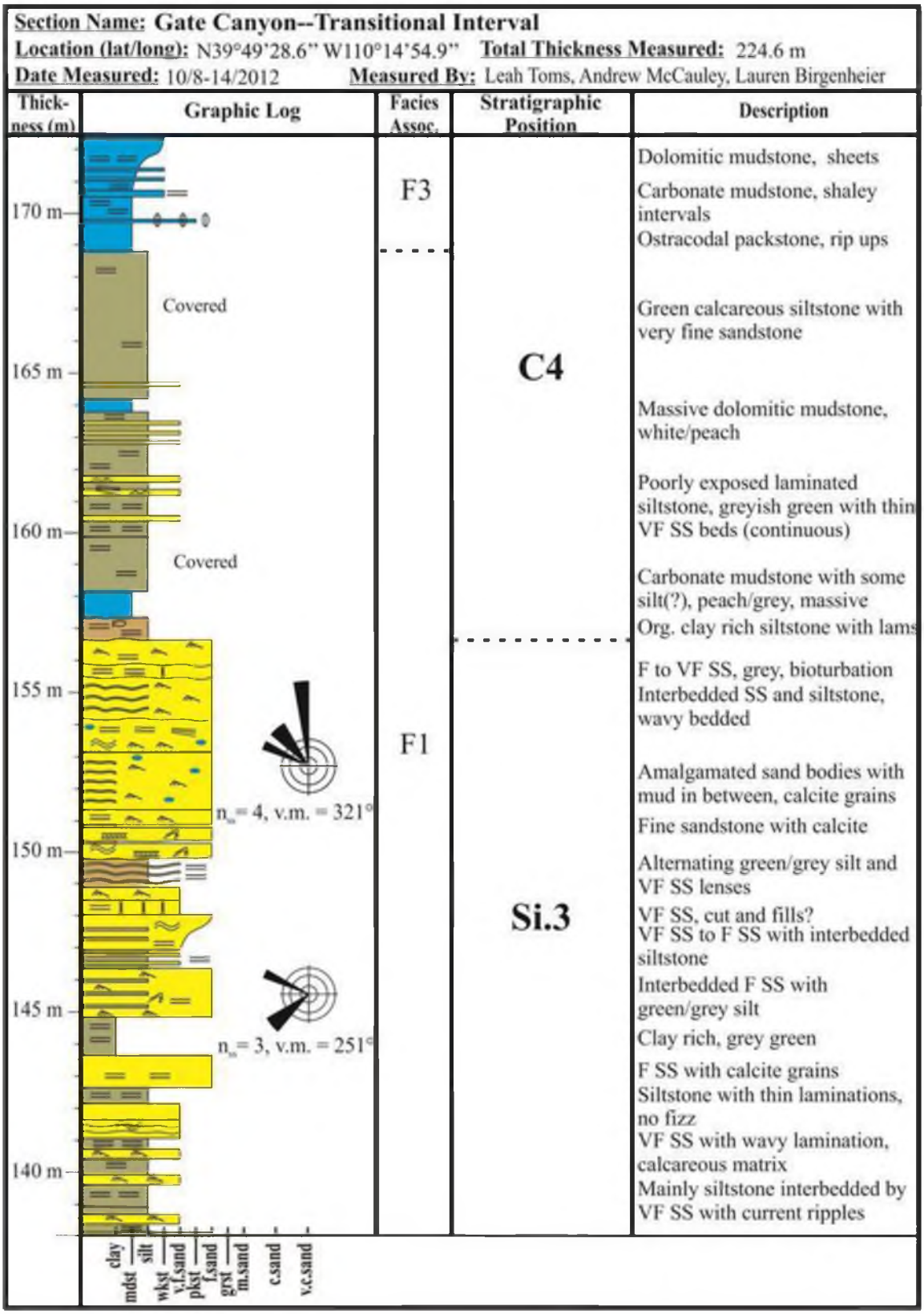
Section Name: Gate Canyon--Transitional Interval
Location (lat/long): N39°49'28.6" W110°14'54.9" Total Thickness Measured: 224.6 m
Date Measured: 10/8-14/2012 Measured By: Leah Toms, Andrew McCauley, Lauren Birgenheier
Thick-ness (m)
Graphic Log
Facies Assoc.
Stratigraphic Position
Description
170 m
165 m
160 m
155 m
150 m
145 m
140 m
Covered
Covered
F3
F1
C4
Si.3
Dolomitic mudstone, sheets
Carbonate mudstone, shaley intervals
Ostracodal packstone, rip ups
Green calcareous siltstone with very fine sandstone
Massive dolomitic mudstone, white/peach
Poorly exposed laminated siltstone, greyish green with thin VF SS beds (continuous)
Carbonate mudstone with some silt(?), peach/grey, massive
Org. clay rich siltstone with lams
F to VF SS, grey, bioturbation
Interbedded SS and siltstone, wavy bedded
Amalgamated sand bodies with mud in between, calcite grains
Fine sandstone with calcite
Alternating green/grey silt and VF SS lenses
VF SS, cut and fills?
VF SS to F SS with interbedded siltstone
Interbedded F SS with green/grey silt
Clay rich, grey green
F SS with calcite grains
Siltstone with thin laminations, no fizz
VF SS with wavy lamination, calcareous matrix
Mainly siltstone interbedded by VF SS with current ripples
n = 4, v.m. = 321°
n = 3, v.m. = 251°
clay
silt
mdst
wkst
v.f.sand
pkst
f.sand
grst
m.sand
c.sand
v.c.sand

Section Name: Gate Canyon--Transitional Interval
Location (lat/long): N39°49'28.6" W110°14'54.9" **Total Thickness Measured:** 224.6 m
Date Measured: 10/8-14/2012 **Measured By:** Leah Toms, Andrew McCauley, Lauren Birgenheier

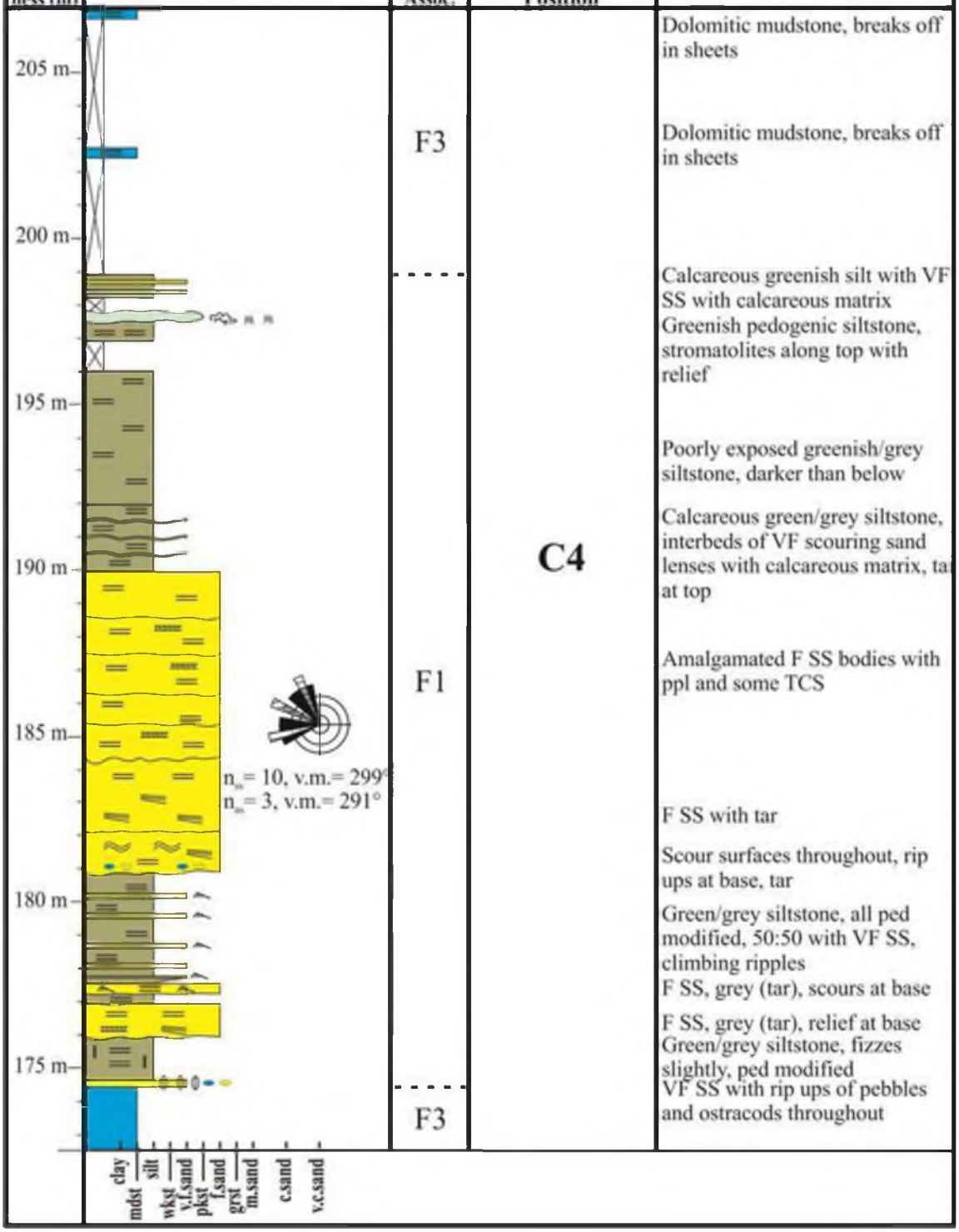

Section Name: Gate Canyon--Transitional Interval
Location (lat/long): N39°49'28.6" W110°14'54.9" **Total Thickness Measured:** 224.6 m
Date Measured: 10/8-14/2012 **Measured By:** Leah Toms, Andrew McCauley, Lauren Birgenheier

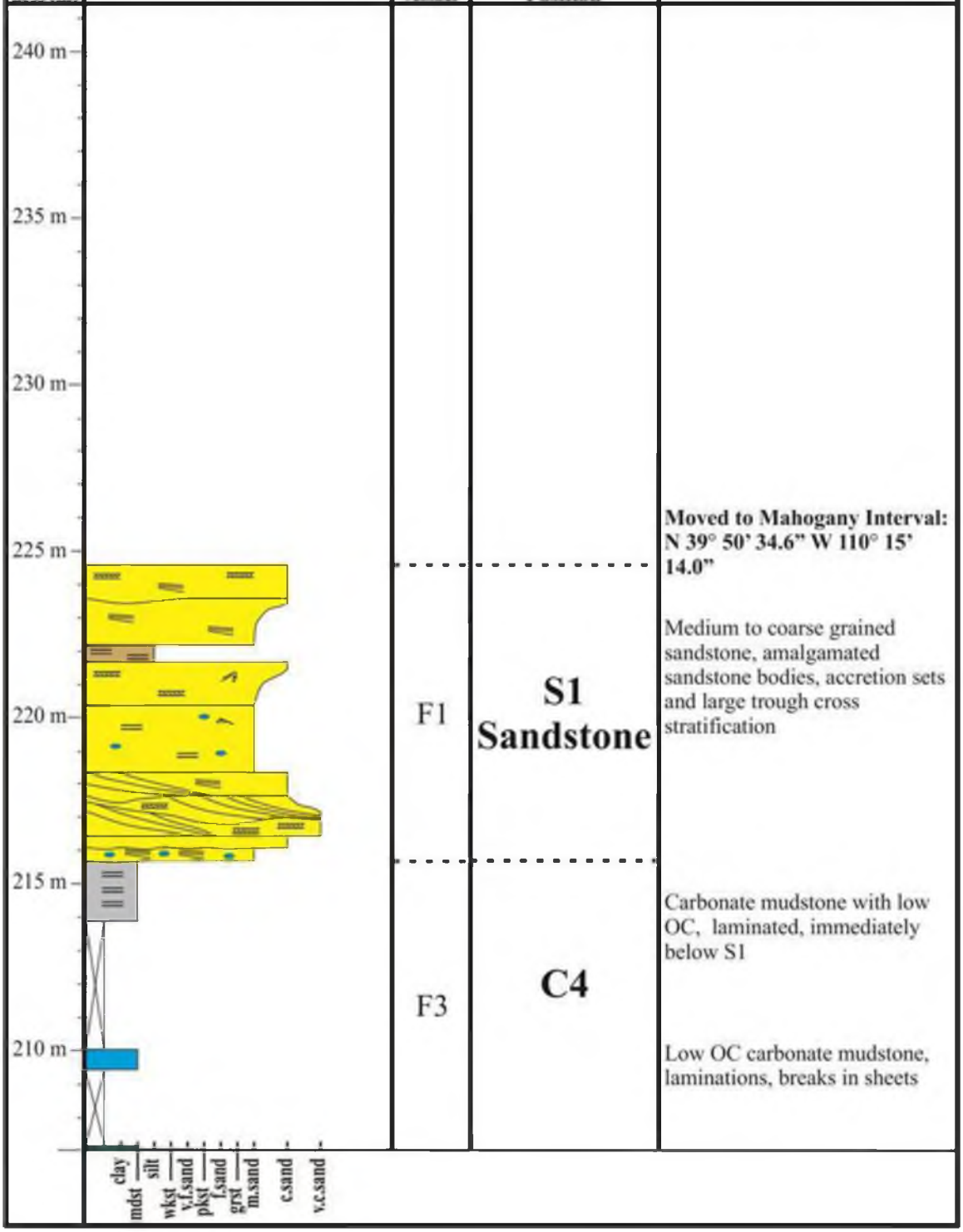

Section Name: Gate Canyon--Mahogany Interval
Location (lat/long): N39°50'37.3" W110°15'08.4" **Total Thickness Measured:** 31.54 m
Date Measured: 5/9/2013 **Measured By:** Leah Toms and Paul Thomas

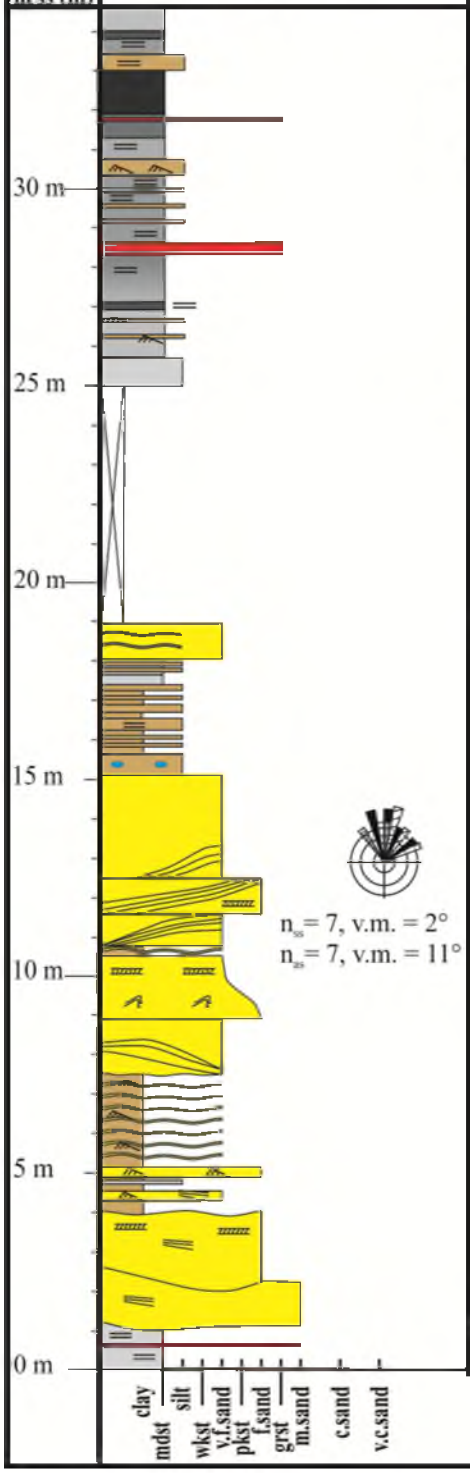

Facies Assoc.	Stratigraphic Position	Description
F3		Mod OC, topped by oil shale
		Silty, Mod OC at base
F4		High OC carbonate mudstone, flakey, tuff
		Brownish siltstone, current ripples
		Mod OC, white on outside, silty
	Curly Tuff	Tuff
		Mod OC to high
		High organic content, white outside, flakey
F3	**Mahogany Zone**	Siltstone, white, sticks out of outcrop; Moved upstream to **N 39 50' 45.2" W 110 15' 00.4"** (followed silt bed)
		VF SS interbedded with wavy siltstone
		Orangish siltstone beds
		Siltstone interbedded
		Dark siltstone with carbonate clasts, relocated up creek: **N 39 50' 42.1", W 110 15' 04.5"**
		F SS, accretion sets towards base
		M SS, some tar, accretionary sets
F1		M-F SS, soft sed deformation near base
	S1 Sandstone	F SS, scours into lower muds
		50:50 mudstone and sandstone, current ripples
		Silty mudstone, flaggy sands in between, with LAL and current
		Fine SS, erosional coarsens upwards
		Medium sandstone, scours into mud below
		White CMS bed

Section Name: Gate Canyon--Mahogany Interval
Location (lat/long): N39°50'37.3" W110°15'08.4" **Total Thickness Measured:** 31.54 m
Date Measured: 5/9/2013 **Measured By:** Leah Toms and Paul Thomas

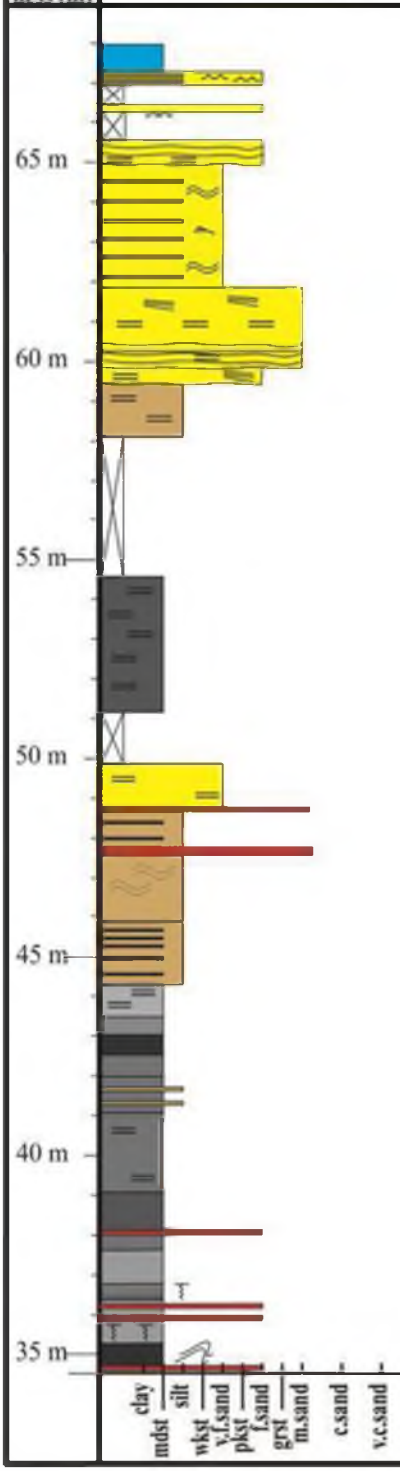

Thickness (m)	Facies Assoc.	Stratigraphic Position	Description
			Moved to HB Interval: N 39° 50' 56.5" W 110° 14' 54.1"
			F SS interbedded with siltstone, more sand than silt, laterally continuous
	F1		F SS with interbeds of siltstone, wavy laminations in sandstone, no scouring
			M-F SS, tar, organic clasts, slightly calcareous
			M-F SS, tar, amalgamated beds
			F SS, scours into lower silt
			Siltstone, moderately organic, weathers into flakes
		S2 Sandstone	
	F4		High OC carbonate mudstone, some places more brown than black
			VF SS, parallel lams
	F1		Siltstone with interbedded mudstone
			Siltstone, brown inside, orange continuous bed within
			Grey siltstone, interbedded with darker flakey mudstone
		Mahogany Oil Shale Bed	Mod OC, dark grey
	F3		High OC, shaley, very dark
			Mod OC, shaley
			Mod OC, with distinct interbeds of siltstone
		Mahogany Zone	Moderate OC
			High OC, shaley, dark
			Mod OC, darker than below, reddish
	F4		High OC carbonate mudstone
			Dark oil shale, high OC, hard, weathers peddy, flakey base, mod OC on top

Section Name: Gate Canyon– R8 Interval
Location (lat/long): N39°50'56.5" W110°14'54.1" **Total Thickness Measured:** 109.75 m
Date Measured: 10/8-14/2012 **Measured By:** Leah Toms and Andrew McCauley

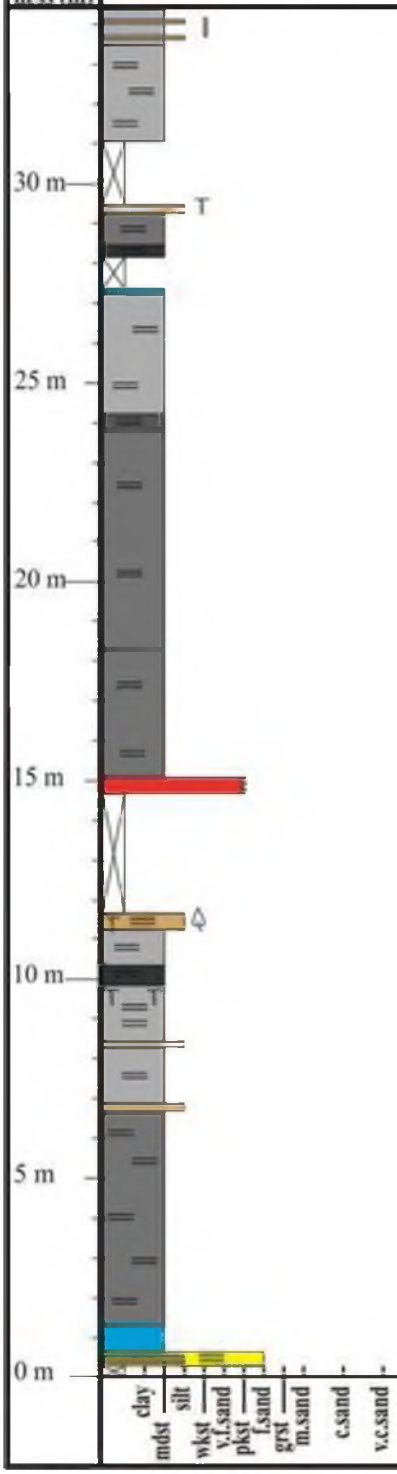

Thickness (m)	Facies Assoc.	Stratigraphic Position	Description
	F3		Moderate OC carbonate mudstone with greyish calcareous siltstone interbeds
			Moderate OC carbonate mudstone
			High to moderate OC carbonate mudstone, topped by greyish calcareous siltstone, orange
	F4		
	F3		Moderate OC carbonate mudstone, topped by white/orange CMS
			High OC carbonate mudstone, flakey
			Moderate OC carbonate mudstone, slightly higher than below
	F4	**R8**	Moderate OC carbonate mudstone, not super flakey
		Wavy Tuff	Weathered layer, peachish/grey
			Greyish siltstone, calcareous, weathers orange, organic matter
	F3		Moderate to high OC carbonate mudstone
			Greyish siltstone, calcareous, weathers orange, synoresis
			Moderate OC carbonate mudstone, brown
	F4		Greyish siltstone, calcareous, weathers orange
			High OC carbonate mudstone, flakey, decreases in OC slightly upwards
			White/peach dolomitic mudstone
			F SS interbedded with siltstone

Section Name: Gate Canyon– R8 Interval
Location (lat/long): N39°50'56.5" W110°14'54.1" **Total Thickness Measured:** 109.75 m
Date Measured: 10/8-14/2012 **Measured By:** Leah Toms and Andrew McCauley

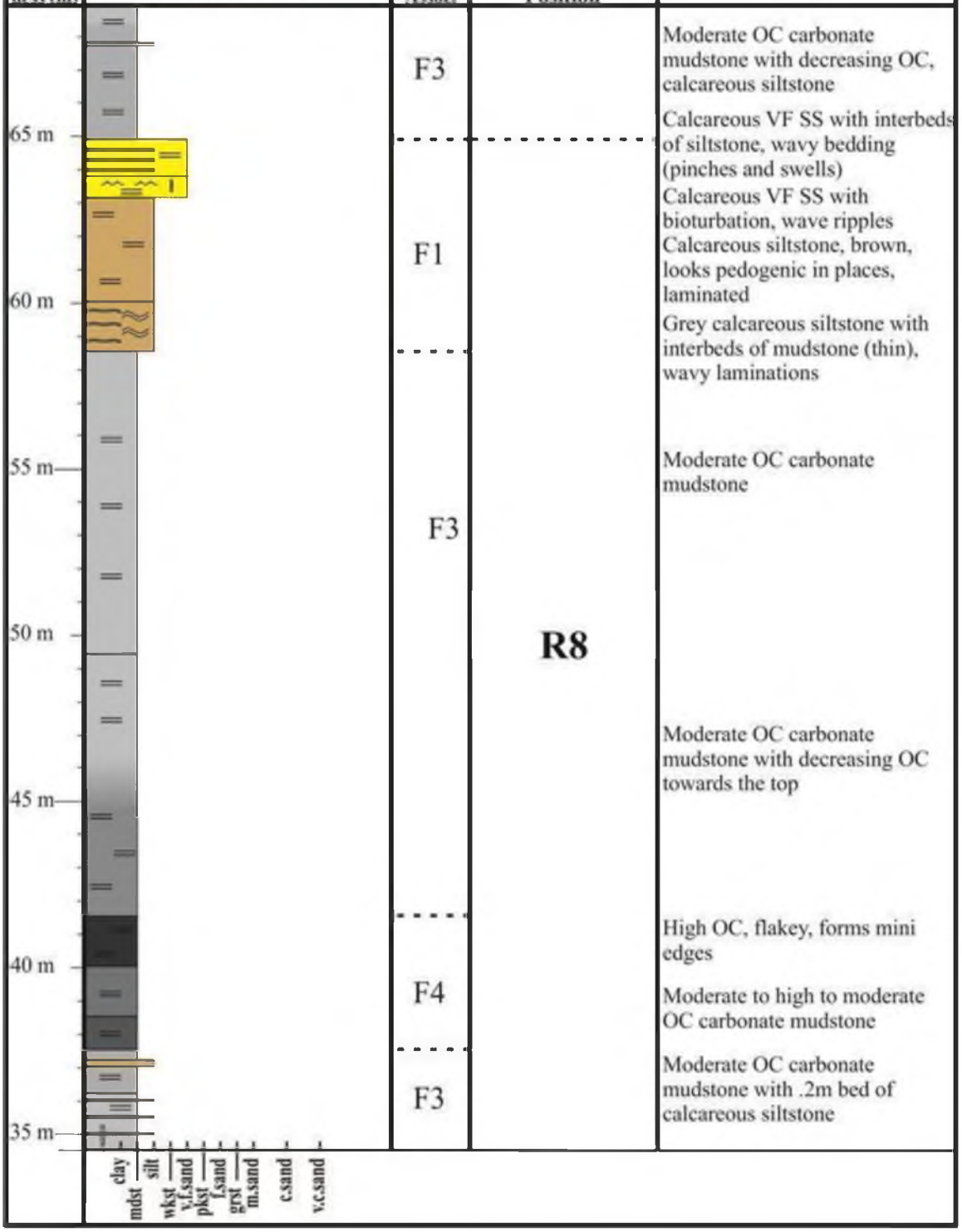

Section Name: Gate Canyon– R8 Interval
Location (lat/long): N39°50'56.5" W110°14'54.1" **Total Thickness Measured:** 109.75 m
Date Measured: 10/8-14/2012 **Measured By:** Leah Toms and Andrew McCauley

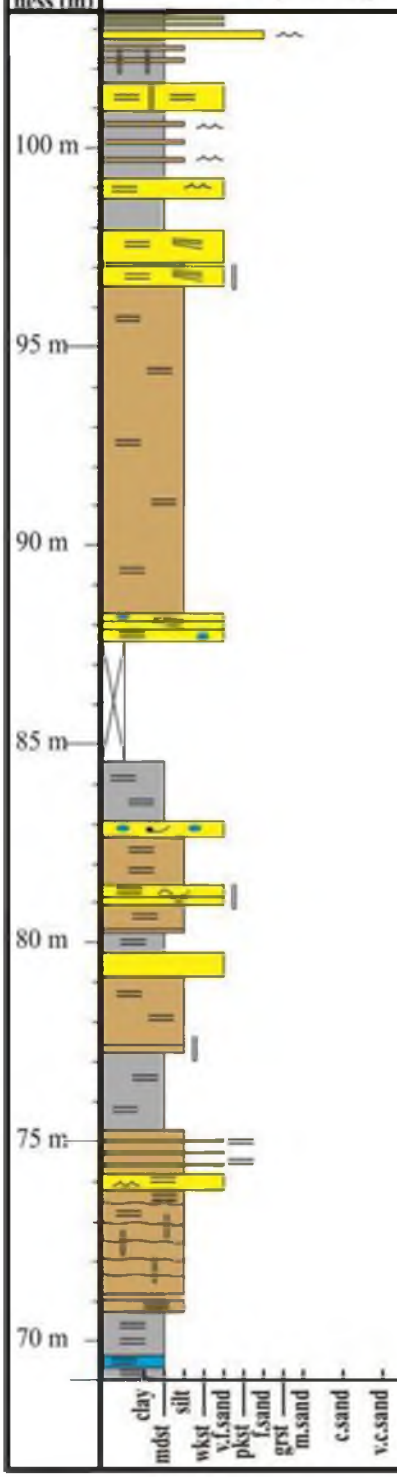

Thickness (m)	Facies Assoc.	Stratigraphic Position	Description
	F3	Horse Bench	Calcareous F SS Moderate OC carbonate mudstone with interbedded calcareous siltstone Grey calcareous VF SS with PPL Moderate OC carbonate mudstone interbedded and silt Grey calcareous VF SS Moderate OC CMS
	F1		Calcareous VF SS, blocky, PPL to LAL, wavy beds along top Calcareous VF SS (grey) with burrows, blocky Calcareous siltstone varying from well cemented to flakey, pedogenic, dark band running through middle Calcareous VF SS beds with rip ups, LAL, possible burrows at top
	F3		Moderate OC carbonate mudstone
	F1		Calcareous siltstone, peddy in places, burrows at base, topped by calcareous VF SS Moderate OC carbonate mudstone Grey calcareous VF SS with bioturbation and wavy beds Calcareous siltstone, looks pedogenic in some places
	F3		Moderate OC carbonate mudstone
	F1		Grey calcareous VF SS interbedded with siltstone Blocky calcareous VF SS with PPL Calcareous siltstone, pedogenic in some places, brown Calcareous siltstone, thin laminations
	F3		Moderate OC carbonate mudstone

Section Name: Gate Canyon– R8 Interval
Location (lat/long): N39°50'56.5" W110°14'54.1" **Total Thickness Measured:** 109.75 m
Date Measured: 10/8-14/2012 **Measured By:** Leah Toms and Andrew McCauley

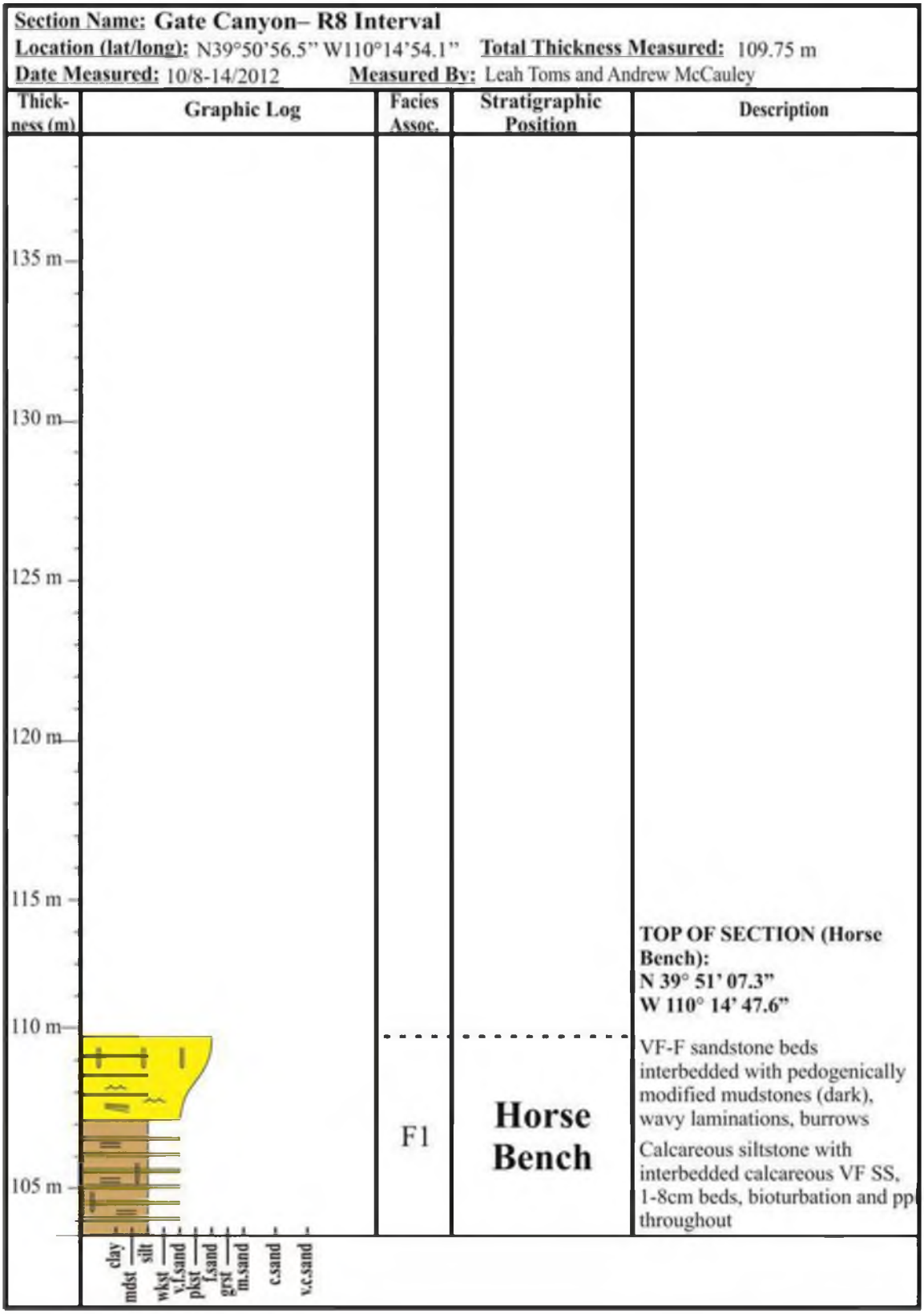

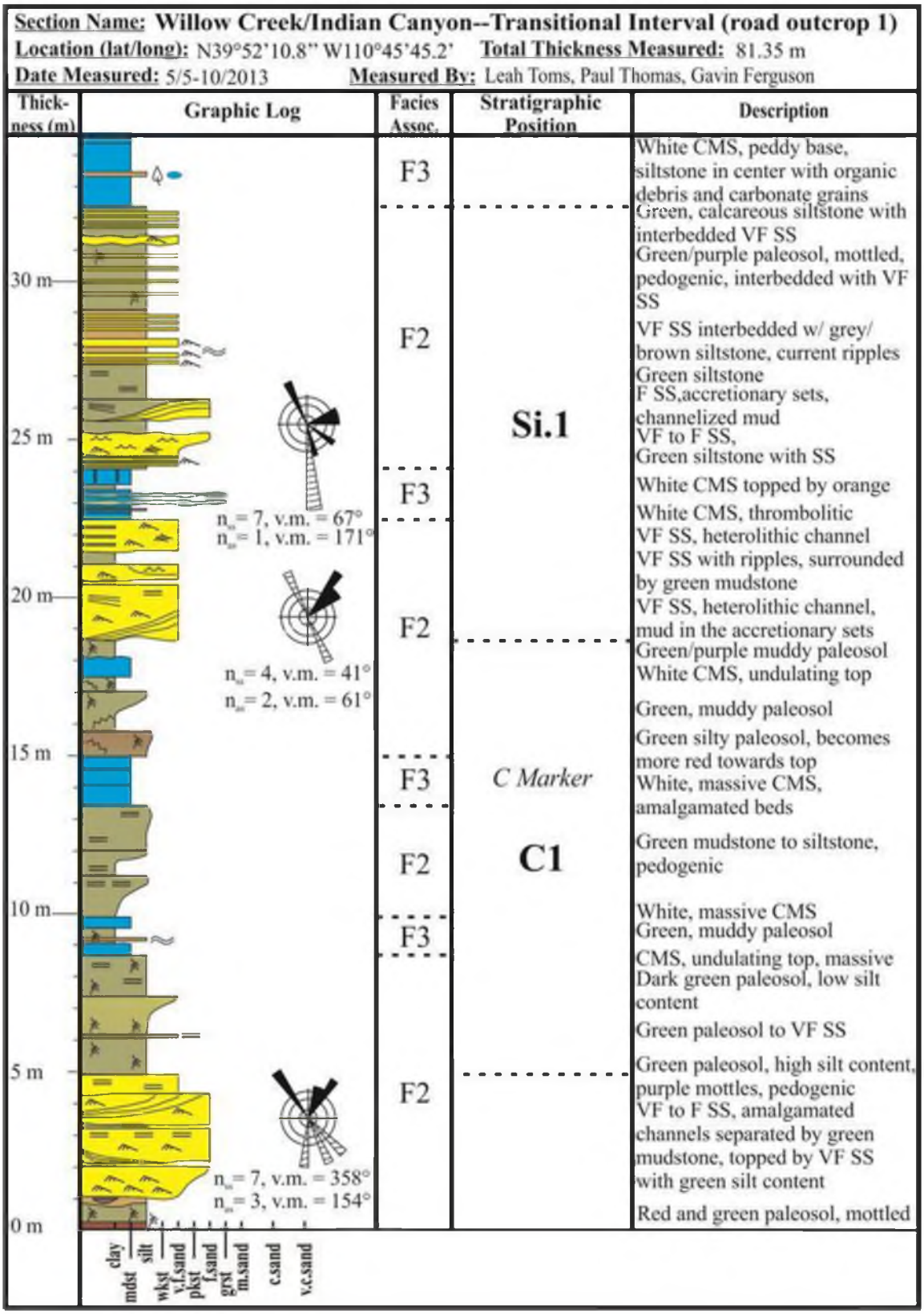
Section Name: Willow Creek/Indian Canyon--Transitional Interval (road outcrop 1)
Location (lat/long): N39°52'10.8" W110°45'45.2' Total Thickness Measured: 81.35 m
Date Measured: 5/5-10/2013 Measured By: Leah Toms, Paul Thomas, Gavin Ferguson
Thick-ness (m)
Graphic Log
Facies Assoc.
Stratigraphic Position
Description
30 m
25 m
20 m
15 m
10 m
5 m
0 m
F3
F2
F3
F2
F3
F2
F3
F2
Si.1
C Marker
C1
White CMS, peddy base, siltstone in center with organic debris and carbonate grains
Green, calcareous siltstone with interbedded VF SS
Green/purple paleosol, mottled, pedogenic, interbedded with VF SS
VF SS interbedded w/ grey/ brown siltstone, current ripples
Green siltstone
F SS,accretionary sets, channelized mud
VF to F SS,
Green siltstone with SS
White CMS topped by orange
White CMS, thrombolitic
VF SS, heterolithic channel
VF SS with ripples, surrounded by green mudstone
VF SS, heterolithic channel, mud in the accretionary sets
Green/purple muddy paleosol
White CMS, undulating top
Green, muddy paleosol
Green silty paleosol, becomes more red towards top
White, massive CMS, amalgamated beds
Green mudstone to siltstone, pedogenic
White, massive CMS
Green, muddy paleosol
CMS, undulating top, massive
Dark green paleosol, low silt content
Green paleosol to VF SS
Green paleosol, high silt content, purple mottles, pedogenic
VF to F SS, amalgamated channels separated by green mudstone, topped by VF SS with green silt content
Red and green paleosol, mottled
n = 7, v.m. = 67°
n = 1, v.m. = 171°
n = 4, v.m. = 41°
n = 2, v.m. = 61°
n = 7, v.m. = 358°
n = 3, v.m. = 154°
clay
mdst
silt
wkst
v.f.sand
pkst
f.sand
grst
m.sand
c.sand
v.c.sand

Section Name: Willow Creek/Indian Canyon--Transitional Interval (road outcrop 1)
Location (lat/long): N39°52'10.8" W110°45'45.2' **Total Thickness Measured:** 81.35 m
Date Measured: 5/5-10/2013 **Measured By:** Leah Toms, Paul Thomas, Gavin Ferguson

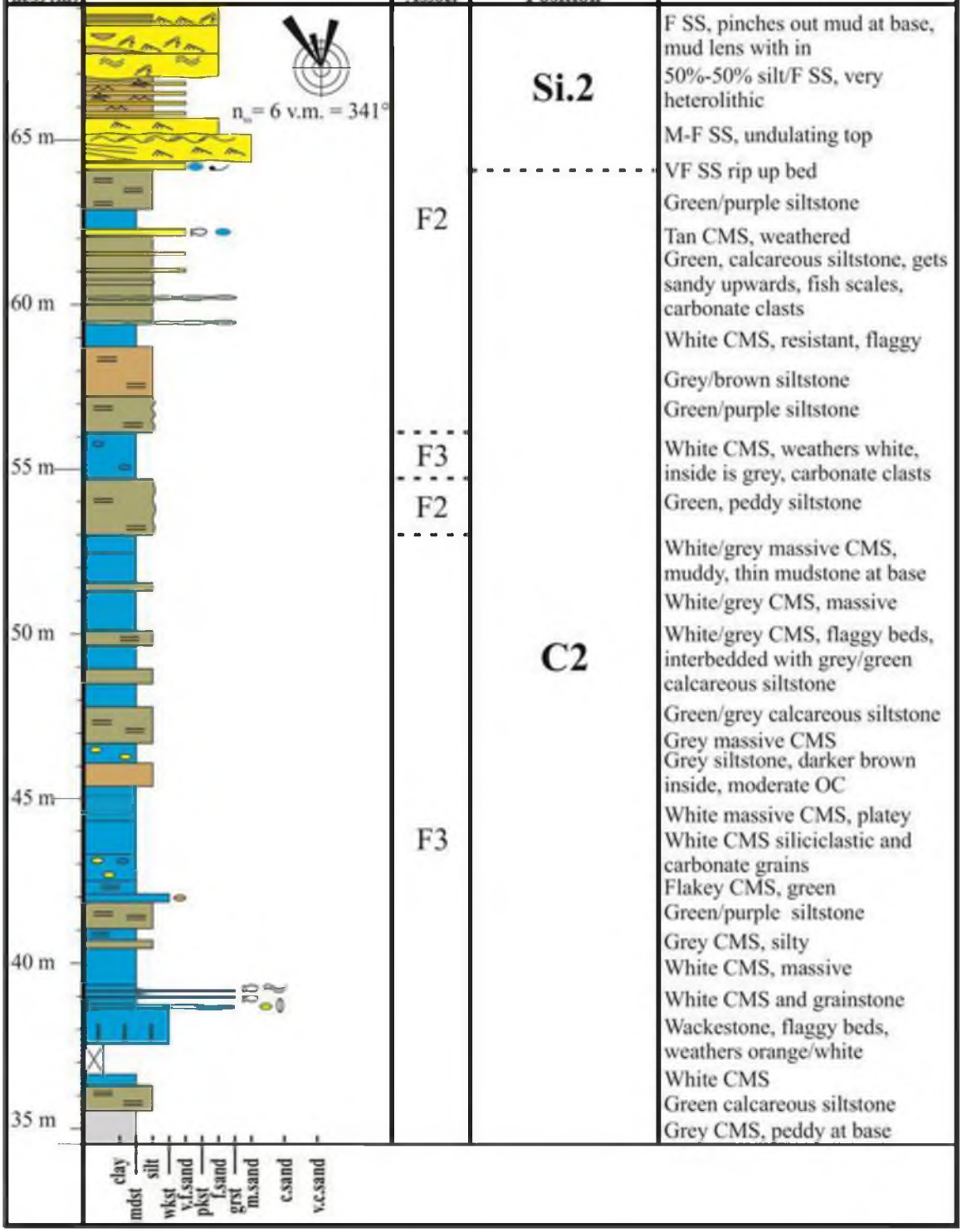

Thickness (m)	Facies Assoc.	Stratigraphic Position	Description
		Si.2	F SS, pinches out mud at base, mud lens with in
			50%-50% silt/F SS, very heterolithic
			M-F SS, undulating top
			VF SS rip up bed
	F2		Green/purple siltstone
			Tan CMS, weathered
			Green, calcareous siltstone, gets sandy upwards, fish scales, carbonate clasts
			White CMS, resistant, flaggy
			Grey/brown siltstone
			Green/purple siltstone
	F3		White CMS, weathers white, inside is grey, carbonate clasts
	F2		Green, peddy siltstone
		C2	White/grey massive CMS, muddy, thin mudstone at base
			White/grey CMS, massive
			White/grey CMS, flaggy beds, interbedded with grey/green calcareous siltstone
			Green/grey calcareous siltstone
			Grey massive CMS
			Grey siltstone, darker brown inside, moderate OC
	F3		White massive CMS, platey
			White CMS siliciclastic and carbonate grains
			Flakey CMS, green
			Green/purple siltstone
			Grey CMS, silty
			White CMS, massive
			White CMS and grainstone
			Wackestone, flaggy beds, weathers orange/white
			White CMS
			Green calcareous siltstone
			Grey CMS, peddy at base

Section Name: Willow Creek/Indian Canyon--Transitional Interval (road outcrop 1)
Location (lat/long): N39°52'10.8" W110°45'45.2' **Total Thickness Measured:** 81.35 m
Date Measured: 5/5-10/2013 **Measured By:** Leah Toms, Paul Thomas, Gavin Ferguson

Thick-ness (m)	Graphic Log	Facies Assoc.	Stratigraphic Position	Description
100 m				
95 m				
90 m				
85 m				
	21.5 m			**Finished at:** **N 39° 52' 23.1"** **W 110° 45' 45.3"**
				3 VF friable orange SS, variable thicknesses, interbedded with green siltstone
80 m				Green, calcareous siltstone, pedogenic, pyrite, white blobs
				VF SS, similar to sands below, has orange nodules
				Grey siltstone to VF SS, orange nodules and pyrite, some larger white clasts
75 m		F2	**Si.2**	Dark purple/green siltstone
				VF SS lens, more tan mud at base and grades into sand
				Purple/green calcareous siltstone; VF SS, more sand than silt, mottled, burrows and roots
				VF SS, organic matter, orange bed at base
70 m				
69 m				F SS, interbeds of siltstone

clay | silt | mdst | wkst | v.f.sand | pkst | f.sand | grst | m.sand | c.sand | v.c.sand

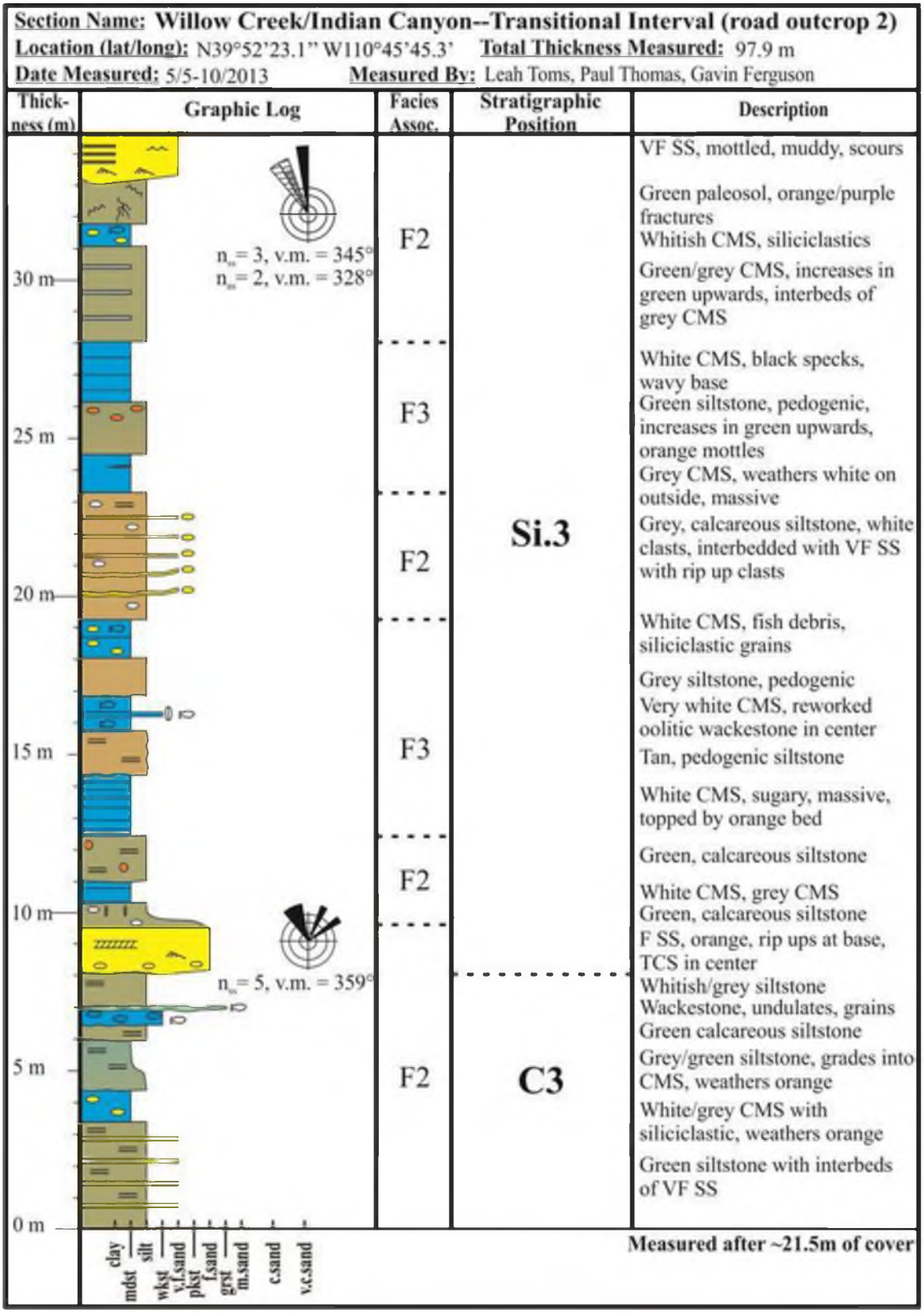
Section Name: Willow Creek/Indian Canyon--Transitional Interval (road outcrop 2)
Location (lat/long): N39°52'23.1" W110°45'45.3' Total Thickness Measured: 97.9 m
Date Measured: 5/5-10/2013 Measured By: Leah Toms, Paul Thomas, Gavin Ferguson
Thick-ness (m)
Graphic Log
Facies Assoc.
Stratigraphic Position
Description
30 m
25 m
20 m
15 m
10 m
5 m
0 m
n = 3, v.m. = 345°
n = 2, v.m. = 328°
n = 5, v.m. = 359°
F2
F3
F2
F3
F2
F2
Si.3
C3
VF SS, mottled, muddy, scours
Green paleosol, orange/purple fractures
Whitish CMS, siliciclastics
Green/grey CMS, increases in green upwards, interbeds of grey CMS
White CMS, black specks, wavy base
Green siltstone, pedogenic, increases in green upwards, orange mottles
Grey CMS, weathers white on outside, massive
Grey, calcareous siltstone, white clasts, interbedded with VF SS with rip up clasts
White CMS, fish debris, siliciclastic grains
Grey siltstone, pedogenic
Very white CMS, reworked oolitic wackestone in center
Tan, pedogenic siltstone
White CMS, sugary, massive, topped by orange bed
Green, calcareous siltstone
White CMS, grey CMS
Green, calcareous siltstone
F SS, orange, rip ups at base, TCS in center
Whitish/grey siltstone
Wackestone, undulates, grains
Green calcareous siltstone
Grey/green siltstone, grades into CMS, weathers orange
White/grey CMS with siliciclastic, weathers orange
Green siltstone with interbeds of VF SS
Measured after ~21.5m of cover
clay
mdst
silt
wkst
v.f.sand
pkst
f.sand
grst
m.sand
c.sand
v.c.sand

Section Name: Willow Creek/Indian Canyon--Transitional Interval (road outcrop 2)
Location (lat/long): N39°52'23.1" W110°45'45.3' **Total Thickness Measured:** 97.9 m
Date Measured: 5/5-10/2013 **Measured By:** Leah Toms, Paul Thomas, Gavin Ferguson

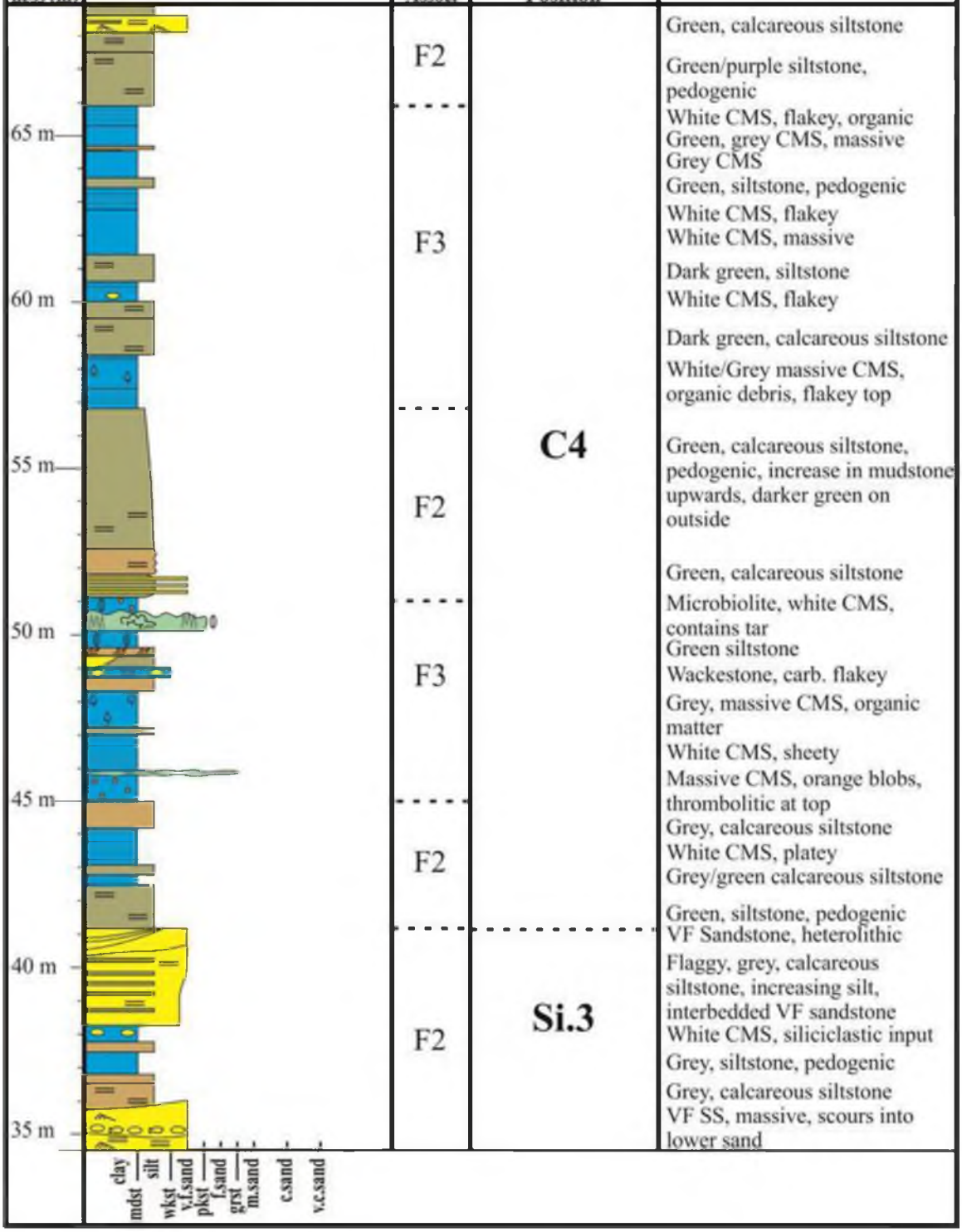

Section Name: Willow Creek/Indian Canyon--Transitional Interval (road outcrop 2)
Location (lat/long): N39°52'23.1" W110°45'45.3' **Total Thickness Measured:** 97.9 m
Date Measured: 5/5-10/2013 **Measured By:** Leah Toms, Paul Thomas, Gavin Ferguson

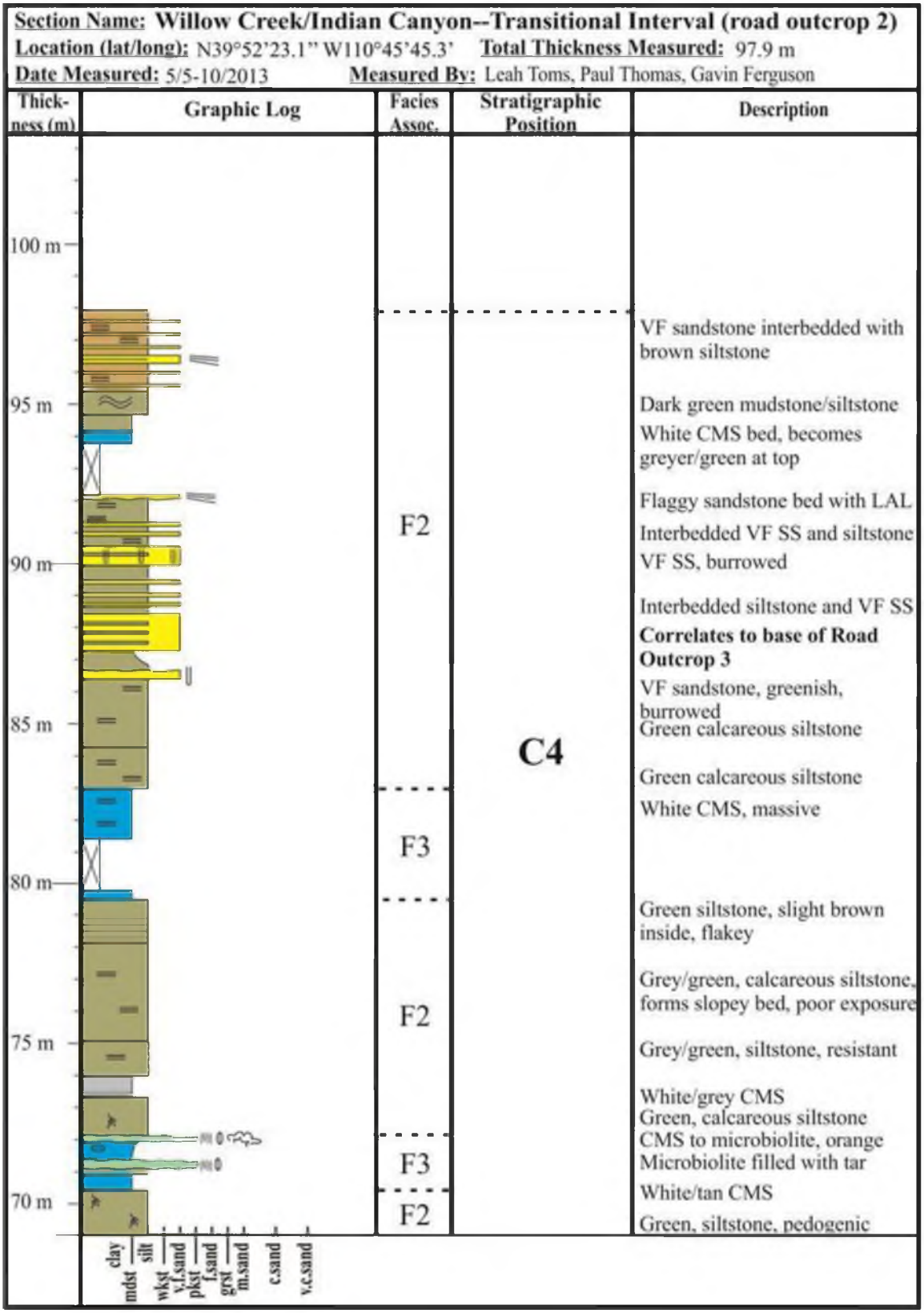

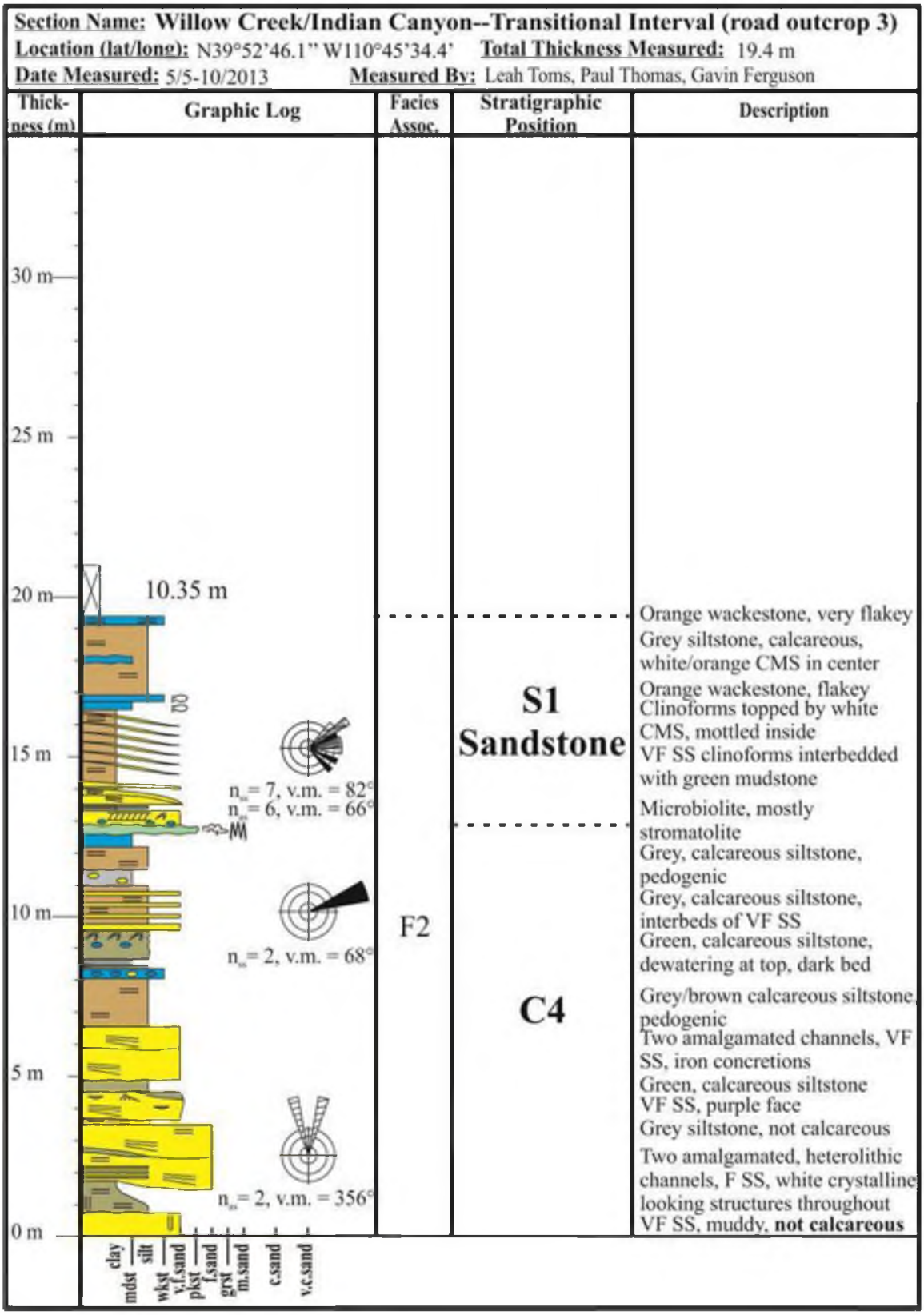
Section Name: Willow Creek/Indian Canyon--Transitional Interval (road outcrop 3)
Location (lat/long): N39°52'46.1" W110°45'34.4'
Total Thickness Measured: 19.4 m
Date Measured: 5/5-10/2013
Measured By: Leah Toms, Paul Thomas, Gavin Ferguson
Thick-ness (m)
Graphic Log
Facies Assoc.
Stratigraphic Position
Description
30 m
25 m
20 m
15 m
10 m
5 m
0 m
10.35 m
n = 7, v.m. = 82°
n = 6, v.m. = 66°
n = 2, v.m. = 68°
n = 2, v.m. = 356°
F2
S1 Sandstone
C4
Orange wackestone, very flakey
Grey siltstone, calcareous, white/orange CMS in center
Orange wackestone, flakey
Clinoforms topped by white CMS, mottled inside
VF SS clinoforms interbedded with green mudstone
Microbiolite, mostly stromatolite
Grey, calcareous siltstone, pedogenic
Grey, calcareous siltstone, interbeds of VF SS
Green, calcareous siltstone, dewatering at top, dark bed
Grey/brown calcareous siltstone, pedogenic
Two amalgamated channels, VF SS, iron concretions
Green, calcareous siltstone
VF SS, purple face
Grey siltstone, not calcareous
Two amalgamated, heterolithic channels, F SS, white crystalline looking structures throughout
VF SS, muddy, not calcareous
clay
mdst
silt
wkst
v.f.sand
pkst
f.sand
grst
m.sand
c.sand
v.c.sand

Section Name: Willow Creek/Indian Canyon--Mahogany Interval (road outcrop 4)
Location (lat/long): N39°52'43.5" W110°45'23.2" **Total Thickness Measured:** 28.3 m
Date Measured: 5/5-10/2013 **Measured By:** Leah Toms, Paul Thomas, Gavin Ferguson

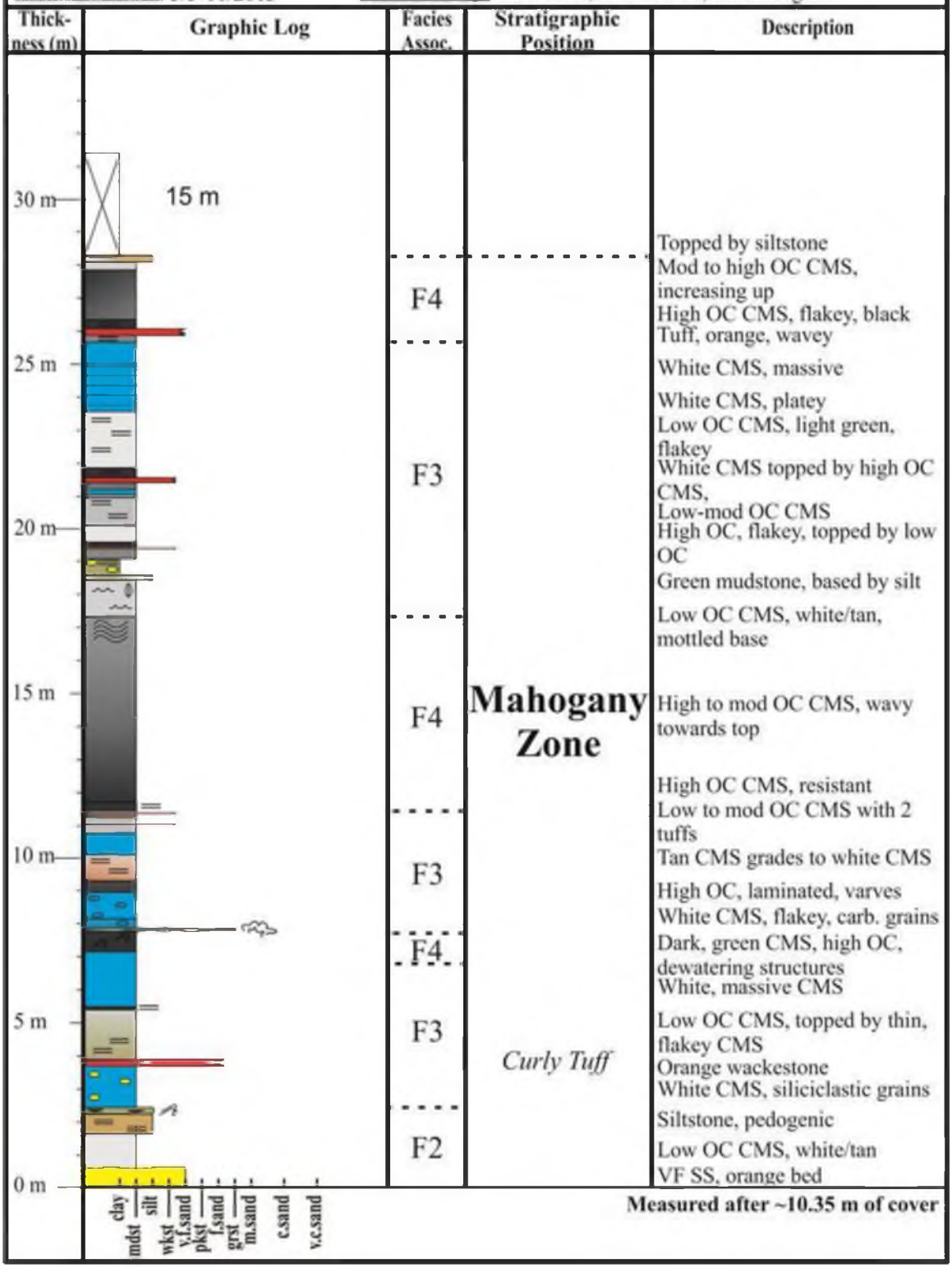

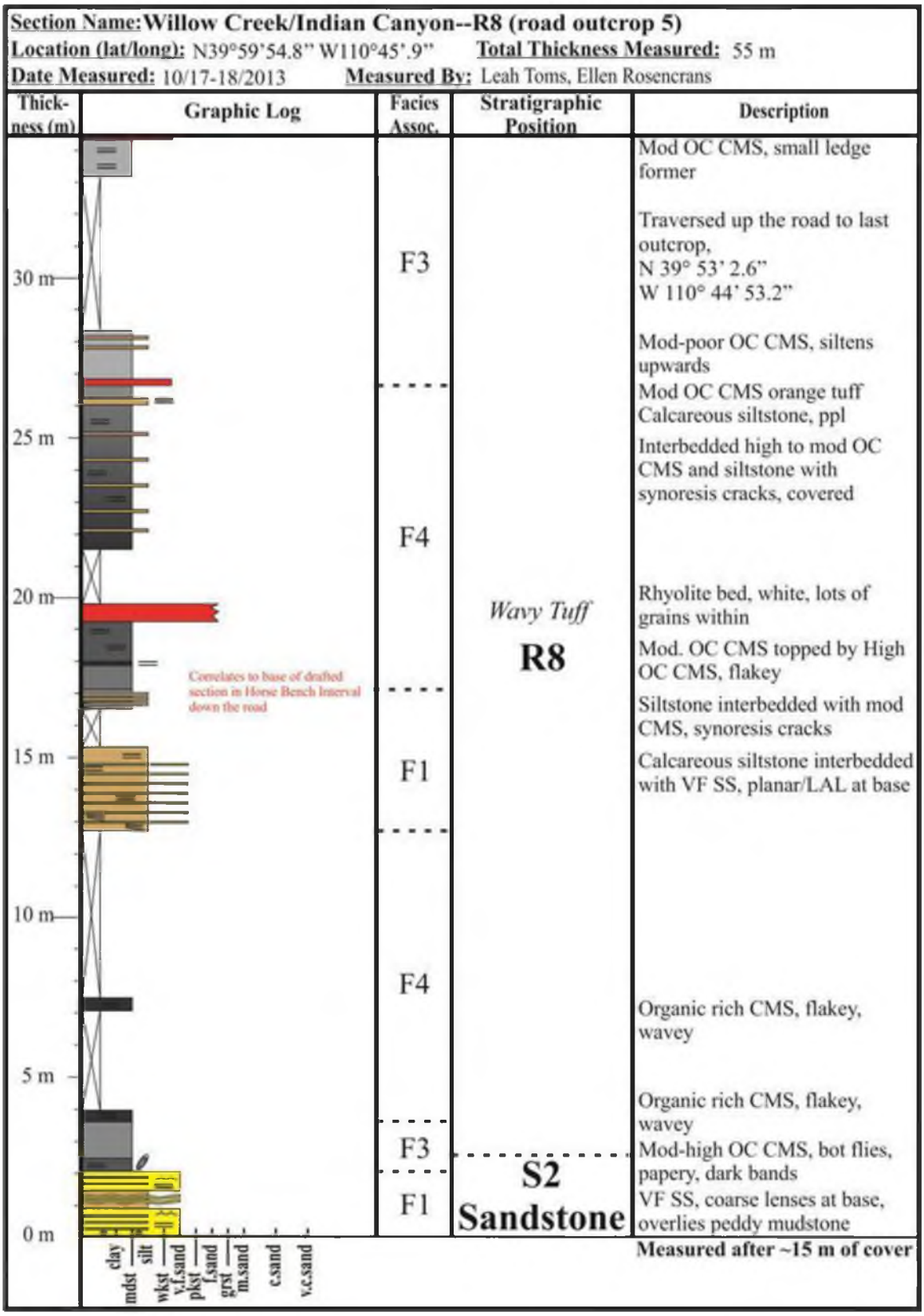
Section Name: Willow Creek/Indian Canyon--R8 (road outcrop 5)
Location (lat/long): N39°59'54.8" W110°45'.9"
Total Thickness Measured: 55 m
Date Measured: 10/17-18/2013
Measured By: Leah Toms, Ellen Rosencrans
Thick-ness (m)
Graphic Log
Facies Assoc.
Stratigraphic Position
Description
30 m
25 m
20 m
15 m
10 m
5 m
0 m
F3
F4
F1
F4
F3
F1
Wavy Tuff
R8
S2
Sandstone
Correlates to base of drafted section in Horse Bench Interval down the road
Mod OC CMS, small ledge former
Traversed up the road to last outcrop,
N 39° 53' 2.6"
W 110° 44' 53.2"
Mod-poor OC CMS, siltens upwards
Mod OC CMS orange tuff
Calcareous siltstone, ppl
Interbedded high to mod OC CMS and siltstone with synoresis cracks, covered
Rhyolite bed, white, lots of grains within
Mod. OC CMS topped by High OC CMS, flakey
Siltstone interbedded with mod CMS, synoresis cracks
Calcareous siltstone interbedded with VF SS, planar/LAL at base
Organic rich CMS, flakey, wavey
Organic rich CMS, flakey, wavey
Mod-high OC CMS, bot flies, papery, dark bands
VF SS, coarse lenses at base, overlies peddy mudstone
Measured after ~15 m of cover
clay
silt
mdst
wkst
v.f.sand
pkst
f.sand
grst
m.sand
c.sand
v.c.sand

Section Name: Willow Creek/Indian Canyon--R8 (road outcrop 5)
Location (lat/long): N39°59'54.8" W110°45'.9" **Total Thickness Measured:** 55 m
Date Measured: 10/17-18/2013 **Measured By:** Leah Toms, Ellen Rosencrans

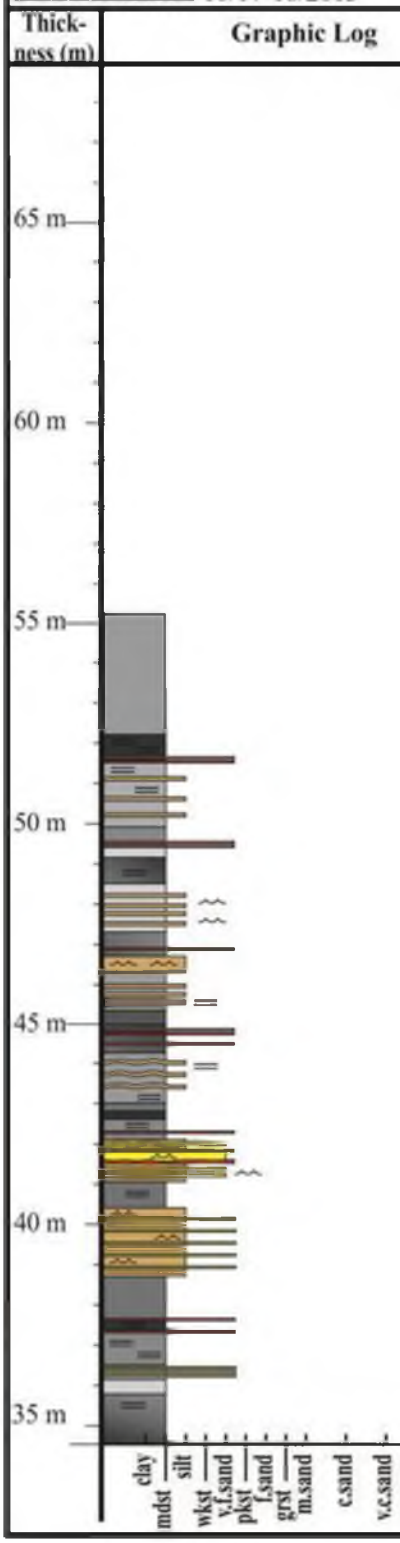

Thickness (m)	Graphic Log	Facies Assoc.	Stratigraphic Position	Description
				N 39° 53' 9.5" W 110° 44' 51.7" at summit of 191
				Mod OC CMS, forms ledge
				Black flakey CMS
				Low-mod OC CMS interbedded siltstone
				Mod-high OC CMS
		F3		High OC CMS, black
				CMS and siltstone, whitish
				Mod OC CMS
				Calcareous siltstone
				Interbedded CMS and siltstone
			R8	High OC CMS, peddy
				High OC CMS, becomes flakey
				Mod OC CMS
				High OC CMS, flakey
				Mod. OC CMS
				Interbedded SS and siltstone
		F1		Mod rich CMS
				VF SS, interbedded with siltstone, contains pyrite
				Mod OC CMS
		F3		High OC CMS, flakey, wavey
				Low OC CMS, interbeds of VF SS
				Mod OC CMS

Section Name: Willow Creek/Indian Canyon--R8 Interval (outcrop 6)
Location (lat/long): N39°54'43.6" W110°42'16.1" **Total Thickness Measured:** 109.4 m
Date Measured: 5/5-10/2013 **Measured By:** Leah Toms, Paul Thomas

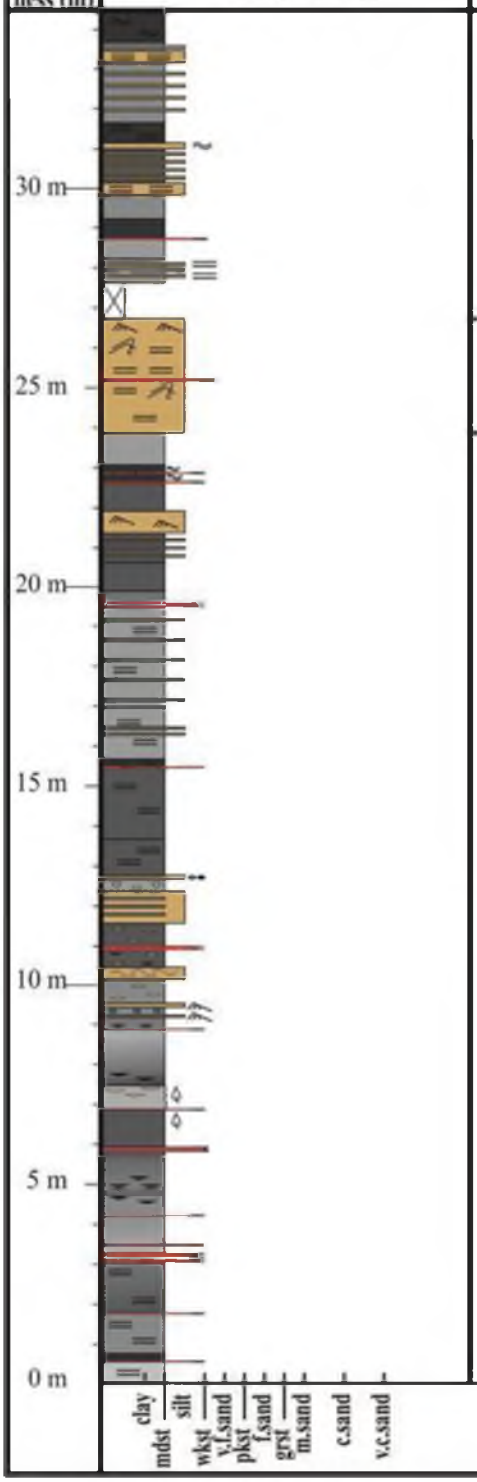

Thickness (m)	Facies Assoc.	Stratigraphic Position	Description
	F4	R8	High OC CMS, black, flakey, wavy
			Low-mod OC CMS mixed with grey siltstone
			High OC CMS, black, flakey
			High OC CMS
			Mod-high OC CMS, brown, slopey
			Low-mod OC CMS
			Grey calcareous siltstone mixed with CMS
	F1		Grey calcareous siltstone, resistant, peddy, iron concretions
			Grey calcareous siltstone
			Low to Mod OC CMS, reddish
			High OC CMS, black, flakey
			Grey calcareous siltstone
			Mod OC CMS
			Mod-high OC CMS, black
			Mod OC CMS, red
			More siltstone, weathers white on outside
			Mod OC CMS, red, silty
			High OC CMS, black and flakey wavey
			Mod OC CMS, red
			Mod OC CMS, red, based by silt
	F4		Calcareous siltstone, synoresis cracks
			High OC CMS
			High OC CMS
			Red/brown CMS, mixed with siltstone
			Mod-low OC CMS, less OC upwards
			Mod-Low OC CMS, red, black lenses
			Mod OC CMS, black lenses and organic matter
			Low OC to mod OC CMS upwards
			Tuff with orange band
			Mod OC, less OC upwards
			Mod OC CMS, grey
			High OC CMS, black, flakey
			Low OC CMS

Outcrop immediately past mile marker 270 on Willow Creek/Indian Canyon Road; Parking N39°54'36.8" W110°42' 09.5"

Section Name: Willow Creek/Indian Canyon--R8 Interval (outcrop 6)
Location (lat/long): N39°54'43.6" W110°42'16.1" **Total Thickness Measured:** 109.4 m
Date Measured: 5/5-10/2013 **Measured By:** Leah Toms, Paul Thomas

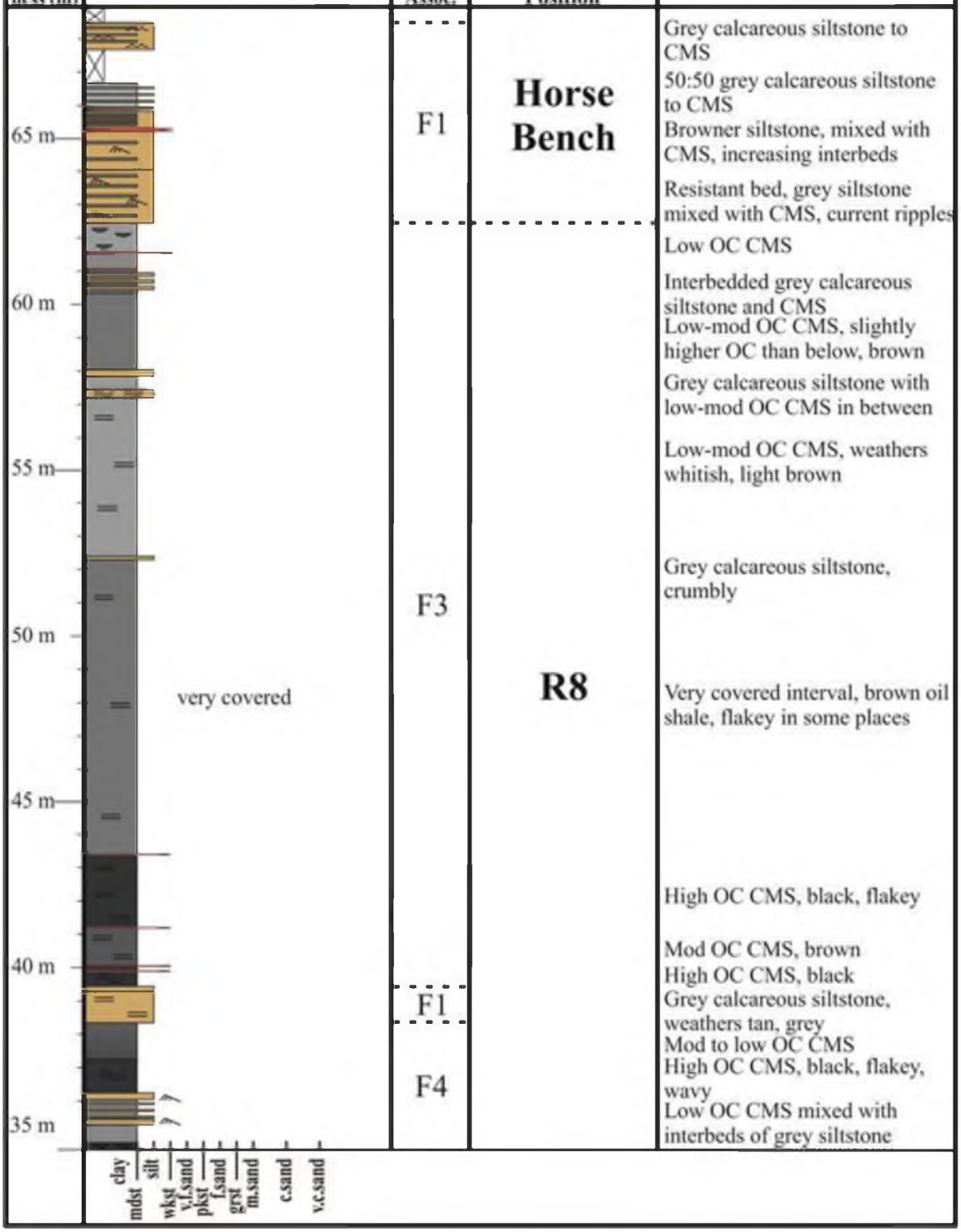

Section Name: Willow Creek/Indian Canyon--R8 Interval (outcrop 6)
Location (lat/long): N39°54'43.6" W110°42'16.1" **Total Thickness Measured:** 109.4 m
Date Measured: 5/5-10/2013 **Measured By:** Leah Toms, Paul Thomas

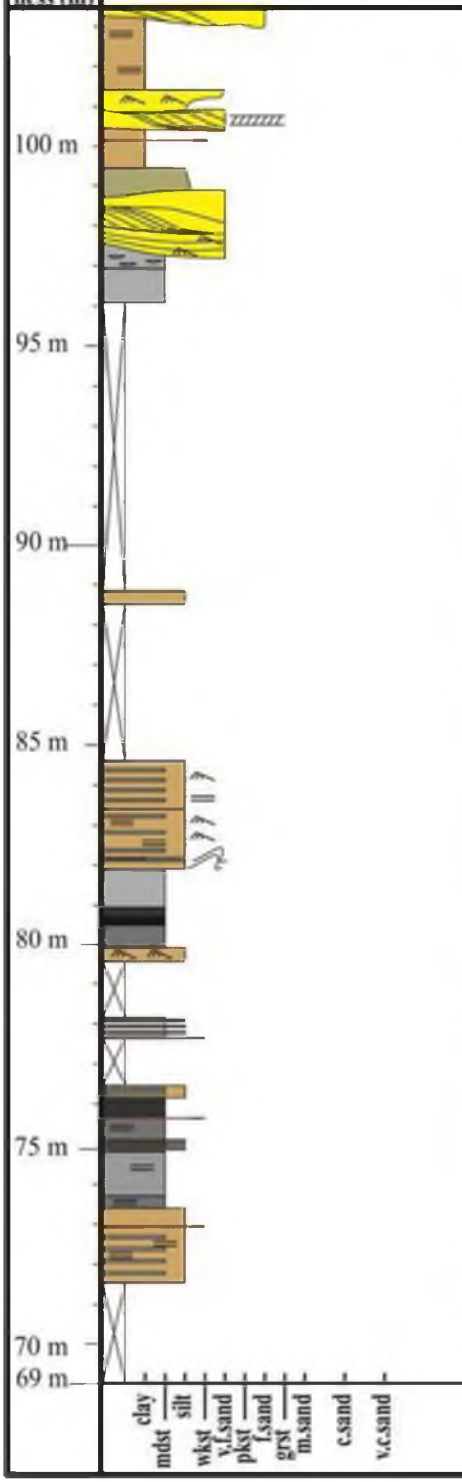

Section Name: Willow Creek/Indian Canyon--R8 Interval (outcrop 6)
Location (lat/long): N39°54'43.6" W110°42'16.1" **Total Thickness Measured:** 109.4 m
Date Measured: 5/5-10/2013 **Measured By:** Leah Toms, Paul Thomas

Thick-ness (m)	Graphic Log	Facies Assoc.	Stratigraphic Position	Description
135 m				
130 m				
125 m				
120 m				
115 m				
110 m				**Top of Indian Canyon: N 39° 54' 48.6" W 110° 42' 15.6"**
				Coarse lithic SS, fractures filled with tar, capped by siltstone and then flakey/muddy siltstone
	n_u = 12, v.m. = 46° n_u = 8, v.m. = 64°	F3	**Horse Bench**	F SS, clinoform set, mud filled clinoforms
105 m				Another channel cutting down through lower mud
				Sandstone with accretion sets

clay | silt | mdst | wkst | v.f.sand | pkst | f.sand | grst | m.sand | c.sand | v.c.sand

Section Name: Henderson 3 Core
Location (lat/long): N39°56'18.7" W110°13'45.3" **Total Thickness Measured:** 362 ft
Date Measured: 11/7-14/2012 **Measured By:** Leah Toms

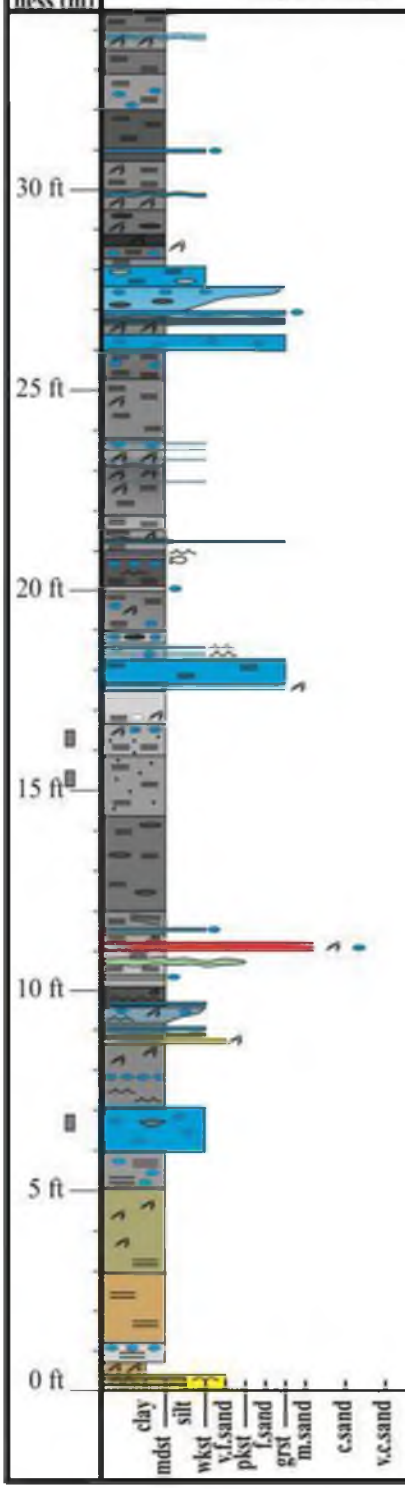

Thickness (m)	Facies Assoc.	Stratigraphic Position	Description
	F4	C4	Varying OC carbonate mudstone, random interbeds of wackestone/reworked carbonate, SSD, laminated
			CMS, coarsens into grainstone, topped by wackestone
	F3		Interbedded CMS and grainstone
			Mod OC CMS, decreasing OC
			Dark brown CMS, mod/high OC
	F4		Interbedded wackestone and CMS
			Mod OC CMS
			Mod OC CMS, increasing OC
			Mod OC CMS, increasing OC
			Low OC CMS, carbonate rip-ups
			Interbedded CMS/grainstone
			Low OC CMS
			Low OC CMS, marcasite
			Low OC CMS, marcasite throughout
			Mod OC CMS, higher OC lenses
			Green tuff with white CMS within, SSD
	F3		Mod OC CMS
			Interbedded CMS/wackestone
			Mod OC, carbonate clasts, rip ups at base, topped by VF SS
			Intraclastic wackestone
			Mod OC CMS, some brecciation
			Low OC CMS, green
			Mod OC CMS, brown
			Low OC CMS
			Ripple cross laminated VF SS

Section Name: Henderson 3 Core
Location (lat/long): N39°56'18.7" W110°13'45.3" **Total Thickness Measured:** 362 ft
Date Measured: 11/7-14/2012 **Measured By:** Leah Toms

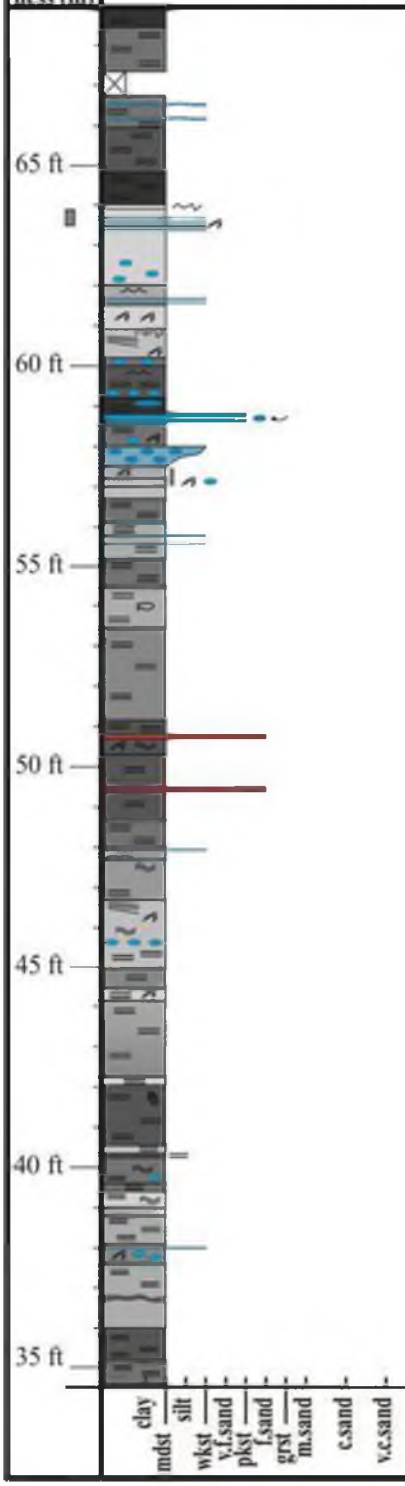

Thickness (m)	Facies Assoc.	Stratigraphic Position	Description
	F4	C4	Black CMS, high OC
			Brown CMS, mod/high OC, thin laminations, pyrite crystals
			Brown CMS, high OC, SSD
			High OC, brown
			Black CMS, high OC
	F3		Tan/orange OC CMS, wackestone in center
			Low OC CMS w/ wackestone
			Whiter CMS, fish debris
			White CMS, low OC
			Mod OC, dark laminations
			Packstone with CMS rip-ups, wackestone lense
			Grey CMS to wackestone
			Tan CMS, low OC, high OC CMS, wackestone laminations
			Brown CMS, mod/high OC
			Grey CMS, mod OC, fish debris, PPL
			Tan/brown thinly laminated CMS, mod OC
	F4		High OC CMS, very reworked at base through SSD
			High OC CMS, dark
			High OC CMS, dark and tan laminations, PPL
			Higher OC than below, mod OC, rip-ups
	F3		Tan CMS, low OC, black CMS interbeds
			Tan CMS to high OC CMS
			Mod/high OC CMS, thin laminations, decreasing OC
	F4		High OC CMS, thin laminations, bot flies, SSD
			Mod/high OC CMS, brown, thin laminations
			Tan laminations, mod OC CMS
	F3		Tan, mod OC CMS
			Mod OC CMS, carbonate clasts
			Mod OC CMS, rich area in middle, some layers have pyrite
	F4		High OC CMS, thin laminations, LAL at base

Section Name: Henderson 3 Core
Location (lat/long): N39°56'18.7" W110°13'45.3" **Total Thickness Measured:** 362 ft
Date Measured: 11/7-14/2012 **Measured By:** Leah Toms

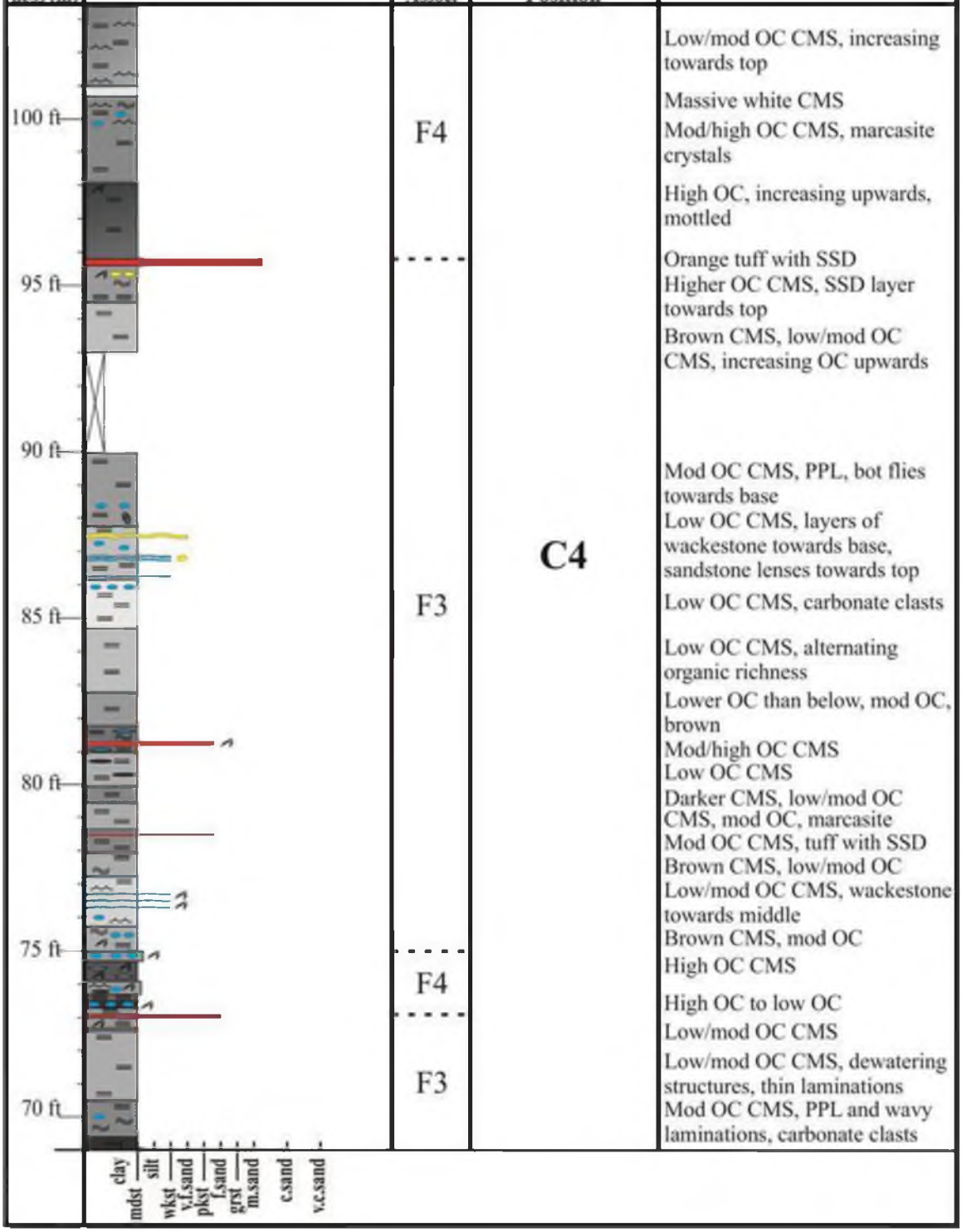

Thickness (m)	Facies Assoc.	Stratigraphic Position	Description
			Low/mod OC CMS, increasing towards top
			Massive white CMS
	F4		Mod/high OC CMS, marcasite crystals
			High OC, increasing upwards, mottled
			Orange tuff with SSD
			Higher OC CMS, SSD layer towards top
			Brown CMS, low/mod OC CMS, increasing OC upwards
			Mod OC CMS, PPL, bot flies towards base
		C4	Low OC CMS, layers of wackestone towards base, sandstone lenses towards top
	F3		Low OC CMS, carbonate clasts
			Low OC CMS, alternating organic richness
			Lower OC than below, mod OC, brown
			Mod/high OC CMS
			Low OC CMS
			Darker CMS, low/mod OC CMS, mod OC, marcasite
			Mod OC CMS, tuff with SSD
			Brown CMS, low/mod OC
			Low/mod OC CMS, wackestone towards middle
			Brown CMS, mod OC
	F4		High OC CMS
			High OC to low OC
			Low/mod OC CMS
	F3		Low/mod OC CMS, dewatering structures, thin laminations
			Mod OC CMS, PPL and wavy laminations, carbonate clasts

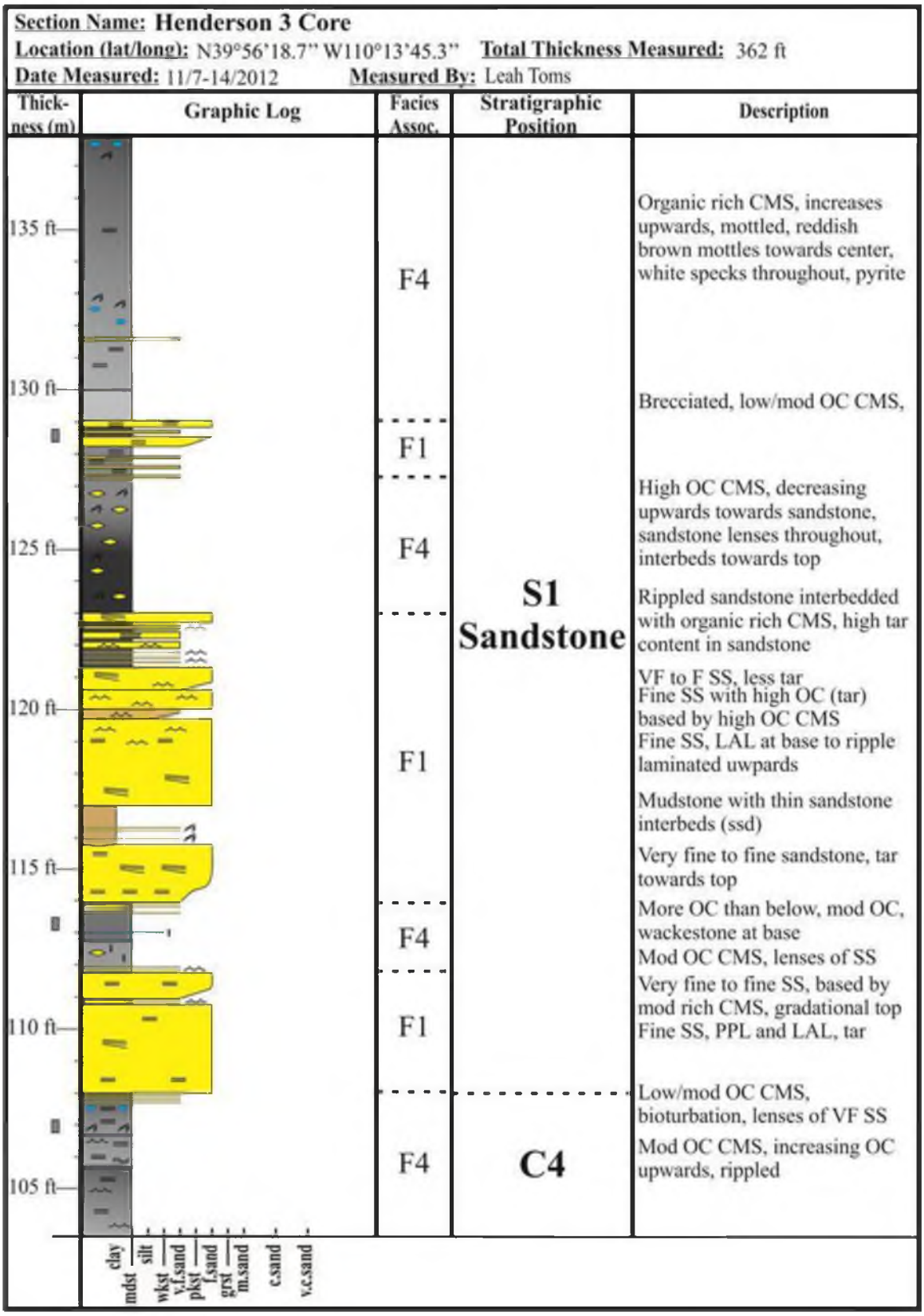
Section Name: Henderson 3 Core
Location (lat/long): N39°56'18.7" W110°13'45.3"
Total Thickness Measured: 362 ft
Date Measured: 11/7-14/2012
Measured By: Leah Toms
Thick-ness (m)
Graphic Log
Facies Assoc.
Stratigraphic Position
Description
135 ft
130 ft
125 ft
120 ft
115 ft
110 ft
105 ft
F4
F1
F4
F1
F4
F1
F4
S1 Sandstone
C4
Organic rich CMS, increases upwards, mottled, reddish brown mottles towards center, white specks throughout, pyrite
Brecciated, low/mod OC CMS,
High OC CMS, decreasing upwards towards sandstone, sandstone lenses throughout, interbeds towards top
Rippled sandstone interbedded with organic rich CMS, high tar content in sandstone
VF to F SS, less tar
Fine SS with high OC (tar) based by high OC CMS
Fine SS, LAL at base to ripple laminated uwpards
Mudstone with thin sandstone interbeds (ssd)
Very fine to fine sandstone, tar towards top
More OC than below, mod OC, wackestone at base
Mod OC CMS, lenses of SS
Very fine to fine SS, based by mod rich CMS, gradational top
Fine SS, PPL and LAL, tar
Low/mod OC CMS, bioturbation, lenses of VF SS
Mod OC CMS, increasing OC upwards, rippled
clay
mdst
silt
wkst
v.f.sand
pkst
f.sand
grst
m.sand
c.sand
v.c.sand

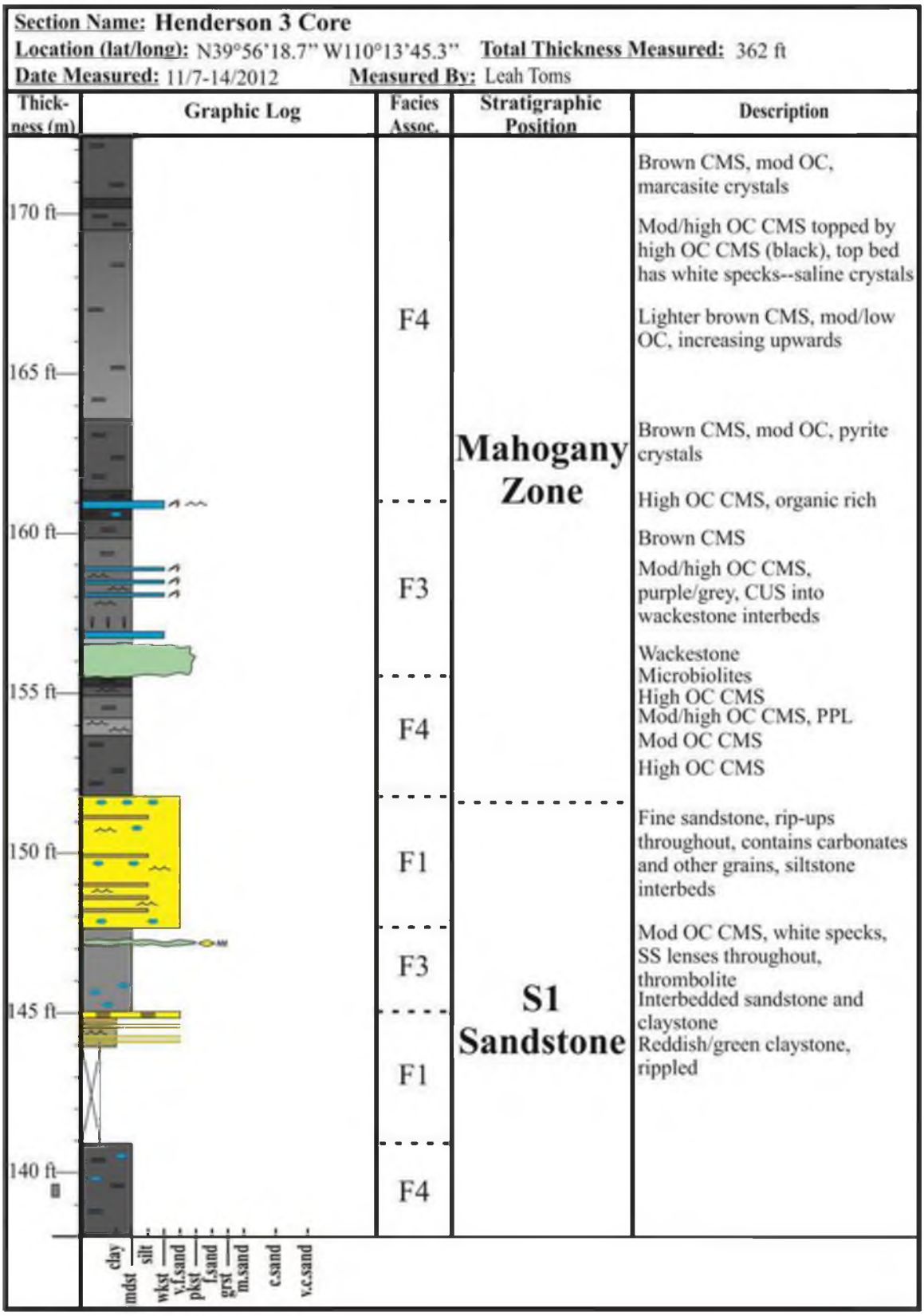
Section Name: Henderson 3 Core
Location (lat/long): N39°56'18.7" W110°13'45.3"
Total Thickness Measured: 362 ft
Date Measured: 11/7-14/2012
Measured By: Leah Toms
Thick-ness (m)
Graphic Log
Facies Assoc.
Stratigraphic Position
Description
170 ft
165 ft
160 ft
155 ft
150 ft
145 ft
140 ft
F4
F3
F4
F1
F3
F1
F4
Mahogany Zone
S1 Sandstone
Brown CMS, mod OC, marcasite crystals
Mod/high OC CMS topped by high OC CMS (black), top bed has white specks--saline crystals
Lighter brown CMS, mod/low OC, increasing upwards
Brown CMS, mod OC, pyrite crystals
High OC CMS, organic rich
Brown CMS
Mod/high OC CMS, purple/grey, CUS into wackestone interbeds
Wackestone
Microbiolites
High OC CMS
Mod/high OC CMS, PPL
Mod OC CMS
High OC CMS
Fine sandstone, rip-ups throughout, contains carbonates and other grains, siltstone interbeds
Mod OC CMS, white specks, SS lenses throughout, thrombolite
Interbedded sandstone and claystone
Reddish/green claystone, rippled
clay
silt
mdst
wkst
v.f.sand
pkst
f.sand
grst
m.sand
c.sand
v.c.sand

Section Name: Henderson 3 Core
Location (lat/long): N39°56'18.7" W110°13'45.3" **Total Thickness Measured:** 362 ft
Date Measured: 11/7-14/2012 **Measured By:** Leah Toms

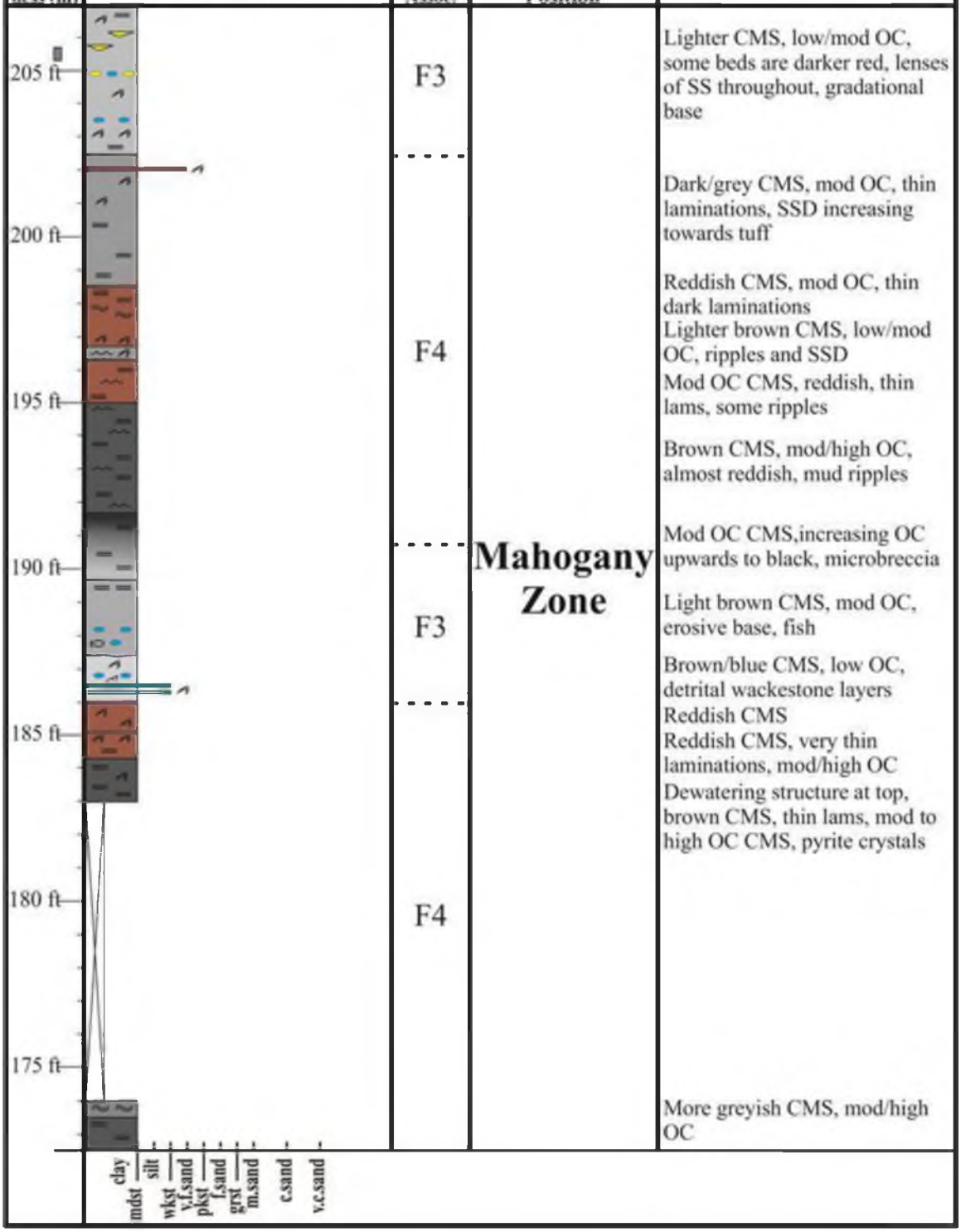

Section Name: Henderson 3 Core
Location (lat/long): N39°56'18.7" W110°13'45.3" **Total Thickness Measured:** 362 ft
Date Measured: 11/7-14/2012 **Measured By:** Leah Toms

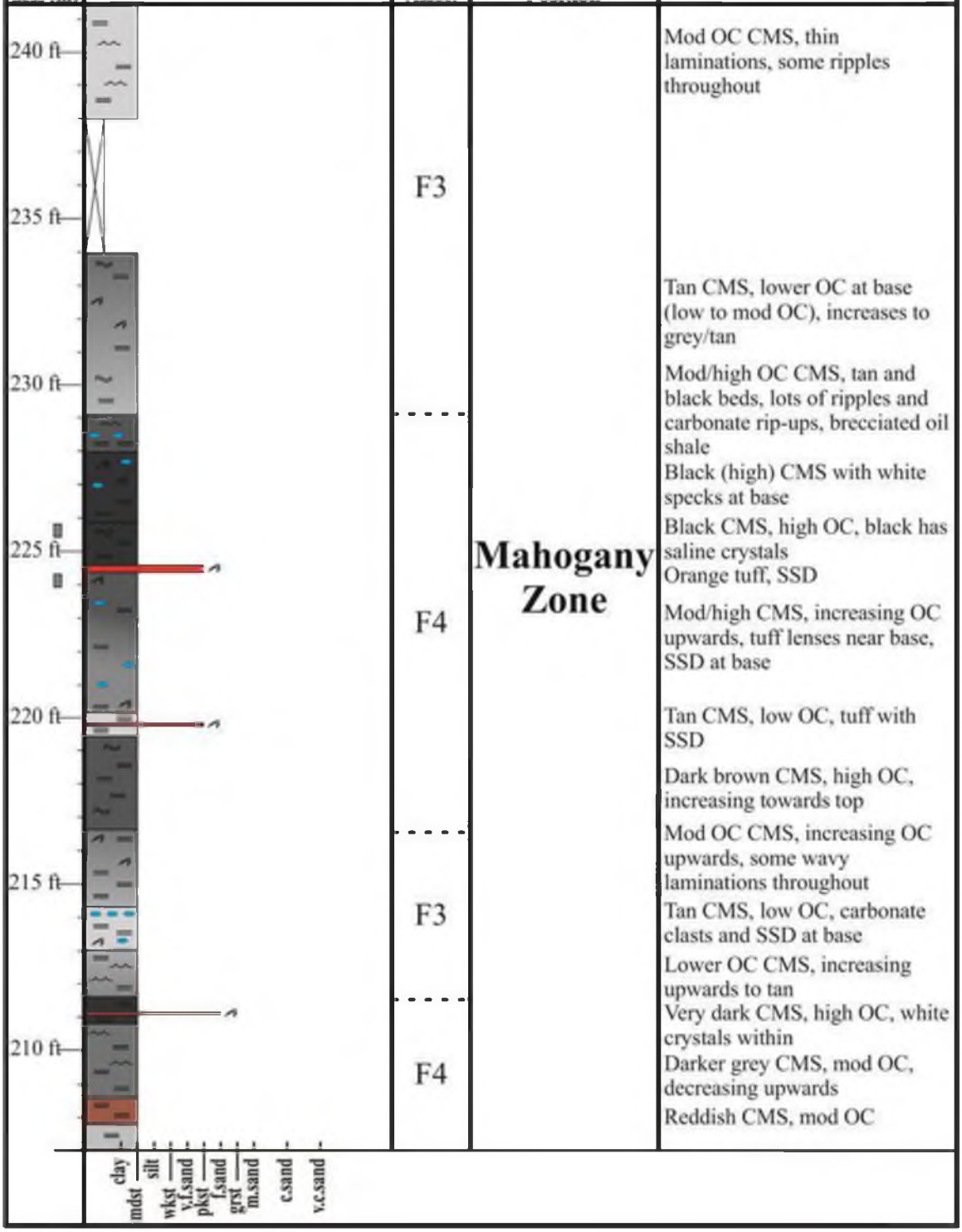

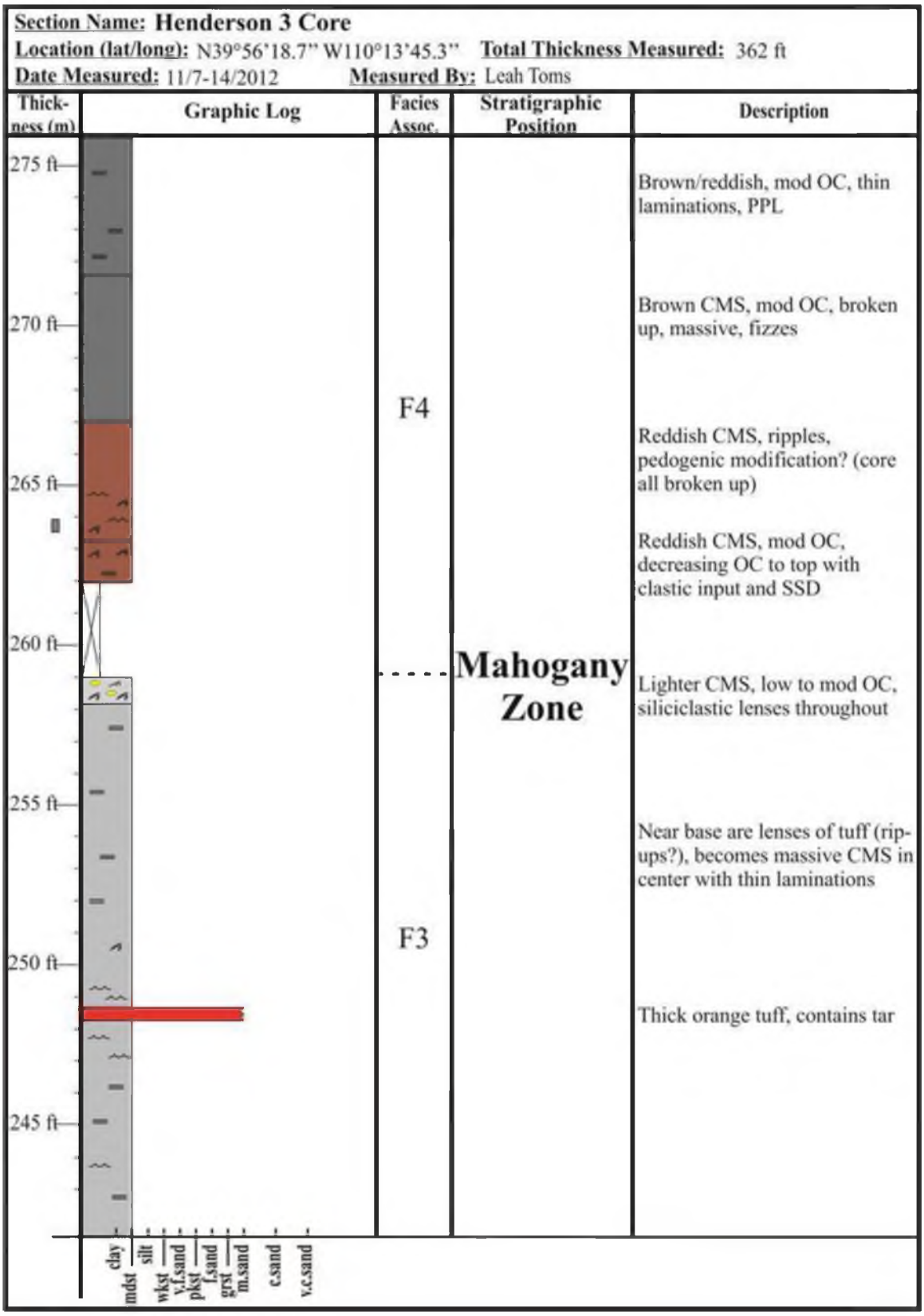
Section Name: Henderson 3 Core
Location (lat/long): N39°56'18.7" W110°13'45.3"
Total Thickness Measured: 362 ft
Date Measured: 11/7-14/2012
Measured By: Leah Toms
Thick-ness (m)
Graphic Log
Facies Assoc.
Stratigraphic Position
Description
275 ft
270 ft
265 ft
260 ft
255 ft
250 ft
245 ft
F4
F3
Mahogany Zone
Brown/reddish, mod OC, thin laminations, PPL
Brown CMS, mod OC, broken up, massive, fizzes
Reddish CMS, ripples, pedogenic modification? (core all broken up)
Reddish CMS, mod OC, decreasing OC to top with clastic input and SSD
Lighter CMS, low to mod OC, siliciclastic lenses throughout
Near base are lenses of tuff (rip-ups?), becomes massive CMS in center with thin laminations
Thick orange tuff, contains tar
clay
silt
mdst
wkst
v.f.sand
pkst
f.sand
grst
m.sand
c.sand
v.c.sand

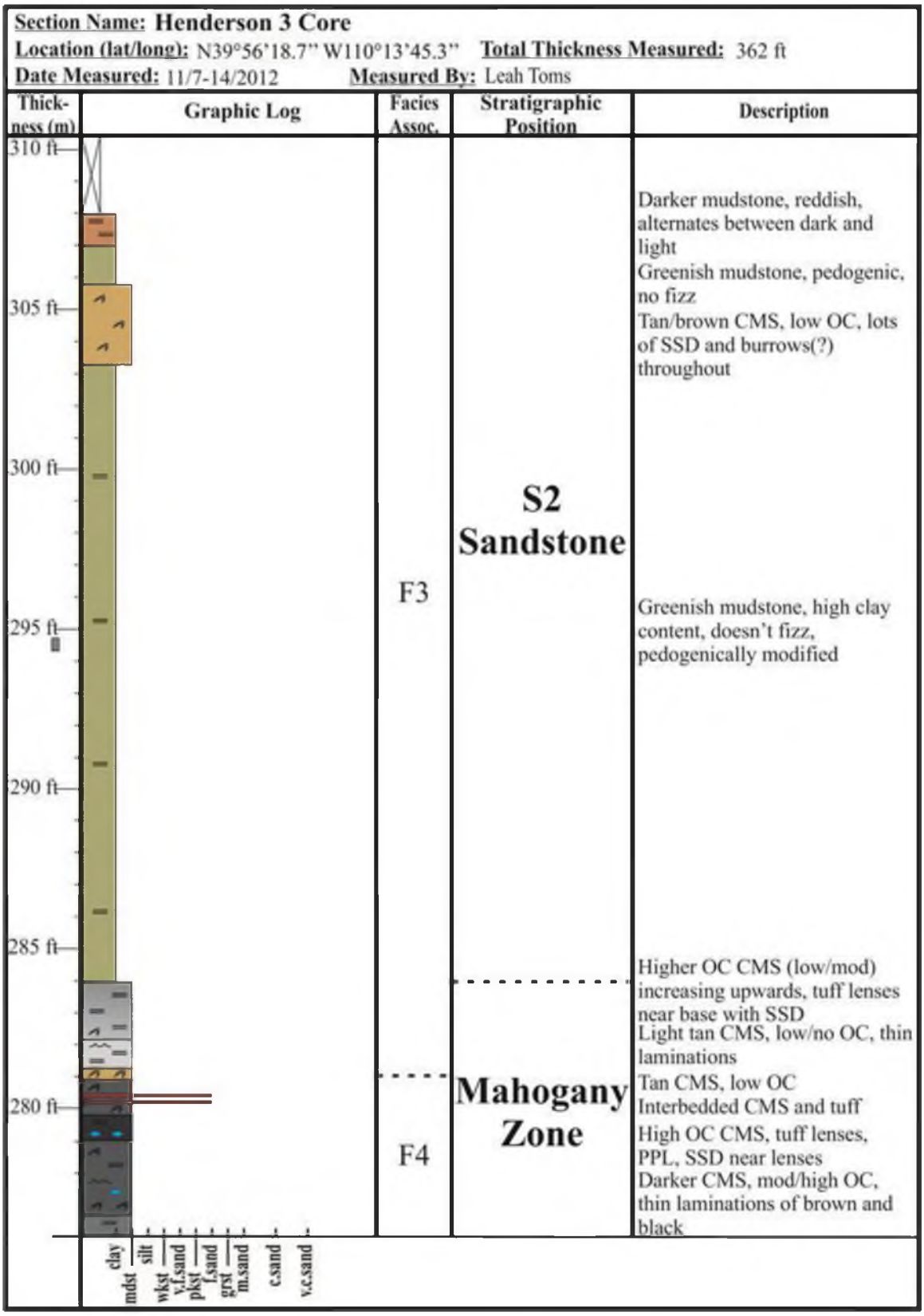
Section Name: Henderson 3 Core
Location (lat/long): N39°56'18.7" W110°13'45.3"
Total Thickness Measured: 362 ft
Date Measured: 11/7-14/2012
Measured By: Leah Toms
Thick-ness (m)
Graphic Log
Facies Assoc.
Stratigraphic Position
Description
310 ft
305 ft
300 ft
295 ft
290 ft
285 ft
280 ft
Darker mudstone, reddish, alternates between dark and light
Greenish mudstone, pedogenic, no fizz
Tan/brown CMS, low OC, lots of SSD and burrows(?) throughout
S2 Sandstone
F3
Greenish mudstone, high clay content, doesn't fizz, pedogenically modified
Higher OC CMS (low/mod) increasing upwards, tuff lenses near base with SSD
Light tan CMS, low/no OC, thin laminations
Tan CMS, low OC
Interbedded CMS and tuff
Mahogany Zone
F4
High OC CMS, tuff lenses, PPL, SSD near lenses
Darker CMS, mod/high OC, thin laminations of brown and black
clay
mdst
silt
wkst
v.f.sand
pkst
f.sand
grst
m.sand
c.sand
v.c.sand

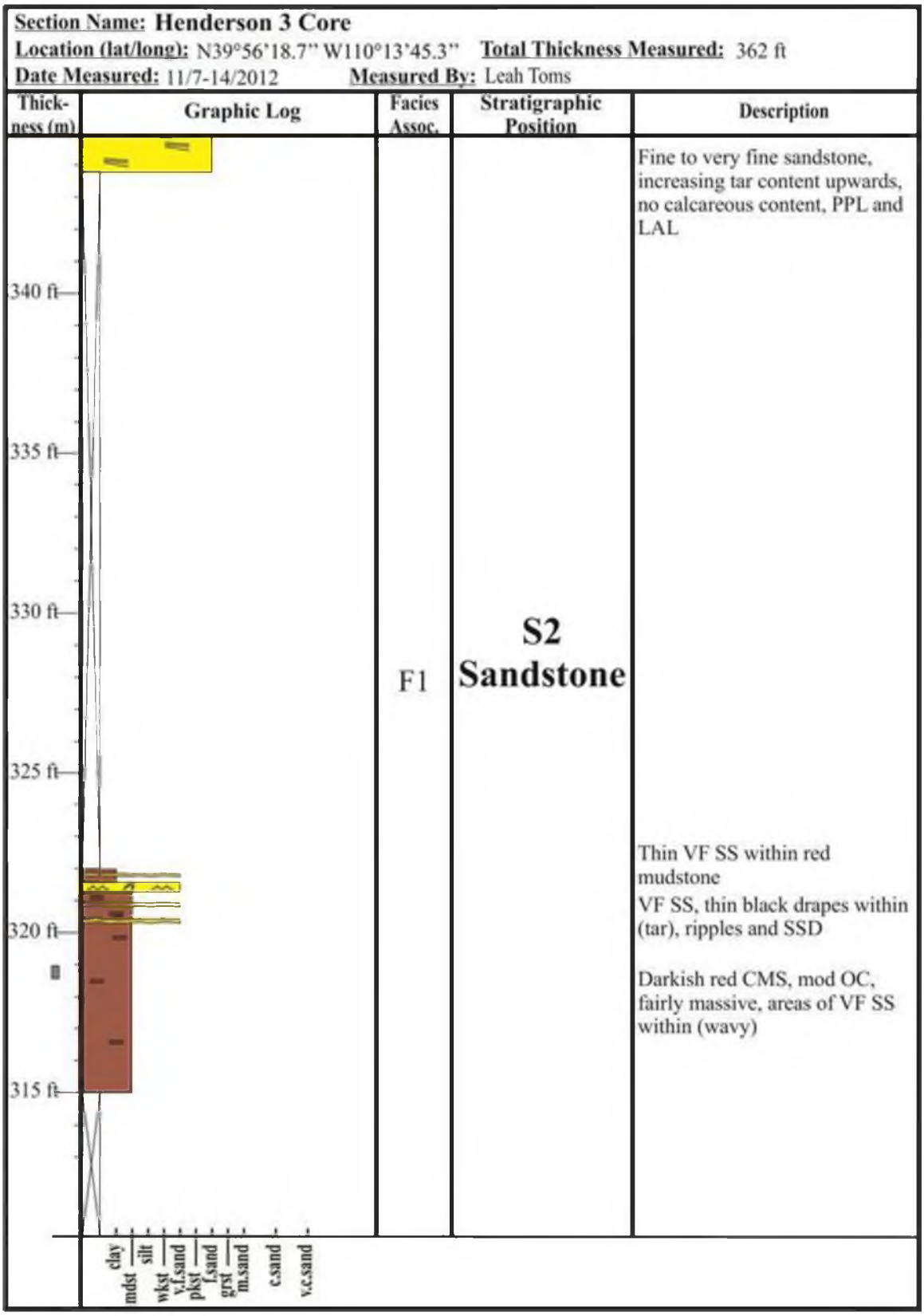
Section Name: Henderson 3 Core
Location (lat/long): N39°56'18.7" W110°13'45.3"
Total Thickness Measured: 362 ft
Date Measured: 11/7-14/2012
Measured By: Leah Toms
Thick-ness (m)
Graphic Log
Facies Assoc.
Stratigraphic Position
Description
340 ft
335 ft
330 ft
325 ft
320 ft
315 ft
F1
S2 Sandstone
Fine to very fine sandstone, increasing tar content upwards, no calcareous content, PPL and LAL
Thin VF SS within red mudstone
VF SS, thin black drapes within (tar), ripples and SSD
Darkish red CMS, mod OC, fairly massive, areas of VF SS within (wavy)
clay
mdst
silt
wkst
v.f.sand
pkst
f.sand
grst
m.sand
c.sand
v.c.sand

Section Name: Henderson 3 Core
Location (lat/long): N39°56'18.7" W110°13'45.3" **Total Thickness Measured:** 362 ft
Date Measured: 11/7-14/2012 **Measured By:** Leah Toms

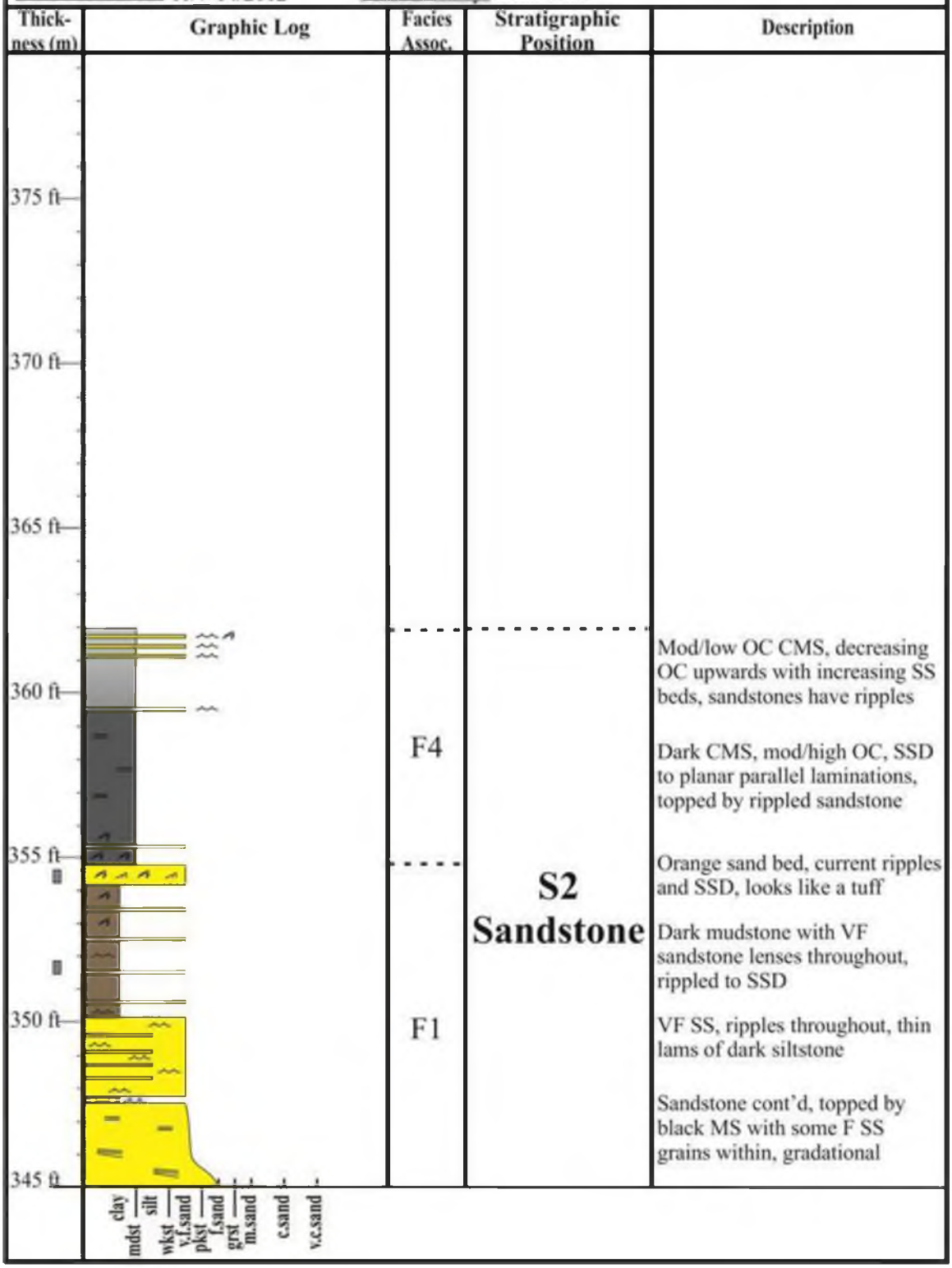

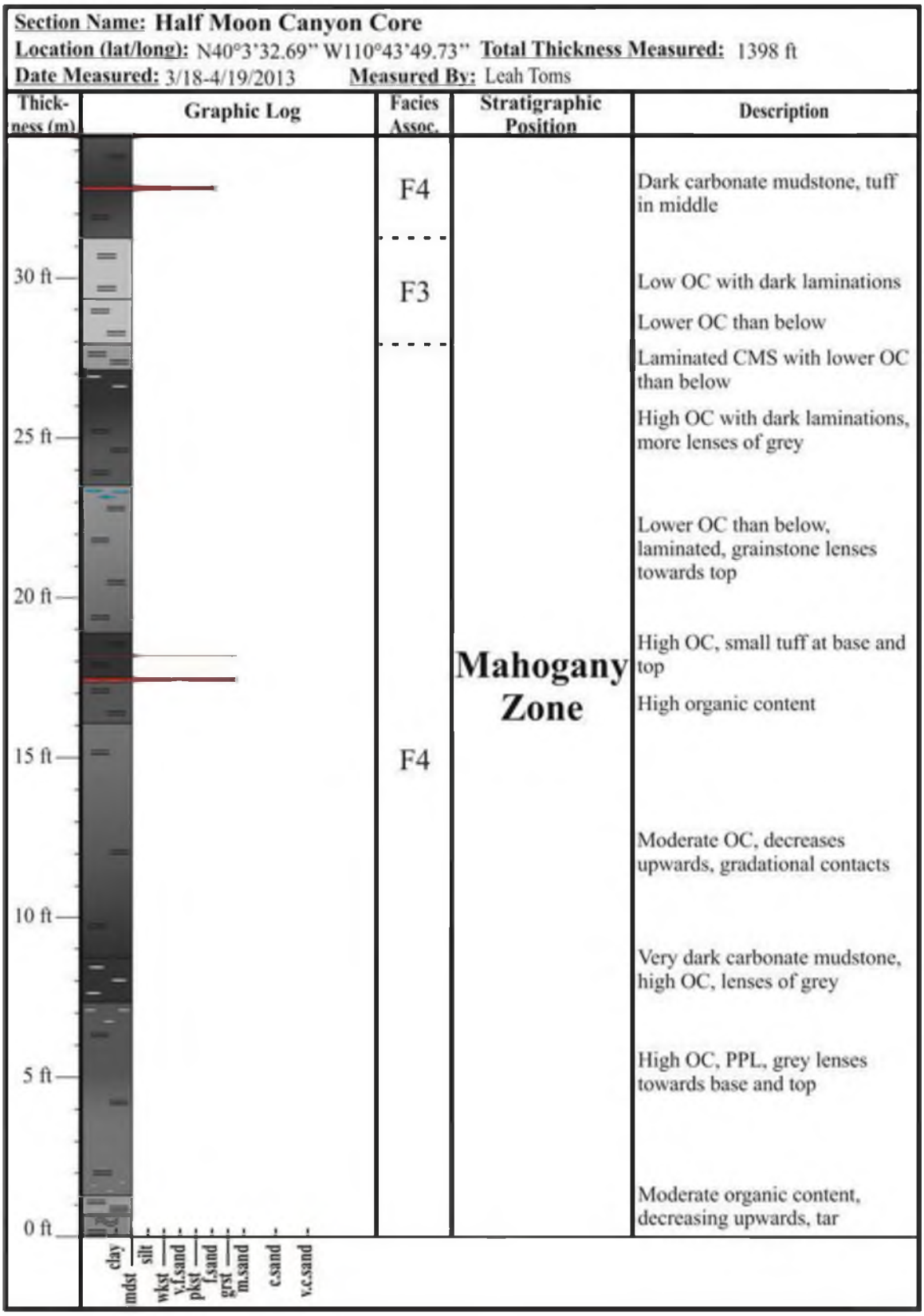
Section Name: Half Moon Canyon Core
Location (lat/long): N40°3'32.69" W110°43'49.73" Total Thickness Measured: 1398 ft
Date Measured: 3/18-4/19/2013 Measured By: Leah Toms
Thick-ness (m)
Graphic Log
Facies Assoc.
Stratigraphic Position
Description
30 ft
25 ft
20 ft
15 ft
10 ft
5 ft
0 ft
F4
F3
F4
Mahogany Zone
Dark carbonate mudstone, tuff in middle
Low OC with dark laminations
Lower OC than below
Laminated CMS with lower OC than below
High OC with dark laminations, more lenses of grey
Lower OC than below, laminated, grainstone lenses towards top
High OC, small tuff at base and top
High organic content
Moderate OC, decreases upwards, gradational contacts
Very dark carbonate mudstone, high OC, lenses of grey
High OC, PPL, grey lenses towards base and top
Moderate organic content, decreasing upwards, tar
clay
silt
mdst
wkst
v.f.sand
pkst
f.sand
grst
m.sand
c.sand
v.c.sand

Section Name: Half Moon Canyon Core
Location (lat/long): N40°3'32.69" W110°43'49.73" **Total Thickness Measured:** 1398 ft
Date Measured: 3/18-4/19/2013 **Measured By:** Leah Toms

Thickness (m)	Graphic Log	Facies Assoc.	Stratigraphic Position	Description
65 ft		F4	Mahogany Zone	Light CMS with low OC Reddish carbonate mudstone (degraded oil shale), increasing OC upwards
60 ft				Mod OC CMS, reddish towards base with white specks
55 ft				Overall increasing OC towards top, minor tuff lenses
50 ft				
45 ft				Mod to low OC CMS, dark laminations
40 ft				Very high OC CMS Slight less OC than below, reddish, grey specks throughout Darker CMS, reddish, tuff in middle Mod to high OC, small tuff lenses
35 ft				

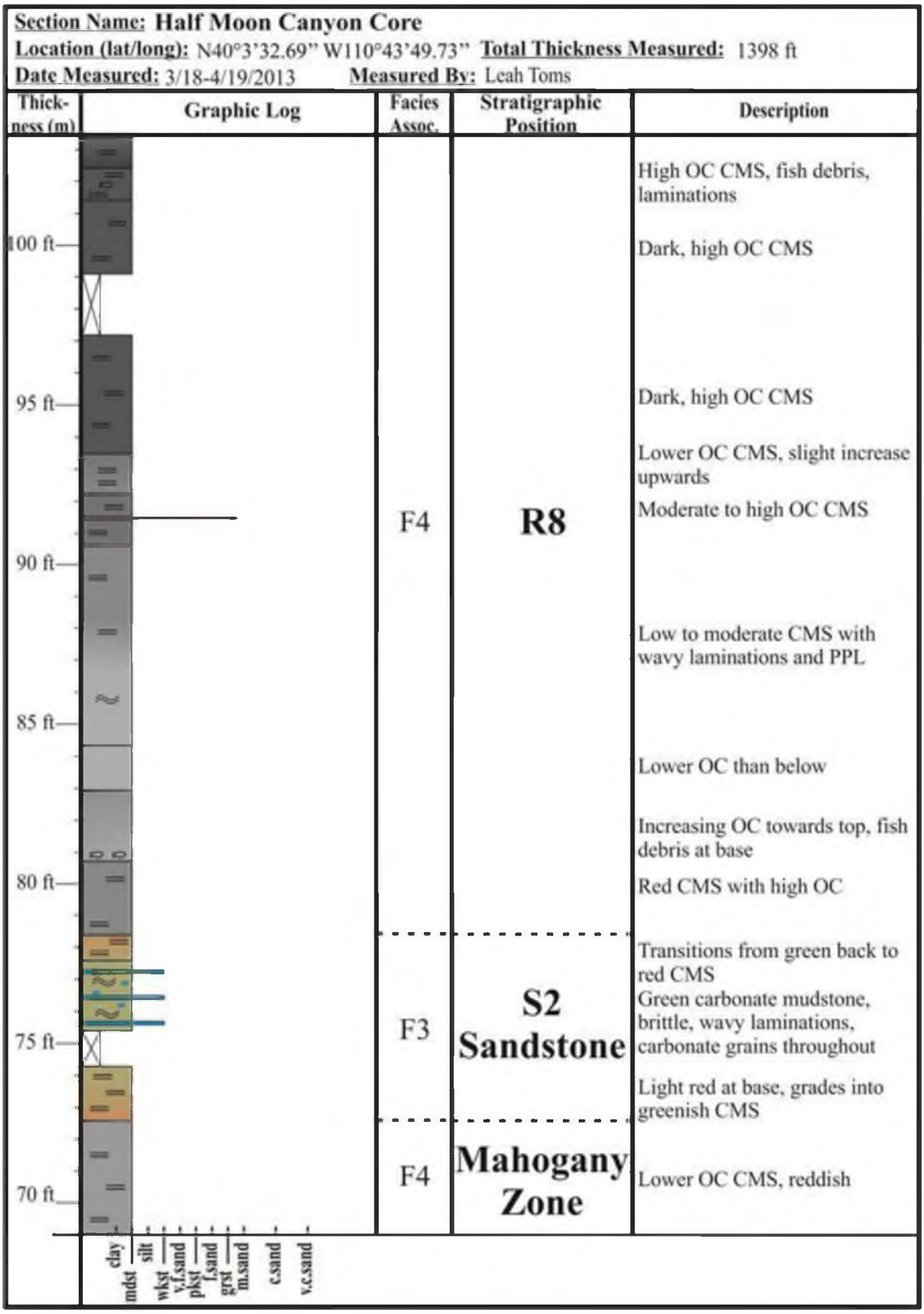
Section Name: Half Moon Canyon Core
Location (lat/long): N40°3'32.69" W110°43'49.73" Total Thickness Measured: 1398 ft
Date Measured: 3/18-4/19/2013 Measured By: Leah Toms
Thick-ness (m)
Graphic Log
Facies Assoc.
Stratigraphic Position
Description
100 ft
95 ft
90 ft
85 ft
80 ft
75 ft
70 ft
High OC CMS, fish debris, laminations
Dark, high OC CMS
Dark, high OC CMS
Lower OC CMS, slight increase upwards
Moderate to high OC CMS
F4
R8
Low to moderate CMS with wavy laminations and PPL
Lower OC than below
Increasing OC towards top, fish debris at base
Red CMS with high OC
Transitions from green back to red CMS
Green carbonate mudstone, brittle, wavy laminations, carbonate grains throughout
F3
S2 Sandstone
Light red at base, grades into greenish CMS
F4
Mahogany Zone
Lower OC CMS, reddish
clay
mdst
silt
wkst
v.f.sand
pkst
f.sand
grst
m.sand
c.sand
v.c.sand

Section Name: Half Moon Canyon Core
Location (lat/long): N40°3'32.69" W110°43'49.73" **Total Thickness Measured:** 1398 ft
Date Measured: 3/18-4/19/2013 **Measured By:** Leah Toms

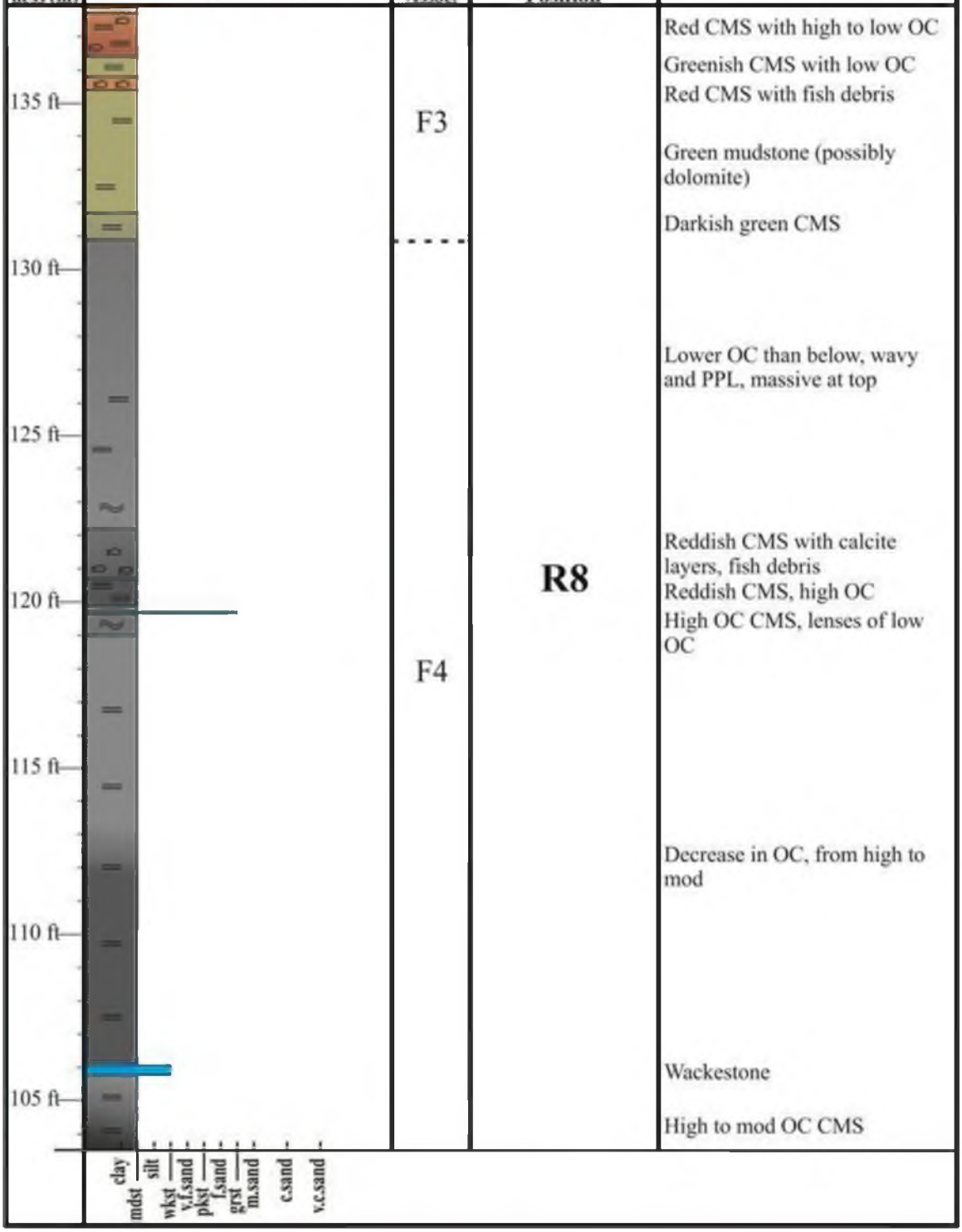

Section Name: Half Moon Canyon Core
Location (lat/long): N40°3'32.69" W110°43'49.73" **Total Thickness Measured:** 1398 ft
Date Measured: 3/18-4/19/2013 **Measured By:** Leah Toms

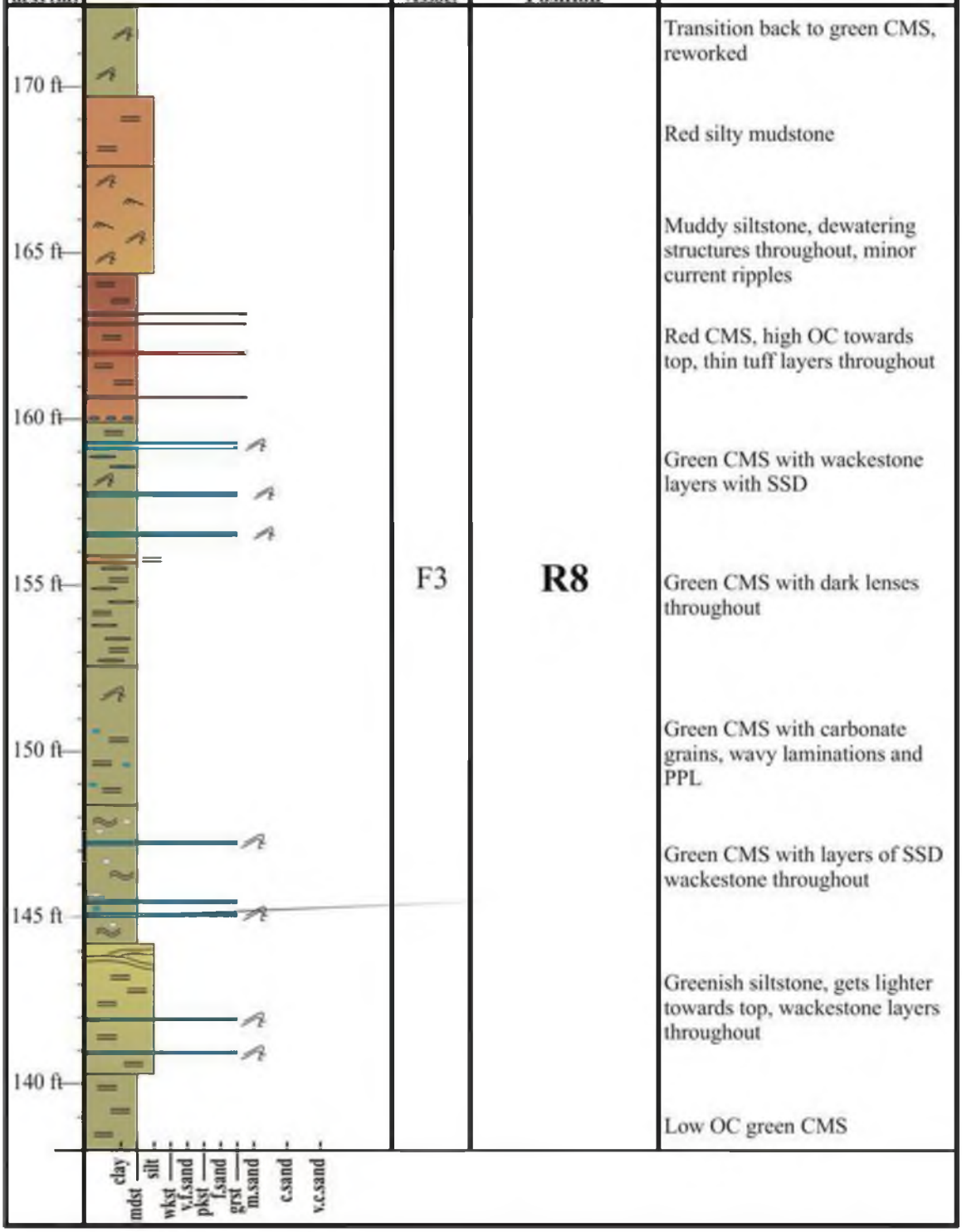

Section Name: Half Moon Canyon Core
Location (lat/long): N40°3'32.69" W110°43'49.73" **Total Thickness Measured:** 1398 ft
Date Measured: 3/18-4/19/2013 **Measured By:** Leah Toms

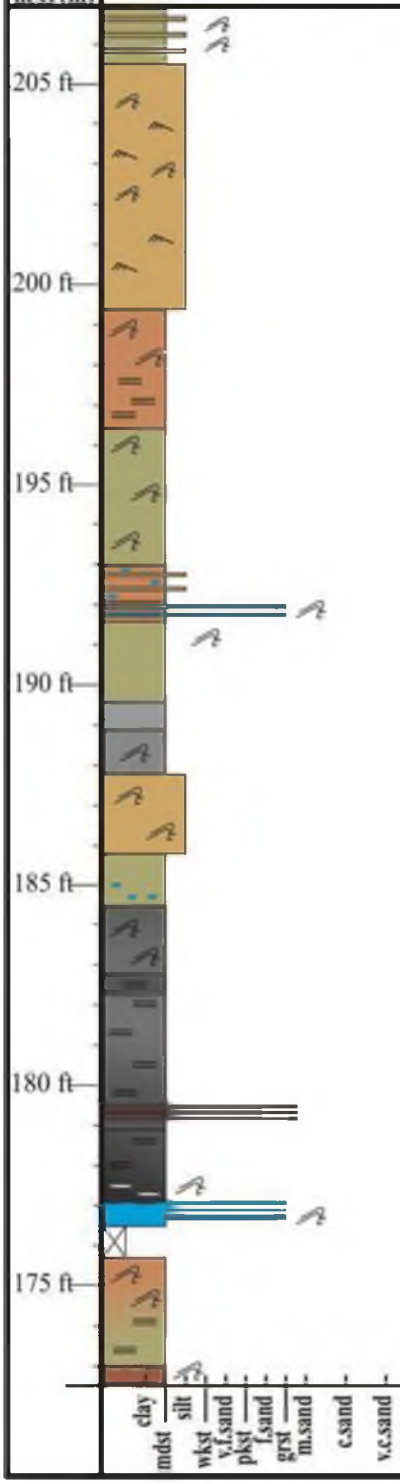

Thickness (m)	Facies Assoc.	Stratigraphic Position	Description
	F1	R8	Greensih CMS with white lenses throughout, also layers of siltstone
			Siltstone with CMS, current ripples, rip up mud clasts, SSD
			Reddish CMS with dewatering features
	F3		Greenish CMS with SSD, carbonate clasts
			Reddish CMS with siltstone layers and wackestone layers,
			Greenish CMS with red layer towards top, SSD
			Moderate OC from grey to red, SSD
	F1		Siltstone with calcite lenses, organic rich, SSD
			Greenish CMS, massive, carbonate grains throughout
			High OC CMS with SSD
			Higher OC CMS
	F4		Lower OC than below, goes from high to mod with PPL
			Dark red CMS with high OC
			Wackestone to grainstone at top, SSD
	F3		Greenish CMS to red, SSD towards top
			Red CMS

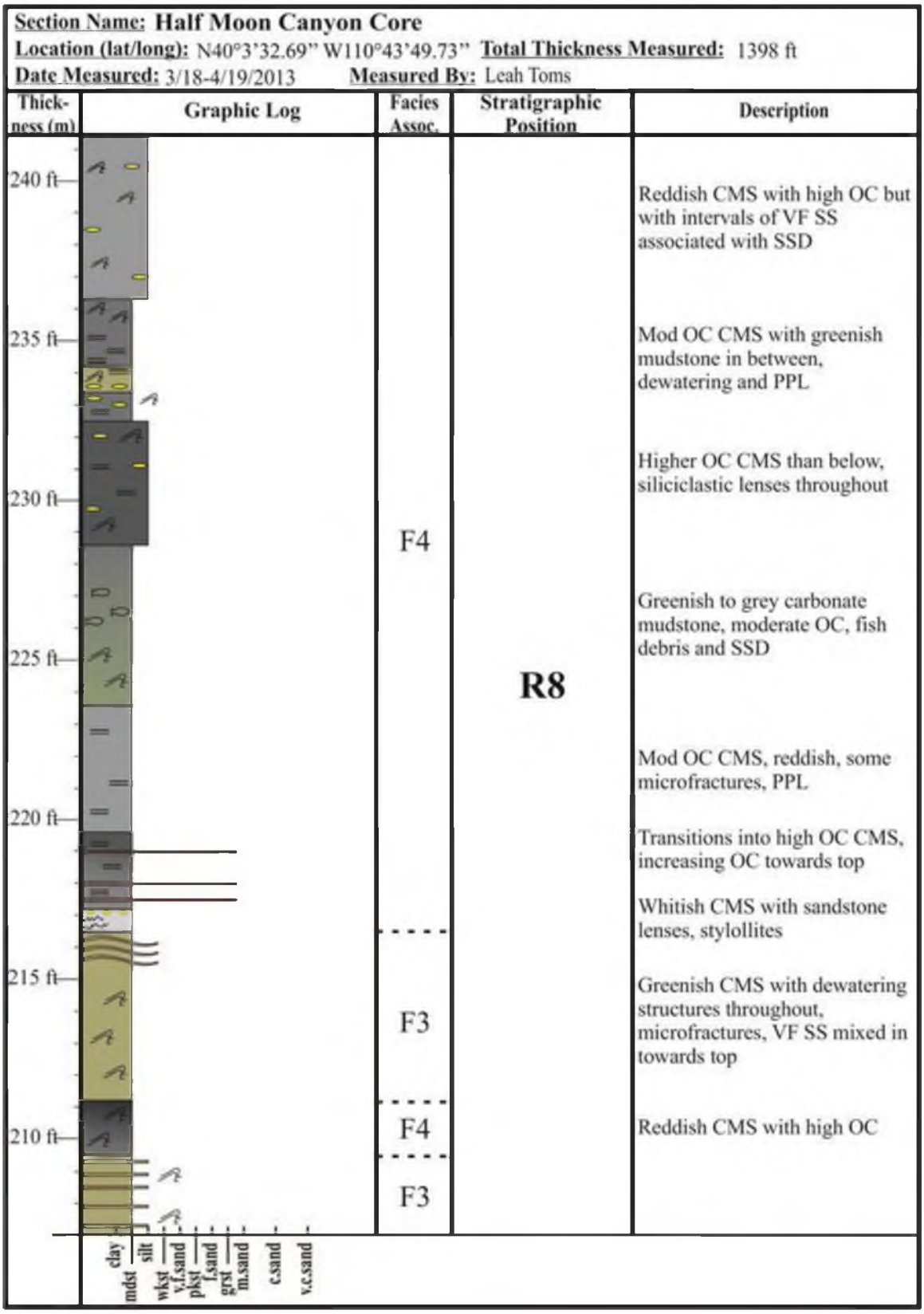
Section Name: Half Moon Canyon Core
Location (lat/long): N40°3'32.69" W110°43'49.73" Total Thickness Measured: 1398 ft
Date Measured: 3/18-4/19/2013 Measured By: Leah Toms
Thick-ness (m)
Graphic Log
Facies Assoc.
Stratigraphic Position
Description
240 ft
235 ft
230 ft
225 ft
220 ft
215 ft
210 ft
F4
F3
F4
F3
R8
Reddish CMS with high OC but with intervals of VF SS associated with SSD
Mod OC CMS with greenish mudstone in between, dewatering and PPL
Higher OC CMS than below, siliciclastic lenses throughout
Greenish to grey carbonate mudstone, moderate OC, fish debris and SSD
Mod OC CMS, reddish, some microfractures, PPL
Transitions into high OC CMS, increasing OC towards top
Whitish CMS with sandstone lenses, stylollites
Greenish CMS with dewatering structures throughout, microfractures, VF SS mixed in towards top
Reddish CMS with high OC
clay
silt
mdst
wkst
v.f.sand
pkst
f.sand
grst
m.sand
c.sand
v.c.sand

Section Name: Half Moon Canyon Core
Location (lat/long): N40°3'32.69" W110°43'49.73" **Total Thickness Measured:** 1398 ft
Date Measured: 3/18-4/19/2013 **Measured By:** Leah Toms

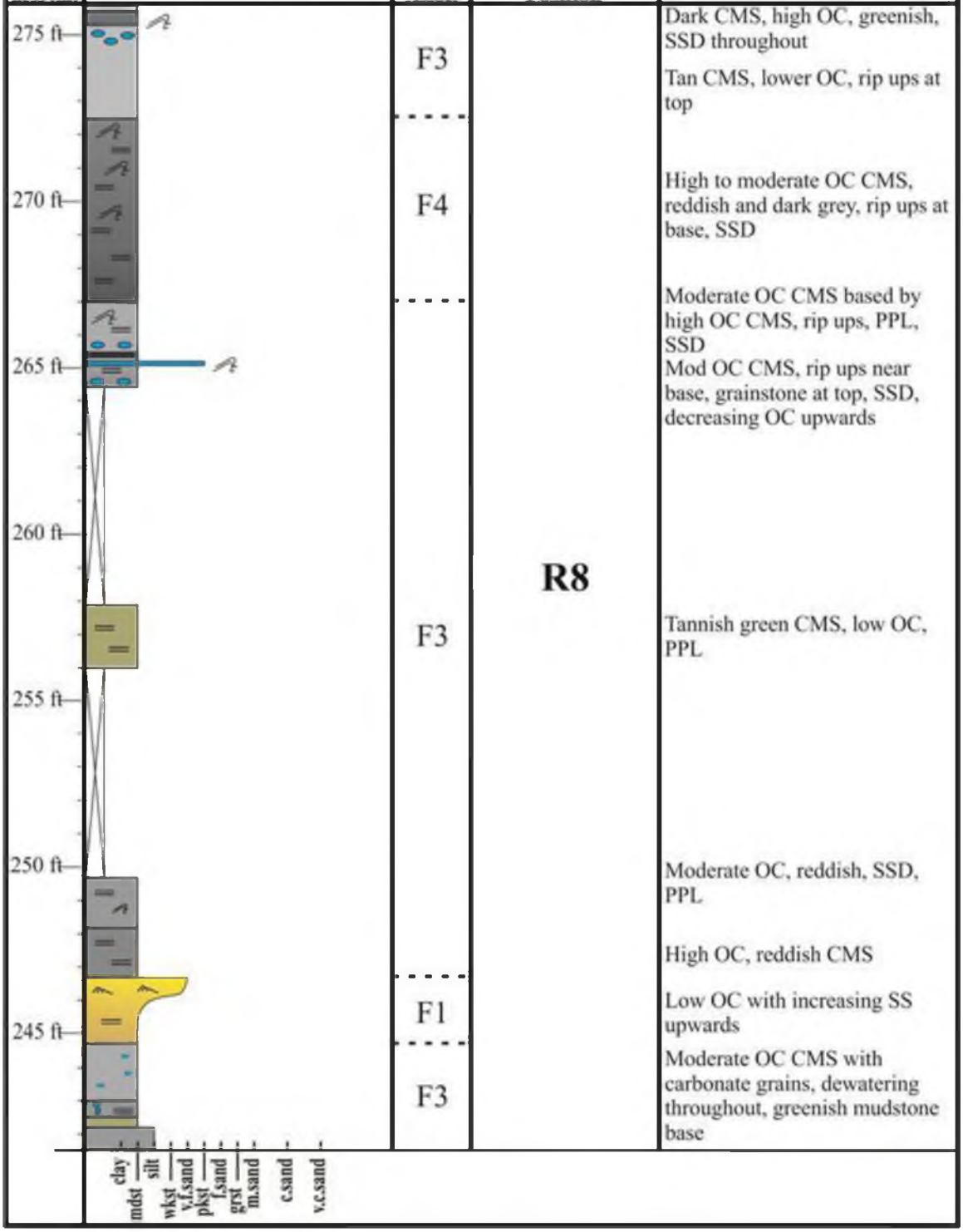

Section Name: Half Moon Canyon Core
Location (lat/long): N40°3'32.69" W110°43'49.73" **Total Thickness Measured:** 1398 ft
Date Measured: 3/18-4/19/2013 **Measured By:** Leah Toms

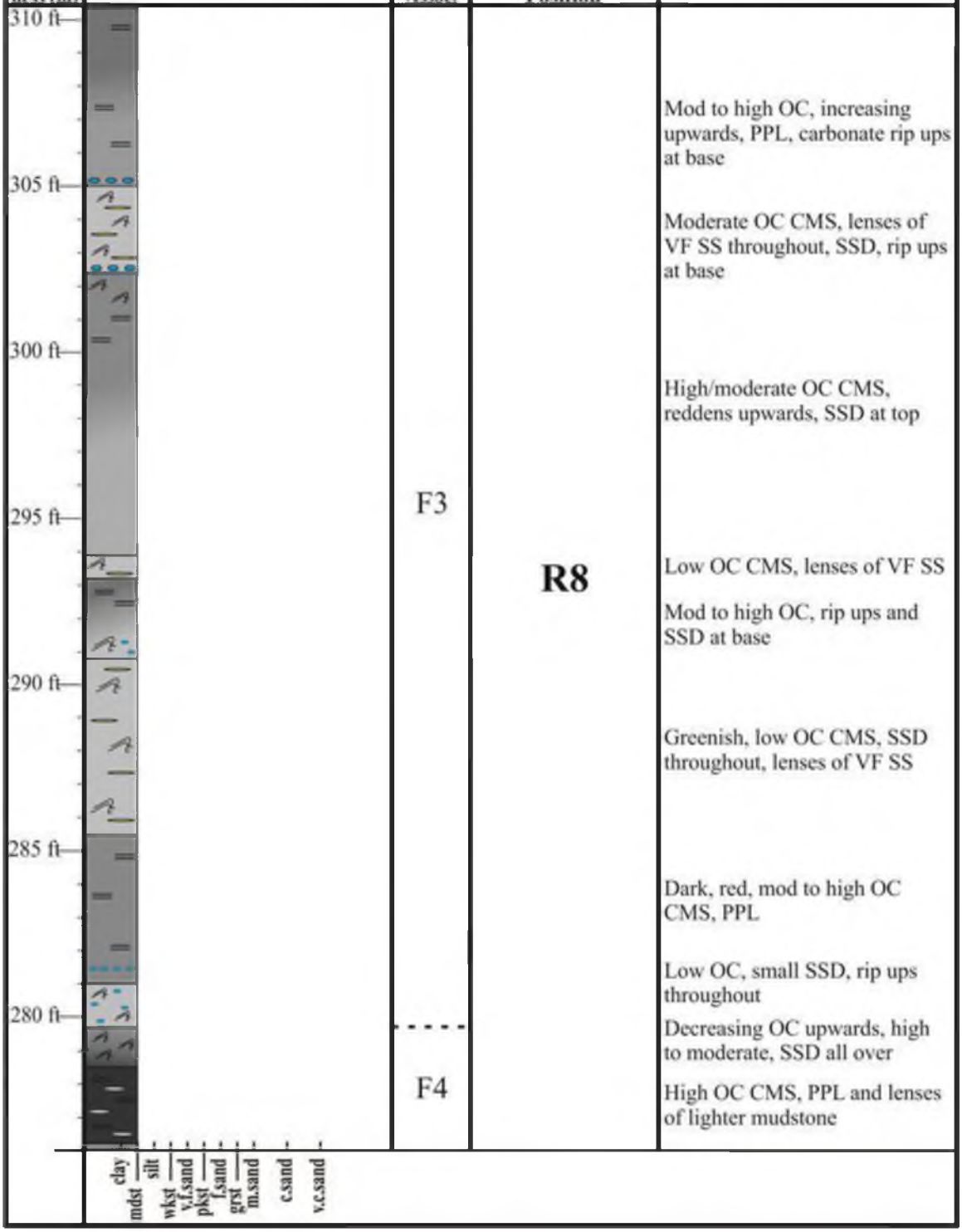

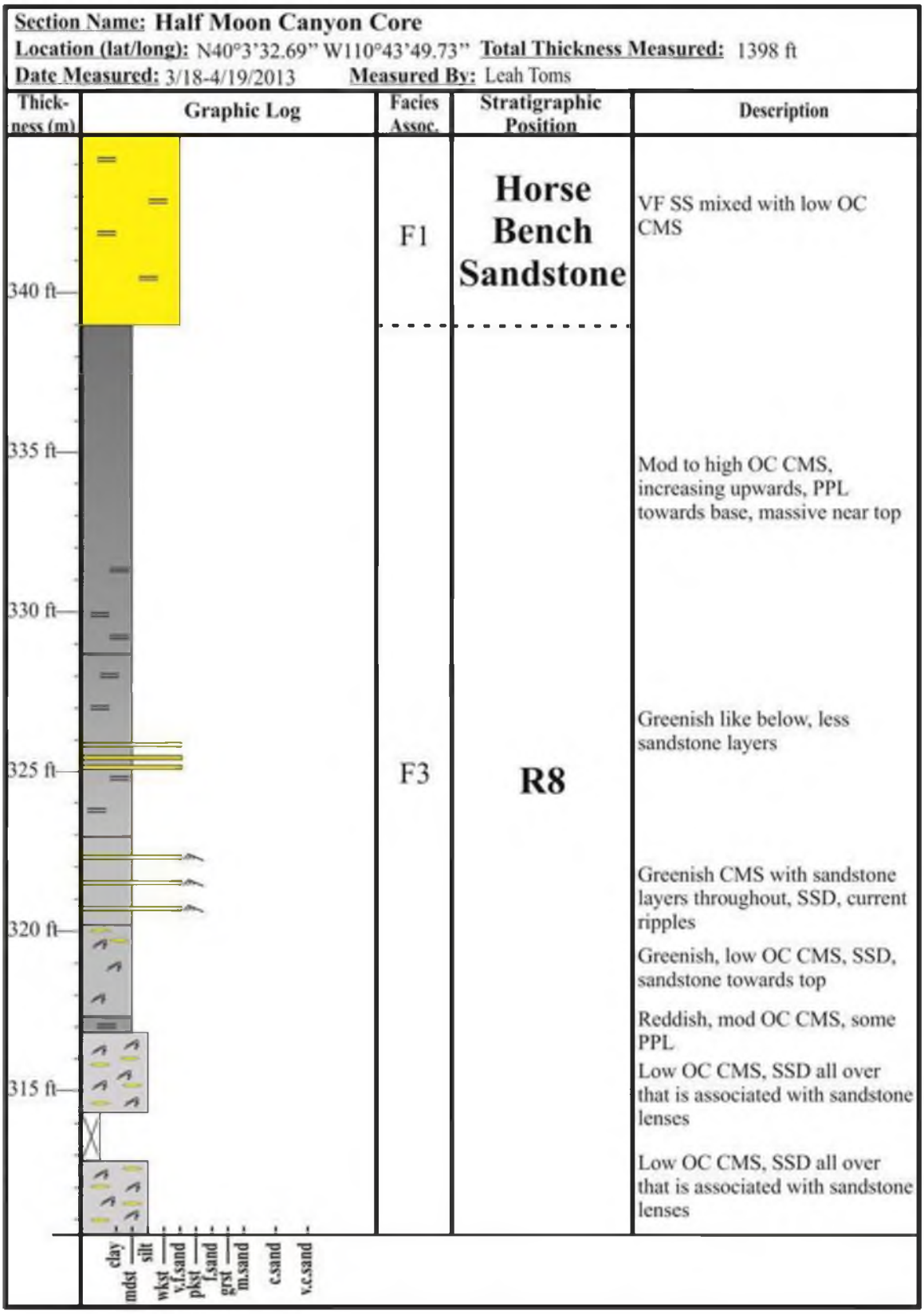
Section Name: Half Moon Canyon Core
Location (lat/long): N40°3'32.69" W110°43'49.73" Total Thickness Measured: 1398 ft
Date Measured: 3/18-4/19/2013 Measured By: Leah Toms
Thick-ness (m)
Graphic Log
Facies Assoc.
Stratigraphic Position
Description
340 ft
335 ft
330 ft
325 ft
320 ft
315 ft
F1
F3
Horse Bench Sandstone
R8
VF SS mixed with low OC CMS
Mod to high OC CMS, increasing upwards, PPL towards base, massive near top
Greenish like below, less sandstone layers
Greenish CMS with sandstone layers throughout, SSD, current ripples
Greenish, low OC CMS, SSD, sandstone towards top
Reddish, mod OC CMS, some PPL
Low OC CMS, SSD all over that is associated with sandstone lenses
Low OC CMS, SSD all over that is associated with sandstone lenses
clay
silt
mdst
wkst
v.f.sand
pkst
f.sand
grst
m.sand
c.sand
v.c.sand

Section Name: Half Moon Canyon Core
Location (lat/long): N40°3'32.69" W110°43'49.73" **Total Thickness Measured:** 1398 ft
Date Measured: 3/18-4/19/2013 **Measured By:** Leah Toms

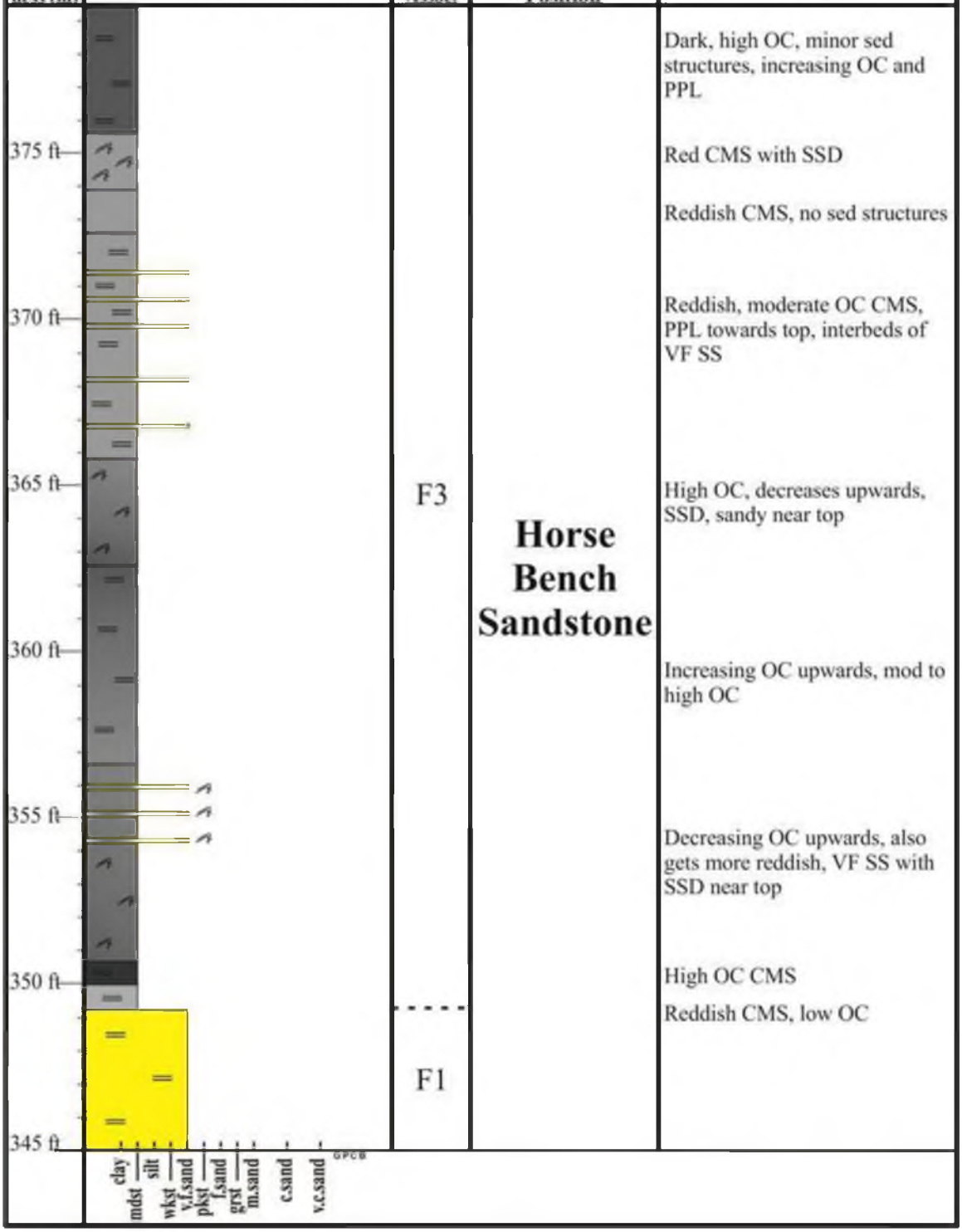

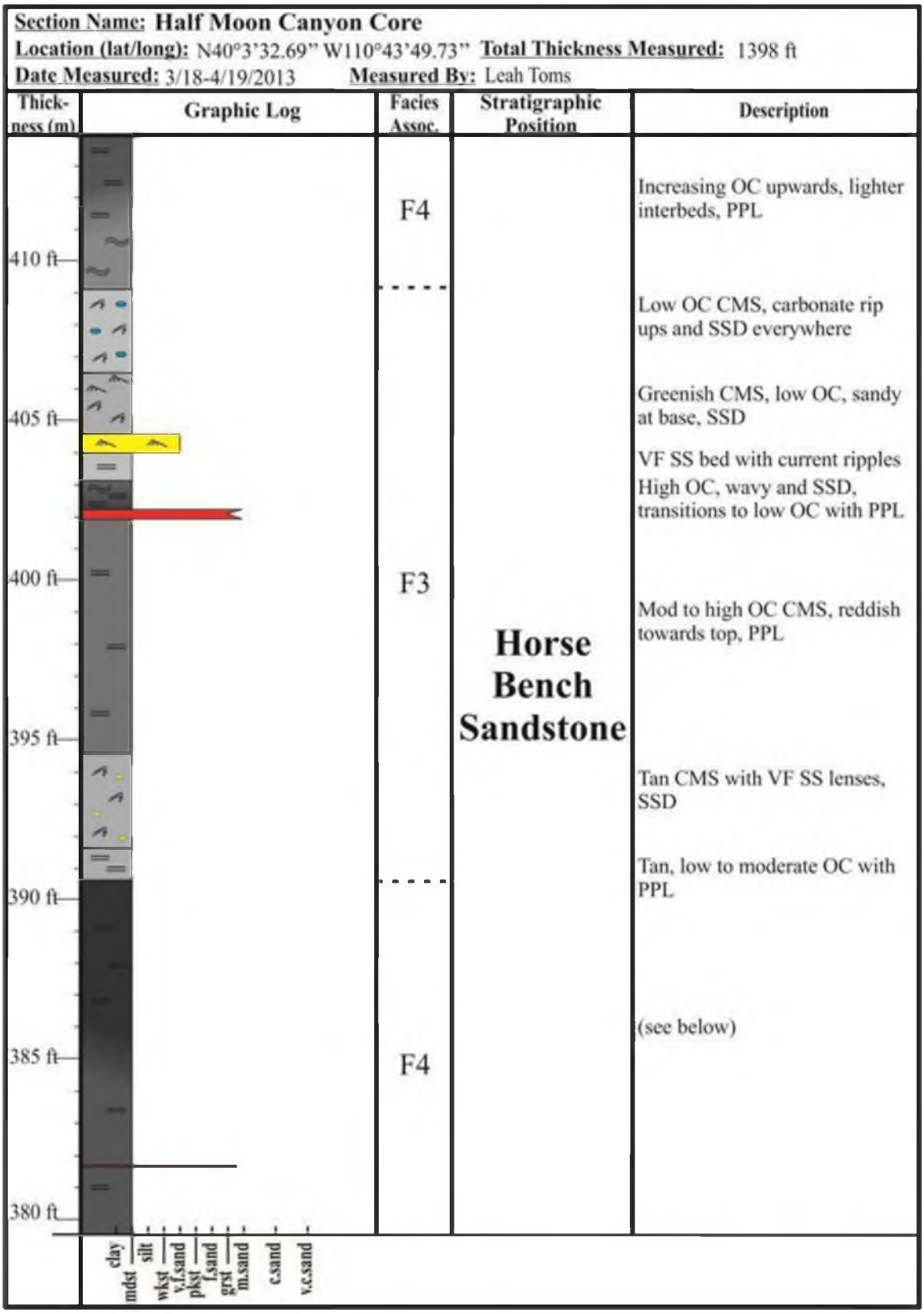
Section Name: Half Moon Canyon Core
Location (lat/long): N40°3'32.69" W110°43'49.73" Total Thickness Measured: 1398 ft
Date Measured: 3/18-4/19/2013 Measured By: Leah Toms
Thick-ness (m)
Graphic Log
Facies Assoc.
Stratigraphic Position
Description
410 ft
405 ft
400 ft
395 ft
390 ft
385 ft
380 ft
F4
F3
F4
Horse Bench Sandstone
Increasing OC upwards, lighter interbeds, PPL
Low OC CMS, carbonate rip ups and SSD everywhere
Greenish CMS, low OC, sandy at base, SSD
VF SS bed with current ripples
High OC, wavy and SSD, transitions to low OC with PPL
Mod to high OC CMS, reddish towards top, PPL
Tan CMS with VF SS lenses, SSD
Tan, low to moderate OC with PPL
(see below)
clay
mdst
silt
wkst
v.f.sand
pkst
f.sand
grst
m.sand
c.sand
v.c.sand

Section Name: Half Moon Canyon Core
Location (lat/long): N40°3'32.69" W110°43'49.73" **Total Thickness Measured:** 1398 ft
Date Measured: 3/18-4/19/2013 **Measured By:** Leah Toms

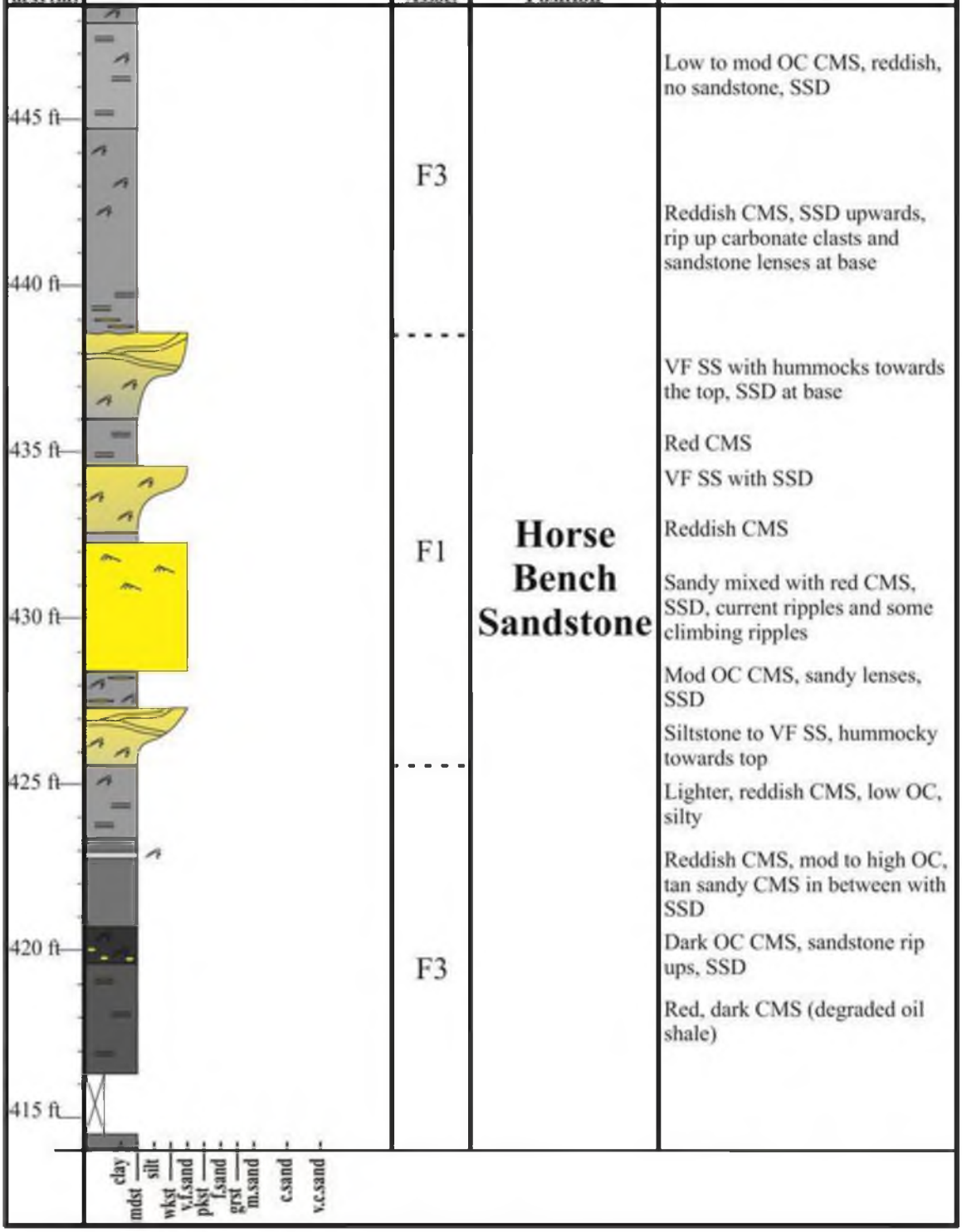

Section Name: Half Moon Canyon Core
Location (lat/long): N40°3'32.69" W110°43'49.73" **Total Thickness Measured:** 1398 ft
Date Measured: 3/18-4/19/2013 **Measured By:** Leah Toms

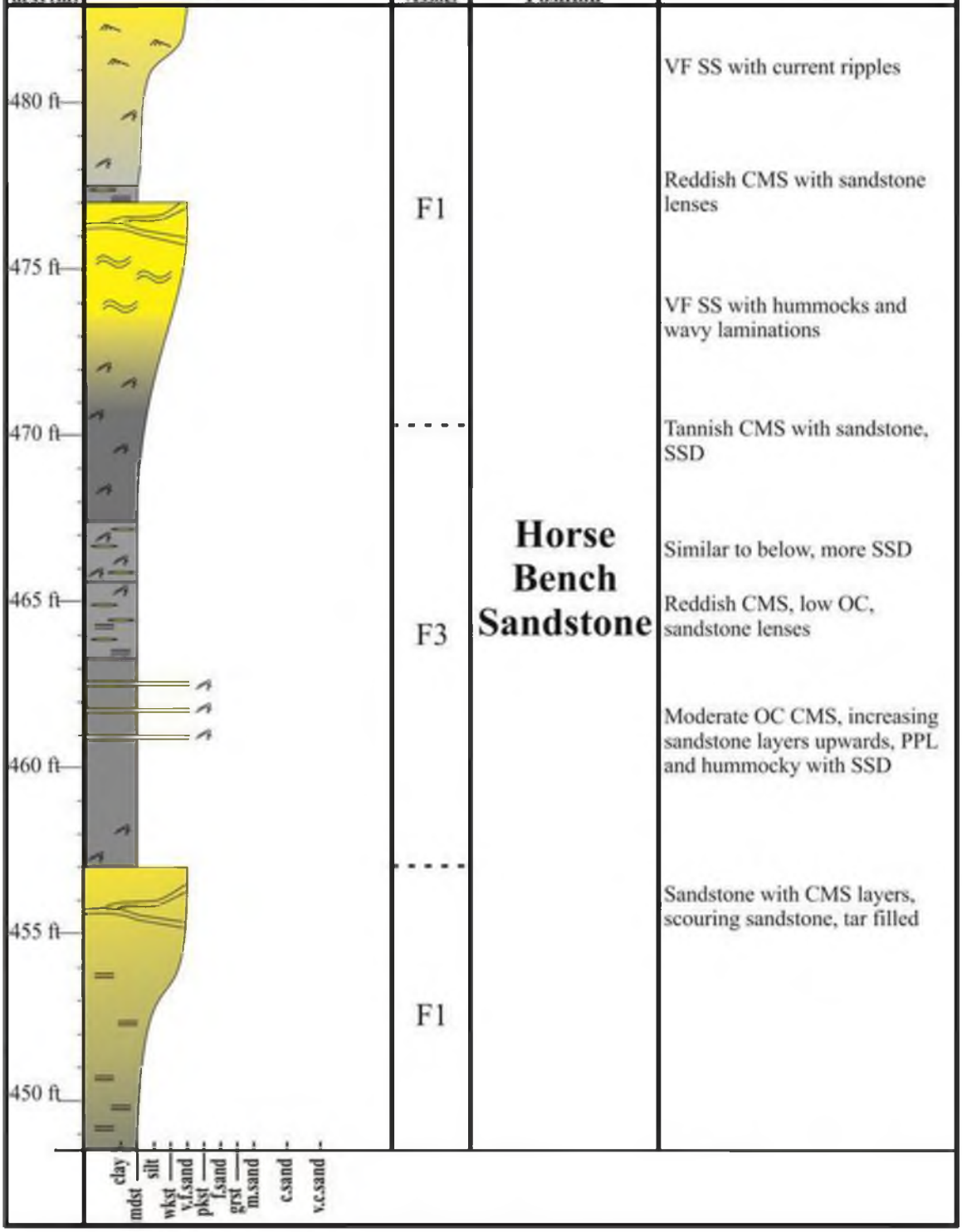

Section Name: Half Moon Canyon Core
Location (lat/long): N40°3'32.69" W110°43'49.73" **Total Thickness Measured:** 1398 ft
Date Measured: 3/18-4/19/2013 **Measured By:** Leah Toms

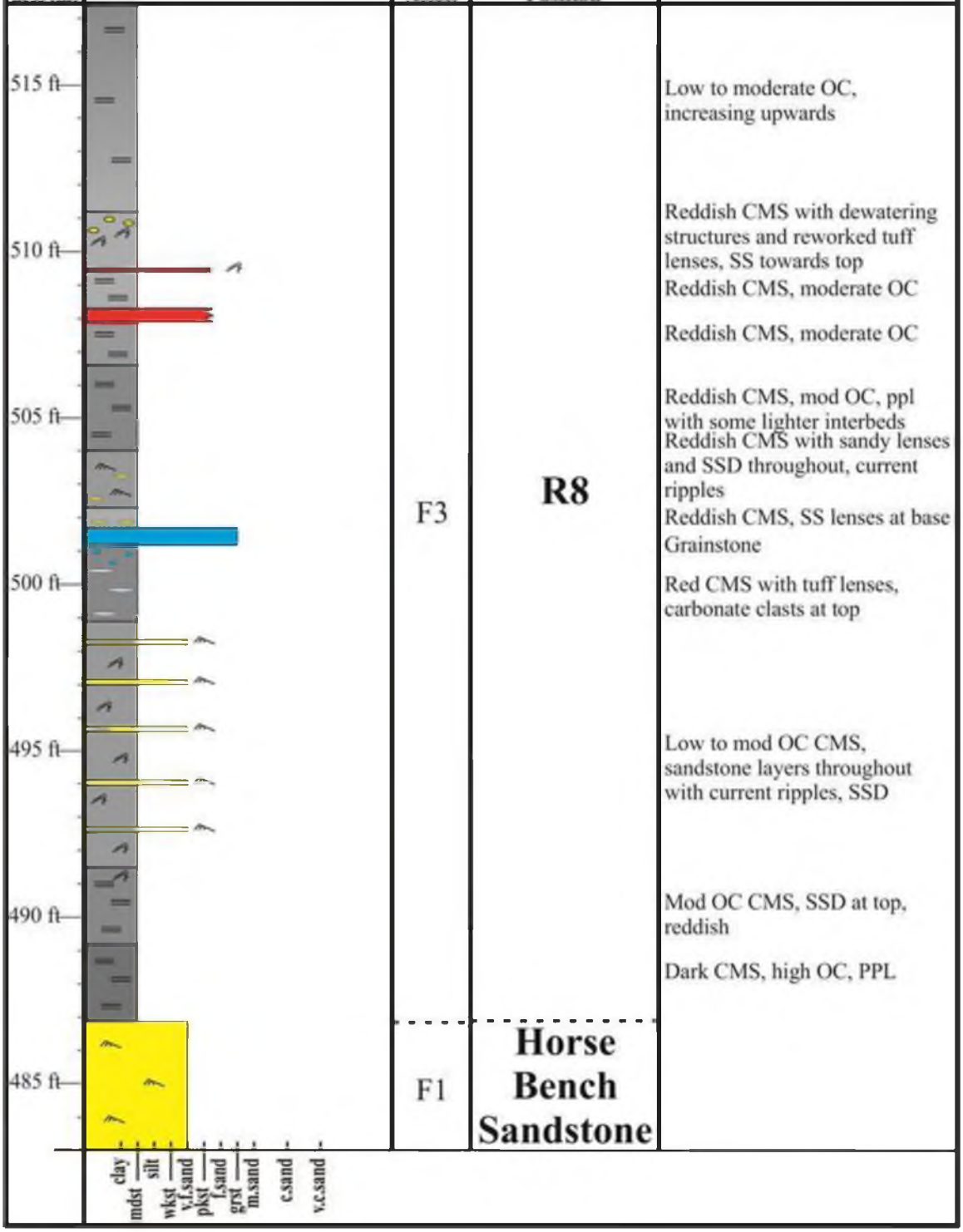

Section Name: Half Moon Canyon Core
Location (lat/long): N40°3'32.69" W110°43'49.73" **Total Thickness Measured:** 1398 ft
Date Measured: 3/18-4/19/2013 **Measured By:** Leah Toms

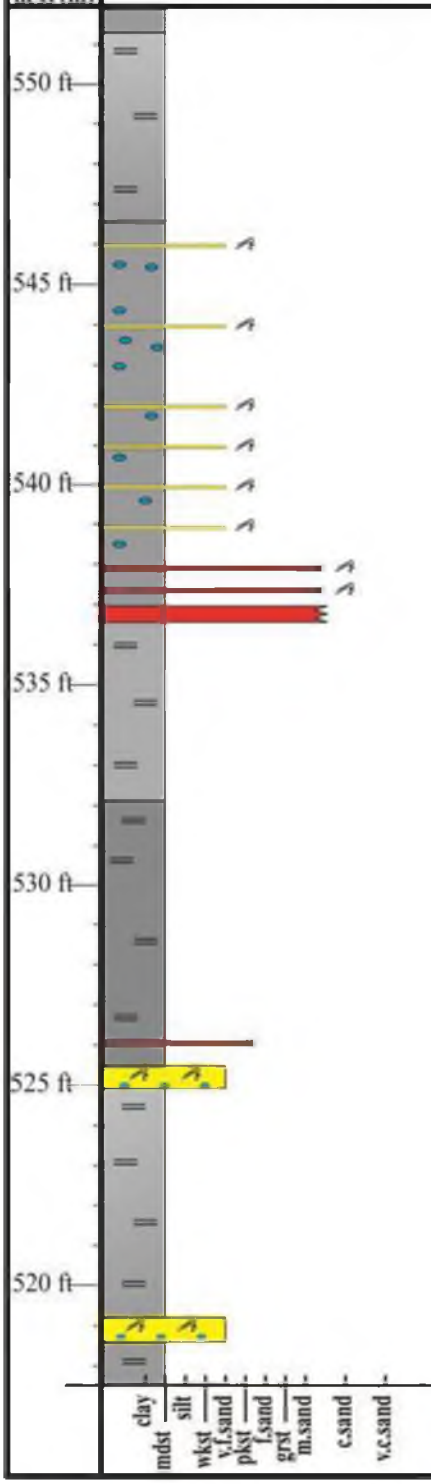

Thickness (m)	Graphic Log	Facies Assoc.	Stratigraphic Position	Description
				Decreasing OC upwards, low to mod OC
				Mod OC CMS, layers of VF SS associated with dewatering, also carbonate rip ups
				Tuff with crystallization (rhyolite?)
		F3	R8	Reddish CMS, mod OC, lighter interbeds
				Greyish red CMS with mod to high OC
				VF SS and siltstone with SSD, based by carbonate rip ups
				Greenish to red with lighter interbeds, low OC CMS
				VF SS and siltstone with SSD, based by carbonate rip ups

Section Name: Half Moon Canyon Core
Location (lat/long): N40°3'32.69" W110°43'49.73" **Total Thickness Measured:** 1398 ft
Date Measured: 3/18-4/19/2013 **Measured By:** Leah Toms

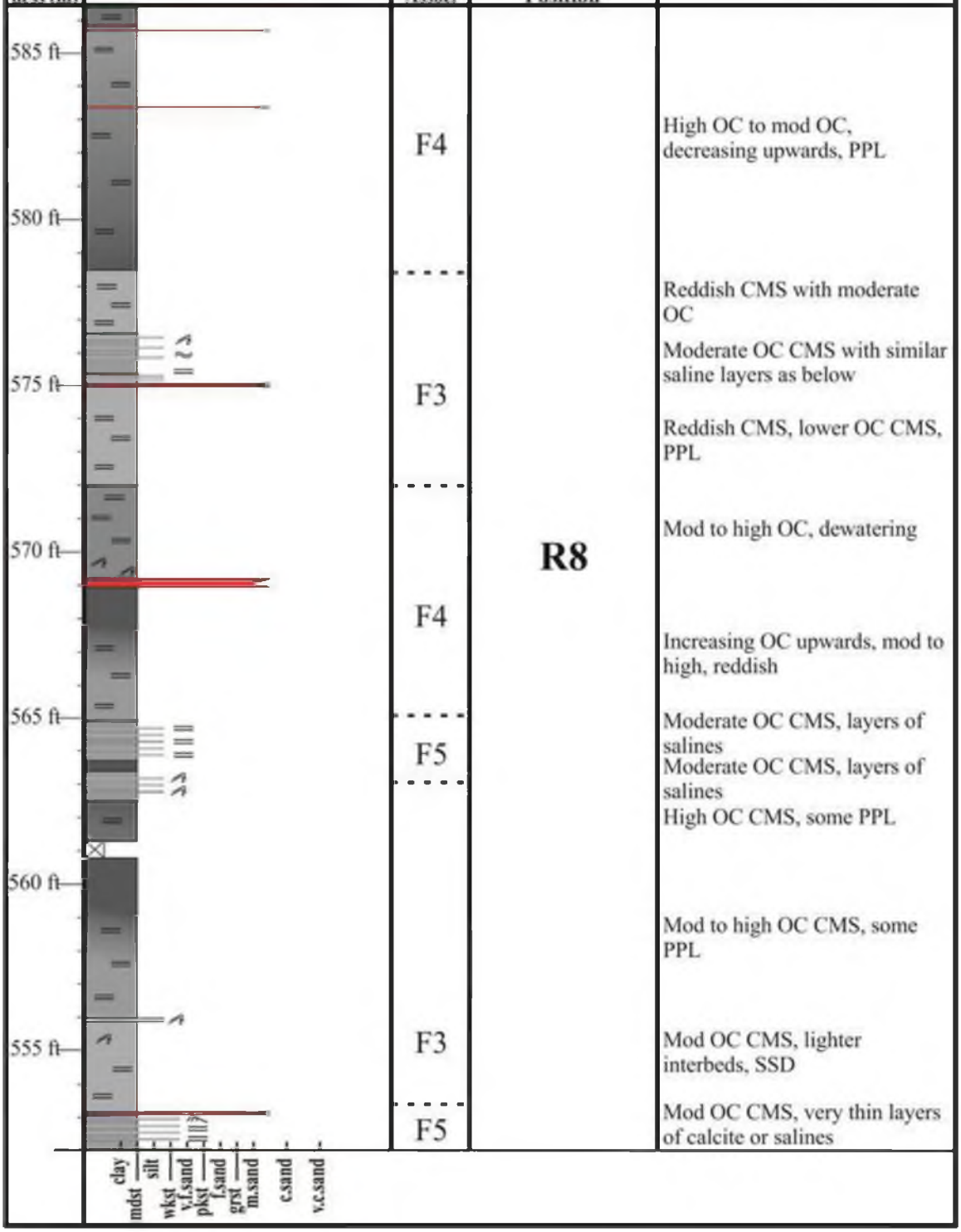

Section Name: Half Moon Canyon Core
Location (lat/long): N40°3'32.69" W110°43'49.73" **Total Thickness Measured:** 1398 ft
Date Measured: 3/18-4/19/2013 **Measured By:** Leah Toms

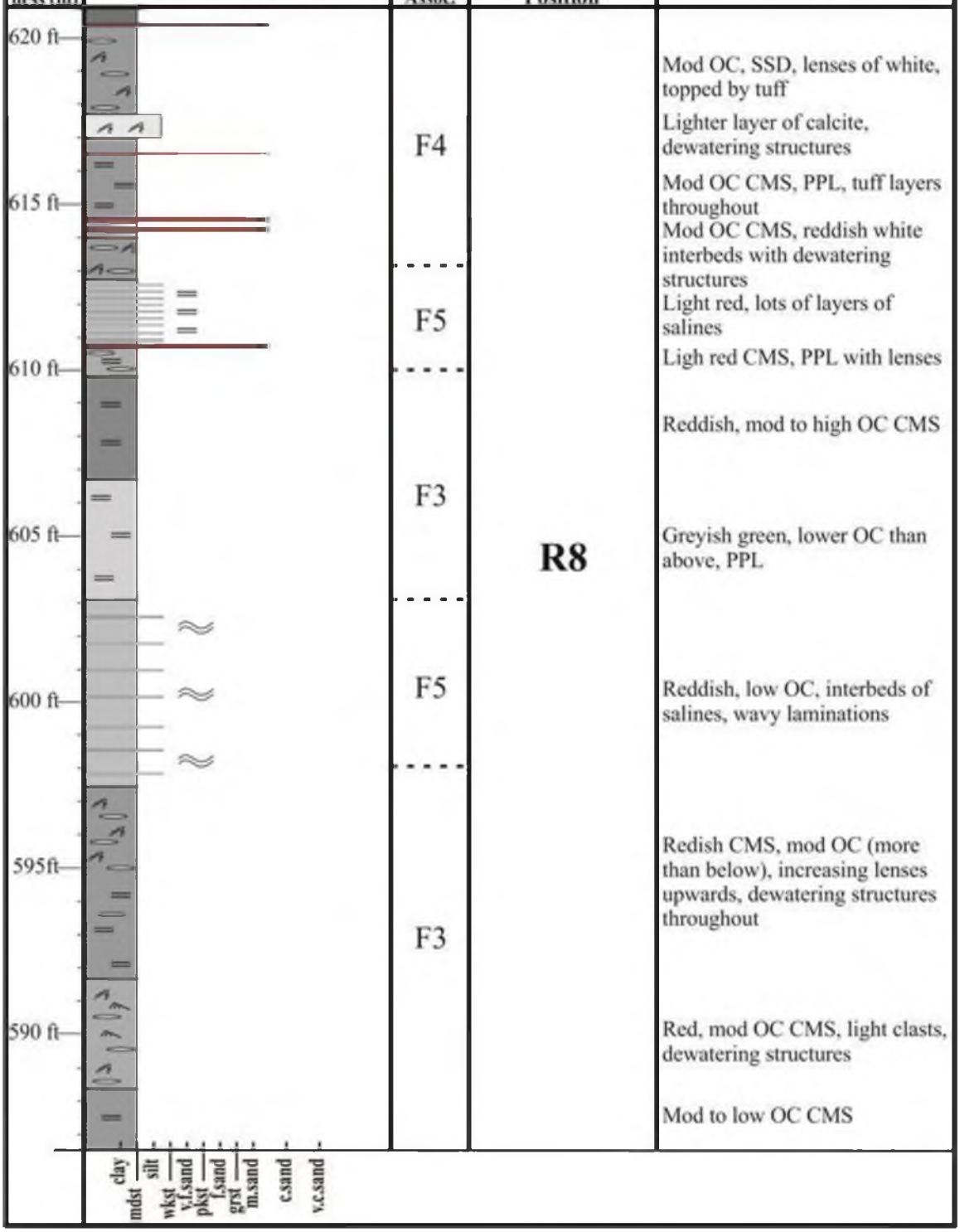

Section Name: Half Moon Canyon Core
Location (lat/long): N40°3'32.69" W110°43'49.73" **Total Thickness Measured:** 1398 ft
Date Measured: 3/18-4/19/2013 **Measured By:** Leah Toms

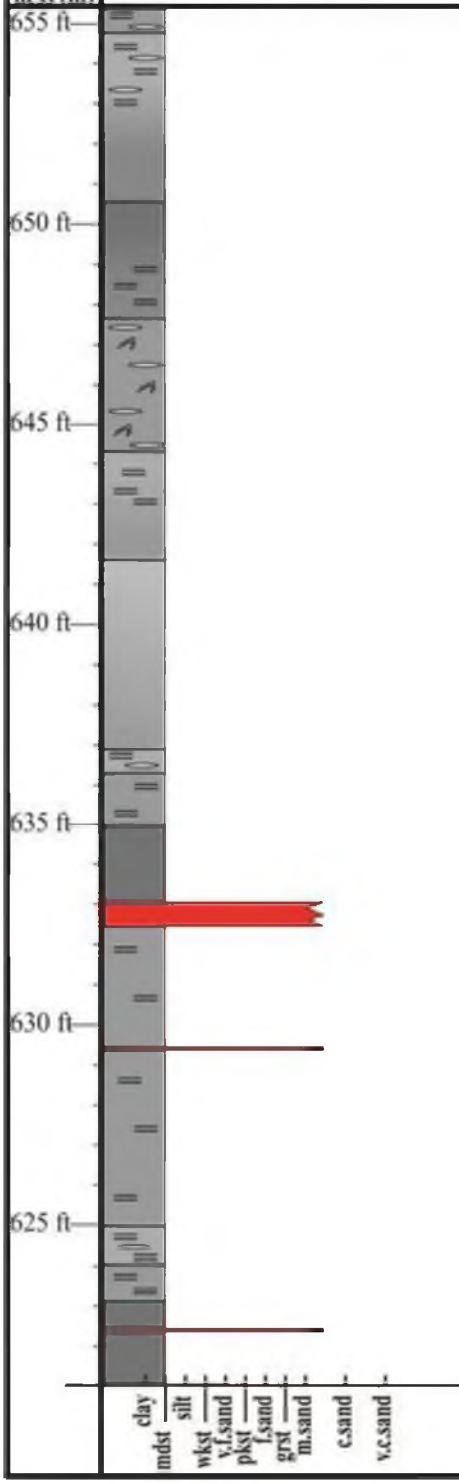

Thickness (m)	Graphic Log	Facies Assoc.	Stratigraphic Position	Description
		F4	R8	Reddish/grey CMS, lenses and interbeds of salines throughout
				Reddish CMS, mod OC, decreases upwards, lighter beds upwards, lenses at top
				Greenish grey, mod OC, increases upwards, PPL towards base
				Red with white/grey lenses, mod OC, SSD
				Mod OC CMS, reddens upwards, decreasing OC upwards
				Mod OC, decreases upwards, massive
				Lighter CMS, red with lighter interbeds, lenses
				Mod CMS, reddish, PPL
				Greyish CMS, mod to high OC
				Rhyolite
				Mod OC CMS, reddish, lenses throughout
				Mod OC CMS, PPL and lenses
				Reddish CMS, mod OC
				Greyish green CMS, mod to high OC CMS

Section Name: Half Moon Canyon Core
Location (lat/long): N40°3'32.69" W110°43'49.73" **Total Thickness Measured:** 1398 ft
Date Measured: 3/18-4/19/2013 **Measured By:** Leah Toms

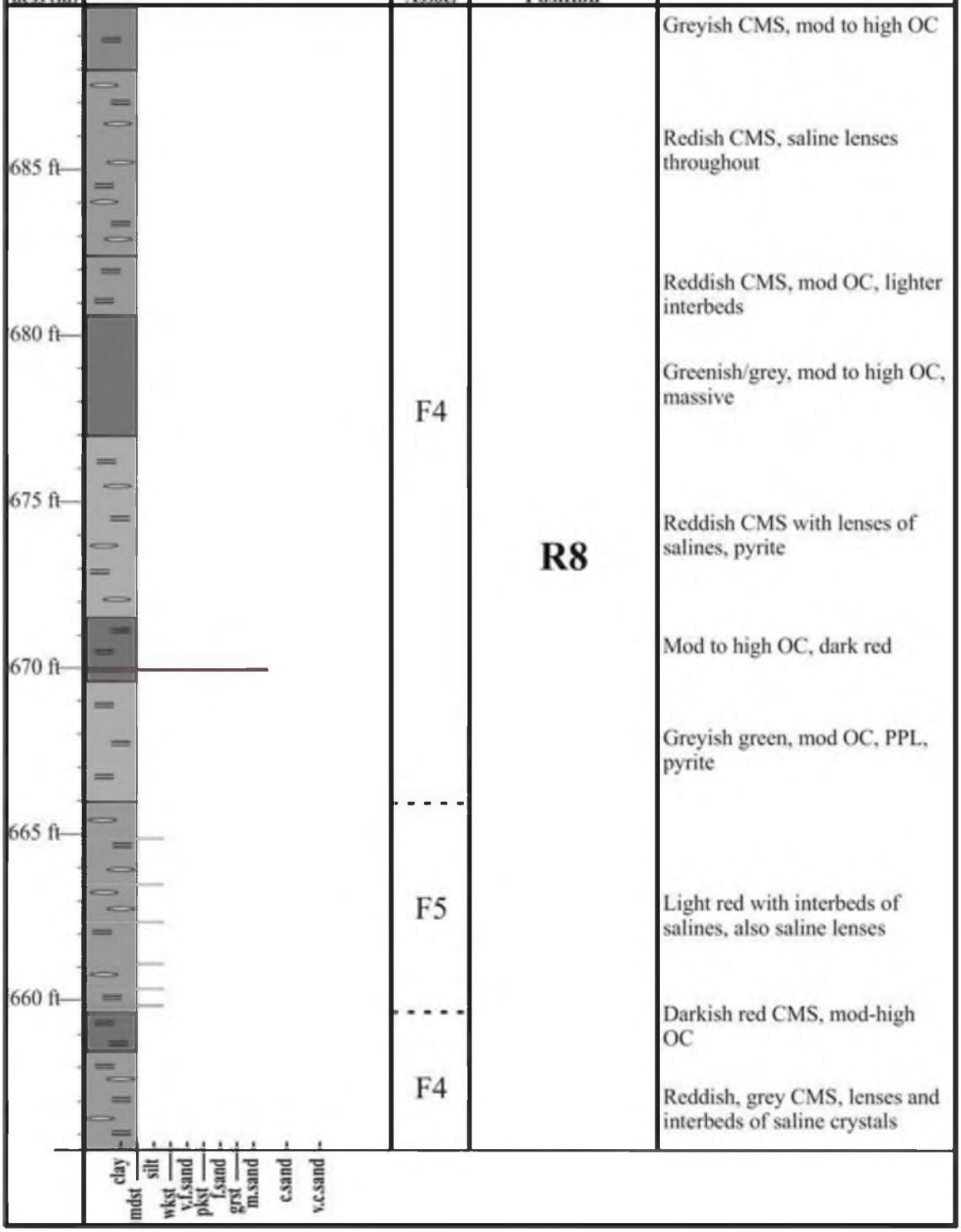

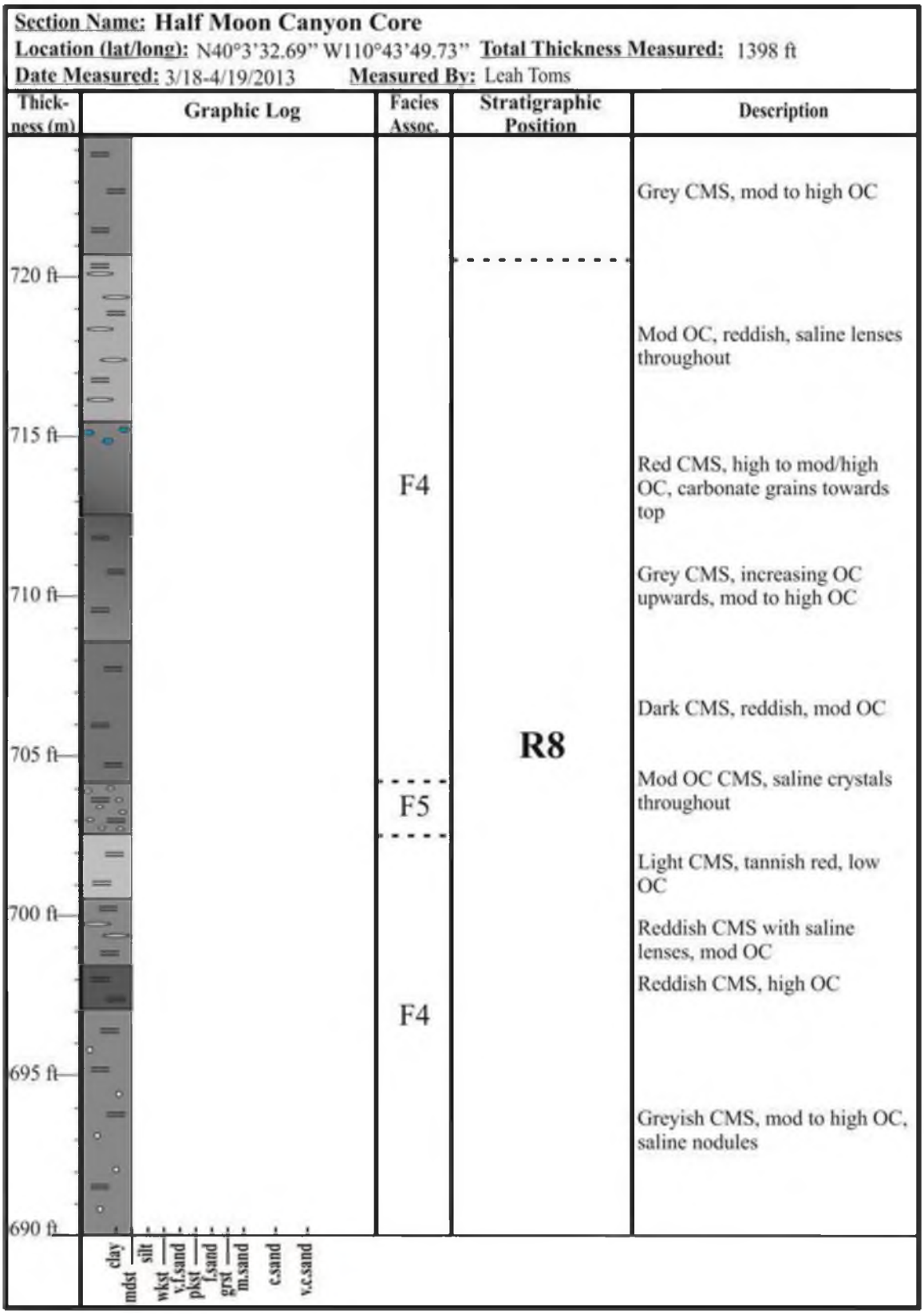
Section Name: Half Moon Canyon Core
Location (lat/long): N40°3'32.69" W110°43'49.73" Total Thickness Measured: 1398 ft
Date Measured: 3/18-4/19/2013 Measured By: Leah Toms
Thick-ness (m)
Graphic Log
Facies Assoc.
Stratigraphic Position
Description
720 ft
715 ft
710 ft
705 ft
700 ft
695 ft
690 ft
F4
F5
F4
R8
Grey CMS, mod to high OC
Mod OC, reddish, saline lenses throughout
Red CMS, high to mod/high OC, carbonate grains towards top
Grey CMS, increasing OC upwards, mod to high OC
Dark CMS, reddish, mod OC
Mod OC CMS, saline crystals throughout
Light CMS, tannish red, low OC
Reddish CMS with saline lenses, mod OC
Reddish CMS, high OC
Greyish CMS, mod to high OC, saline nodules
clay
mdst
silt
wkst
v.f.sand
pkst
f.sand
grst
m.sand
c.sand
v.c.sand

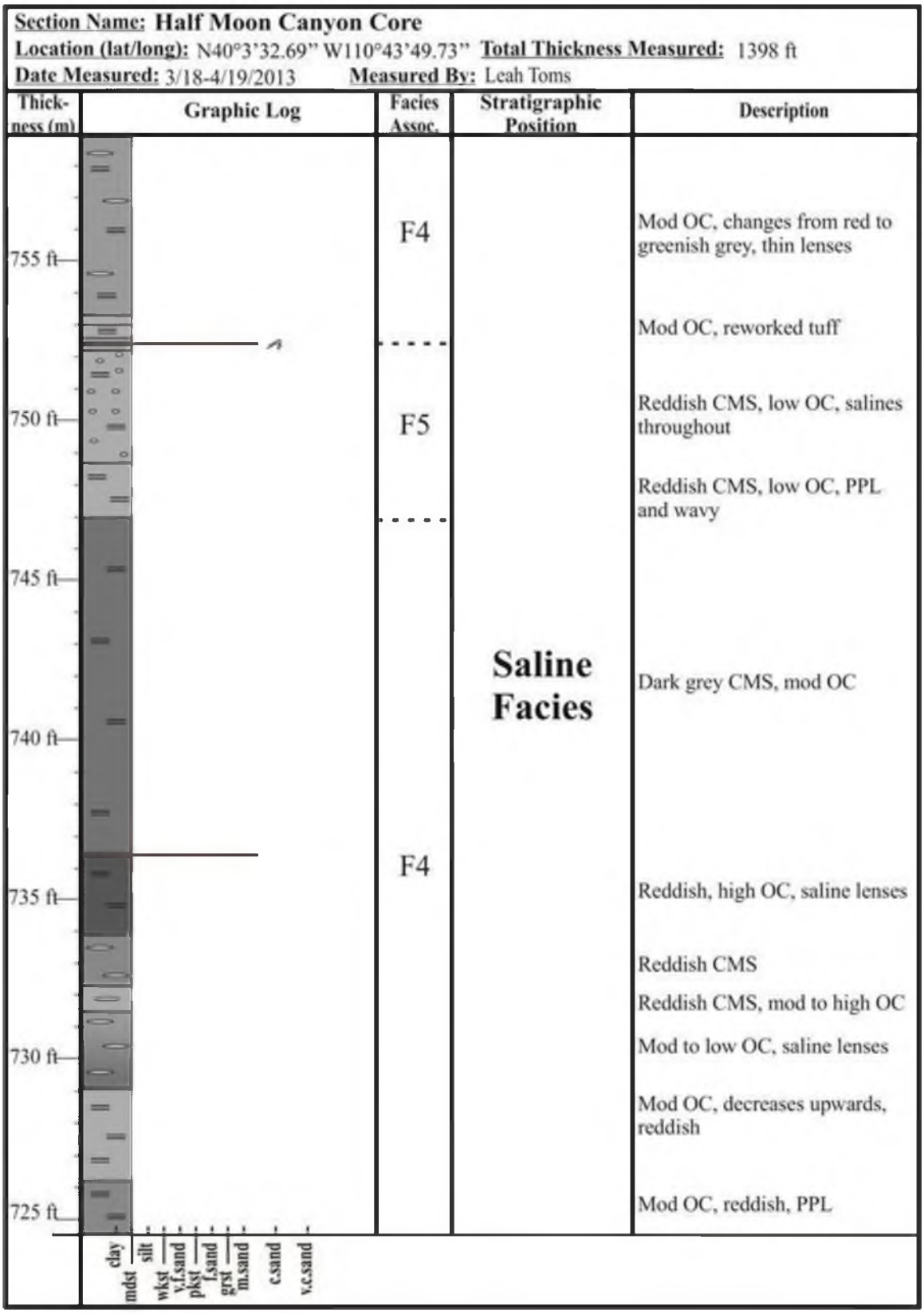
Section Name: Half Moon Canyon Core
Location (lat/long): N40°3'32.69" W110°43'49.73" Total Thickness Measured: 1398 ft
Date Measured: 3/18-4/19/2013 Measured By: Leah Toms
Thick-ness (m)
Graphic Log
Facies Assoc.
Stratigraphic Position
Description
755 ft
750 ft
745 ft
740 ft
735 ft
730 ft
725 ft
F4
F5
F4
Saline Facies
Mod OC, changes from red to greenish grey, thin lenses
Mod OC, reworked tuff
Reddish CMS, low OC, salines throughout
Reddish CMS, low OC, PPL and wavy
Dark grey CMS, mod OC
Reddish, high OC, saline lenses
Reddish CMS
Reddish CMS, mod to high OC
Mod to low OC, saline lenses
Mod OC, decreases upwards, reddish
Mod OC, reddish, PPL
clay
mdst
silt
wkst
v.f.sand
pkst
f.sand
grst
m.sand
c.sand
v.c.sand

Section Name: Half Moon Canyon Core
Location (lat/long): N40°3'32.69" W110°43'49.73" **Total Thickness Measured:** 1398 ft
Date Measured: 3/18-4/19/2013 **Measured By:** Leah Toms

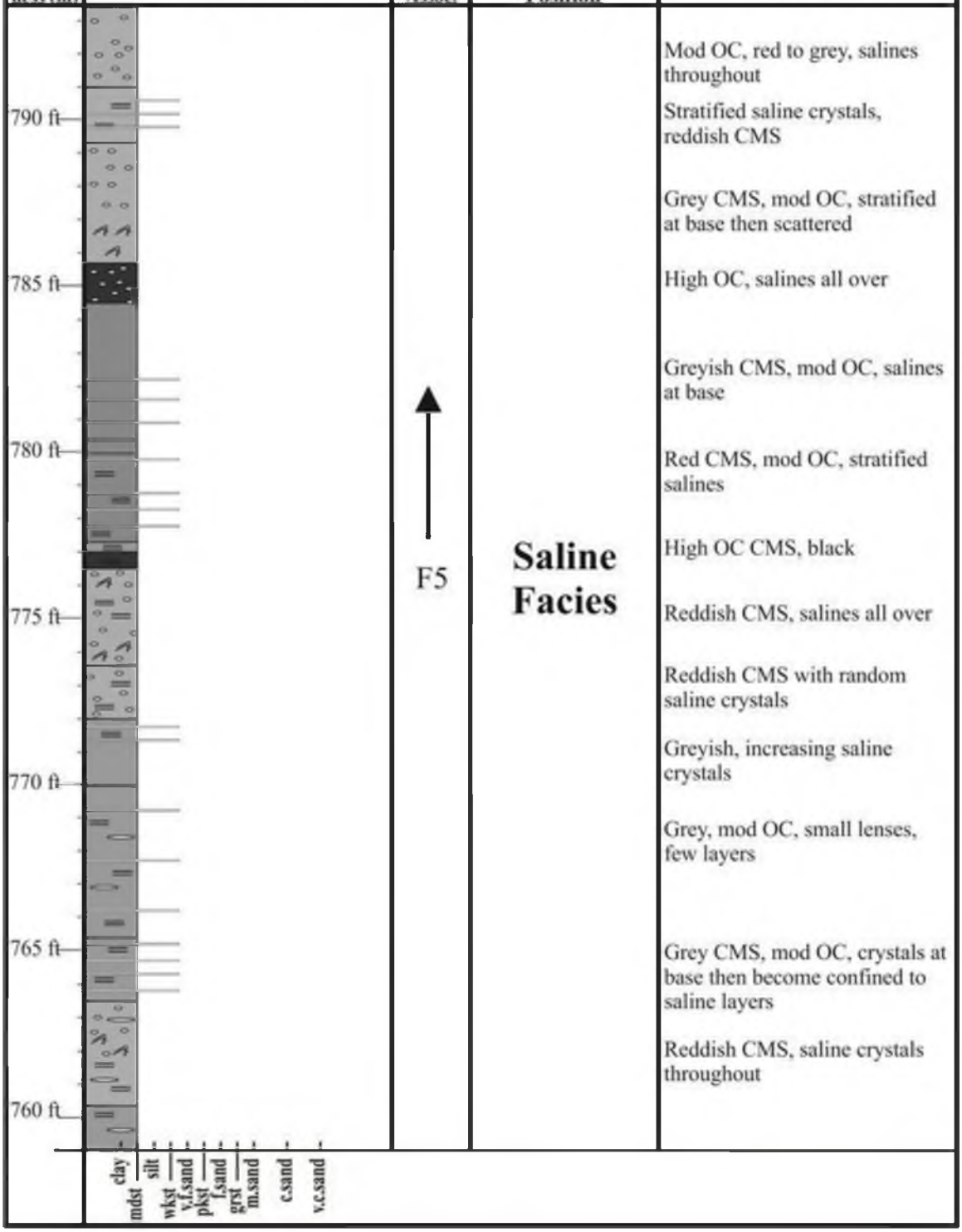

Section Name: Half Moon Canyon Core
Location (lat/long): N40°3'32.69" W110°43'49.73" **Total Thickness Measured:** 1398 ft
Date Measured: 3/18-4/19/2013 **Measured By:** Leah Toms

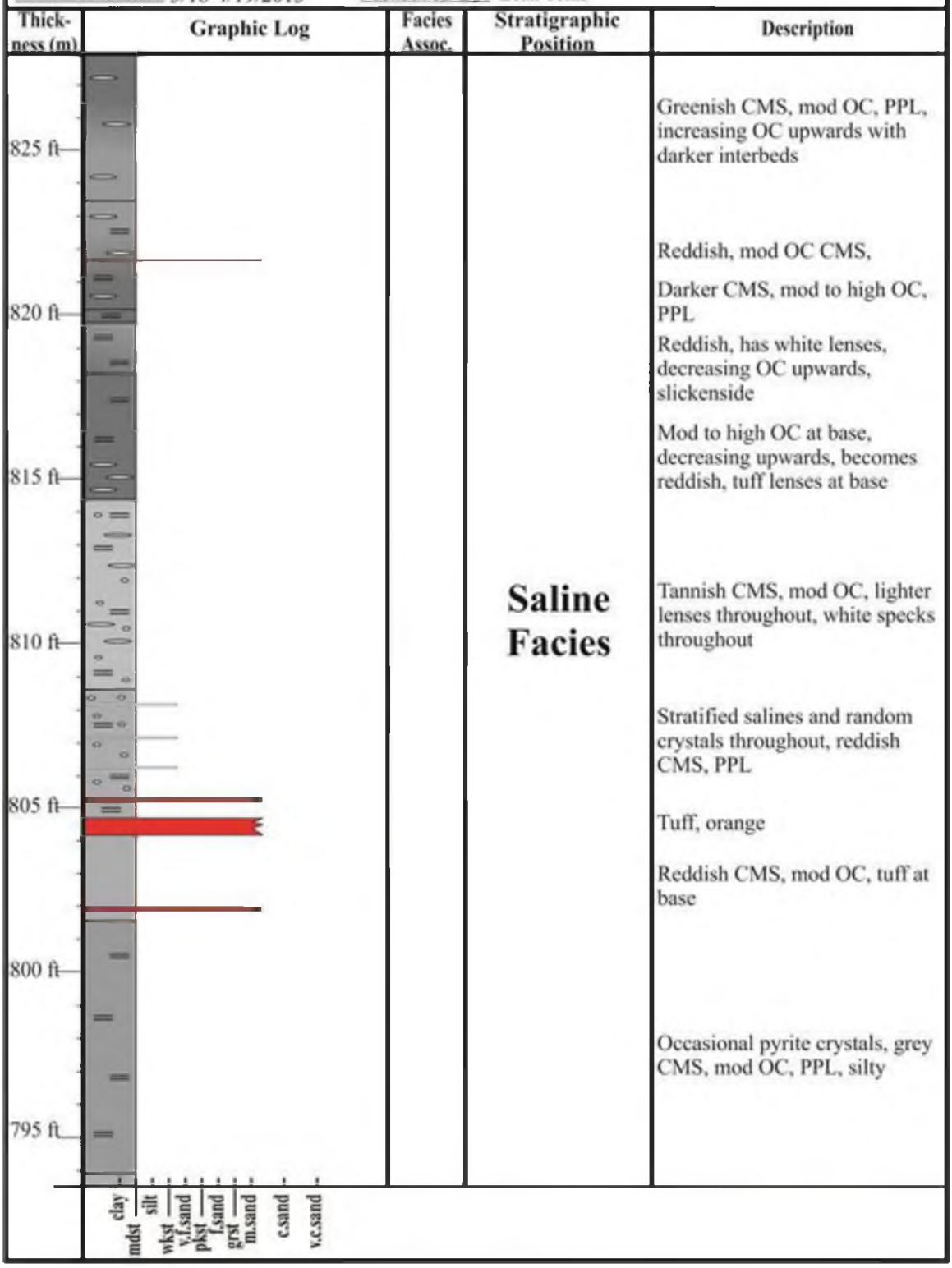

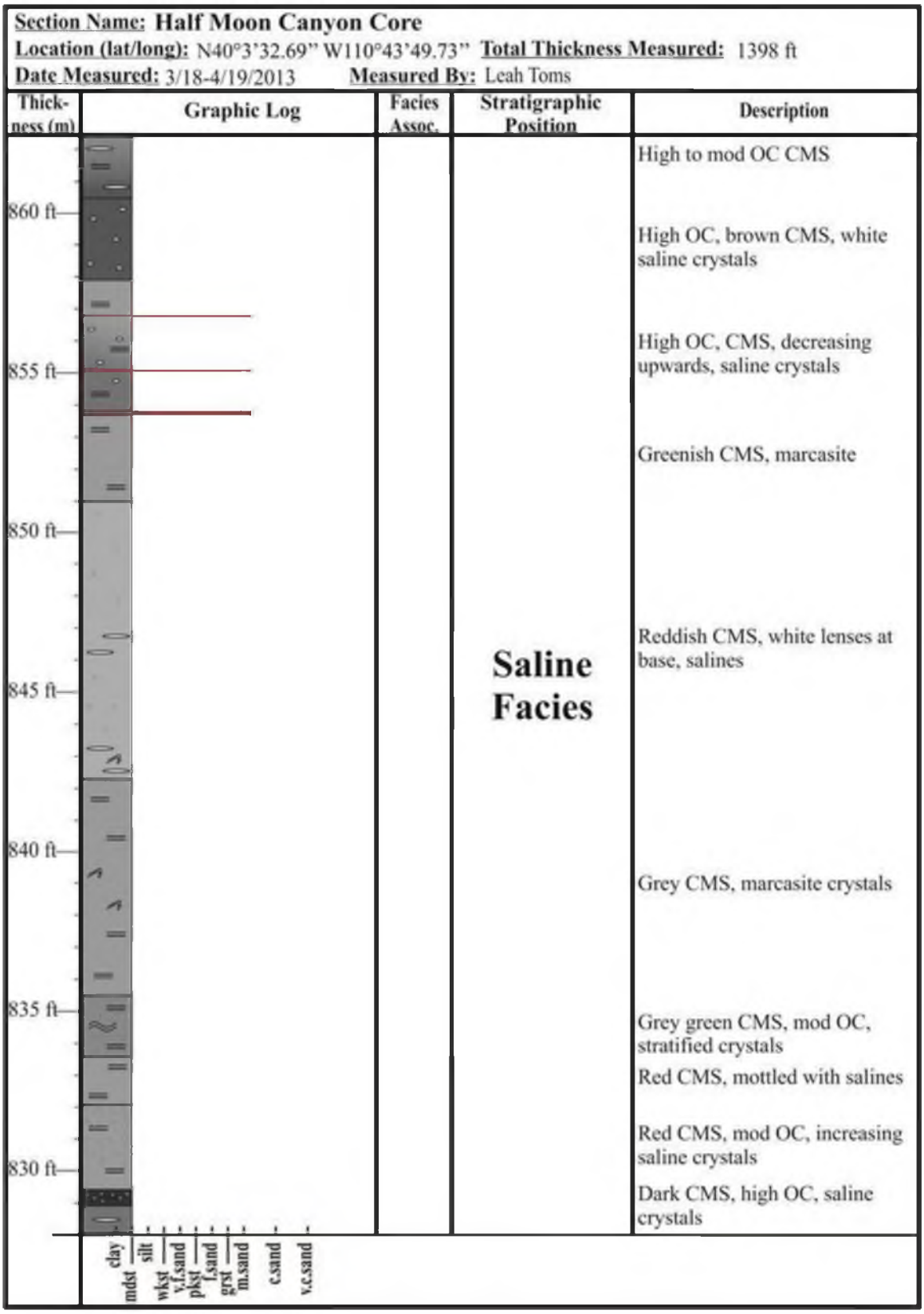
Section Name: Half Moon Canyon Core
Location (lat/long): N40°3'32.69" W110°43'49.73" Total Thickness Measured: 1398 ft
Date Measured: 3/18-4/19/2013 Measured By: Leah Toms
Thick-ness (m)
Graphic Log
Facies Assoc.
Stratigraphic Position
Description
860 ft
855 ft
850 ft
845 ft
840 ft
835 ft
830 ft
Saline Facies
High to mod OC CMS
High OC, brown CMS, white saline crystals
High OC, CMS, decreasing upwards, saline crystals
Greenish CMS, marcasite
Reddish CMS, white lenses at base, salines
Grey CMS, marcasite crystals
Grey green CMS, mod OC, stratified crystals
Red CMS, mottled with salines
Red CMS, mod OC, increasing saline crystals
Dark CMS, high OC, saline crystals
clay
mdst
silt
wkst
v.f.sand
pkst
f.sand
grst
m.sand
c.sand
v.c.sand

Section Name: Half Moon Canyon Core
Location (lat/long): N40°3'32.69" W110°43'49.73" **Total Thickness Measured:** 1398 ft
Date Measured: 3/18-4/19/2013 **Measured By:** Leah Toms

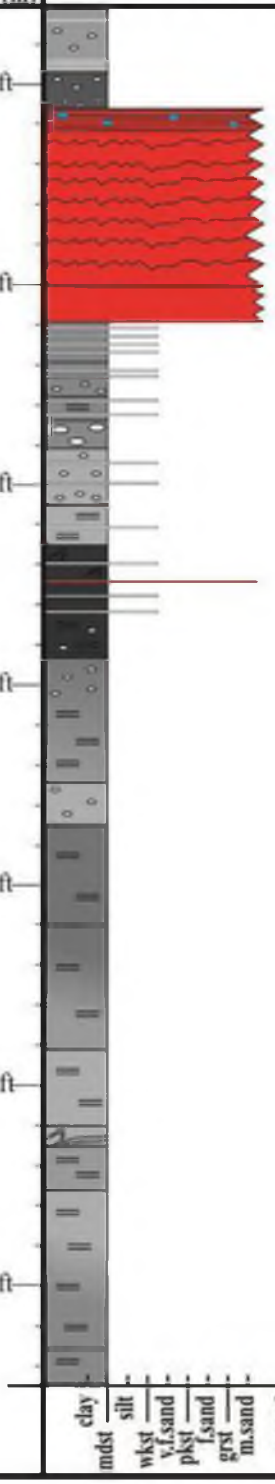

Thickness (m)	Graphic Log	Facies Assoc.	Stratigraphic Position	Description
		F6	**Saline Facies**	Mod OC CMS, stratified and crystals
				High OC CMS, saline crystals
				Carbonate clasts throughout top
				Rhyolite, large crystals, stratified going upwards (reworked/settling), towards top it becomes mixed with dark CMS
				Mod OC brown CMS, stratified crystals
				Mod OC brown CMS
				Mod OC brown, PPL
				Mod OC, brown, large voids
				Grey CMS, varies from stratified salines to crystals
				Mod OC tan CMS, PPL, no crystals
				High OC CMS, SSD
				High OC CMS, crystals to stratified salines
				Mod CMS, increasing upwards, saline crystals upwards
				Mod OC, saline crystals increase
				Mod to high OC CMS, brown, PPL
				Increasing OC upwards, mod to high
				Mod OC, tan CMS, PPL
				Grey with tan beds, cross cutting
				Grey, interbeds of lighter mud at base
				Decreasing OC upwards, from high to mod, tuff lenses
				High OC, brown CMS, white specks all over, PPL

Section Name: Half Moon Canyon Core
Location (lat/long): N40°3'32.69" W110°43'49.73" **Total Thickness Measured:** 1398 ft
Date Measured: 3/18-4/19/2013 **Measured By:** Leah Toms

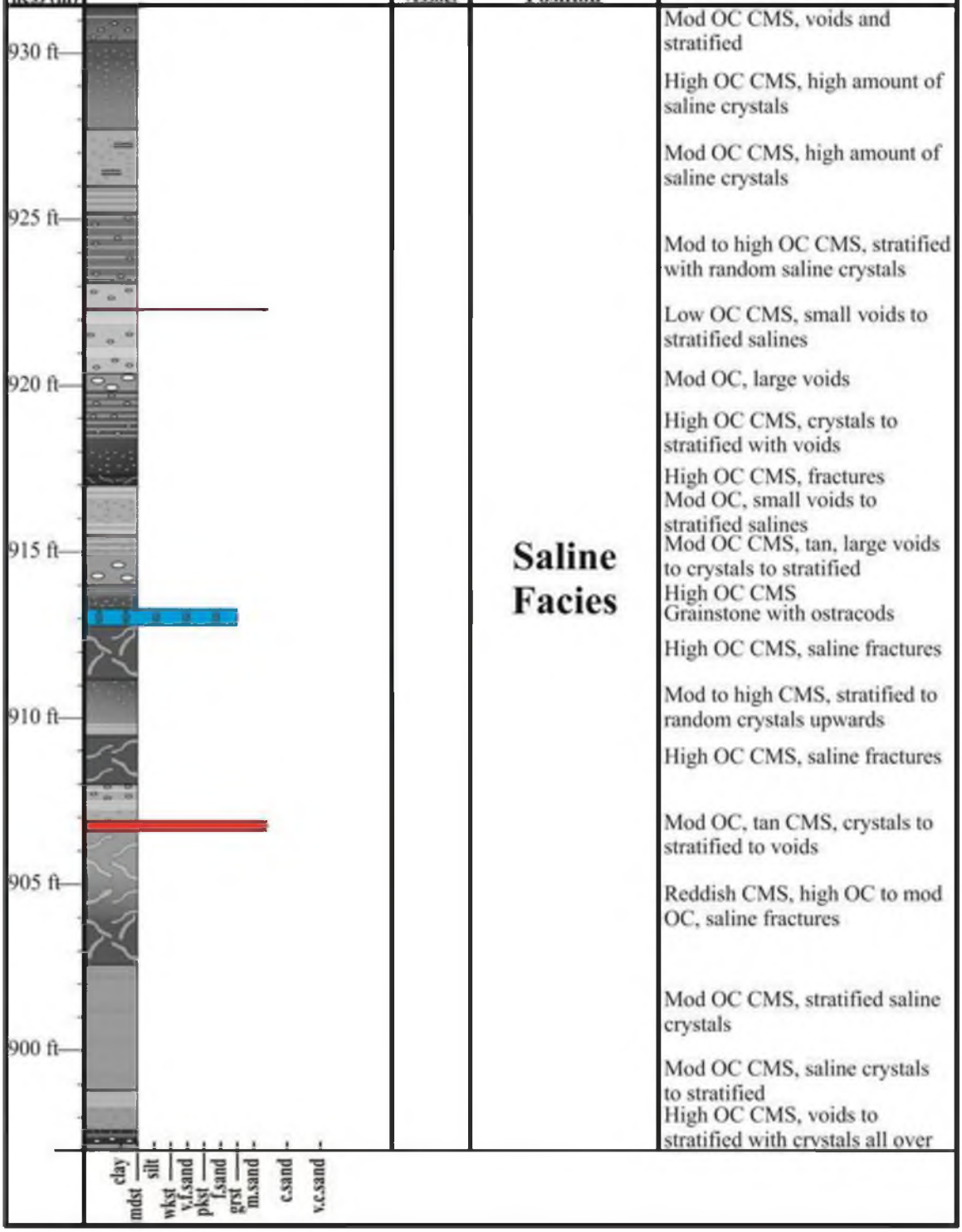

Section Name: Half Moon Canyon Core
Location (lat/long): N40°3'32.69" W110°43'49.73" **Total Thickness Measured:** 1398 ft
Date Measured: 3/18-4/19/2013 **Measured By:** Leah Toms

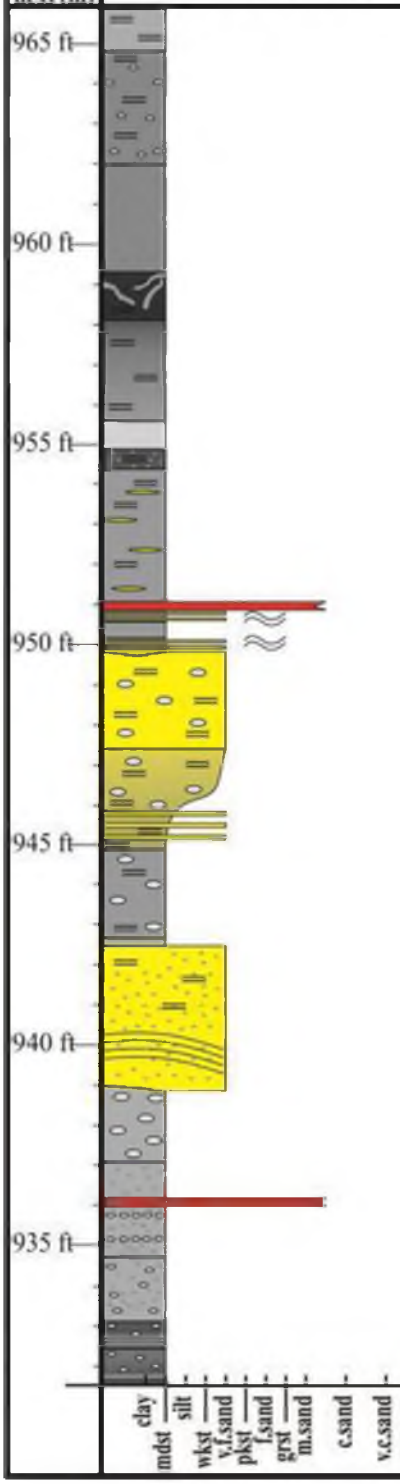

Thickness (m)	Graphic Log	Facies Assoc.	Stratigraphic Position	Description
			Saline Facies	Mod OC CMS, PPL
				Mod OC CMS, small voids
				Mod CMS with saline crystals
				Red CMS, high OC to mod, fractures
				Mod to high OC increasing upwards
				Low OC CMS
				High OC CMS, reddish, saline crystals
				Grey CMS, with mod OC, some lenses of VF SS
				Reddish, thin sandstone beds, wavy
				VF SS with large voids
				VF SS with large voids, dark sandstone
				Mod OC CMS, large voids
				VF SS, saline crystals throughout
				Mod OC CMS, large voids
				Grey CMS, crystals
				Mod OC, stratified and dense crystals
				Mod OC CMS, tan, small voids and dense crystals throughout
				Mod OC, stratified to crystals

Section Name: Half Moon Canyon Core
Location (lat/long): N40°3'32.69" W110°43'49.73" **Total Thickness Measured:** 1398 ft
Date Measured: 3/18-4/19/2013 **Measured By:** Leah Toms

Thick-ness (m)	Graphic Log	Facies Assoc.	Stratigraphic Position	Description
1000 ft	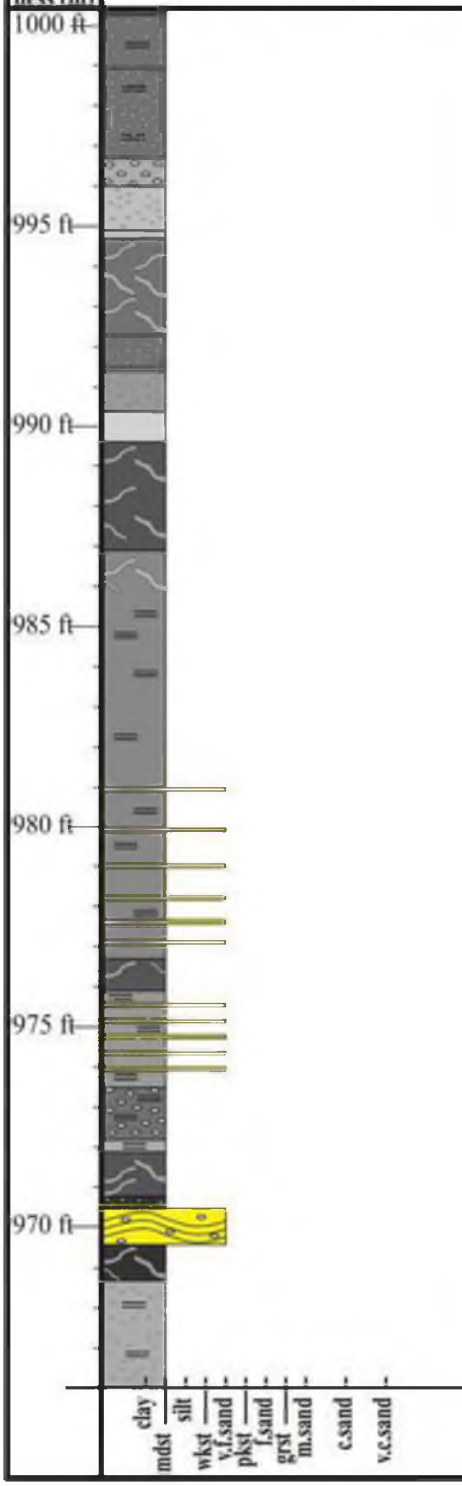		**Saline Facies**	Same as below
				High OC CMS, dense saline crystals
				Low to mod OC CMS, small voids
995 ft				Low OC CMS, saline crystals
				High OC CMS, saline fractures
				Mod to high OC CMS, saline crystals
				Mod OC CMS, saline crystals
990 ft				Low OC CMS
				Mod to high OC CMS, saline fractures
985 ft				
				Mod CMS, VF SS beds towards base, towards top is saline fractures
980 ft				
				Mod to high OC CMS, saline fractures
975 ft				Interbedded CMS and VF SS, saline crystals throughout
				Mod OC CMS, small voids, PPL
				Mod to low OC
				Mod OC, saline fractures
				Red mudstone, high OC, salines
970 ft				Wavy bedded, VF SS, voids
				Dark CMS, saline fractures
				Mod to low OC, saline crystals

clay mdst silt wkst v.f.sand pkst f.sand grst m.sand c.sand v.c.sand

Section Name: Half Moon Canyon Core
Location (lat/long): N40°3'32.69" W110°43'49.73" **Total Thickness Measured:** 1398 ft
Date Measured: 3/18-4/19/2013 **Measured By:** Leah Toms

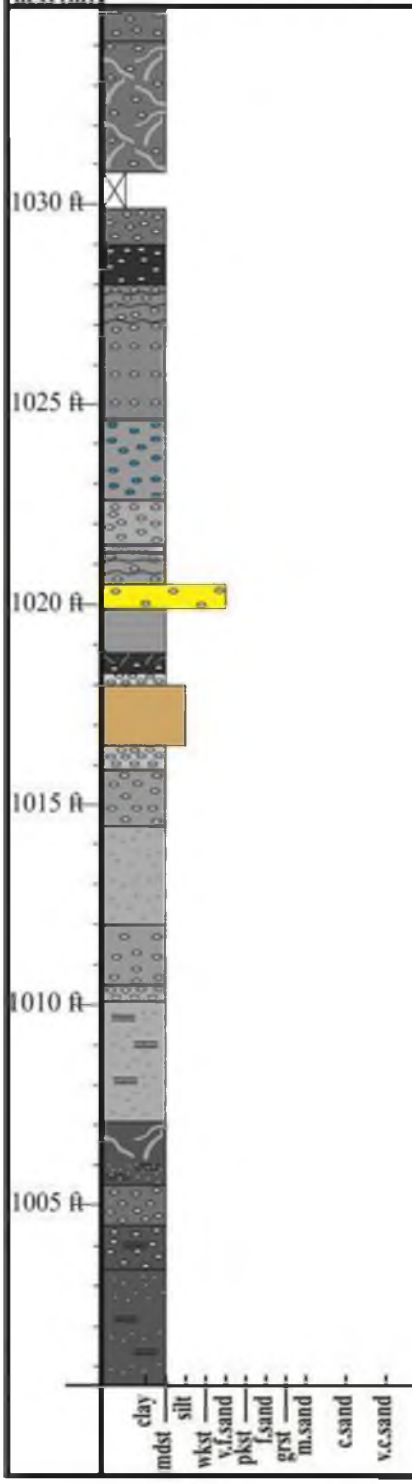

Thickness (m)	Graphic Log	Facies Assoc.	Stratigraphic Position	Description
			Saline Facies	High OC CMS, small voids
				Mod to high OC CMS, saline fractures
				Mod OC CMS, small voids and fractures
				High OC CMS, small voids
				Interbedded red CMS with saline voids
				Reddish CMS, carbonate clasts throughout
				Mod OC CMS, small voids
				Reddish CMS with small voids
				VF SS, saline voids throughout
				Red CMS
				Dark CMS, high OC with small voids
				Reddish, silty CMS, marcasite
				Low OC CMS, small voids
				Mod OC CMS, small voids
				Mod OC CMS, dense saline crystals
				Mod OC CMS, small voids
				Low OC CMS, small voids
				Low OC CMS, dense crystals
				Mod to high OC CMS, saline fractures
				Mod OC CMS, small voids
				Mod to high OC CMS, small voids
				High OC CMS, layers of saline crystals

Section Name: Half Moon Canyon Core
Location (lat/long): N40°3'32.69" W110°43'49.73" **Total Thickness Measured:** 1398 ft
Date Measured: 3/18-4/19/2013 **Measured By:** Leah Toms

Thick-ness (m)	Graphic Log	Facies Assoc.	Stratigraphic Position	Description
1065 ft			**Saline Facies**	Reddish CMS, mod OC Mod to high OC CMS Mod to high OC CMS, saline fractures Reddish CMS, dense saline crystals Mod OC CMS, reddish Mod OC CMS, dense saline crystals Reddish CMS, saline fractures Reddish CMS, dense saline crystals Mod to high OC CMS, dense crystals Mod OC CMS, dense crystals Mod OC CMS, carbonate grains Reddish CMS, saline fractures, mod OC Mod OC CMS Mod OC CMS, saline fractures Grey CMS, dense saline crystals, PPL, carbonate clasts Mod OC CMS, dense saline crystals Mod OC CMS, small voids Low OC CMS, small voids Mod OC CMS, dense saline crystals
1060 ft				
1055 ft				
1050 ft				
1045 ft				
1040 ft				
1035 ft				

Section Name: Half Moon Canyon Core
Location (lat/long): N40°3'32.69" W110°43'49.73" **Total Thickness Measured:** 1398 ft
Date Measured: 3/18-4/19/2013 **Measured By:** Leah Toms

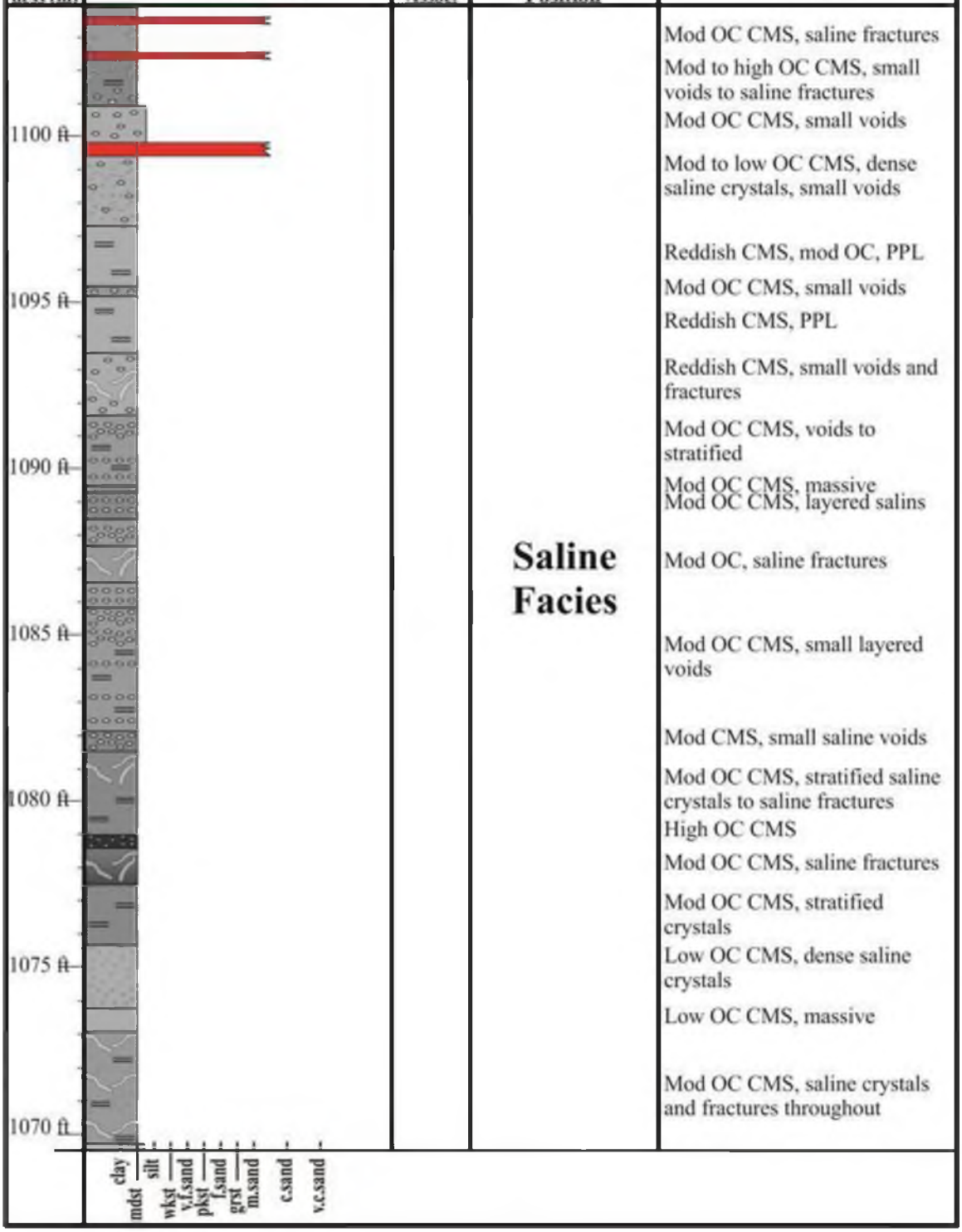

Thick-ness (m)	Graphic Log	Facies Assoc.	Stratigraphic Position	Description
				Mod OC CMS, saline fractures
				Mod to high OC CMS, small voids to saline fractures
				Mod OC CMS, small voids
				Mod to low OC CMS, dense saline crystals, small voids
				Reddish CMS, mod OC, PPL
				Mod OC CMS, small voids
				Reddish CMS, PPL
				Reddish CMS, small voids and fractures
				Mod OC CMS, voids to stratified
				Mod OC CMS, massive
				Mod OC CMS, layered salins
			Saline Facies	Mod OC, saline fractures
				Mod OC CMS, small layered voids
				Mod CMS, small saline voids
				Mod OC CMS, stratified saline crystals to saline fractures
				High OC CMS
				Mod OC CMS, saline fractures
				Mod OC CMS, stratified crystals
				Low OC CMS, dense saline crystals
				Low OC CMS, massive
				Mod OC CMS, saline crystals and fractures throughout

Section Name: Half Moon Canyon Core
Location (lat/long): N40°3'32.69" W110°43'49.73" **Total Thickness Measured:** 1398 ft
Date Measured: 3/18-4/19/2013 **Measured By:** Leah Toms

Thickness (m)	Graphic Log	Facies Assoc.	Stratigraphic Position	Description
	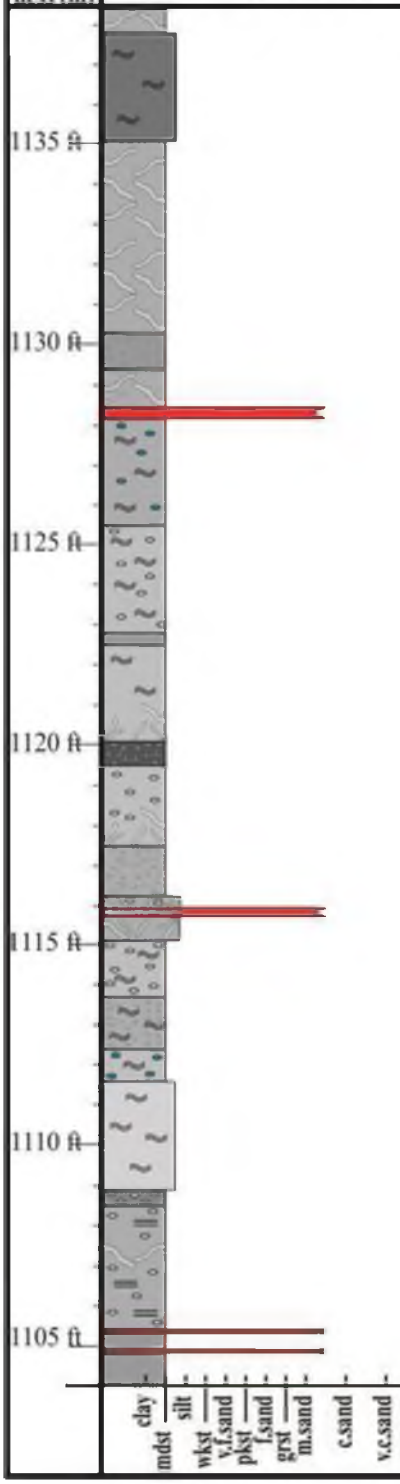		**Saline Facies**	Greyish orange bed (oxidized), possibly volcanic or CMS
				Mod to low OC CMS, saline fractures
				Mod OC CMS, dense saline crystals
				Grey, mod to low OC, saline fractures
				Grey CMS, mod to low OC, wavy laminations, carbonate clasts
				Low OC CMS, voids, wavy lams
				Mod OC CMS, massive
				Mod to low OC CMS, fractures to wavy lams
				High OC CMS, saline crystals
				Low OC CMS, fractures to voids
				Mod OC CMS, saline fractures and voids
				Mod to low OC CMS, voids and wavy lams
				Mod OC CMS, saline crystals
				Low OC CMS, wavy, carbonate clasts
				Low OC CMS mixed with volcanics, wavy
				Mod OC CMS, small voids
				Mod OC CMS, voids and fractures
				Mod OC CMS, massive

Section Name: Half Moon Canyon Core
Location (lat/long): N40°3'32.69" W110°43'49.73" **Total Thickness Measured:** 1398 ft
Date Measured: 3/18-4/19/2013 **Measured By:** Leah Toms

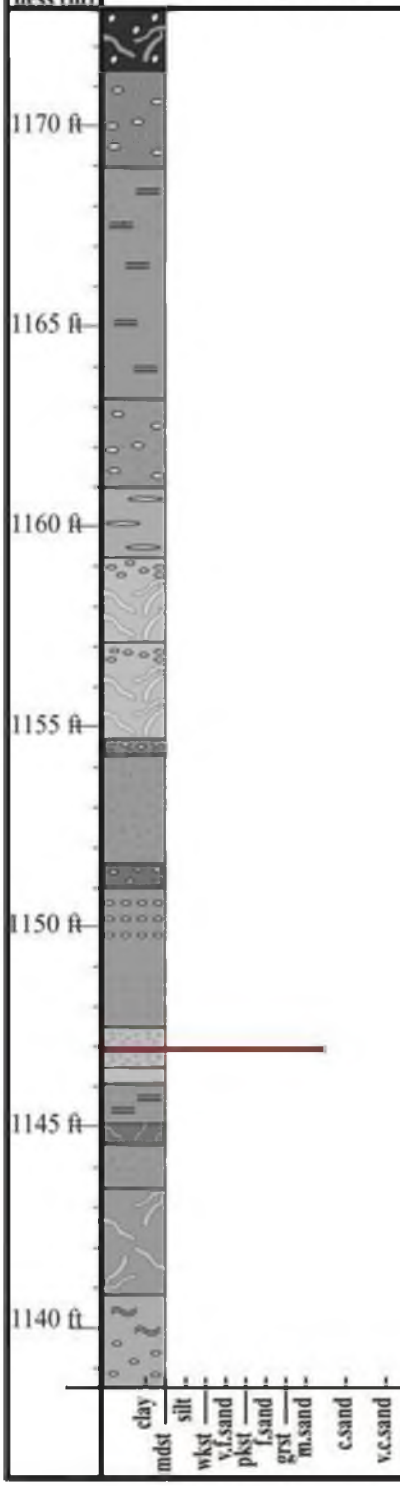

Thickness (m)	Graphic Log	Facies Assoc.	Stratigraphic Position	Description
				High OC CMS, euhedral saline clasts
1170 ft				Mod OC CMS, small voids and saline crystals
				Reddish CMS, PPL, increase in saline crystals upwards
1165 ft				
				Greyish red CMS, saline crystals and saline voids
1160 ft				Greyish CMS, low OC, saline lenses
				Same as below
			Saline Facies	Low OC CMS, saline fractures to small voids
1155 ft				Grey, mod to high OC, orange concretions
				Reddish CMS, mod OC, saline crystals
				Grey, mod to high OC CMS, small voids
1150 ft				Mod OC CMS, small layered saline crystals at base to small voids at top
				Grey CMS with saline crystals
				Greyish CMS
1145 ft				Reddish CMS, stratified saline
				Mod OC CMS, saline fractures
				Mod OC CMS, saline crystals
				Mod OC CMS, saline fractures
1140 ft				Mod to low OC CMS, fractures at base, then small saline voids then wavy laminations

Section Name: Half Moon Canyon Core
Location (lat/long): N40°3'32.69" W110°43'49.73" **Total Thickness Measured:** 1398 ft
Date Measured: 3/18-4/19/2013 **Measured By:** Leah Toms

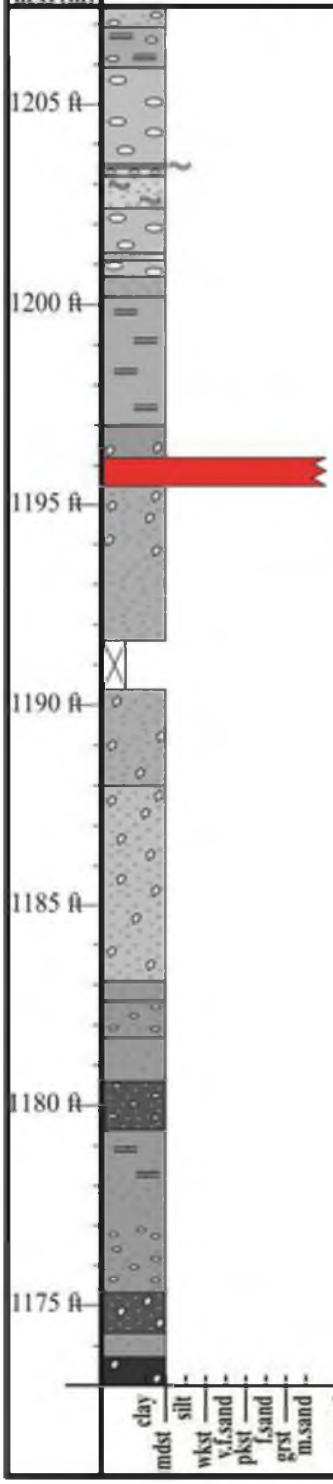

Thick-ness (m)	Graphic Log	Facies Assoc.	Stratigraphic Position	Description
			Saline Facies	Mod OC CMS, reddish, small voids
				Low OC CMS, large voids
				Low OC CMS, wavy, saline crystals
				Mod to low OC CMS, large voids
				Reddish CMS, saline crystals
				Grey to reddish mod OC CMS
				Same as below tuff
				Volcanic, tar inside
				Mod OC CMS, saline crystals, euhedral crystals also
				Mod OC CMS, saline crystals, euhedral crystals
				Mod to low OC CMS, saline crystals and euhedral crystals throughout
				Mod OC CMS, saline crystals
				Mod OC CMS, saline crystals and voids
				Mod OC CMS, saline crystals
				High OC CMS, saline voids, crystals
				Reddish, small saline voids at base, saline crystals throughout
				Black, high OC CMS, euhedral salines
				Low to mod OC, reddish
				High OC CMS, euhedral salines

Section Name: Half Moon Canyon Core
Location (lat/long): N40°3'32.69" W110°43'49.73" **Total Thickness Measured:** 1398 ft
Date Measured: 3/18-4/19/2013 **Measured By:** Leah Toms

Thickness (m)	Graphic Log	Facies Assoc.	Stratigraphic Position	Description
1240 ft	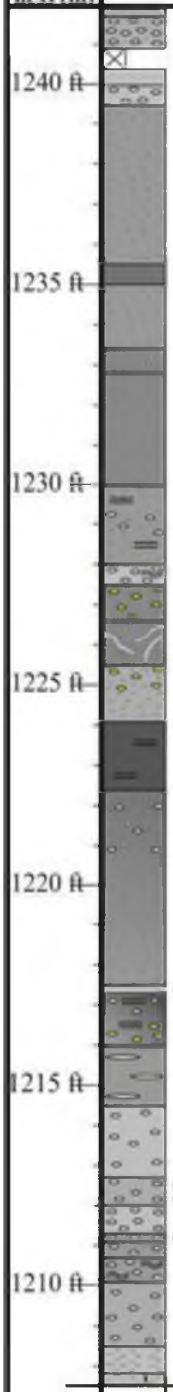		**Saline Facies**	Mod OC CMS, small voids Grey CMS, low OC Grey CMS, low OC, small voids Grey CMS, mod OC, saline crystals Grey CMS, mod to high OC
1235 ft				Grey CMS, mod OC, saline crystals Moderate OC CMS, layers of saline crystals Mod OC CMS, layers of saline crystals
1230 ft				Mod to low OC, saline crystals and voids Low OC CMS, small voids Mod OC CMS, siliciclastics Mod OC CMS, saline fractures
1225 ft				Low to mod OC CMS, saline crystals throughout Grey CMS, high OC, decreasing upwards
1220 ft				Reddish to grey CMS, increasing OC upwards, saline crystals throughout
1215 ft				Mod to high OC CMS, increasing upwards Greyish CMS, mod OC, saline lenses Grey CMS with small voids
1210 ft				Mod OC CMS, wavy, small voids Mod to low OC CMS, small voids Low OC CMS, saline crystals

Section Name: Half Moon Canyon Core
Location (lat/long): N40°3'32.69" W110°43'49.73" **Total Thickness Measured:** 1398 ft
Date Measured: 3/18-4/19/2013 **Measured By:** Leah Toms

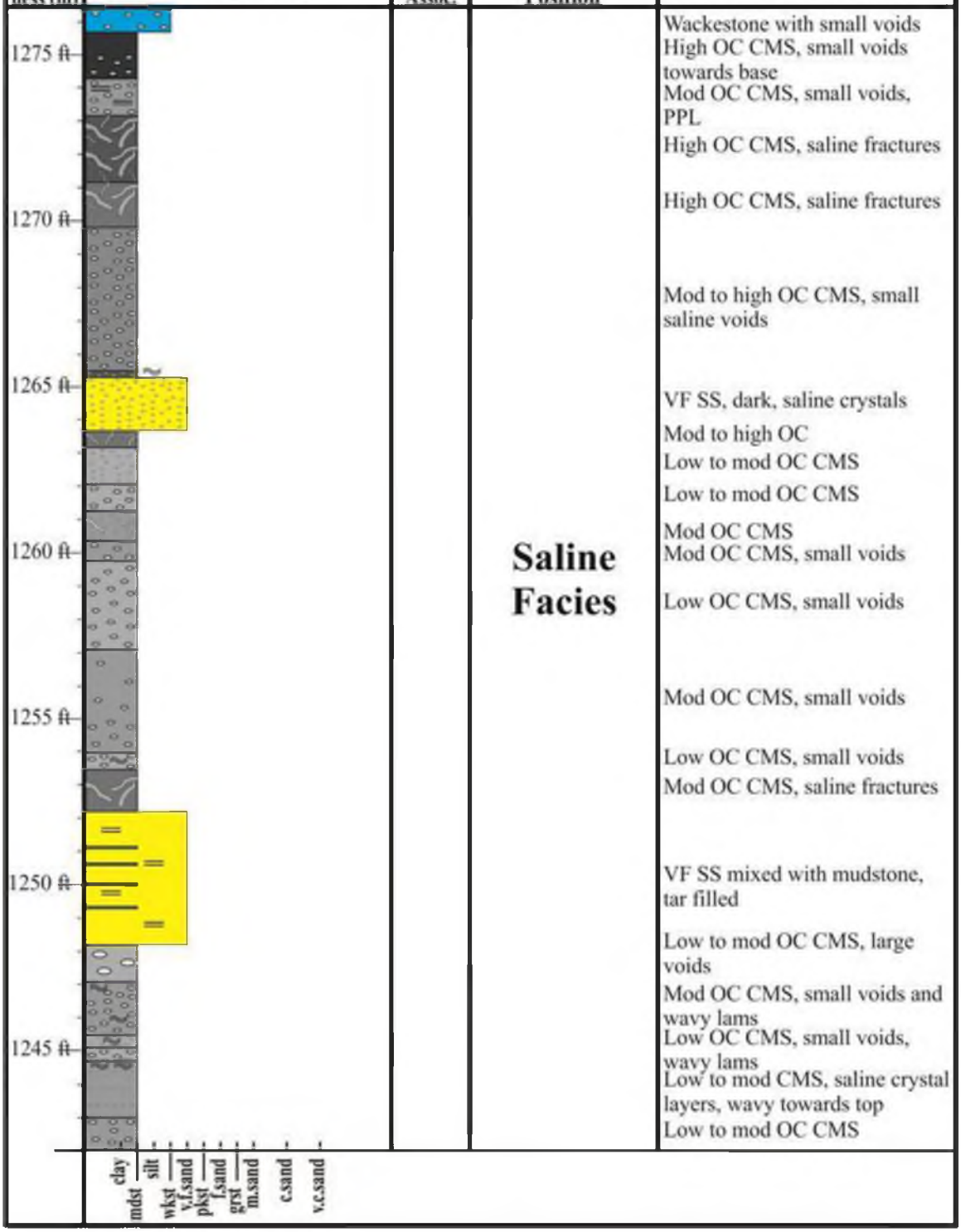

Section Name: Half Moon Canyon Core
Location (lat/long): N40°3'32.69" W110°43'49.73" **Total Thickness Measured:** 1398 ft
Date Measured: 3/18-4/19/2013 **Measured By:** Leah Toms

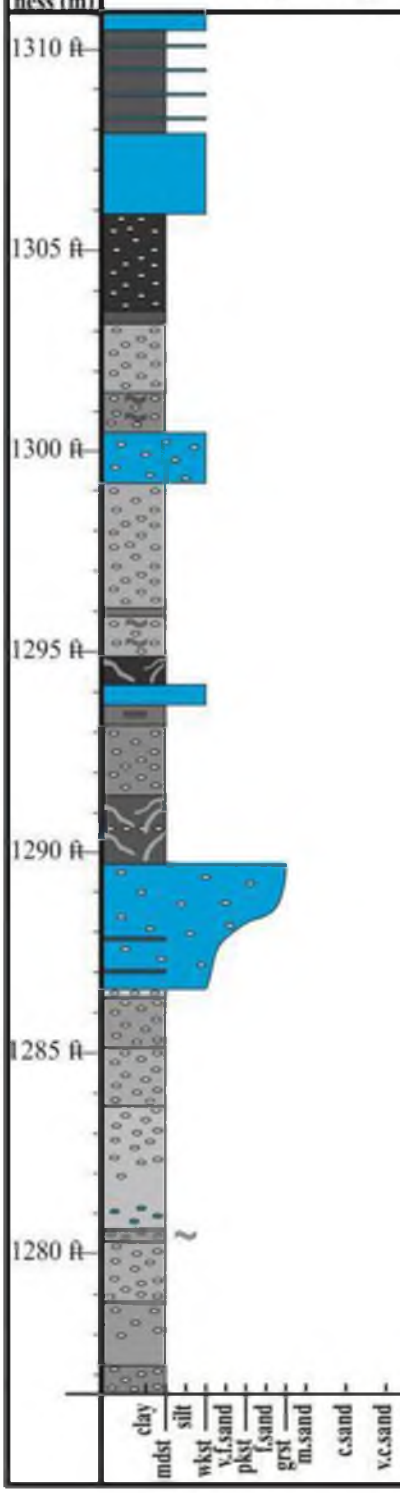

Thickness (m)	Graphic Log	Facies Assoc.	Stratigraphic Position	Description
			Saline Facies	High OC CMS, wackestone beds
				Wackestone
				High OC CMS, small voids
				High OC CMS
				Mod to low OC CMS, small voids
				Mod OC CMS, wavy
				Wackestone, orange mottles throughout
				Mod to low OC CMS, small voids
				Mod OC CMS, small saline voids, wavy
				High OC CMS, saline fractures
				Wackestone
				Moderate to high OC CMS
				High OC CMS, small voids of salines
				High OC CMS, small fractures, saline crystal layer in middle
				Grainstone, small voids throughout
				Mod to low OC CMS, small voids
				Mod to low OC with small saline voids
				Low OC CMS, carbonate clasts towards base and saline voids towards top
				Mod OC CMS, small voids, wavy
				Mod OC CMS, small voids
				Reddish CMS, lenses of carbonate

Section Name: Half Moon Canyon Core
Location (lat/long): N40°3'32.69" W110°43'49.73" **Total Thickness Measured:** 1398 ft
Date Measured: 3/18-4/19/2013 **Measured By:** Leah Toms

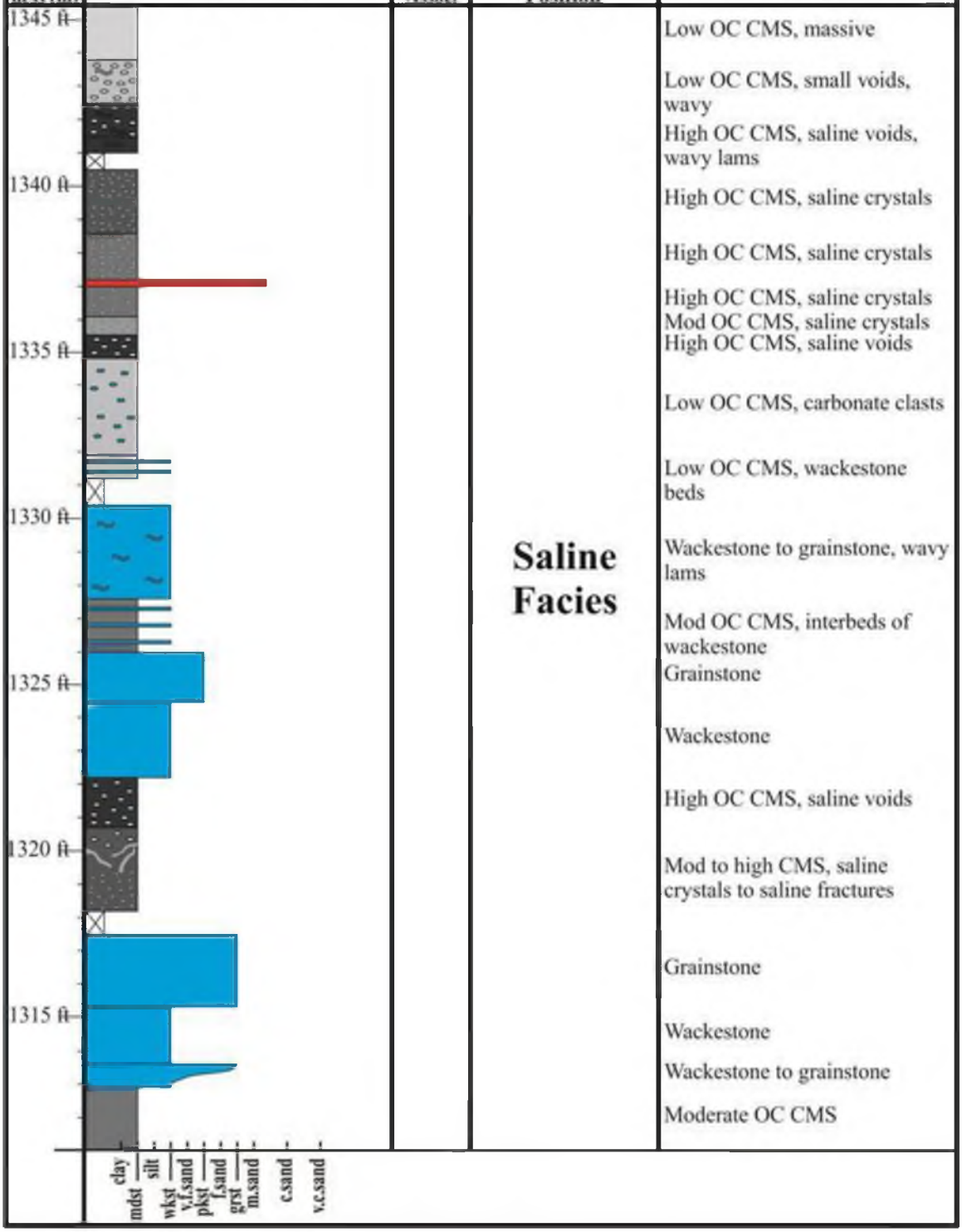

Section Name: Half Moon Canyon Core
Location (lat/long): N40°3'32.69" W110°43'49.73" **Total Thickness Measured:** 1398 ft
Date Measured: 3/18-4/19/2013 **Measured By:** Leah Toms

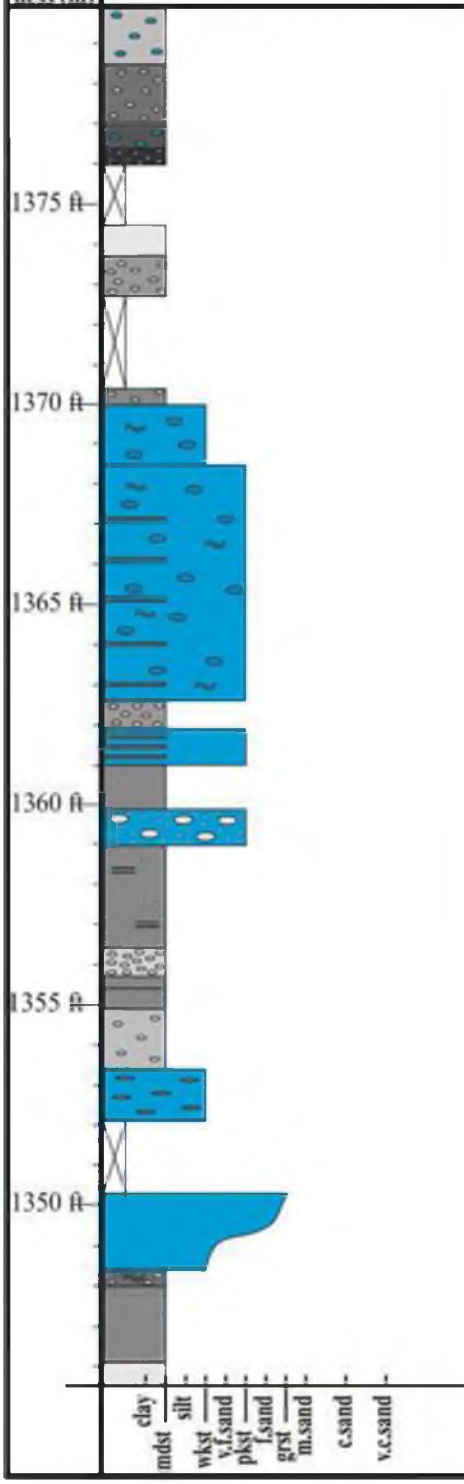

Thickness (m)	Graphic Log	Facies Assoc.	Stratigraphic Position	Description
			Saline Facies	Mod OC CMS with carbonate clasts
				Dark CMS with small saline voids
				Dark CMS, high OC, saline crystals to carbonate clasts
				Low OC CMS, massive, white
				Mod OC CMS, small voids
				Mod OC CMS, small voids
				Wackestone with wavy laminations and carbonate clasts
				Grainstone, carbonate clasts and wavy laminations, interbeds CMS
				Mod OC CMS, small voids
				Grainstone with lenses of CMS
				Mod CMS, massive
				Grainstone with large saline voids
				Mod OC CMS, dense saline crystals
				Low OC CMS, small voids
				Mod OC CMS, saline crystals
				Greyish CMS, orange mottles
				Wackestone with muddy lenses
				White, wackestone to grainstone
				Mod OC CMS, wavy, saline voids
				Mod OC CMS, stratified saline crystals

Section Name: Half Moon Canyon Core
Location (lat/long): N40°3'32.69" W110°43'49.73" **Total Thickness Measured:** 1398 ft
Date Measured: 3/18-4/19/2013 **Measured By:** Leah Toms

Thick-ness (m)	Graphic Log	Facies Assoc.	Stratigraphic Position	Description
1410 ft				
1405 ft				
1400 ft				
1395 ft	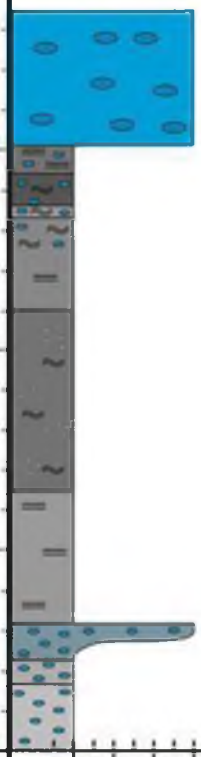		**Saline Facies**	Grainstone with carbonate clasts, whitish tan High OC CMS, carbonate clasts, PPL High OC CMS, carbonate clasts, wavy Mod OC CMS, PPL to wavy laminations, carbonate clasts towards top Mod to high OC CMS, wavy lams, mottles of saline crystals
1390 ft				
1385 ft				Mod OC CMS, PPL CMS to grainstone, carbonate clasts Low to mod OC CMS, carb clasts Low OC CMS, carbonate clasts
1380 ft	clay, silt, mdst, wkst, v.f.sand, pkst, f.sand, grst, m.sand, c.sand, v.c.sand			

APPENDIX C

THIN SECTIONS FROM HENDERSON 3 CORE

Appendix C contains descriptions of the 16 thin sections from the Henderson 3 core. A table is provided that summarizes the thin sections and photomicrographs are included that highlight major observations in each thin section (Table 4, Figures 35 and 36).

Table 4 – Thin section descriptions.

Thin Section Information				
Sample #	Section Depth	Strat. Unit	Lithology	Matrix
1	354.6 ft	S2 S.S.	Fine sandstone with dark mudstone	5-40% micrite
2	352 ft	S2 S.S.	Dark mudstone with very fine sandstone lenses	20-100% micrite
3	319 ft	S2 S.S.	Dark mudstone with very fine sandstone lenses	80% micrite
4	295 ft	S2 S.S.	White/green carb. mudstone	95% micrite
5	264 ft	Mahogany Zone	Tan carb.mudstone, moderately organic	85% micrite
6	226 ft	Mahogany Zone	Dark carb.mudstone, organic rich	90% micrite
7	224.2 ft	Mahogany Zone	Dark carb.mudstone, organic rich with dolomite	60-80% micrite
8	205.5 ft	Mahogany Zone	Tan carb.mudstone, moderately organic	80% micrite

Grain Types				Facies
Quartz	Skeletal Carb.	Non-skeletal Carb.	Other	
Yes	Ostracod debris	Minor dolomite	–	F1.2
Yes	Ostracod debris	–	Micrite clasts	F1.2
Yes	Ostracod debris	Yes, minor	–	F1.2
Yes, minor	Ostracod debris	Abundant dolomite	–	F3.3
Yes	Ostracod debris, minor	Yes, minor	–	F3.3
Yes, minor	–	Precipitated carb. nodules	Micrite clasts	F4.1
Yes, minor	Ostracod debris, minor	Yes, dolomite	Algal mats	F4.1
Yes	Ostracod debris, minor	–	Algal pellets	F4.1

Table 4 – Continued

Thin Section Information			
Sample #	Section Depth	Strat. Unit	Lithology
9	139 ft	S1 S.S.	Dark carb.mudstone, organic rich with saline crystals
10	128.5 ft	S1 S.S.	VF S.S. with organic rich mudstone
11	113.5 ft	S1 S.S.	VF S.S. in organic rich mudstone
12	107 ft	C4	Tan carb.mudstone, moderately organic, lenses of sandstone
13	64 ft	C4	Tan carb.mudstone, moderately organic, carbonate grains
14	16.5 ft	C4	Tan carb.mudstone, moderately organic, marcasite
15	15.5 ft	C4	Tan carb.mudstone, low organic content, marcasite
16	7 ft	C4	Wackestone, rip ups, organic rich lenses

Grain Types					Facies
Matrix	Quartz	Skeletal Carb.	Non-skeletal Carb.	Other	
90% micrite	Yes	Ostracod debris, minor	–	Salines, marcasite	F4.1
< 10% micrite	Yes	Ostracod debris, minor	–	–	F1.2
40% micrite	Yes	Ostracod debris, minor	Yes	–	F1.2
> 90% micrite	Yes	–	–	–	F3.3
50-95 % micrite	Yes	Ostracod debris	Yes, ooids	Micrite clasts	F3.2
80-100 % micrite	Yes	Ostracod debris, minor	–	–	F3.3
50-100 % micrite	Yes	Ostracod debris, minor	–	Marcasite	F3.3
20-85 % micrite	Yes	Ostracod debris	Ooids, stromatolite debris	Micrite clasts	F3.2

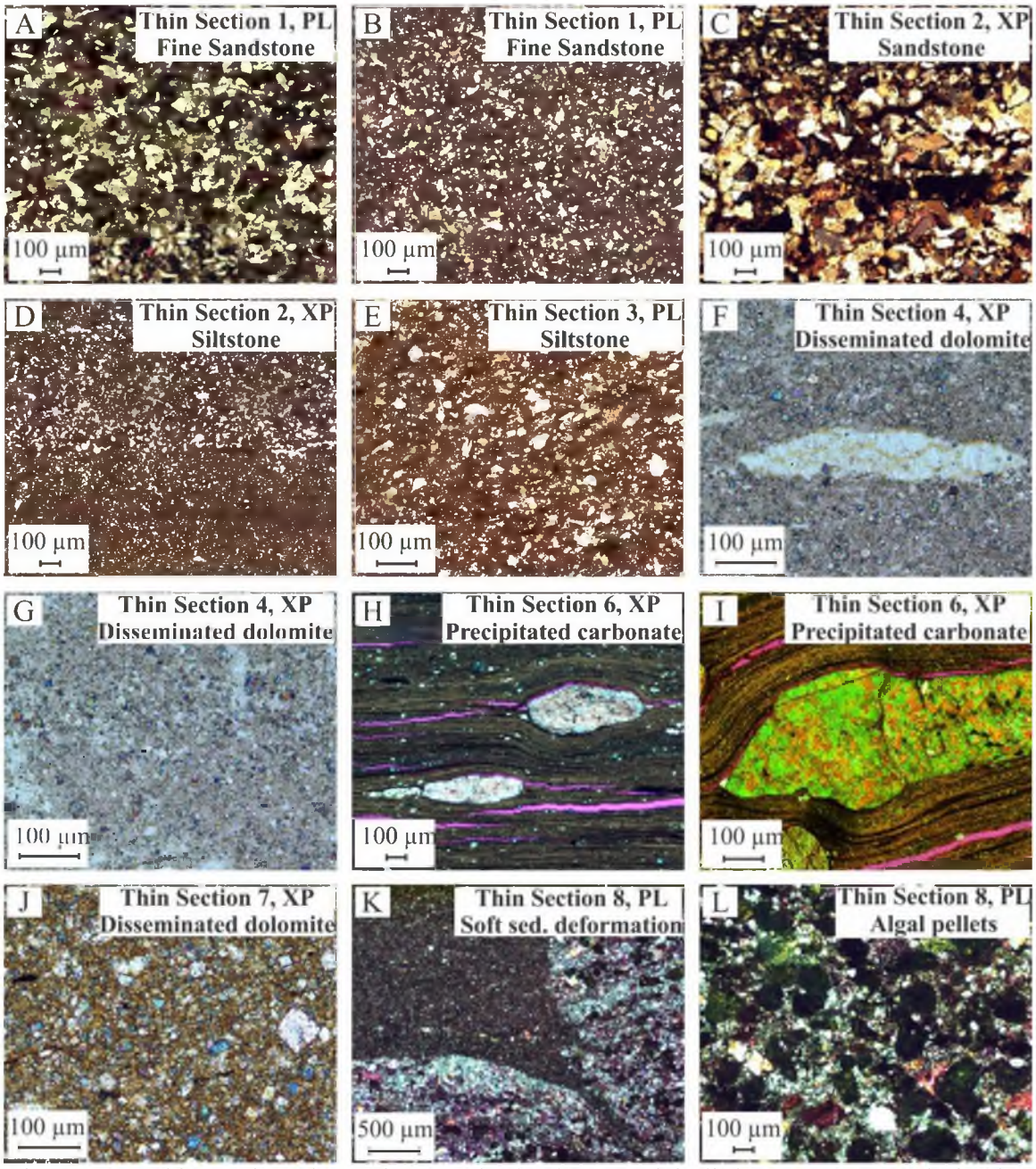

Figure 35 – Thin section photomicrographs (1-8); PL - plain light, XP - cross polarized light.

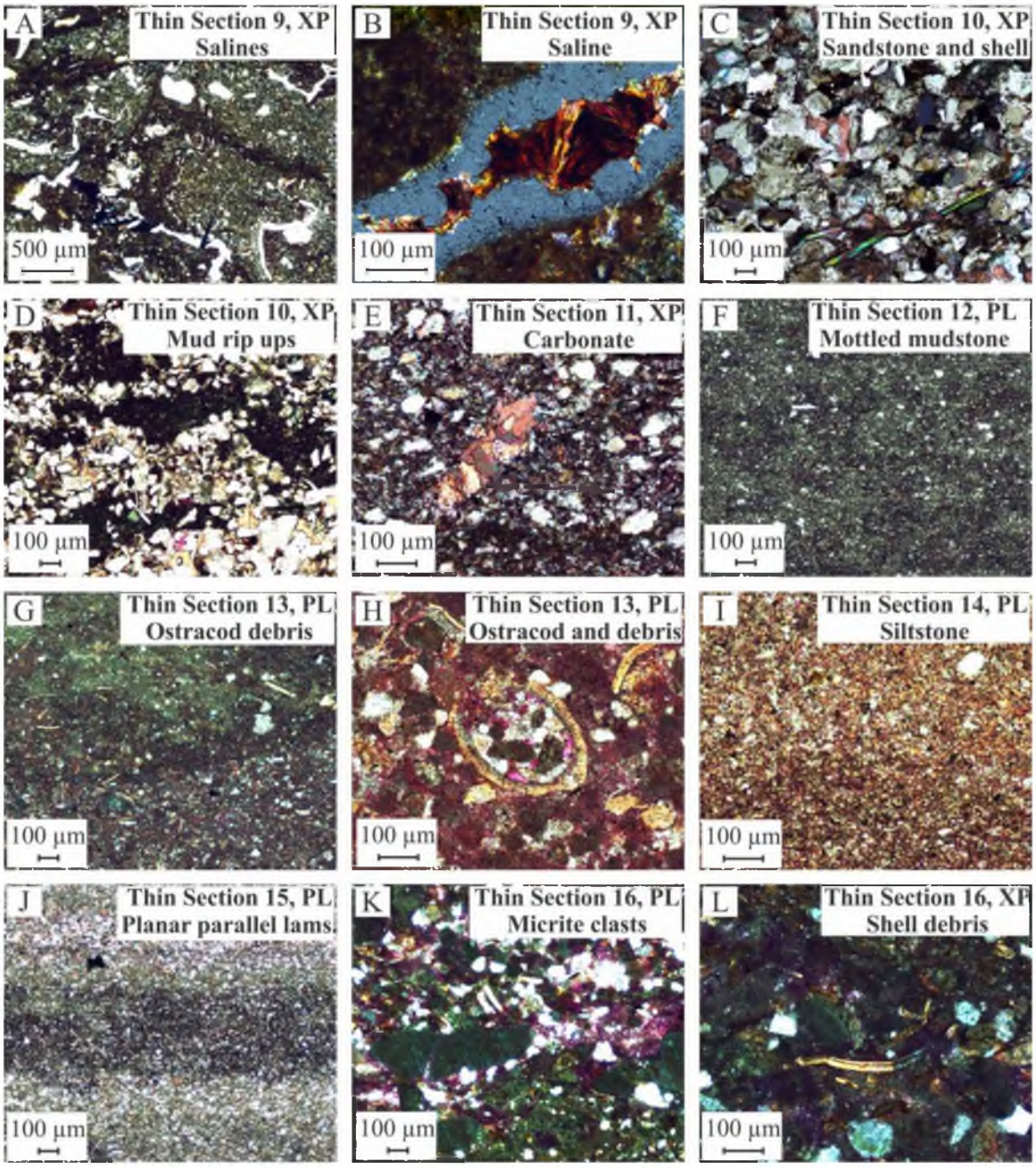

Figure 36 – Thin section photomicrographs (9-16); PL - plain light, XP - cross polarized light.

APPENDIX D

XRF DATA

Appendix D contains scatter plots and depth plots of both XRF data and isotope data of the Henderson 3 core and XRF data of the Half Moon Canyon core.

HENDERSON 3 XRF AND ISOTOPE DATA

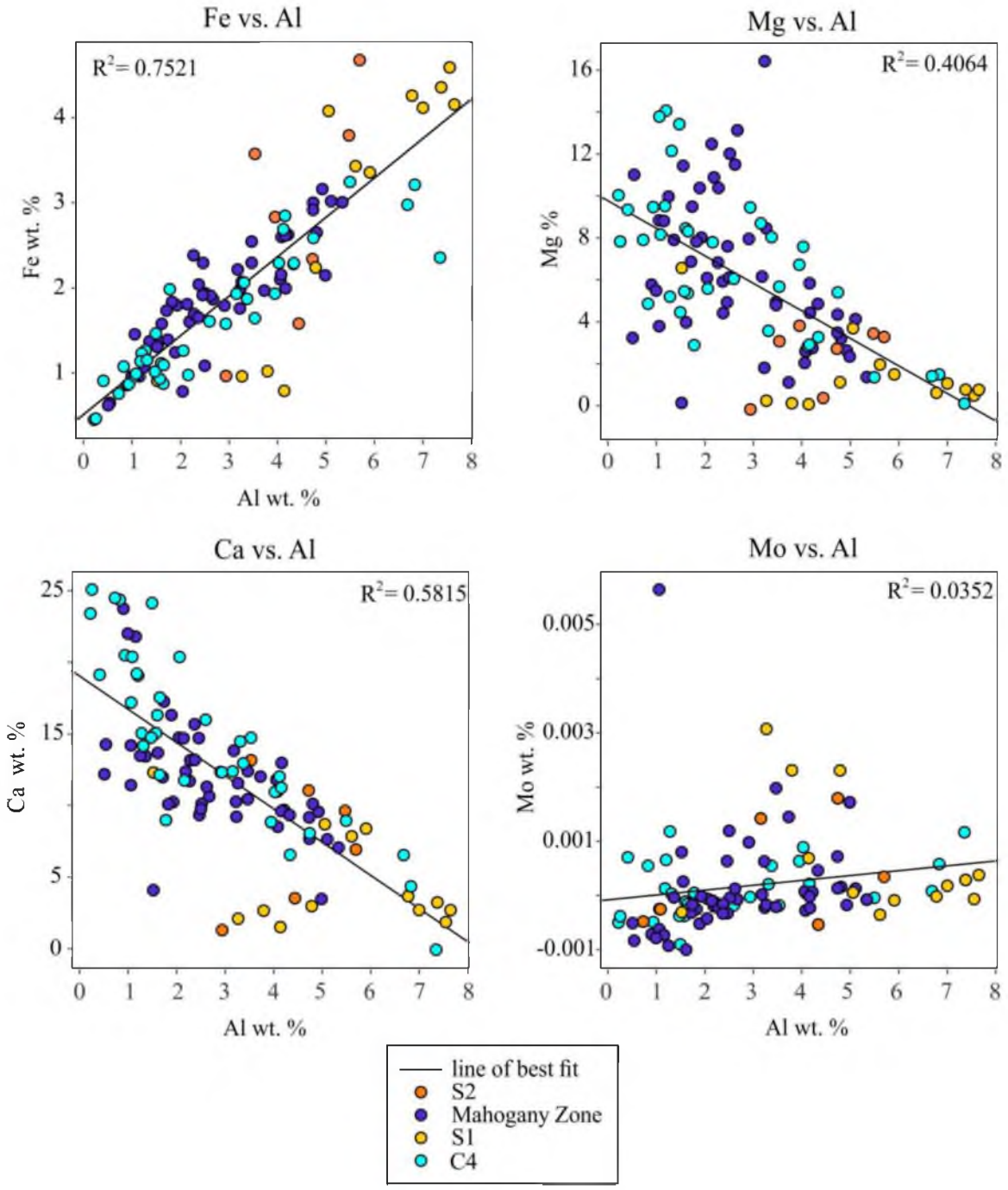
Fe vs. Al
R²= 0.7521
Fe wt. %
Al wt. %
Mg vs. Al
R²= 0.4064
Mg %
Ca vs. Al
R²= 0.5815
Ca wt. %
Mo vs. Al
R²= 0.0352
Mo wt. %
line of best fit
S2
Mahogany Zone
S1
C4

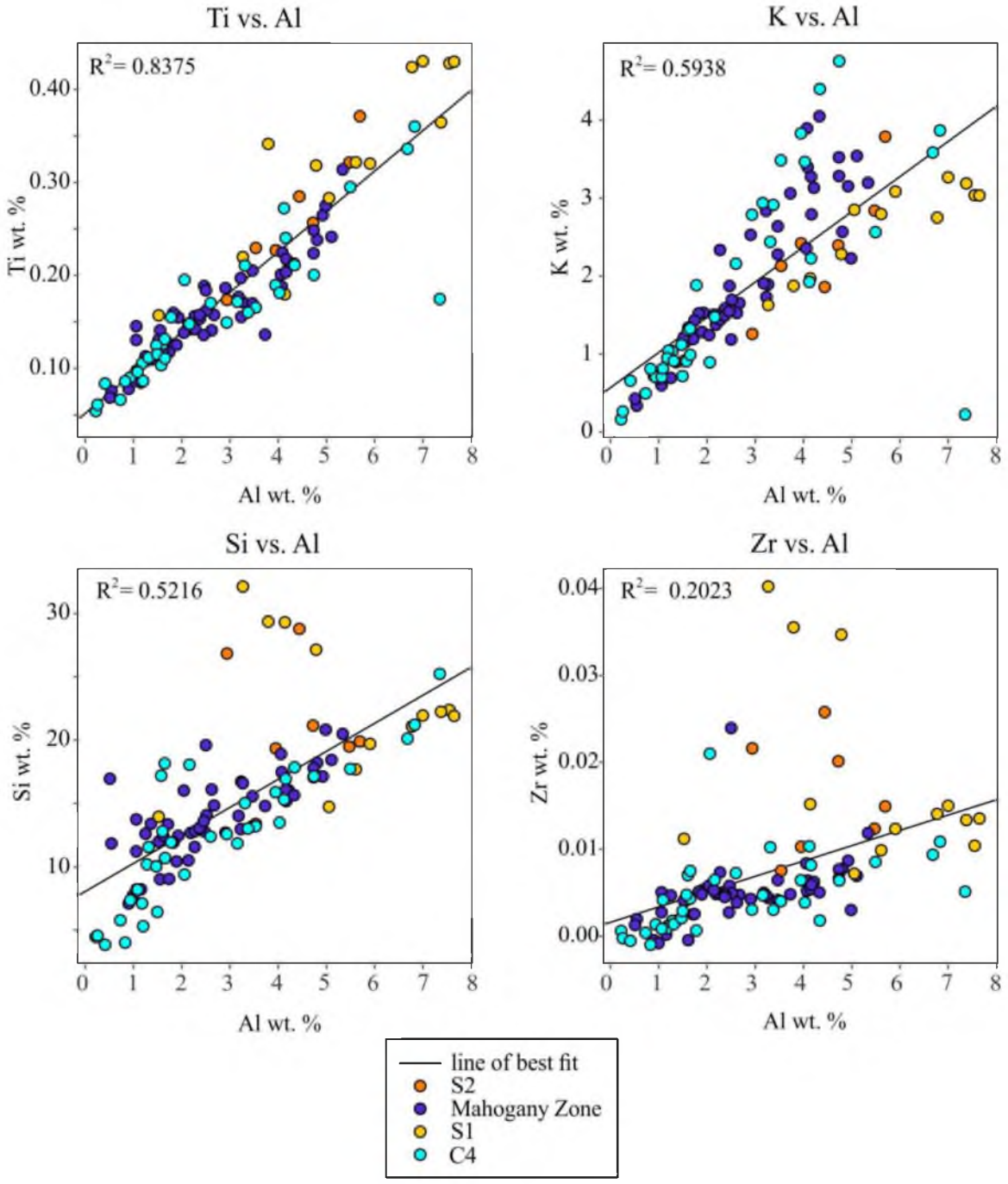
Ti vs. Al
R²= 0.8375
Ti wt. %
Al wt. %
K vs. Al
R²= 0.5938
K wt. %
Al wt. %
Si vs. Al
R²= 0.5216
Si wt. %
Al wt. %
Zr vs. Al
R²= 0.2023
Zr wt. %
Al wt. %
line of best fit
S2
Mahogany Zone
S1
C4

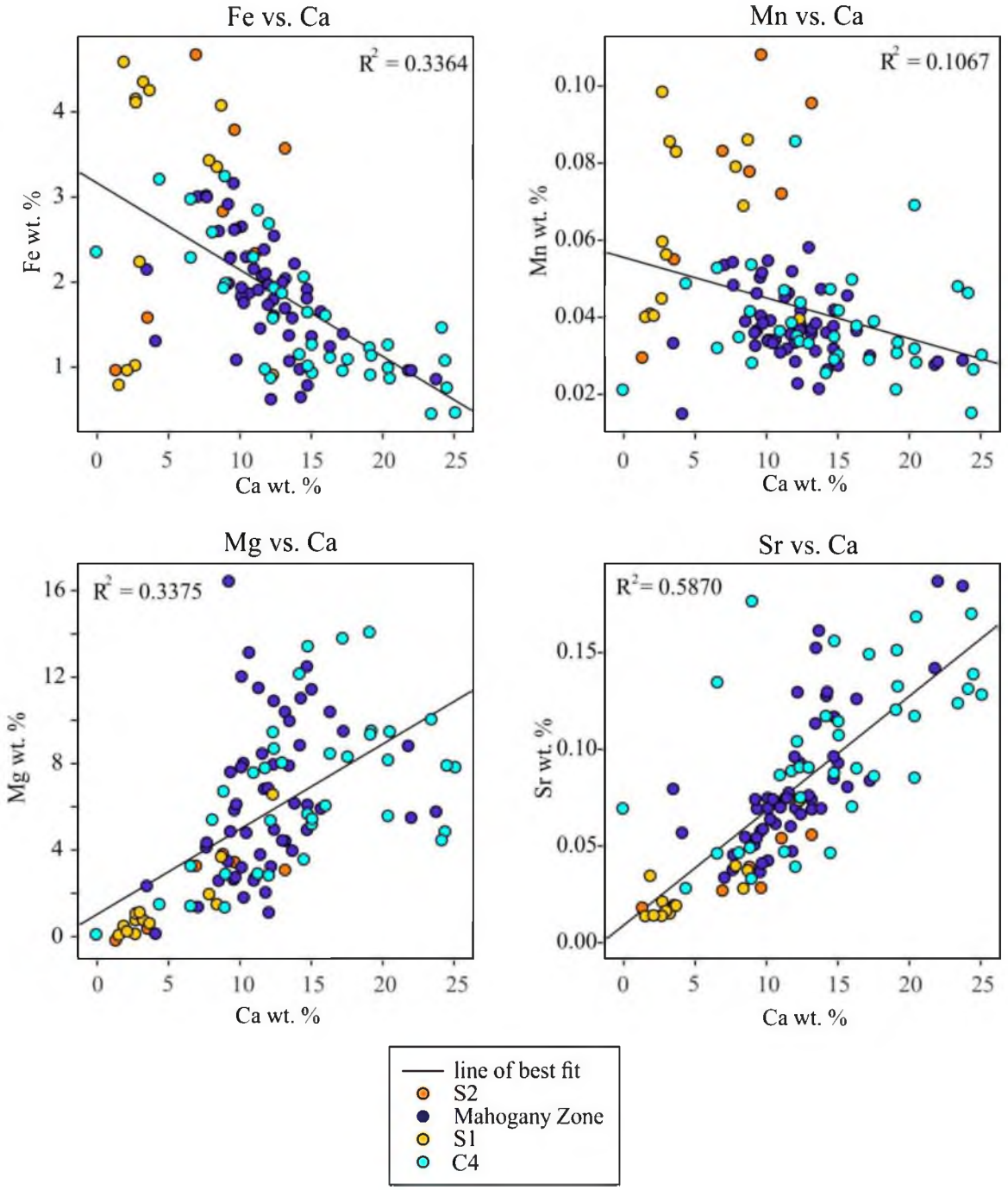
Fe vs. Ca
R² = 0.3364
Fe wt. %
Ca wt. %
Mn vs. Ca
R² = 0.1067
Mn wt. %
Ca wt. %
Mg vs. Ca
R² = 0.3375
Mg wt. %
Ca wt. %
Sr vs. Ca
R²= 0.5870
Sr wt. %
Ca wt. %
line of best fit
S2
Mahogany Zone
S1
C4

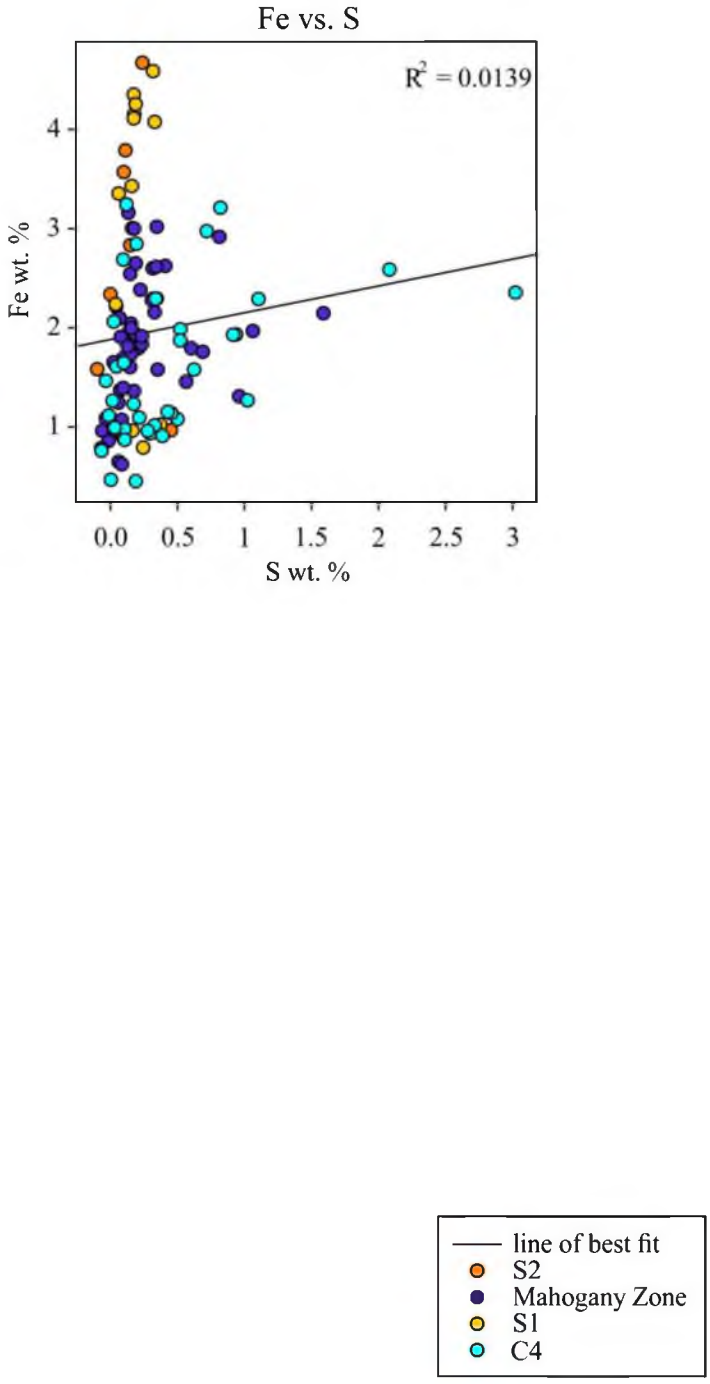
Fe vs. S
$R^2 = 0.0139$
Fe wt. %
S wt. %
0.0
0.5
1
1.5
2
2.5
3
1
2
3
4
line of best fit
S2
Mahogany Zone
S1
C4

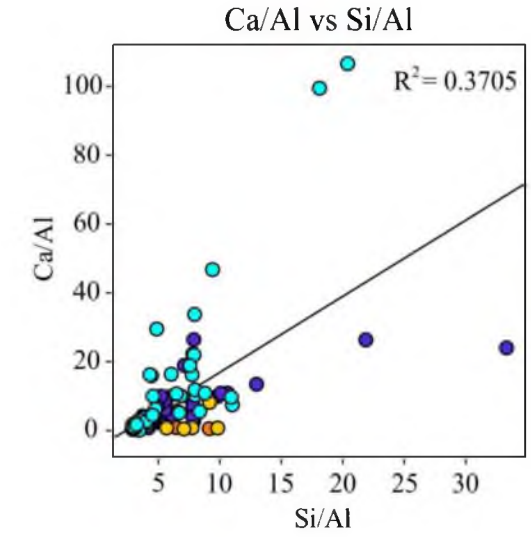
Ca/Al vs Si/Al
R²= 0.3705
Ca/Al
Si/Al
0
20
40
60
80
100
5
10
15
20
25
30

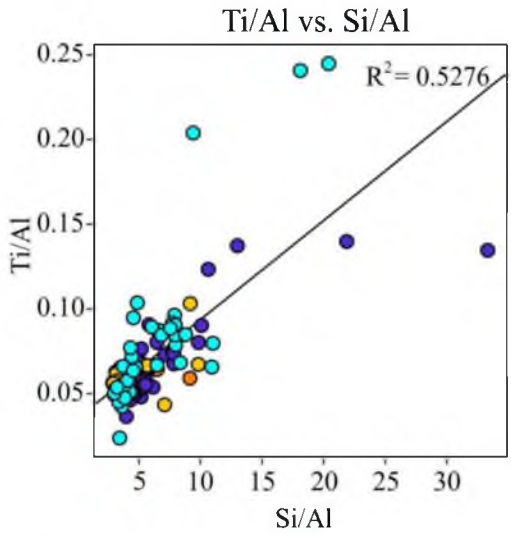
Ti/Al vs. Si/Al
R²= 0.5276
Ti/Al
Si/Al
0.05
0.10
0.15
0.20
0.25
5
10
15
20
25
30

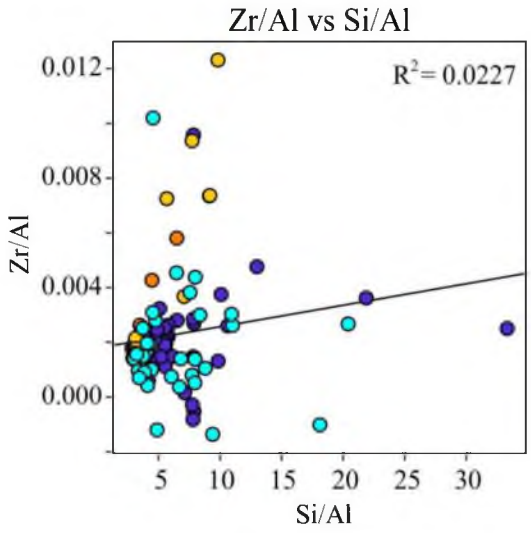
Zr/Al vs Si/Al
R²= 0.0227
Zr/Al
Si/Al
0.000
0.004
0.008
0.012
5
10
15
20
25
30

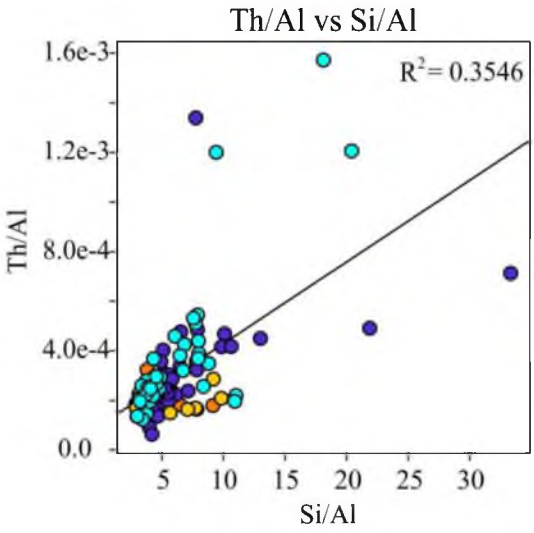
Th/Al vs Si/Al
R²= 0.3546
Th/Al
Si/Al
0.0
4.0e-4
8.0e-4
1.2e-3
1.6e-3
5
10
15
20
25
30

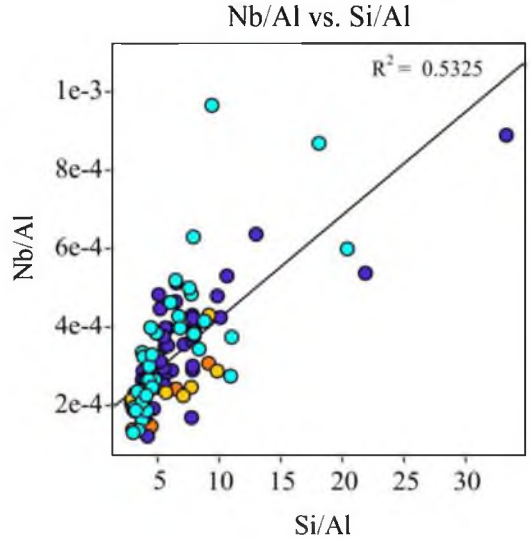
Nb/Al vs. Si/Al
R²= 0.5325
Nb/Al
Si/Al
2e-4
4e-4
6e-4
8e-4
1e-3
5
10
15
20
25
30

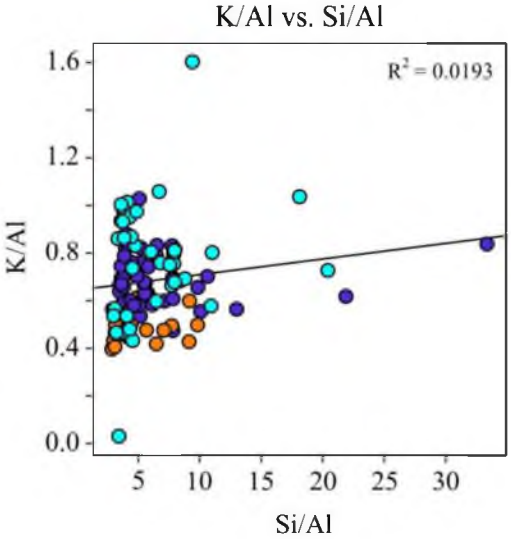
K/Al vs. Si/Al
R²= 0.0193
K/Al
Si/Al
0.0
0.4
0.8
1.2
1.6
5
10
15
20
25
30

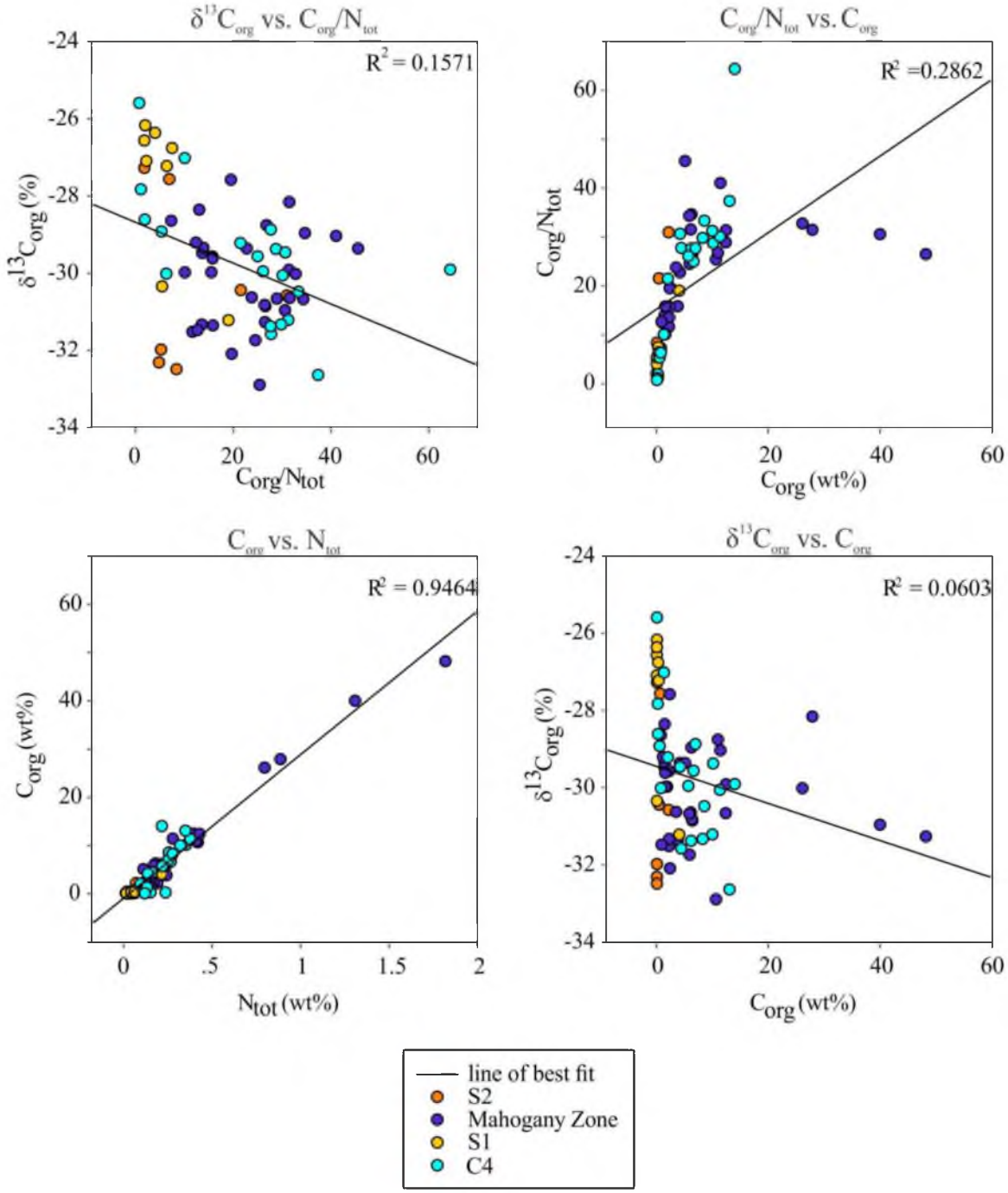
δ13Corg vs. Corg/Ntot
R2 = 0.1571
δ13Corg (%)
Corg/Ntot
Corg/Ntot vs. Corg
R2 =0.2862
Corg/Ntot
Corg (wt%)
Corg vs. Ntot
R2 = 0.9464
Corg (wt%)
Ntot (wt%)
δ13Corg vs. Corg
R2 = 0.0603
δ13Corg (%)
Corg (wt%)
line of best fit
S2
Mahogany Zone
S1
C4

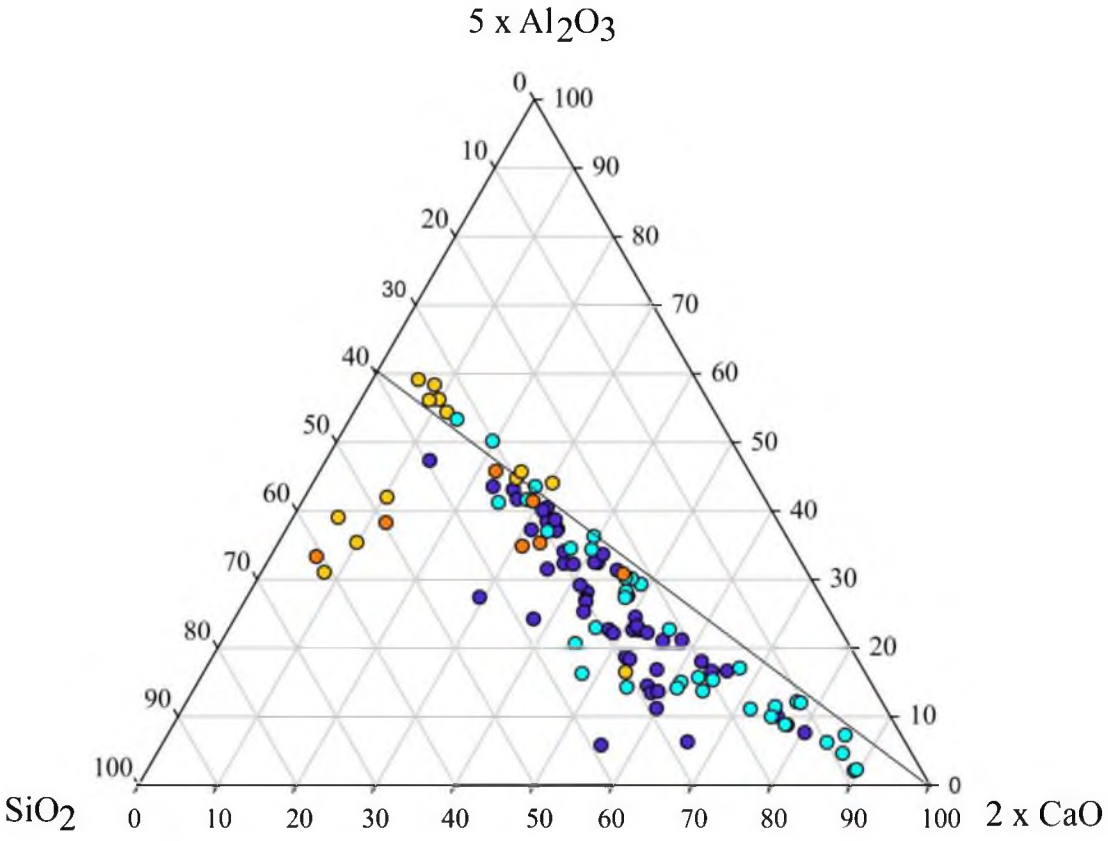
5 x Al2O3
SiO2
2 x CaO
0
10
20
30
40
50
60
70
80
90
100
S2
Mahogany Zone
S1
C4
Trajectory along which low-CaCO3 average shale would be diluted by calcite.

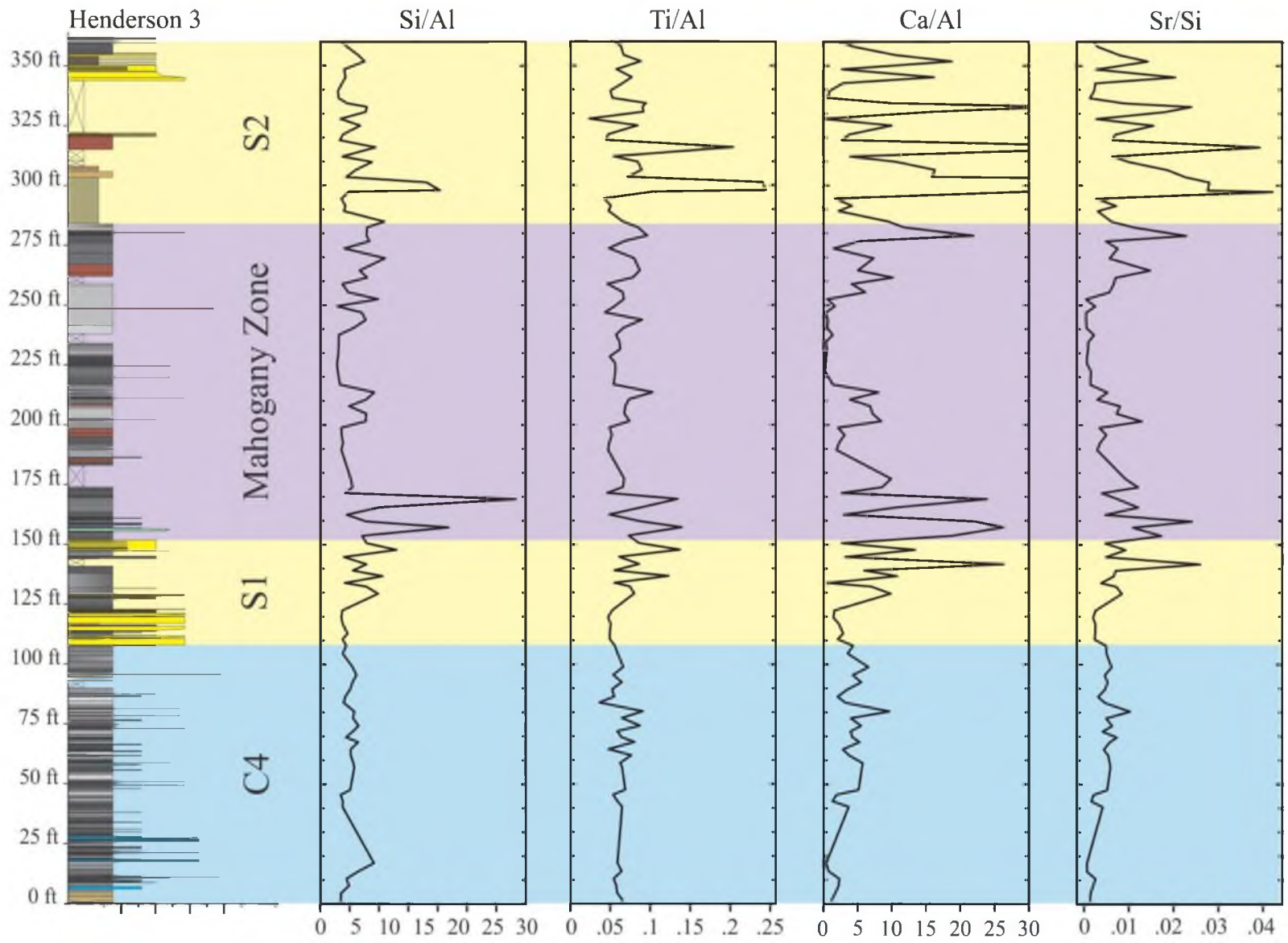
Henderson 3
Si/Al
Ti/Al
Ca/Al
Sr/Si
350 ft
325 ft
300 ft
275 ft
250 ft
225 ft
200 ft
175 ft
150 ft
125 ft
100 ft
75 ft
50 ft
25 ft
0 ft
S2
Mahogany Zone
S1
C4
0 5 10 15 20 25 30
0 .05 .1 .15 .2 .25
0 5 10 15 20 25 30
0 .01 .02 .03 .04

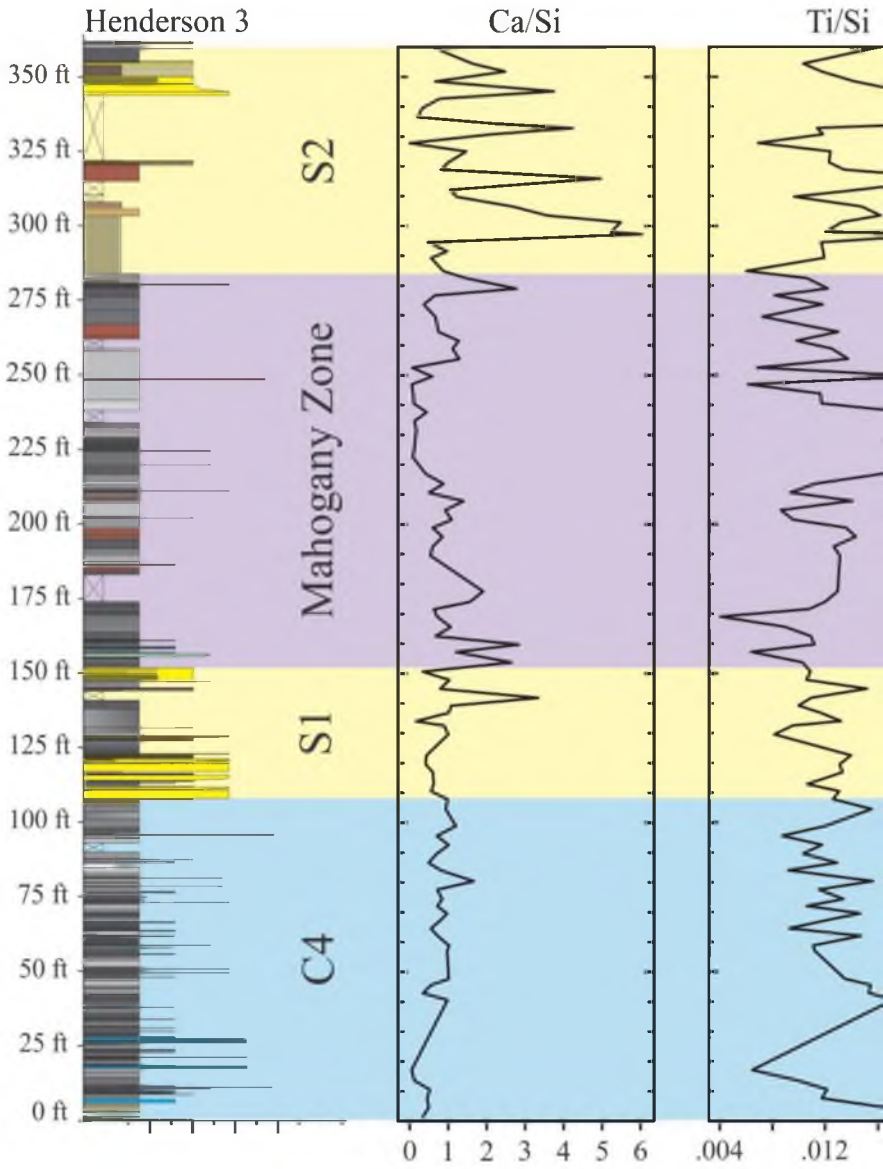
Henderson 3
Ca/Si
Ti/Si
350 ft
325 ft
300 ft
275 ft
250 ft
225 ft
200 ft
175 ft
150 ft
125 ft
100 ft
75 ft
50 ft
25 ft
0 ft
S2
Mahogany Zone
S1
C4
0 1 2 3 4 5 6
.004
.012

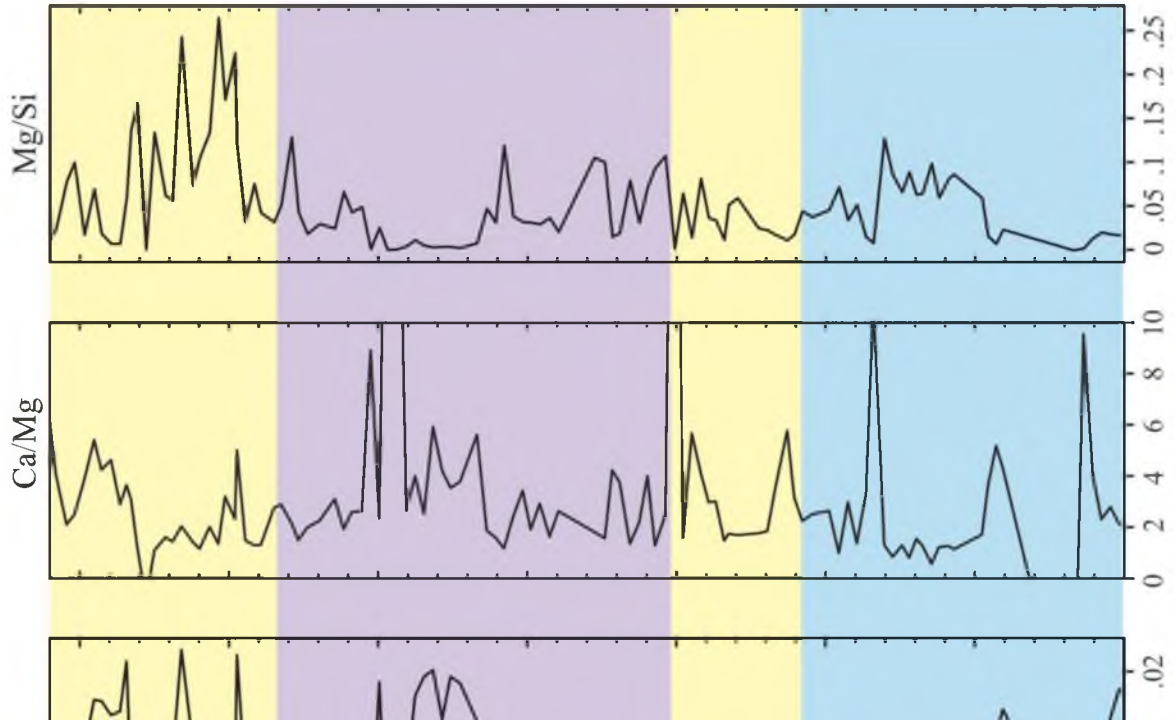
Mg/Si
0
.05
.1
.15
.2
.25
Ca/Mg
0
2
4
6
8
10
.02

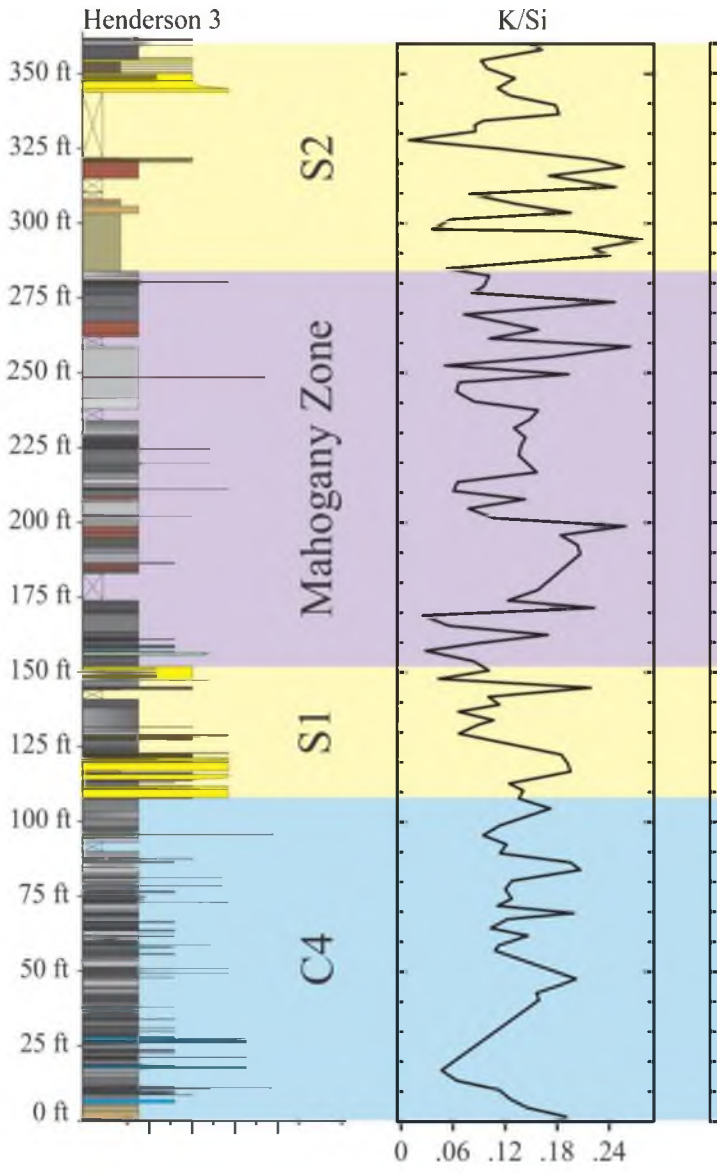
Henderson 3
K/Si
350 ft
325 ft
300 ft
275 ft
250 ft
225 ft
200 ft
175 ft
150 ft
125 ft
100 ft
75 ft
50 ft
25 ft
0 ft
S2
Mahogany Zone
S1
C4
0
.06
.12
.18
.24

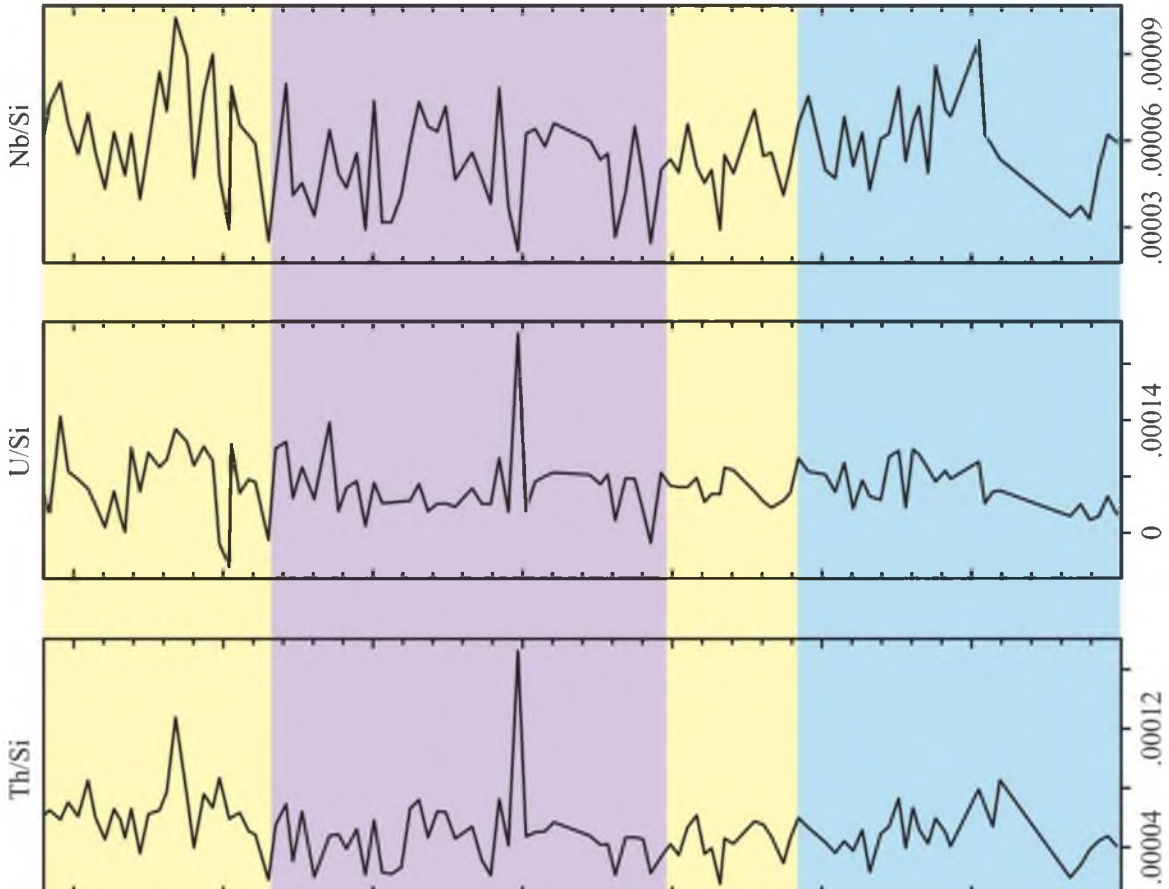
Nb/Si
.00003
.00006
.00009
U/Si
0
.00014
Th/Si
.00004
.00012

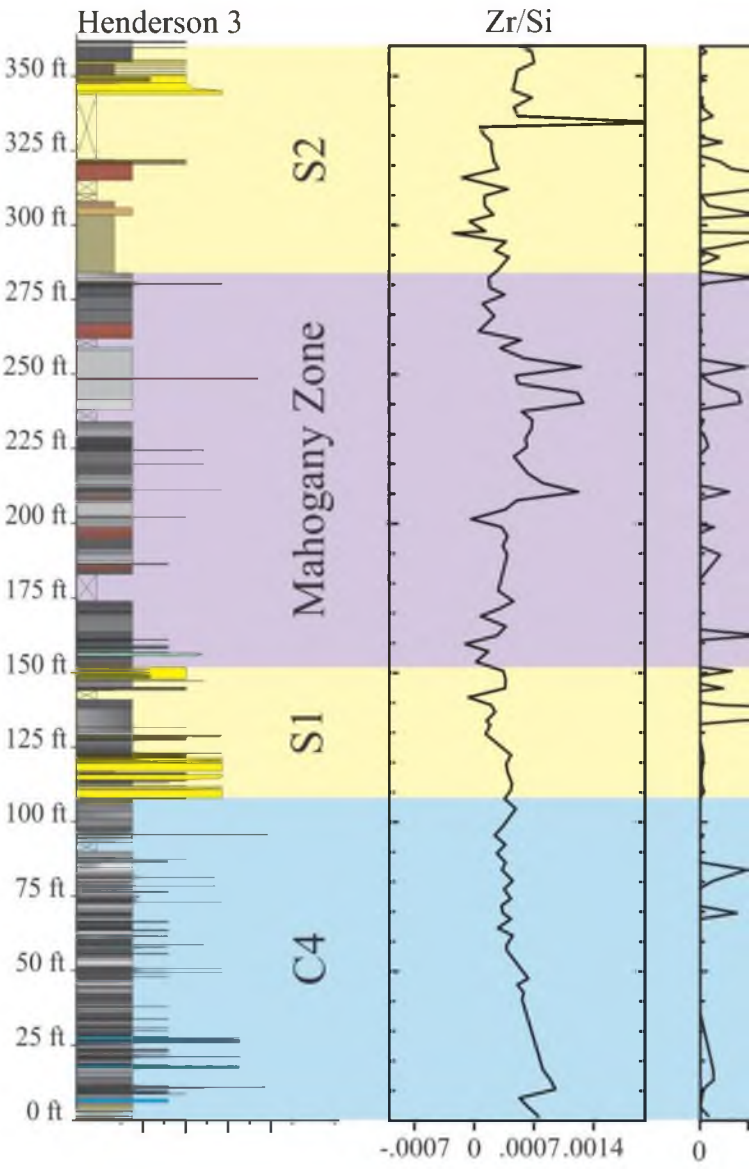
Henderson 3
Zr/Si
350 ft
325 ft
300 ft
275 ft
250 ft
225 ft
200 ft
175 ft
150 ft
125 ft
100 ft
75 ft
50 ft
25 ft
0 ft
S2
Mahogany Zone
S1
C4
-.0007 0 .0007.0014
0

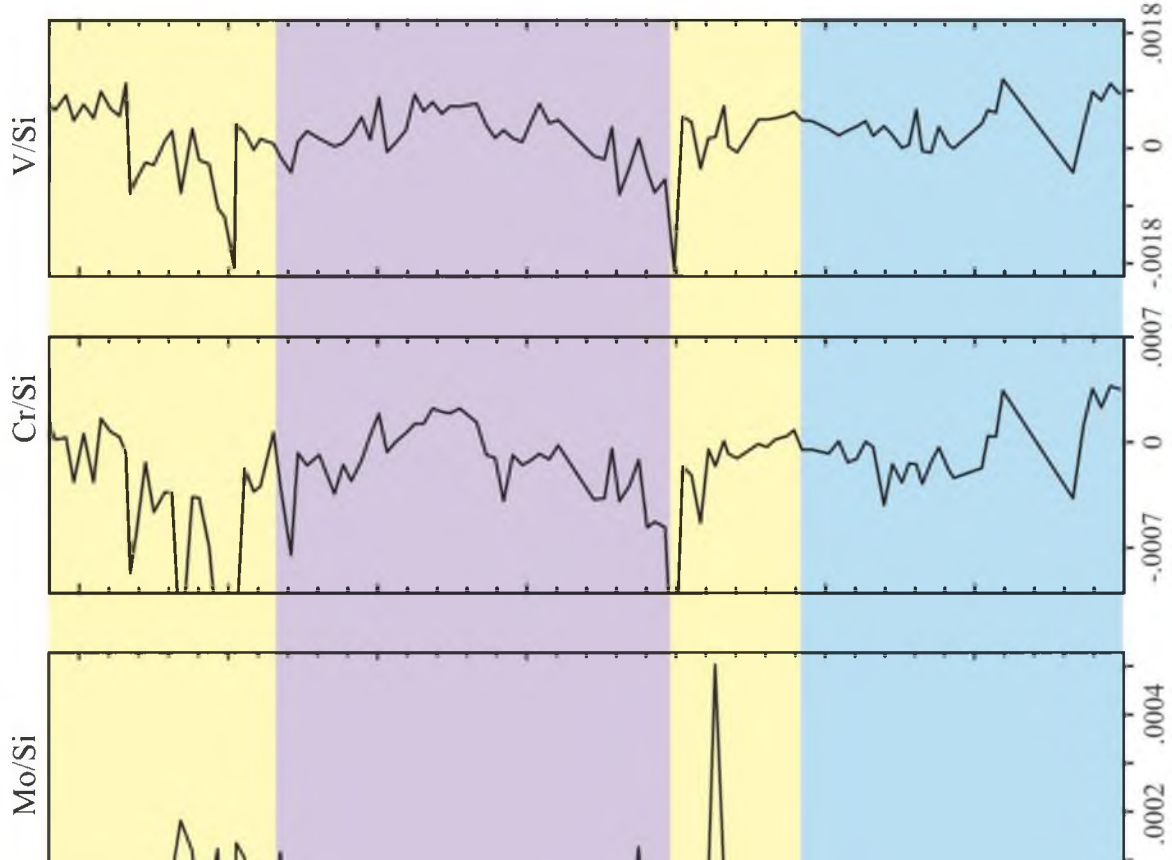
V/Si
.0018
0
-.0018
Cr/Si
.0007
0
-.0007
Mo/Si
.0004
.0002

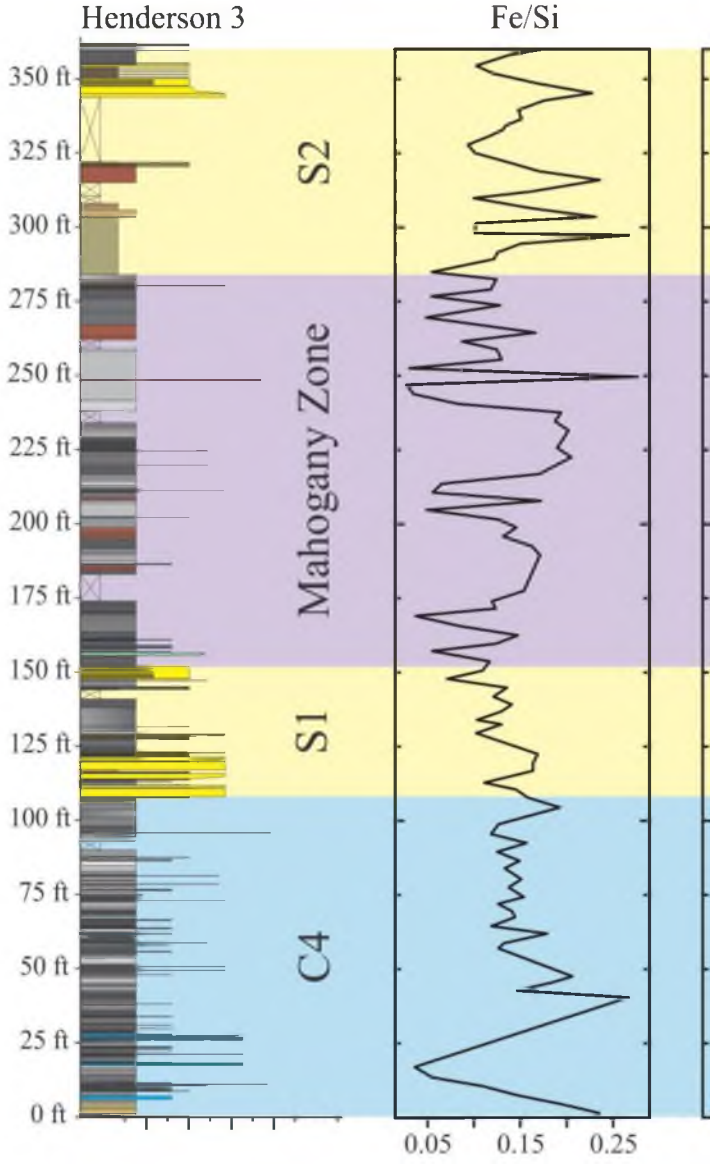
Henderson 3
Fe/Si
350 ft
325 ft
300 ft
275 ft
250 ft
225 ft
200 ft
175 ft
150 ft
125 ft
100 ft
75 ft
50 ft
25 ft
0 ft
S2
Mahogany Zone
S1
C4
0.05
0.15
0.25

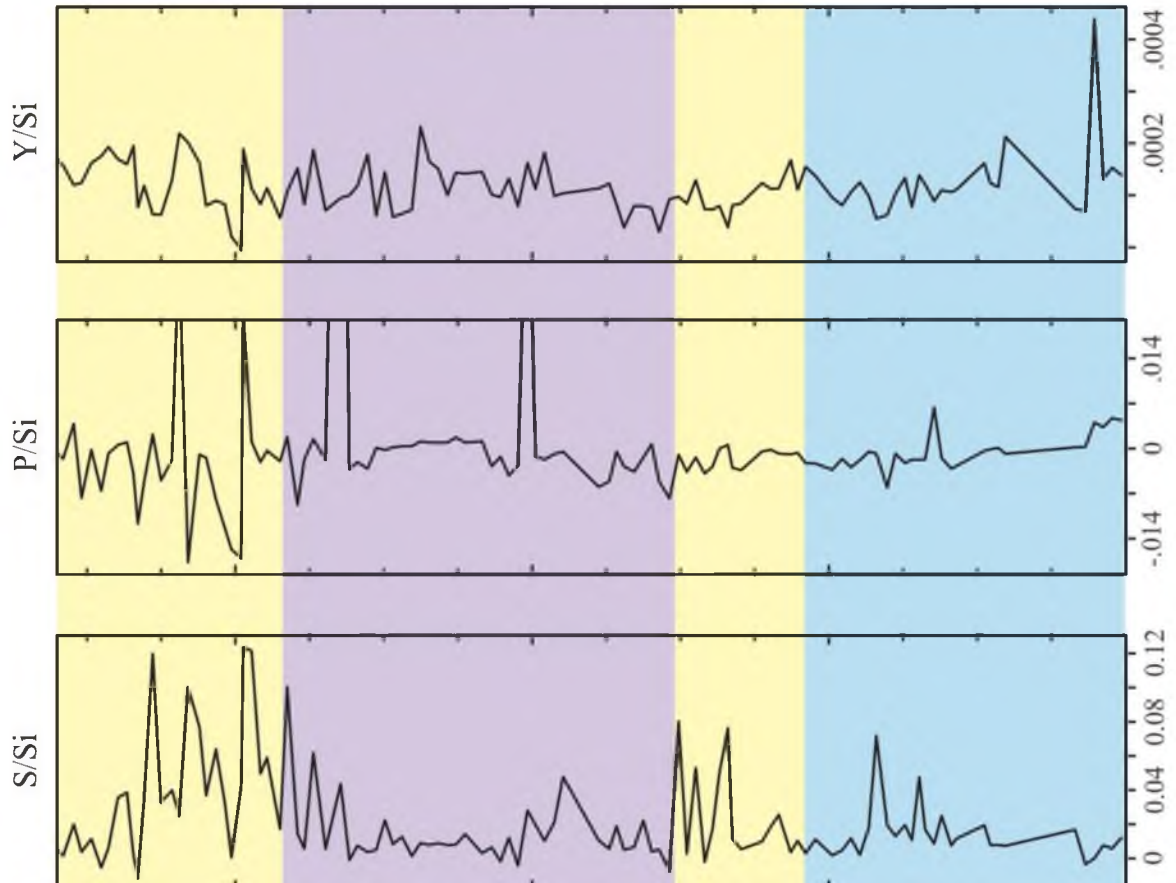
Y/Si
.0004
.0002
P/Si
.014
0
-.014
S/Si
0.12
0.08
0.04
0

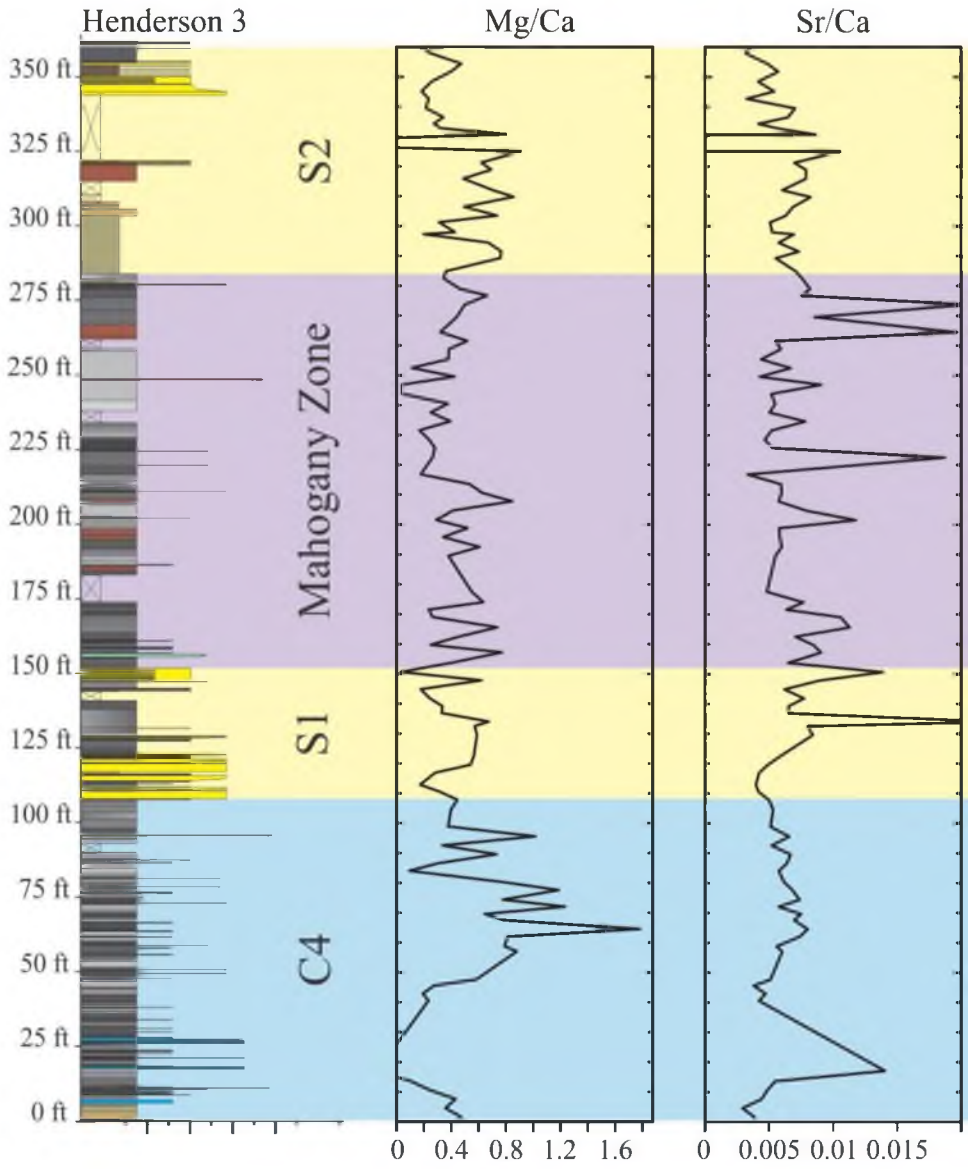
Henderson 3
Mg/Ca
Sr/Ca
350 ft
325 ft
300 ft
275 ft
250 ft
225 ft
200 ft
175 ft
150 ft
125 ft
100 ft
75 ft
50 ft
25 ft
0 ft
S2
Mahogany Zone
S1
C4
0
0.4
0.8
1.2
1.6
0
0.005
0.01
0.015

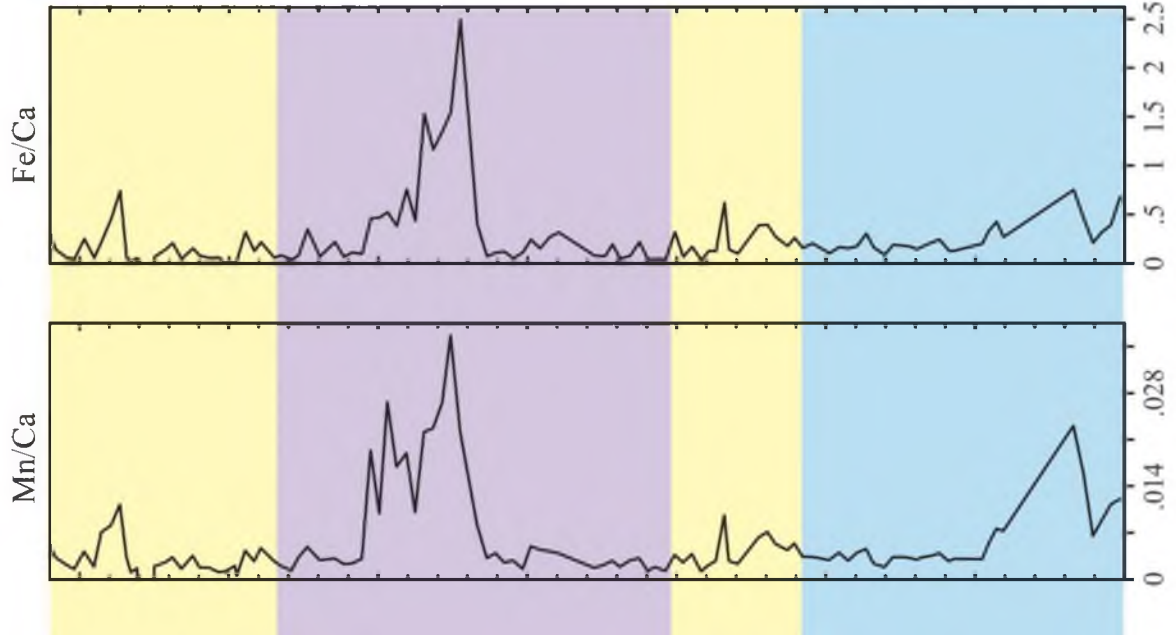
Fe/Ca
0
.5
1
1.5
2
2.5
Mn/Ca
0
.014
.028

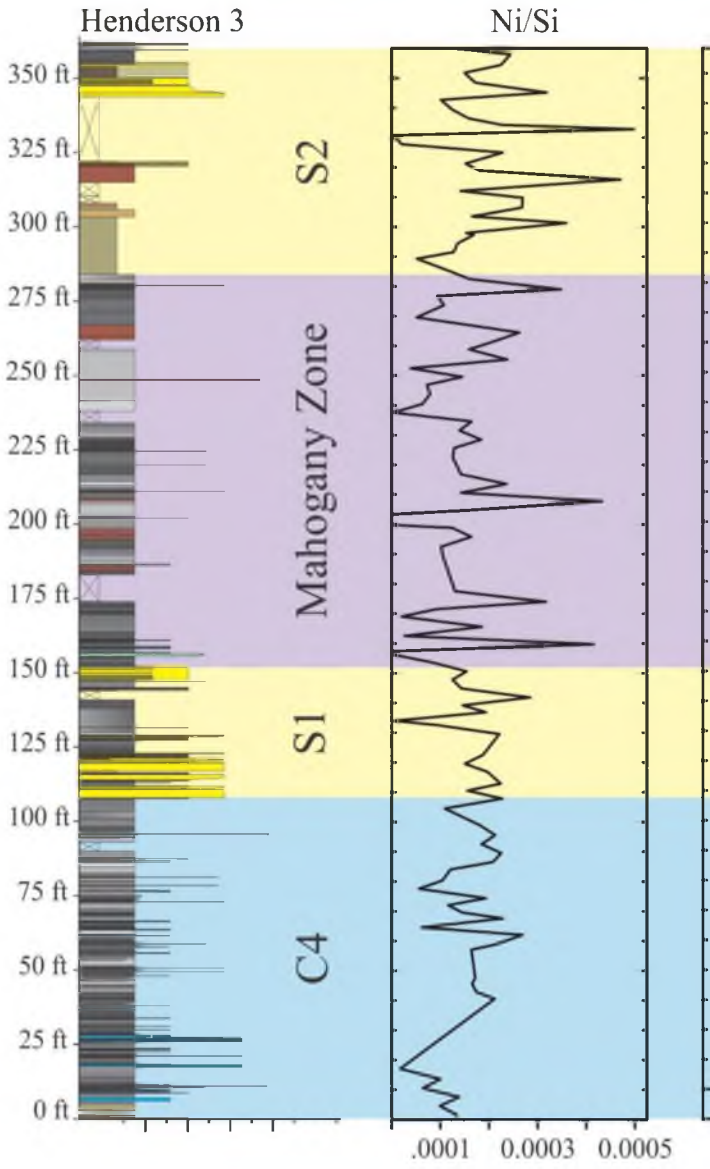
Henderson 3
Ni/Si
350 ft
325 ft
300 ft
275 ft
250 ft
225 ft
200 ft
175 ft
150 ft
125 ft
100 ft
75 ft
50 ft
25 ft
0 ft
S2
Mahogany Zone
S1
C4
.0001
0.0003
0.0005

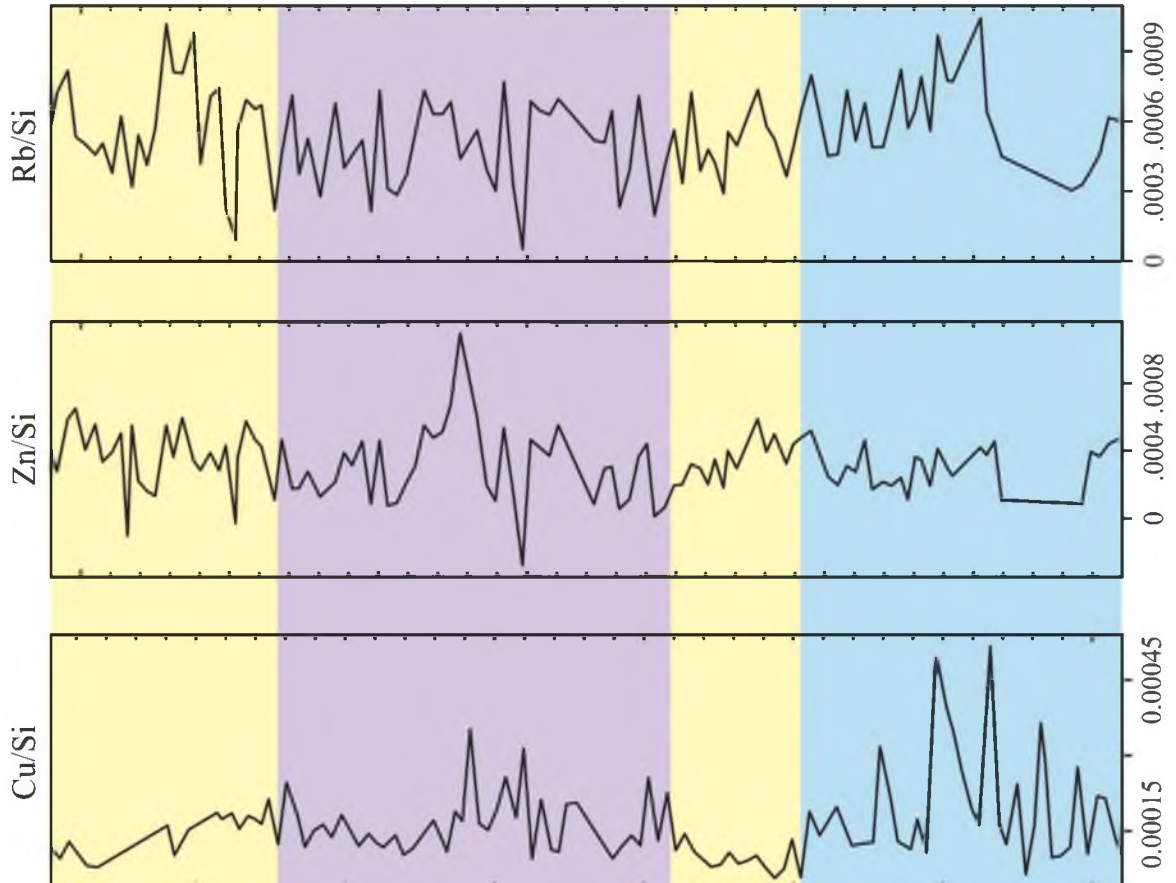
Rb/Si
0
.0003
.0006
.0009
Zn/Si
0
.0004
.0008
Cu/Si
0.00015
0.00045

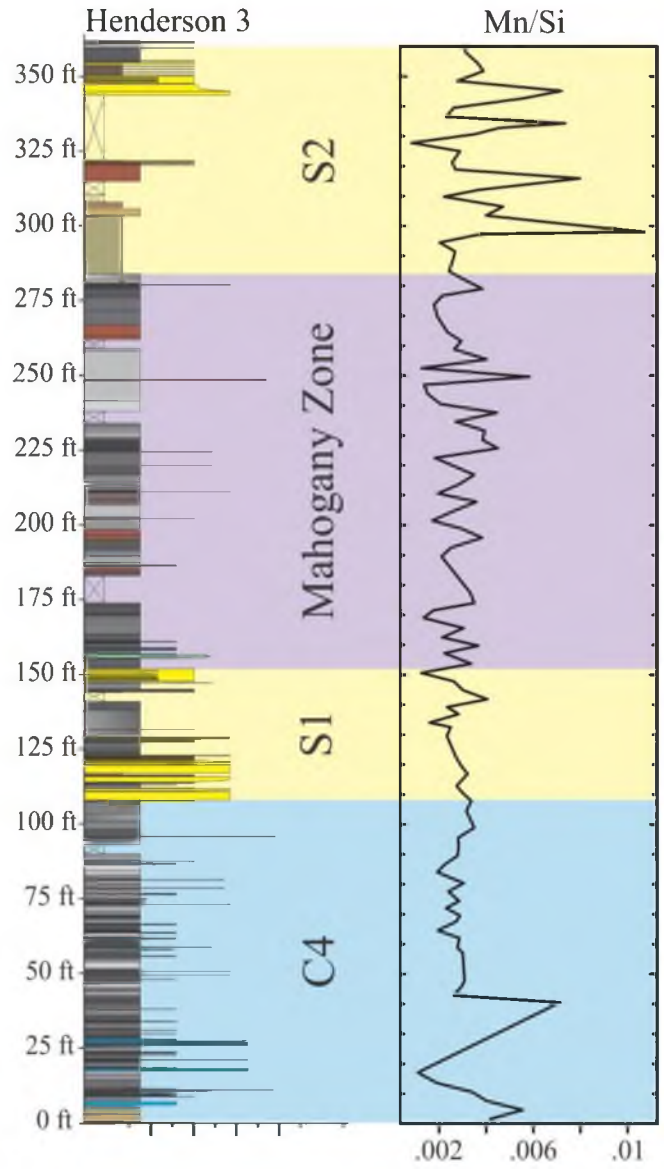
Henderson 3
Mn/Si
350 ft
325 ft
300 ft
275 ft
250 ft
225 ft
200 ft
175 ft
150 ft
125 ft
100 ft
75 ft
50 ft
25 ft
0 ft
S2
Mahogany Zone
S1
C4
.002
.006
.01

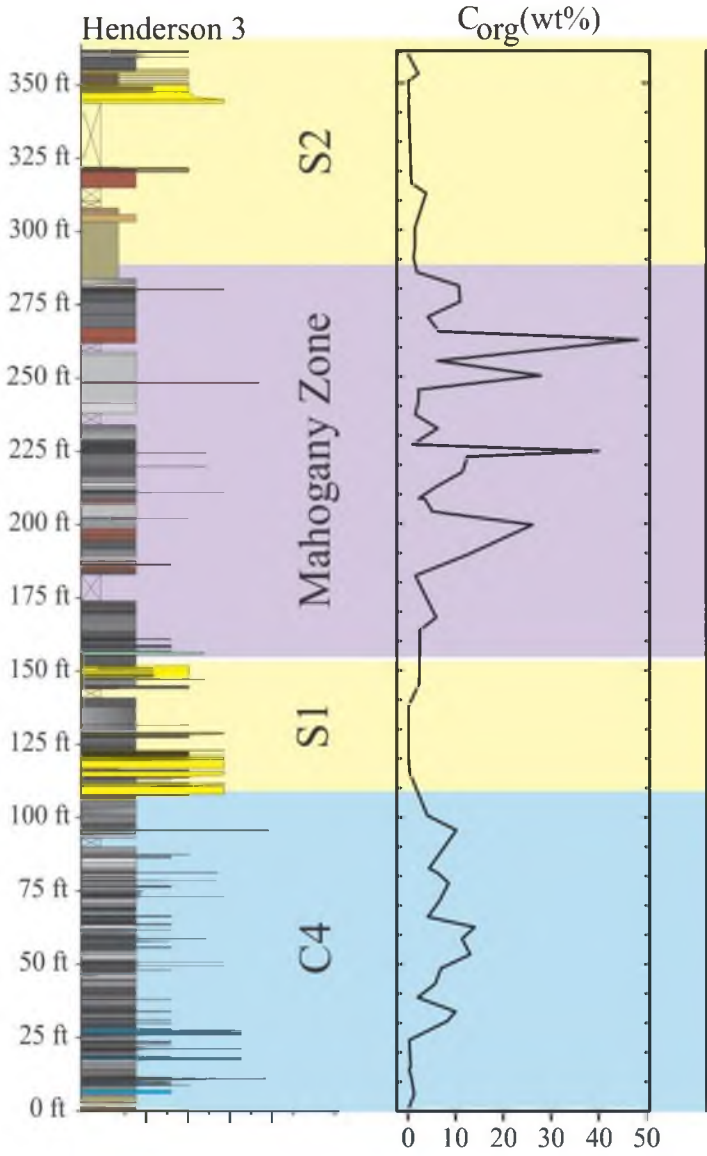
Henderson 3
C_{org}(wt%)
350 ft
325 ft
300 ft
275 ft
250 ft
225 ft
200 ft
175 ft
150 ft
125 ft
100 ft
75 ft
50 ft
25 ft
0 ft
S2
Mahogany Zone
S1
C4
0
10
20
30
40
50

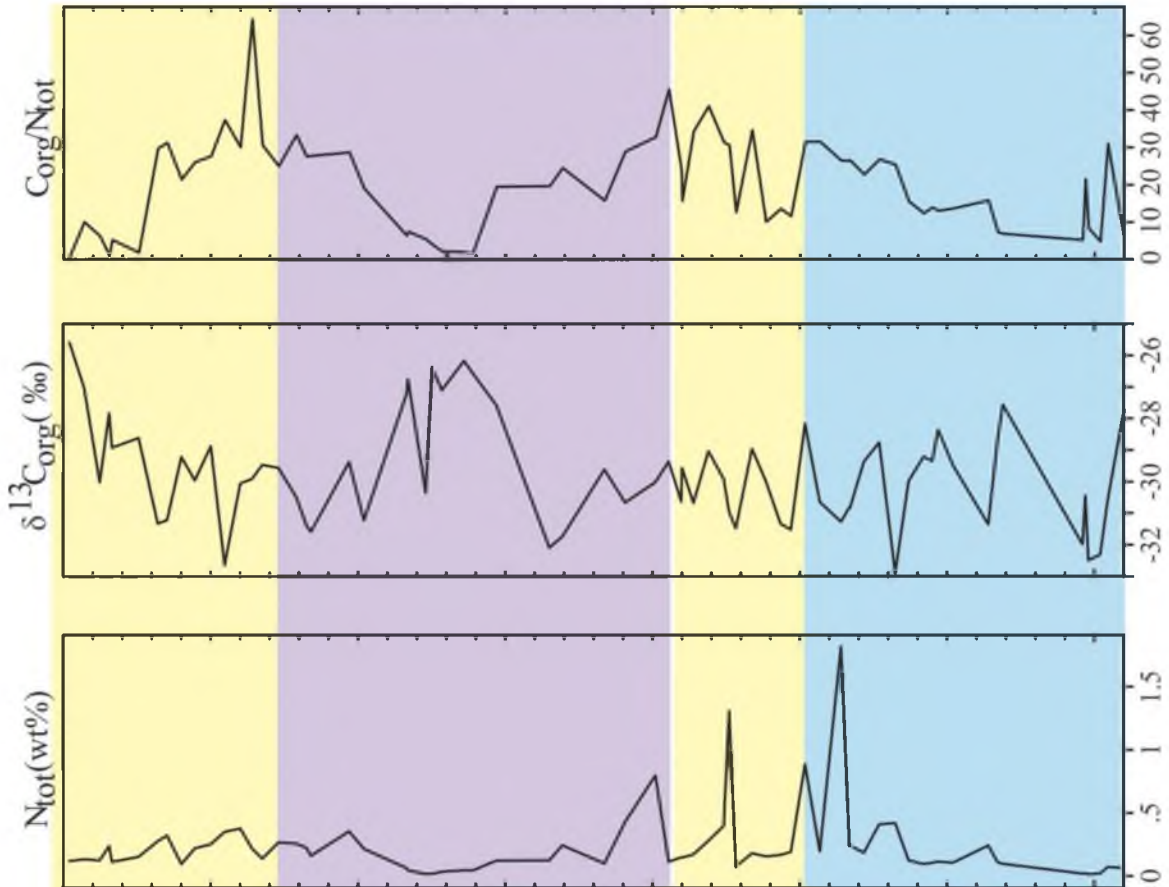
Corg/Ntot
0 10 20 30 40 50 60
δ13Corg(‰)
-32 -30 -28 -26
Ntot(wt%)
0 .5 1 1.5

HALF MOON CANYON XRF DATA

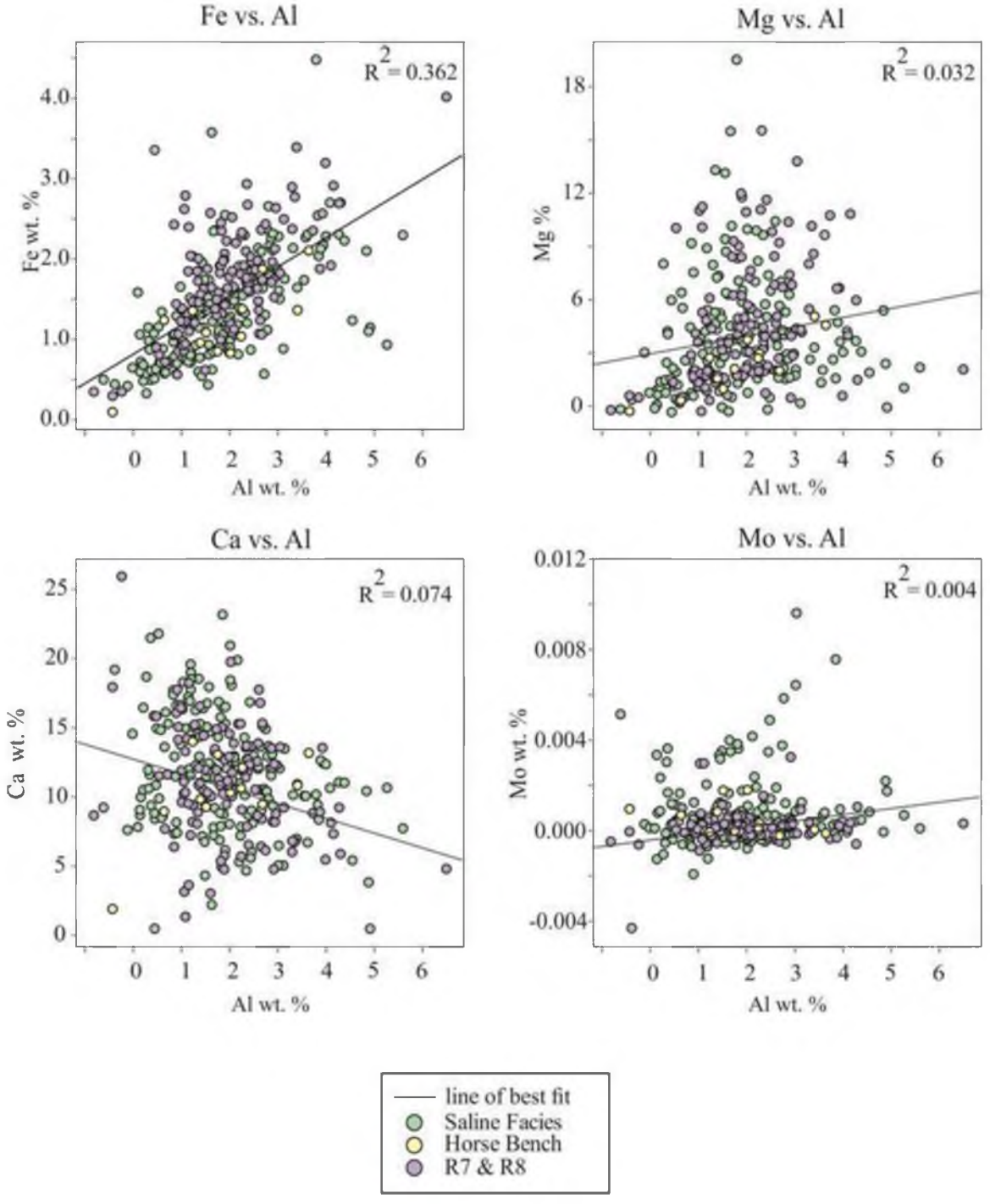
Fe vs. Al
R2 = 0.362
Fe wt. %
Al wt. %
Mg vs. Al
R2 = 0.032
Mg %
Al wt. %
Ca vs. Al
R2 = 0.074
Ca wt. %
Al wt. %
Mo vs. Al
R2 = 0.004
Mo wt. %
Al wt. %
line of best fit
Saline Facies
Horse Bench
R7 & R8

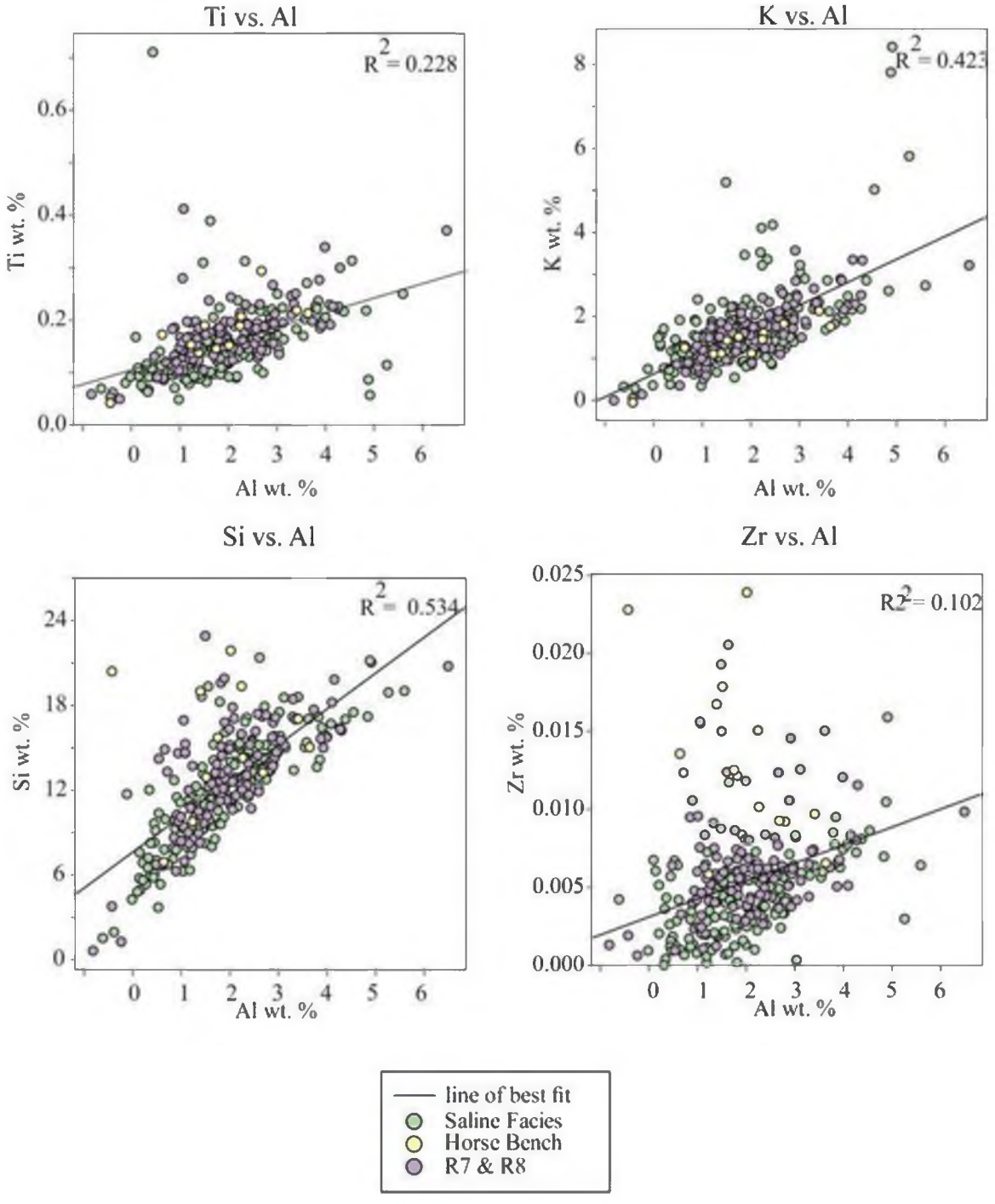
Ti vs. Al
R2 = 0.228
Ti wt. %
Al wt. %
K vs. Al
R2 = 0.423
K wt. %
Al wt. %
Si vs. Al
R2 = 0.534
Si wt. %
Al wt. %
Zr vs. Al
R2 = 0.102
Zr wt. %
Al wt. %
line of best fit
Saline Facies
Horse Bench
R7 & R8

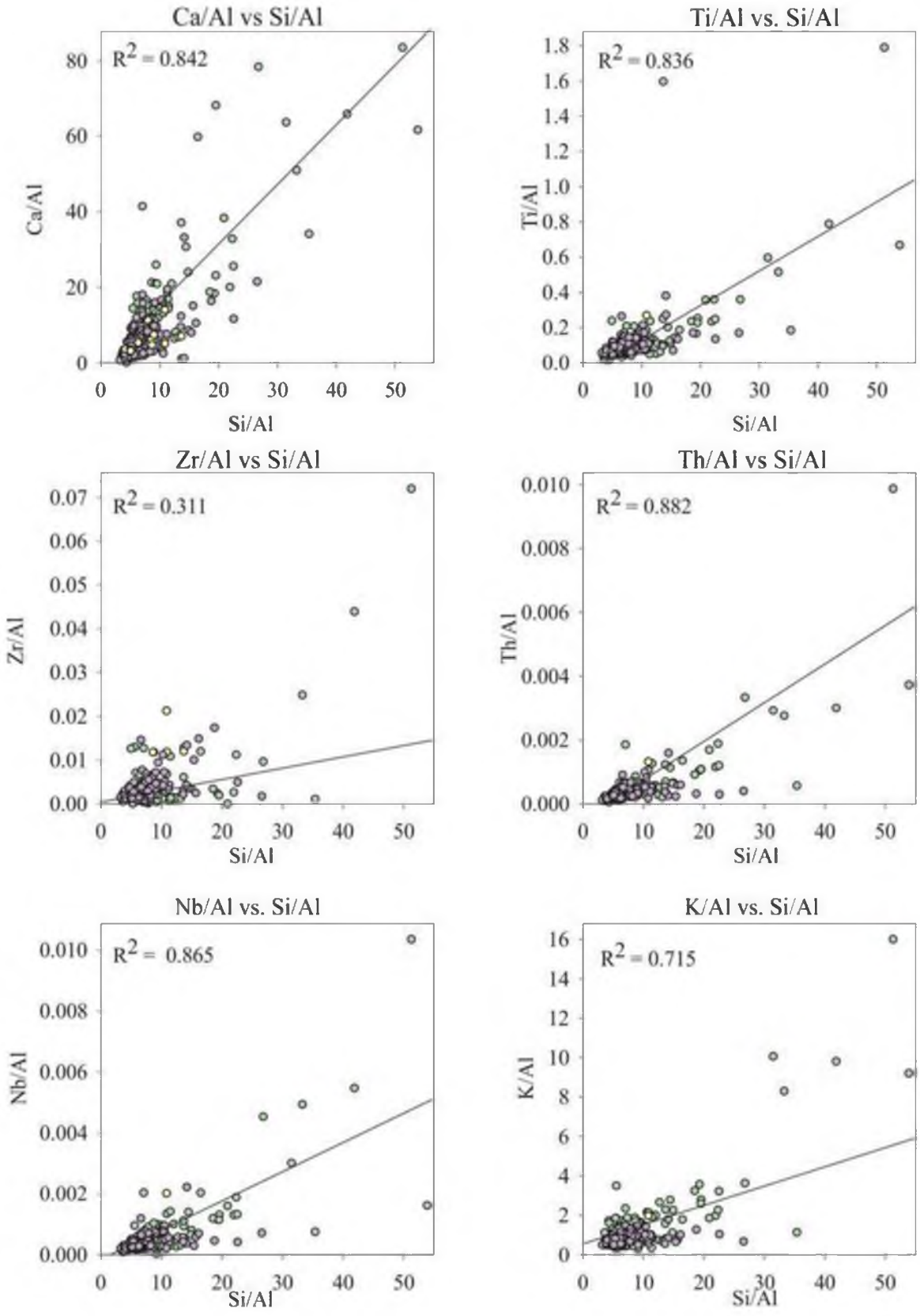
Ca/Al vs Si/Al
R2 = 0.842
Ca/Al
Si/Al
Ti/Al vs. Si/Al
R2 = 0.836
Ti/Al
Si/Al
Zr/Al vs Si/Al
R2 = 0.311
Zr/Al
Si/Al
Th/Al vs Si/Al
R2 = 0.882
Th/Al
Si/Al
Nb/Al vs. Si/Al
R2 = 0.865
Nb/Al
Si/Al
K/Al vs. Si/Al
R2 = 0.715
K/Al
Si/Al

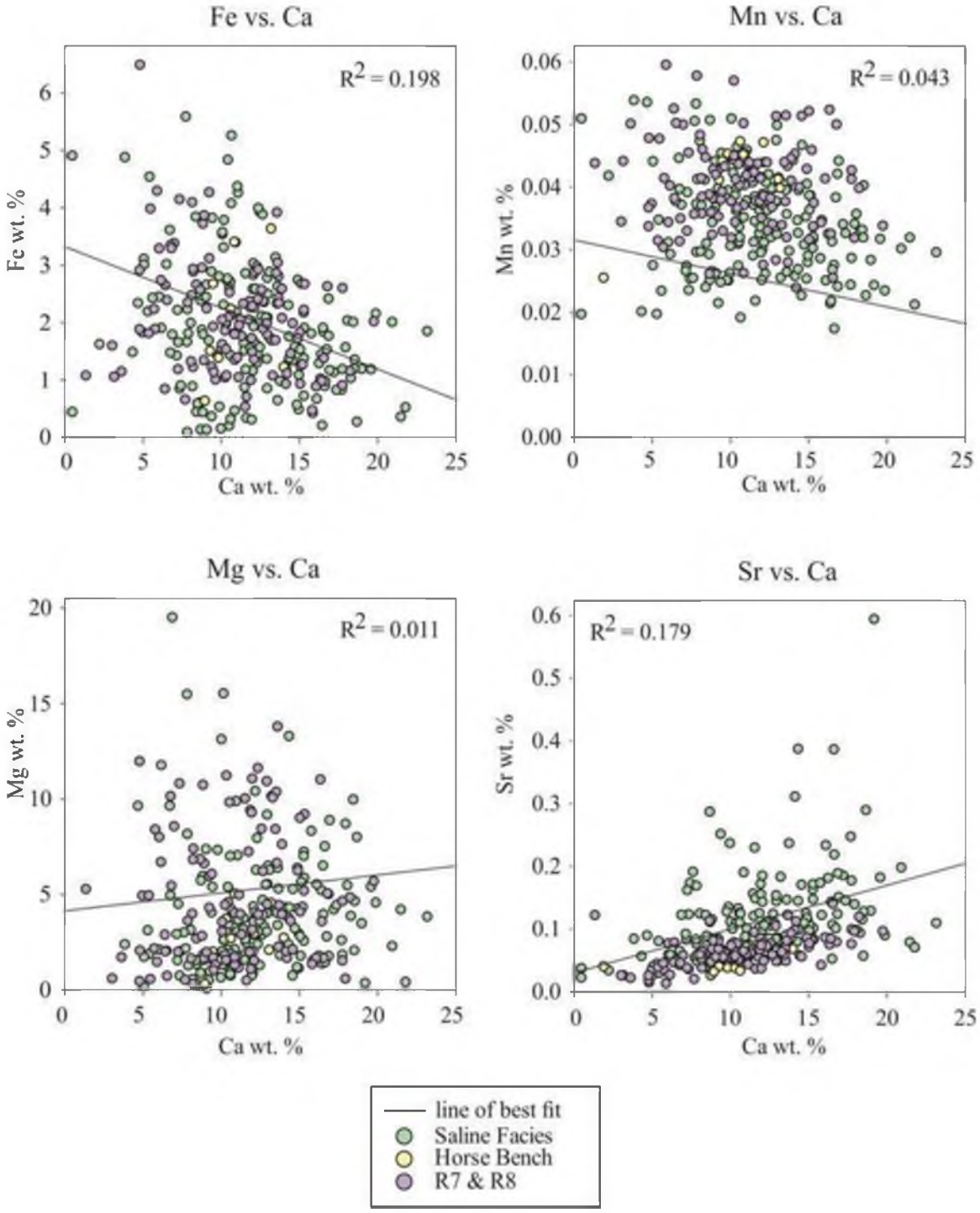
Fe vs. Ca
$R^2 = 0.198$
Fe wt. %
Ca wt. %
Mn vs. Ca
$R^2 = 0.043$
Mn wt. %
Ca wt. %
Mg vs. Ca
$R^2 = 0.011$
Mg wt. %
Ca wt. %
Sr vs. Ca
$R^2 = 0.179$
Sr wt. %
Ca wt. %
line of best fit
Saline Facies
Horse Bench
R7 & R8

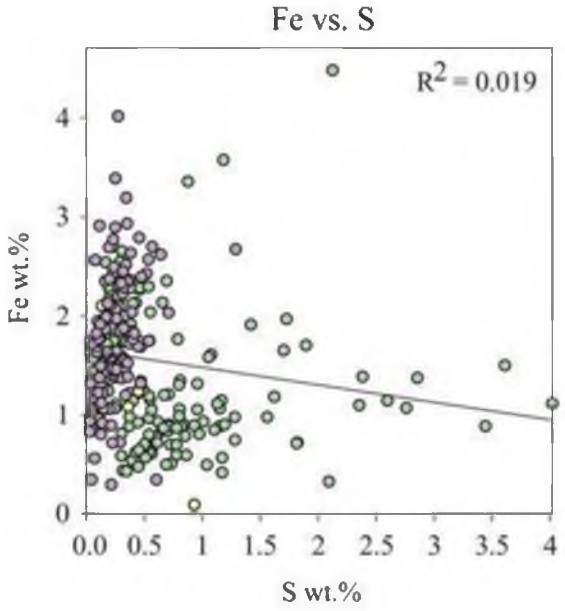
Fe vs. S
$R^2 = 0.019$
Fe wt.%
S wt.%
0
1
2
3
4
0.0
0.5
1
1.5
2
2.5
3
3.5
4

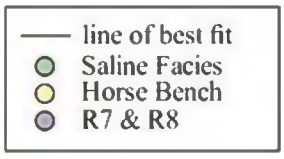
line of best fit
Saline Facies
Horse Bench
R7 & R8

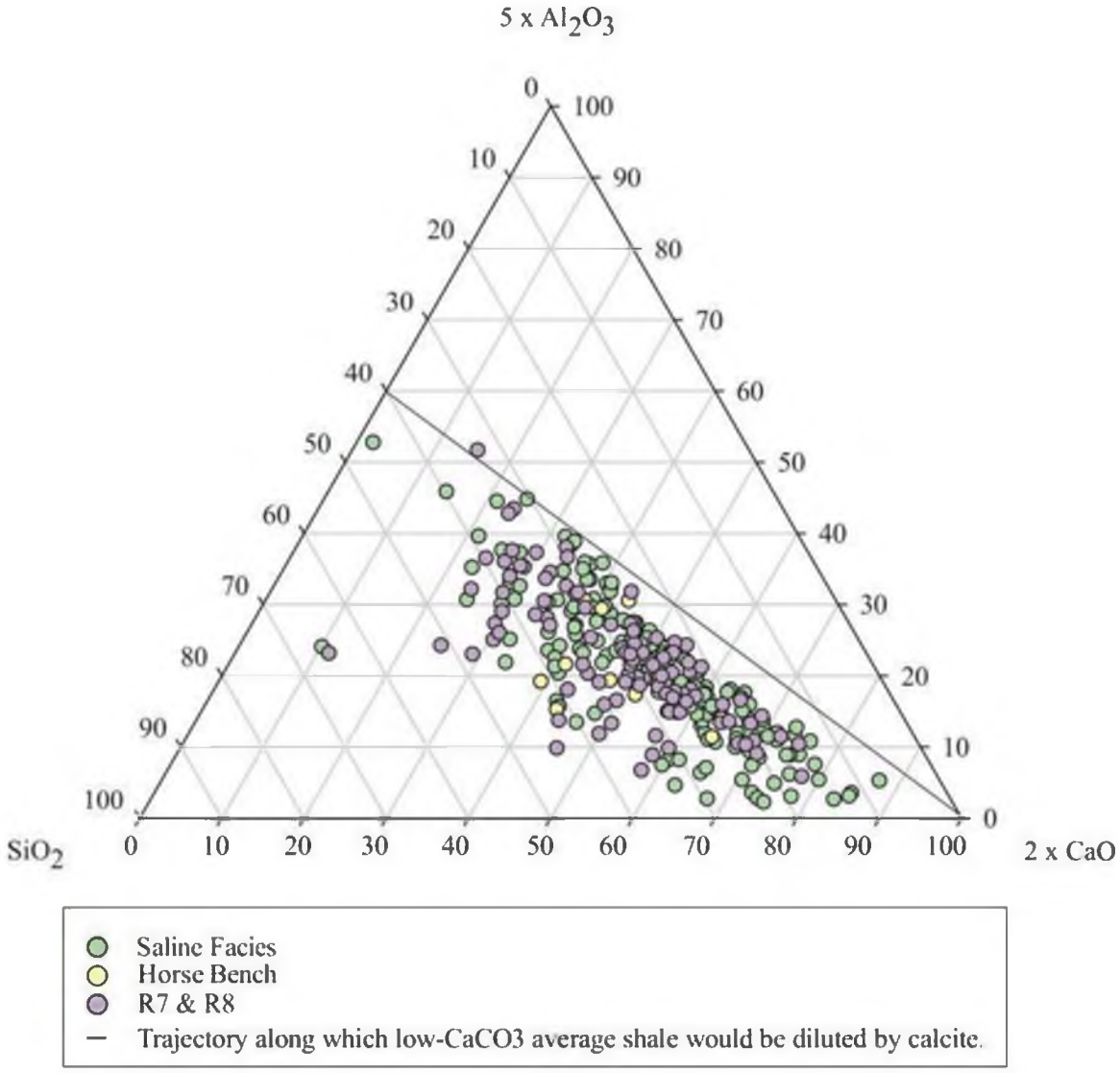
5 x Al2O3
0
100
10
90
20
80
30
70
40
60
50
50
60
40
70
30
80
20
90
10
100
0
SiO2
0 10 20 30 40 50 60 70 80 90 100
2 x CaO
Saline Facies
Horse Bench
R7 & R8
Trajectory along which low-CaCO3 average shale would be diluted by calcite.

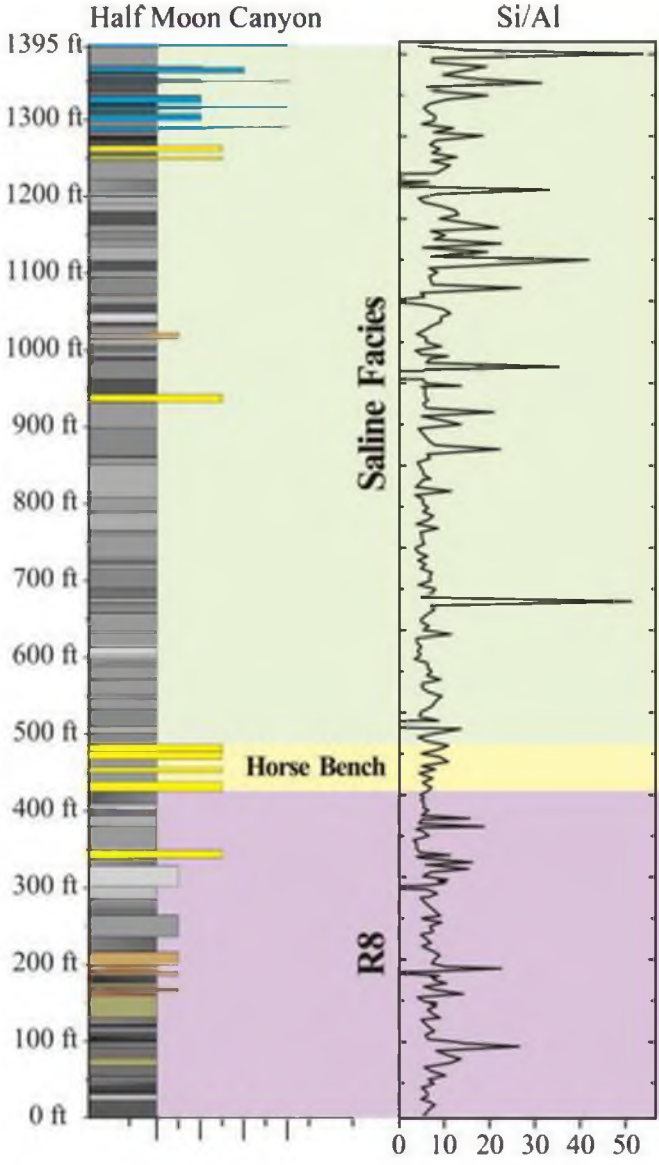
Half Moon Canyon
Si/Al
1395 ft
1300 ft
1200 ft
1100 ft
1000 ft
900 ft
800 ft
700 ft
600 ft
500 ft
400 ft
300 ft
200 ft
100 ft
0 ft
Saline Facies
Horse Bench
R8
0
10
20
30
40
50

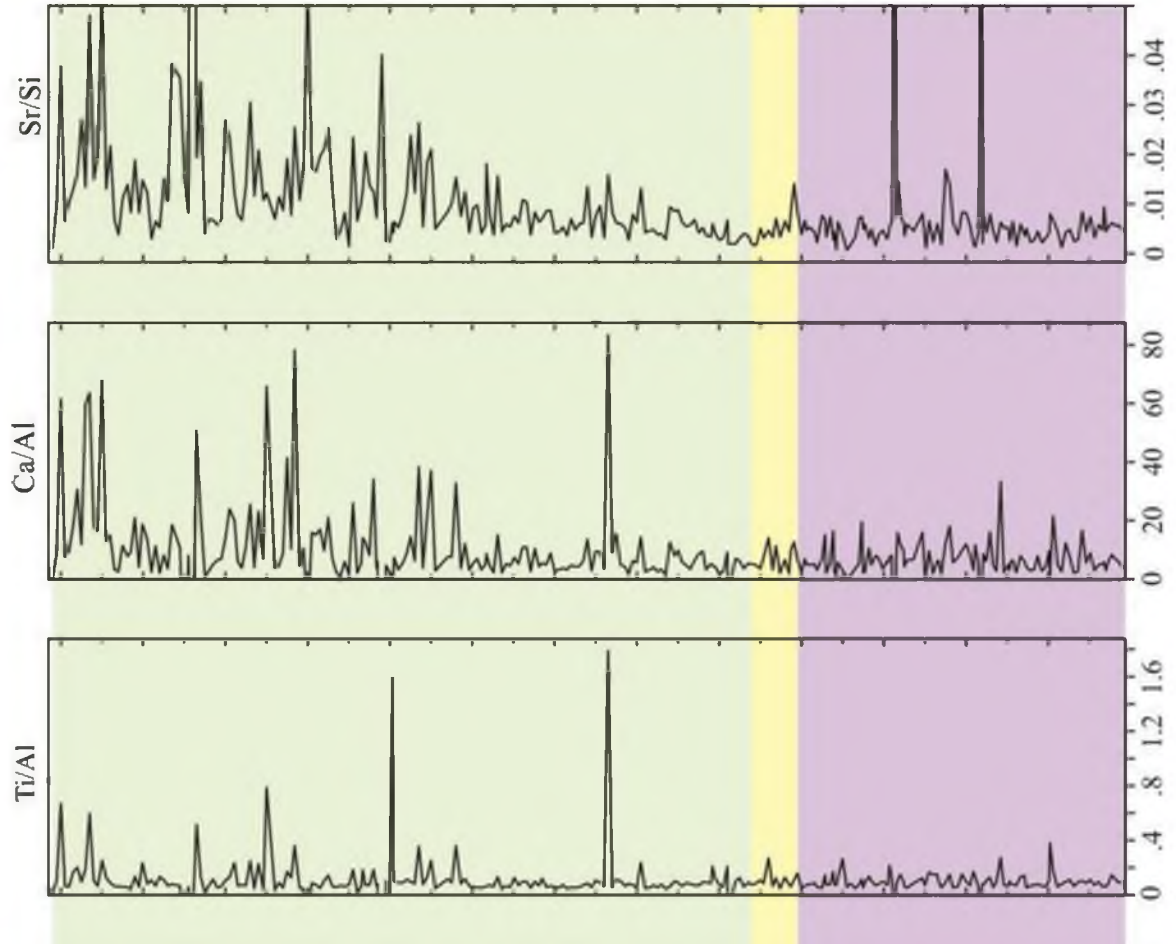
Sr/Si
0
.01
.02
.03
.04
Ca/Al
0
20
40
60
80
Ti/Al
0
.4
.8
1.2
1.6

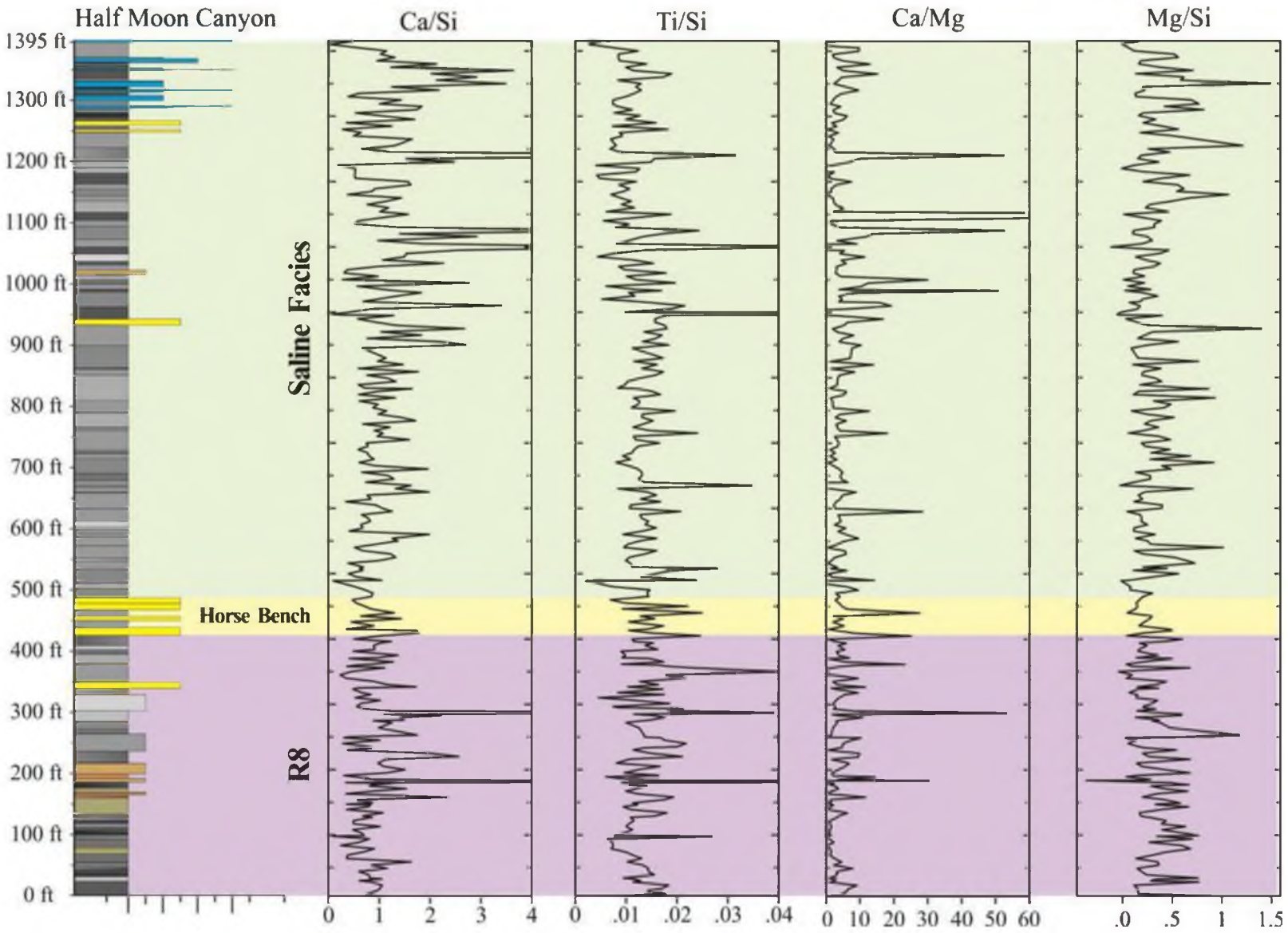
Half Moon Canyon
Ca/Si
Ti/Si
Ca/Mg
Mg/Si
1395 ft
1300 ft
1200 ft
1100 ft
1000 ft
900 ft
800 ft
700 ft
600 ft
500 ft
400 ft
300 ft
200 ft
100 ft
0 ft
Saline Facies
Horse Bench
R8
0 1 2 3 4
0 .01 .02 .03 .04
0 10 20 30 40 50 60
.0 .5 1 1.5

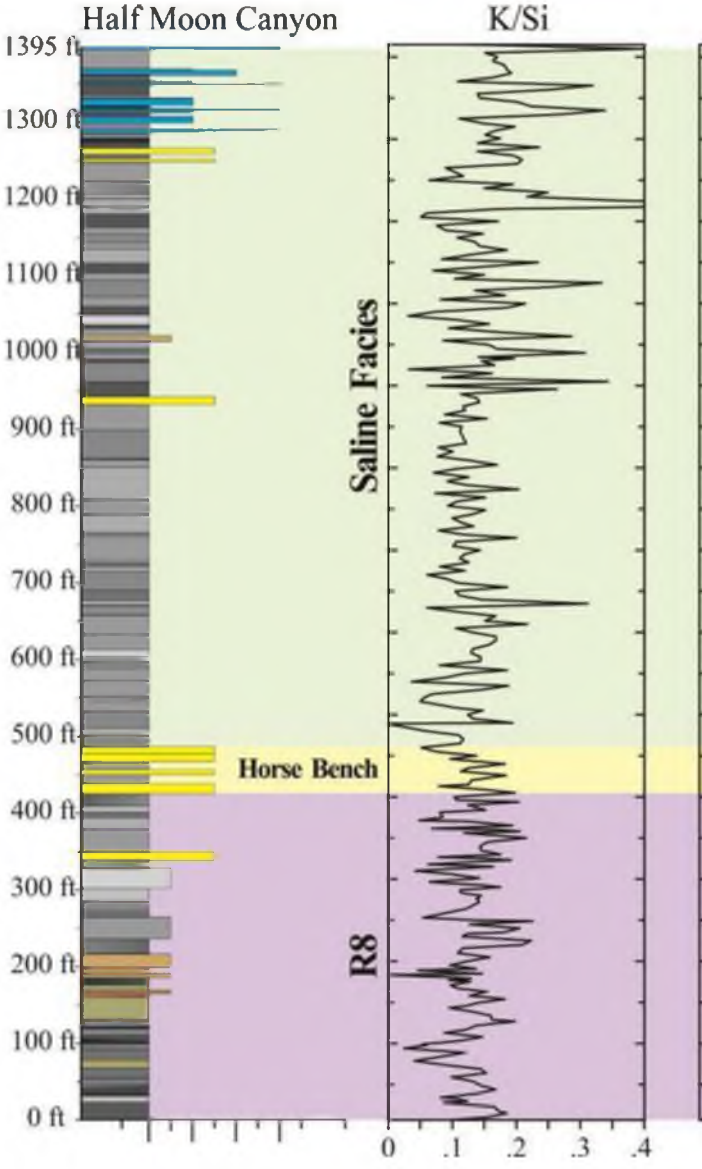
Half Moon Canyon
K/Si
1395 ft
1300 ft
1200 ft
1100 ft
1000 ft
900 ft
800 ft
700 ft
600 ft
500 ft
400 ft
300 ft
200 ft
100 ft
0 ft
Saline Facies
Horse Bench
R8
0
.1
.2
.3
.4

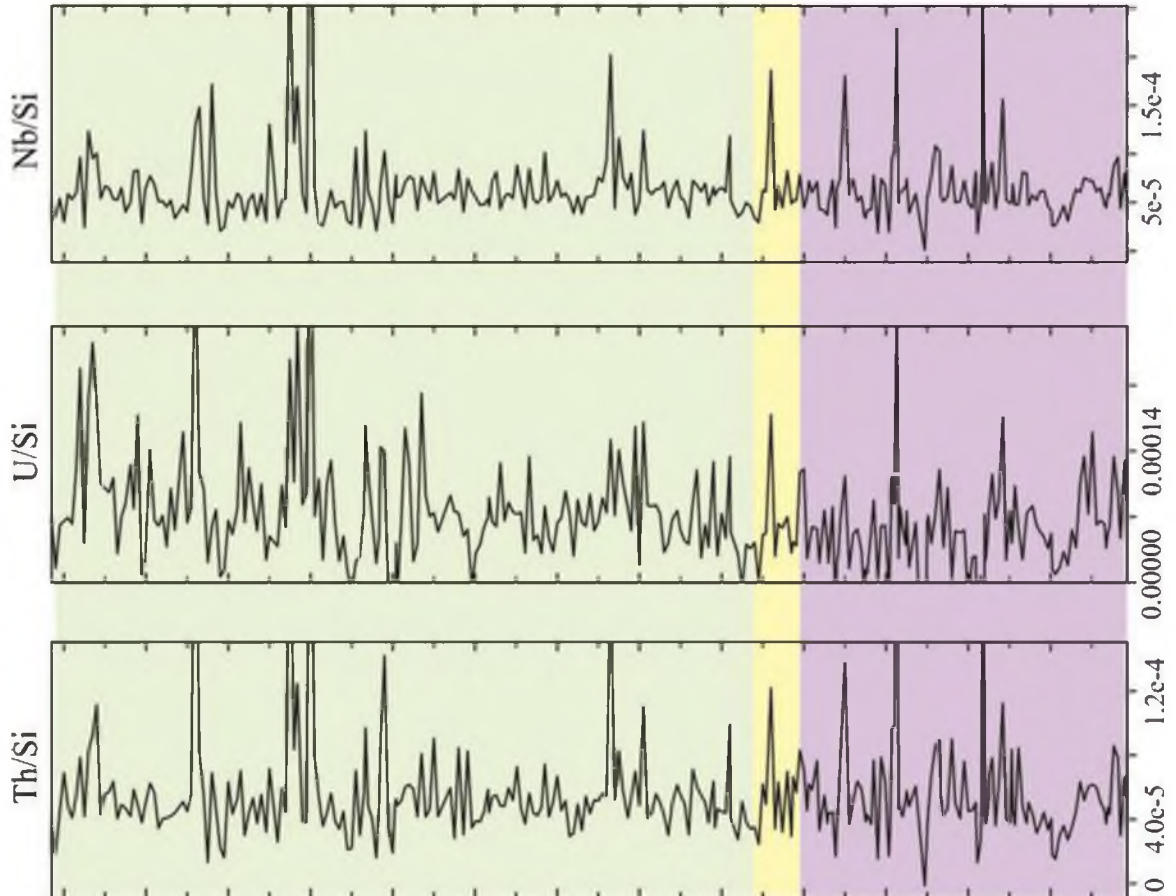
Nb/Si
5e-5
1.5e-4
U/Si
0.00000
0.00014
Th/Si
0
4.0e-5
1.2e-4

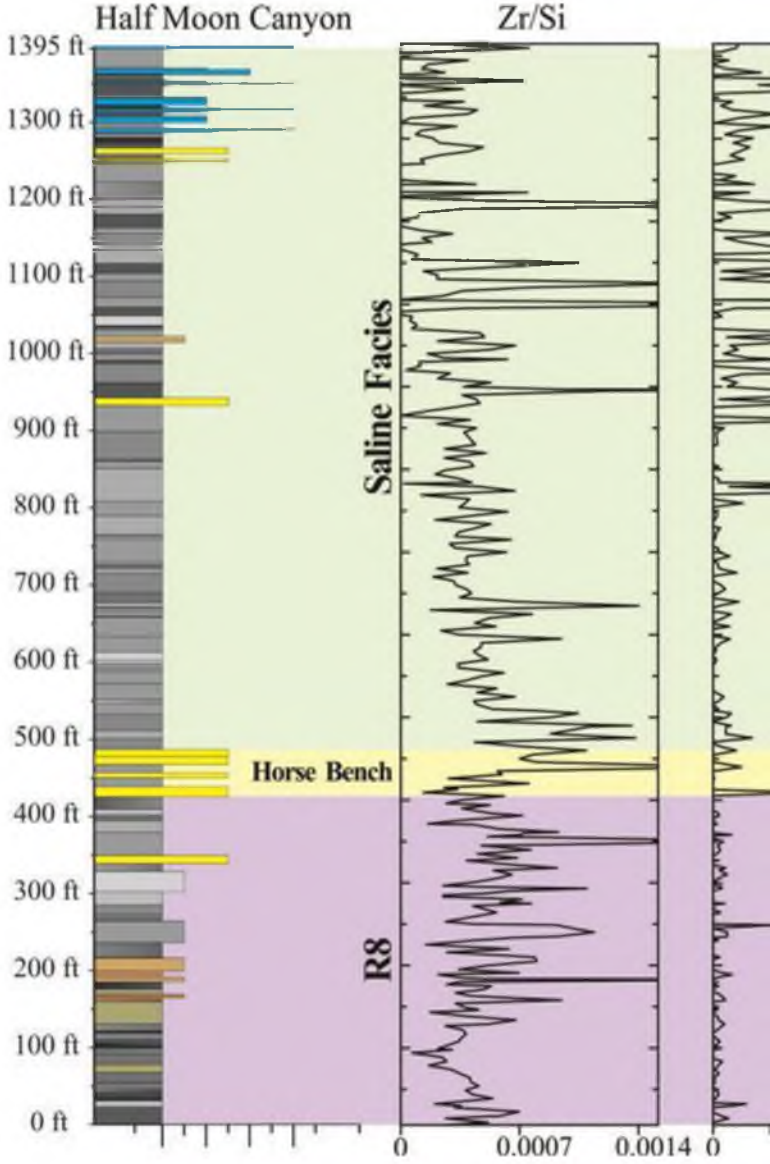
Half Moon Canyon
Zr/Si
1395 ft
1300 ft
1200 ft
1100 ft
1000 ft
900 ft
800 ft
700 ft
600 ft
500 ft
400 ft
300 ft
200 ft
100 ft
0 ft
Saline Facies
Horse Bench
R8
0
0.0007
0.0014
0

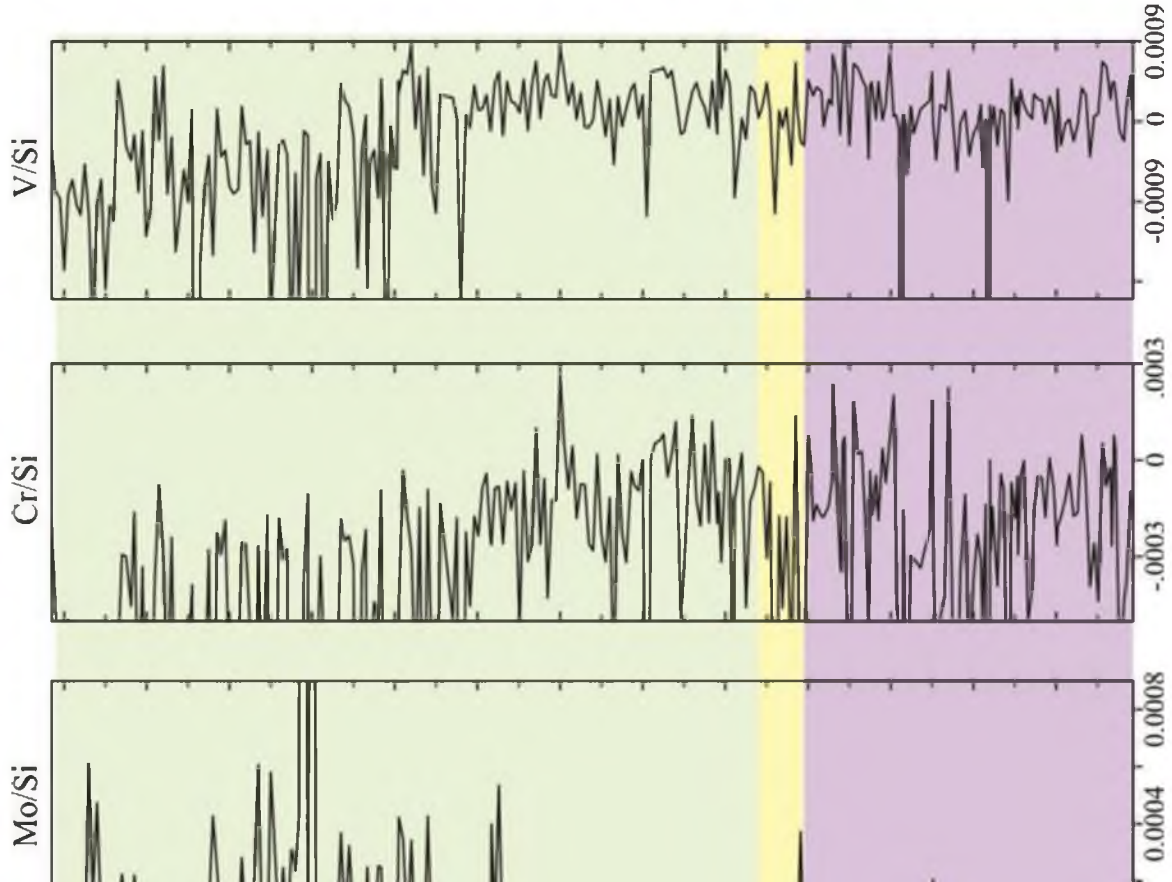
V/Si
0.0009
0
-0.0009
Cr/Si
.0003
0
-.0003
Mo/Si
0.0008
0.0004

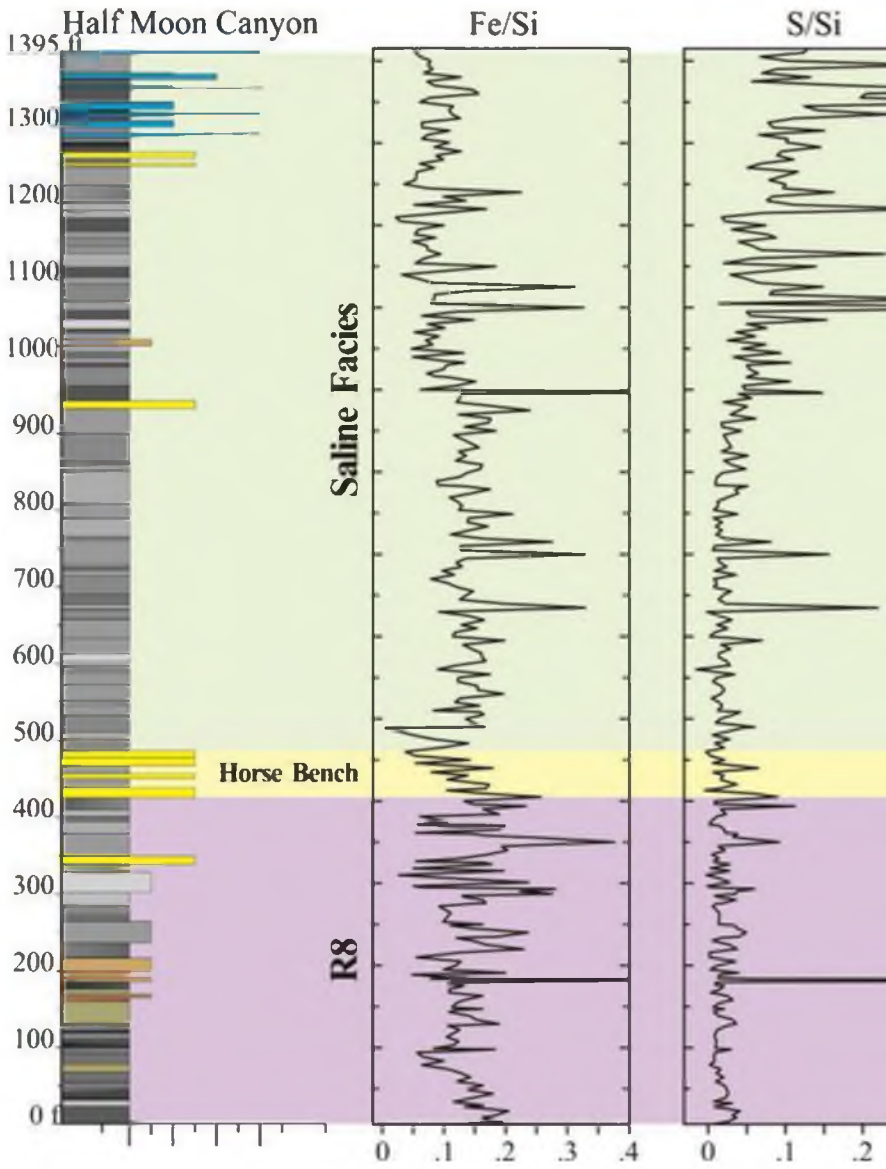
Half Moon Canyon
Fe/Si
S/Si
1395 ft
1300
1200
1100
1000
900
800
700
600
500
400
300
200
100
0 ft
Saline Facies
Horse Bench
R8
0
.1
.2
.3
.4
0
.1
.2

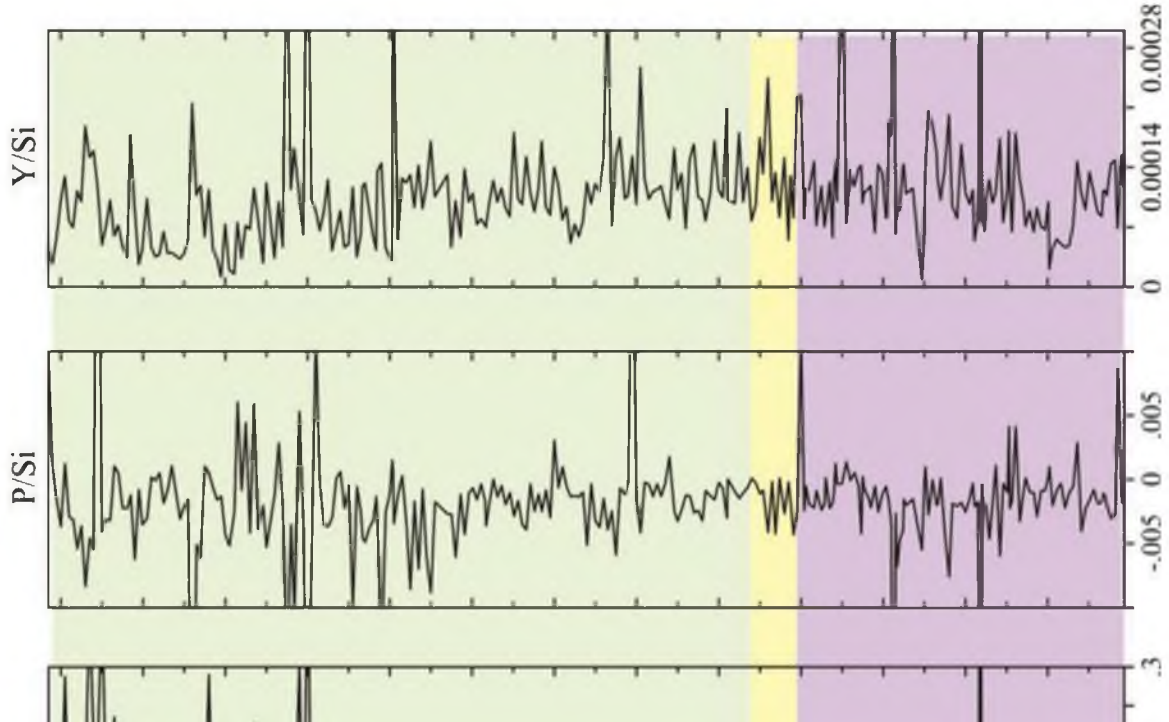
Y/Si
0.00028
0.00014
0
P/Si
.005
0
-.005
.3

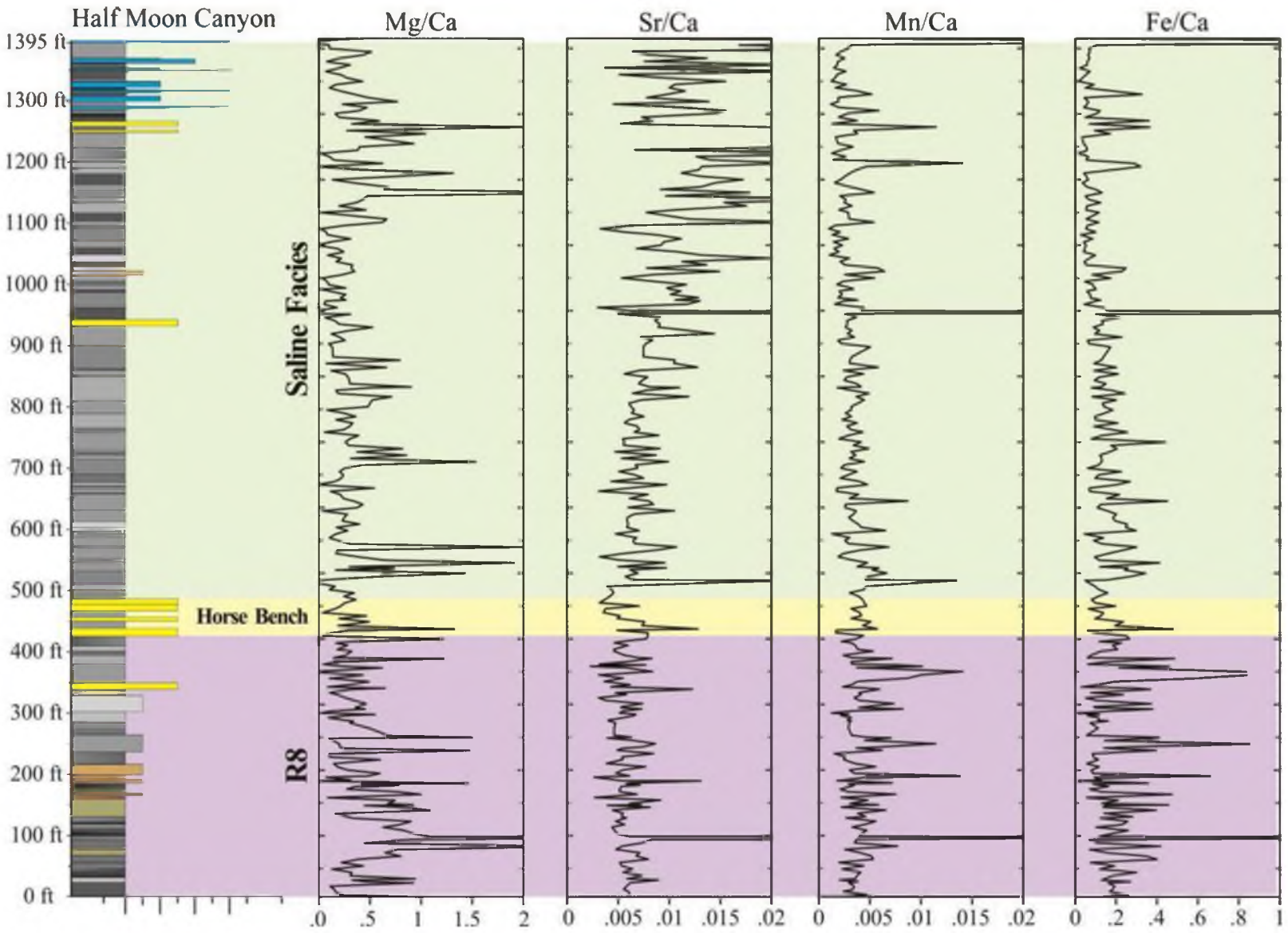
Half Moon Canyon
Mg/Ca
Sr/Ca
Mn/Ca
Fe/Ca
1395 ft
1300 ft
1200 ft
1100 ft
1000 ft
900 ft
800 ft
700 ft
600 ft
500 ft
400 ft
300 ft
200 ft
100 ft
0 ft
Saline Facies
Horse Bench
R8
.0 .5 1 1.5 2
0 .005 .01 .015 .02
0 .005 .01 .015 .02
0 .2 .4 .6 .8 1

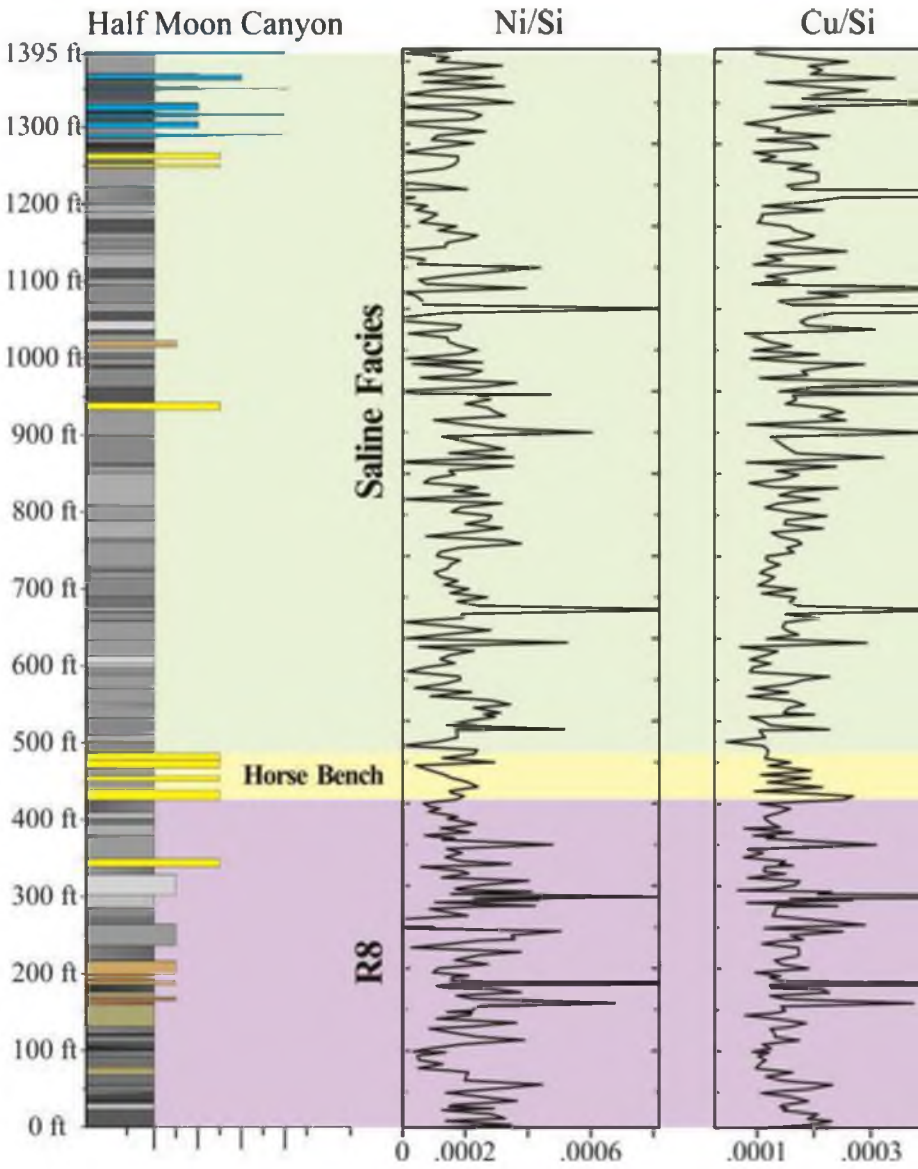
Half Moon Canyon
Ni/Si
Cu/Si
1395 ft
1300 ft
1200 ft
1100 ft
1000 ft
900 ft
800 ft
700 ft
600 ft
500 ft
400 ft
300 ft
200 ft
100 ft
0 ft
Saline Facies
Horse Bench
R8
0
.0002
.0006
.0001
.0003

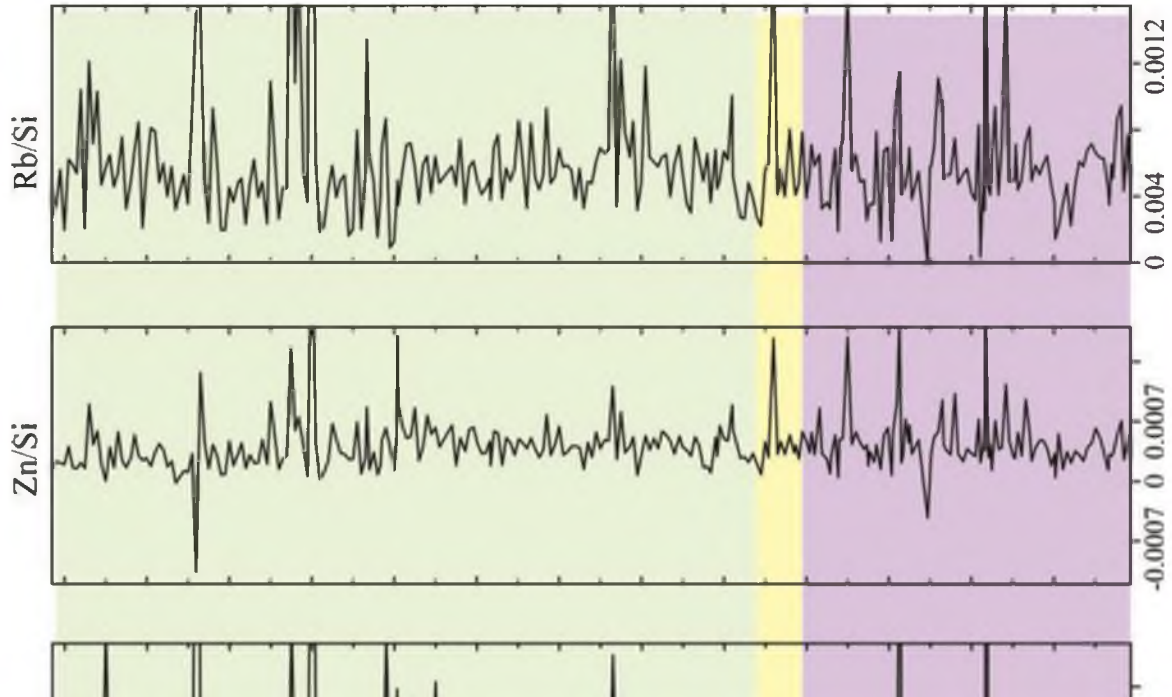
Rb/Si
0.0012
0.004
0
Zn/Si
0.0007
0
-0.0007

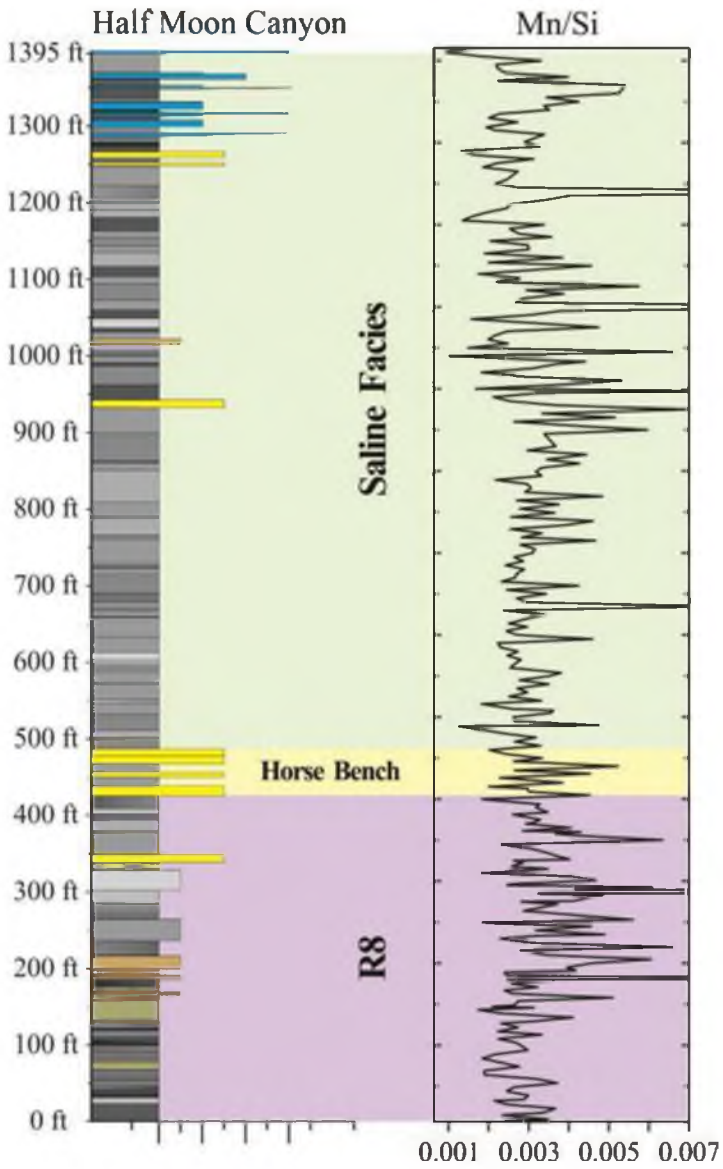
Half Moon Canyon
Mn/Si
1395 ft
1300 ft
1200 ft
1100 ft
1000 ft
900 ft
800 ft
700 ft
600 ft
500 ft
400 ft
300 ft
200 ft
100 ft
0 ft
Saline Facies
Horse Bench
R8
0.001
0.003
0.005
0.007

REFERENCES

Abels, H. A., Clyde, W. C., Gingerich, P. D., Hilgen, F. J., Fricke, H. C., Bowen, G. J., and Lourens, L. J., 2012, Terrestrial carbon isotope excursions and biotic change during Palaeogene hyperthermals: Nature Geosci, v. 5, p. 326-329.

Abels, H. A., Kraus, M. J., and Gingerich, P. D., 2013, Precession-scale cyclicity in the fluvial lower Eocene Willwood Formation of the Bighorn Basin, Wyoming (USA): Sedimentology, v. 60, p. 1467-1483.

Allen, P. A., 1981, Wave-generated structures in the Devonian lacustrine sediments of south-east Shetland and ancient wave conditions: Sedimentology, v. 28, p. 369-379.

Alonso-Zarza, A. M., 2003, Palaeoenvironmental significance of palustrine carbonates and calcretes in the geological record: Earth-Science Reviews, v. 60, p. 261-298.

Alonso-Zarza, A. M., and Tanner, L. H., 2006, Paleoenvironmental record and applications of calcretes and palustrine carbonates: Special Paper - Geological Society of America, v. 416.

Alonso-Zarza, A. M., and Wright, V., 2010, Palustrine carbonates: Developments in Sedimentology, v. 61, p. 103-131.

Anadon, P., Cabrera, L., and Kelts, K., 2009, Lacustrine Facies Analysis: International Association of Sedimentologists (IAS) Special Publication No. 13, v. 30.

Ashley, G. M., Maitima Mworia, J., Muasya, A. M., Owen, R. B., Driese, S. G., Hover, V. C., Renaut, R. W., Goman, M. F., Mathai, S., and Blatt, S. H., 2004, Sedimentation and recent history of a freshwater wetland in a semi-arid environment: Loboi Swamp, Kenya, East Africa: Sedimentology, v. 51, p. 1301-1321.

Aswasereelert, W., Meyers, S. R., Carroll, A. R., Peters, S. E., Smith, M. E., and Feigl, K. L., 2012, Basin-scale cyclostratigraphy of the Green River Formation, Wyoming: Geological Society of America bulletin, v. 125, p. 216-228.

Back, S., Batist, M. D., Strecker, M. R., and Vanhauwaert, P., 1999, Quaternary Depositional Systems in Northern Lake Baikal, Siberia: The Journal of Geology, v. 107, p. 1-12.

Back, S., and Strecker, M. R., 1998, Asymmetric late Pleistocene glaciations in the North basin of the Baikal Rift, Russia: Journal of the Geological Society, v. 155, p. 61-69.

Bader, J. W., 2009, Structural and tectonic evolution of the Douglas Creek arch, the Douglas Creek fault zone, and environs, northwestern Colorado and northeastern Utah: Implications for petroleum accumulation in the Piceance and Uinta basins: Rocky Mountain Geology, v. 44, p. 121-145.

Baskin, R., Wright, V. P., Driscoll, N., Kent, G., and Hepner, G., 2012, Microbial Carbonate Reservoir Characterization, AAPG Hedberg Conference, Houston, Texas.

Bereskin, S. R., Morgan, C. D., and McClure, K. P., 2004, Descriptions, Petrology, Photographs, and Photomicrographs of Core from the Green River Formation, South-Central Uinta Basin, Utah: Miscellaneous Publication - Utah Geological Survey, 0-1 disc.

Birgenheier, L. P., and VandenBerg, M. D., 2011, Core-based integrated sedimentologic, stratigraphic, and geochemical analysis of the oil shale bearing Green River Formation, Uinta Basin, Utah, 1-30 p.

Blakey, R. C., and Ranney, W., 2008, Ancient landscapes of the Colorado Plateau, Grand Canyon Assn.

Bohacs, K. M., Carrol, A. R., Neal, J. E., and Mankiewicz, P. J., 2000, Lake-Basin Type, Source Potential, and Hydrocarbon Character: an Integrated Sequence-Stratigraphic-Geochemical Framework, *in* E. H. Gierlowski-Kordesch, and K. R. Kelts, eds., Lake basins through space and time, AAPG Studies in Geology 46, p. 3-34.

Bowen, G. J., and Beitler Bowen, B., 2008, Mechanisms of PETM global change constrained by a new record from central Utah: Geology, v. 36, p. 379-382.

Brand, L. R., 2002, Lacustrine Deposition in the Bridger Formation: Lake Gosiute Extended: Geological Society of America Abstracts with Programs, p. 557.

Carroll, A. R., and Bohacs, K. M., 1999, Stratigraphic classification of ancient lakes: Balancing tectonic and climatic controls: Geology, v. 27, p. 99-102.

Carroll, A. R., and Bohacs, K. M., 2001, Lake-type controls on petroleum source rock potential in nonmarine basins: AAPG bulletin, v. 85, p. 1033-1053.

Cashion, W. B., 1967, Geology and fuel resources of the Green River Formation, southeastern Uinta Basin, Utah and Colorado: U.S. Geological Survey Professional Paper, v. 548.

Cashion, W. B., 1995, Stratigraphy of the Green River Formation, eastern Uinta Basin, Utah and Colorado - A summary, *in* W. R. Averett, ed., The Green River Formation in Piceance Creek and eastern Uinta Basins, Grand Junction Geological Society, Grand Junction Colorado.

Cohen, A. S., 1989, Facies relationships and sedimentation in large rift lakes and implications for hydrocarbon exploration: examples from Lakes Turkana and Tanganyika: Palaeogeography, Palaeoclimatology, Palaeoecology, v. 70, p. 65-80.

Cohen, A. S., and Thouin, C., 1987, Nearshore carbonate deposits in Lake Tanganyika: Geology, v. 15, p. 414-418.

Davis, S. J., Dickinson, W. R., Gehrels, G. E., Spencer, J. E., Lawton, T. F., and Carroll, A. R., 2010, The Paleogene California River: Evidence of Mojave-Uinta paleodrainage from U-Pb ages of detrital zircons: Geology, v. 38, p. 931-934.

Davis, S. J., Wiegand, B. A., Carroll, A. R., and Chamberlain, C. P., 2008, The effect of drainage reorganization on paleoaltimetry studies: An example from the Paleogene Laramide foreland: Earth and Planetary Science Letters, v. 275, p. 258-268.

Desborough, G. A., 1978, A biogenic-chemical stratified lake model for the origin of oil shale of the Green River Formation: An alternative to the playa-lake model: Geological Society of America Bulletin, v. 89, p. 961-971.

Dickinson, W. R., Lawton, T. F., and Inman, K. F., 1986, Sandstone detrital modes, central Utah foreland region: stratigraphic record of Cretaceous-Paleogene tectonic evolution: Journal of Sedimentary Research, v. 56, p. 276-293.

Dickinson, W. R., Lawton, T. F., Pecha, M., Davis, S. J., Gehrels, G. E., and Young, R. A., 2012, Provenance of the Paleogene Colton Formation (Uinta Basin) and Cretaceous–Paleogene provenance evolution in the Utah foreland: Evidence from U-Pb ages of detrital zircons, paleocurrent trends, and sandstone petrofacies: Geosphere, v. 8, p. 854-880.

Dickinson, W. W., Klute, M. A., Hayes, M. J., Janecke, S. U., Lundin, E. R., McKittrick, M. A., and Olivares, M. D., 1988, Paleogeographic and paleotectonic setting of Laramide sedimentary basins in the central Rocky Mountain region: Geological Society of America bulletin, v. 100, p. 1023-1039.

Driese, S. G., Ashley, G. M., Li, Z.-H., Hover, V. C., and Owen, R. B., 2004, Possible Late Holocene equatorial palaeoclimate record based upon soils spanning the Medieval Warm Period and Little Ice Age, Loboi Plain, Kenya: Palaeogeography, Palaeoclimatology, Palaeoecology, v. 213, p. 231-250.

Dupraz, C., and Visscher, P. T., 2005, Microbial lithification in marine stromatolites and hypersaline mats: Trends in microbiology, v. 13, p. 429-438.

Dyni, J. R., Milton, C., and Cashion Jr, W. B., 1985, The saline facies of the upper part of the Green River Formation near Duchesne, Utah, v. 12, p. 51-60.

Edmonds, D. A., and Slingerland, R. L., 2007, Mechanics of river mouth bar formation: Implications for the morphodynamics of delta distributary networks: Journal of Geophysical Research: Earth Surface, v. 112, p. F02034.

Eugster, H. P., 1986, Lake Magadi, Kenya: a model for rift valley hydrochemistry and sedimentation?: Geological Society, London, Special Publications, v. 25, p. 177-189.

Eugster, H. P., and Hardie, L. A., 1975, Sedimentation in an Ancient Playa-Lake Complex: The Wilkins Peak Member of the Green River Formation of Wyoming: Geological Society of America Bulletin, v. 86, p. 319-334.

Eyles, N., and Clark, B. M., 1986, Significance of hummocky and swaley cross-stratification in late Pleistocene lacustrine sediments of the Ontario basin, Canada: Geology, v. 14, p. 679-682.

Feldmann, M., and McKenzie, J., 1998, Stromatolite-Thrombolite Associations in a Modern Environment, Lee Stocking Island, Bahamas: Palaios, v. 13, p. 201.

Fielding, C. R., Trueman, J. D., and Alexander, J., 2005, Sharp-based, flood-dominated mouth bar sands from the Burdekin River delta of northeastern Australia: Extending the spectrum of mouth-bar facies, geometry, and stacking patterns: Journal of Sedimentary Research, v. 75, p. 55-66.

Flower, R., Mackay, A., Rose, N., Boyle, J., Dearing, J., Appleby, P., Kuzmina, A., and Granina, L., 1995, Sedimentary records of recent environmental change in Lake Baikal, Siberia: The Holocene, v. 5, p. 323-327.

Foreman, B. Z., Heller, P. L., and Clementz, M. T., 2012, Fluvial response to abrupt global warming at the Palaeocene/Eocene boundary: Nature, v. 491, p. 92-95.

Fouch, T. D., 1975, Lithofacies and related hydrocarbon accumulations in Tertiary strata of the western and central Uinta Basin, Utah: Symposium on deep drilling frontiers in the central Rocky Mountains: Rocky Mountain Association of Geologists Special Publication, p. 163-173.

Fouch, T. D., 1976, Revision of the lower part of the Tertiary System in the central and western Uinta basin, Utah.

Franczyk, K. J., and Pitman, J. K., 1991, Latest Cretaceous nonmarine depositional systems in the Wasatch Plateau area: reflections of foreland to intermontane basin transition: Utah Geological Association Publication, v. 19, p. 77-93.

Freytet, P., and Verrecchia, E., 2002, Lacustrine and palustrine carbonate petrography: an overview: Journal of Paleolimnology, v. 27, p. 221-237.

Gierlowski-Kordesch, E., Jacobson, A., Blum, J., and Garćes, B. V., 2008, Watershed reconstruction of a Paleocene–Eocene lake basin using Sr isotopes in carbonate rocks: Geological Society of America Bulletin, v. 120, p. 85-95.

Gierlowski-Kordesch, E. H., 1998, Carbonate deposition in an ephemeral siliciclastic alluvial system: Jurassic Shuttle Meadow Formation, Newark Supergroup, Hartford Basin, USA: Palaeogeography, Palaeoclimatology, Palaeoecology, v. 140, p. 161-184.

Johnson, R., Mercier, T., Brownfield, M., and Self, J., 2010, Assessment of in-place oil shale resources in the Eocene Green River Formation, Uinta Basin, Utah and Colorado: U.S. Geological Survey Digital Data Series, v. 63.

Johnson, R. C., 1985, Early Cenozoic history of the Uinta and Piceance Creek basins, Utah and Colorado, with special reference to the development of Eocene Lake Uinta: Rocky Mountain Section.

Johnson, T. C., Halfman, J. D., Rosendahl, B. R., and Lister, G. S., 1987, Climatic and tectonic effects on sedimentation in a rift-valley lake: Evidence from high-resolution seismic profiles, Lake Turkana, Kenya: Geological Society of America Bulletin, v. 98, p. 439-447.

Jones, B. F., Eugster, H. P., and Rettig, S. L., 1977, Hydrochemistry of the Lake Magadi basin, Kenya: Geochimica et Cosmochimica Acta, v. 41, p. 53-72.

Keighley, D., 2008, A lacustrine shoreface succession in the Albert Formation, Moncton Basin, New Brunswick: Bulletin of Canadian Petroleum Geology, v. 56, p. 235-258.

Keighley, D., Flint, S., Howell, J., Andersson, D., Collins, S., Moscariello, A., and Stone, G., 2002, Surface and Subsurface Correlation of the Green River Formation in Central Nine Mile Canyon, SW Uinta Basin, Carbon and Duchesne Counties, East-Central Utah: Miscellaneous Publication - Utah Geological Survey, 0-1 disc.

Keighley, D., Flint, S., Howell, J., and Moscariello, A., 2003, Sequence Stratigraphy in Lacustrine Basins: A Model for Part of the Green River Formation (Eocene), Southwest Uinta Basin, Utah, U.S.A: Journal of sedimentary research, v. 73, p. 987-1006.

Kelts, K., 1988, Environments of deposition of lacustrine petroleum source rocks: an introduction: Geological Society, London, Special Publications, v. 40, p. 3-26.

Koch, P. L., Clyde, W. C., Hepple, R. P., Fogel, M. L., Wing, S. L., and Zachos, J. C., 2003, Carbon and oxygen isotope records from paleosols spanning in the Paleocene-Eocene boundary, Bighorn Basin, Wyoming, *in* S. L. Wing, P. D. Gingerich, B. Schmitz, and E. Thomas, eds., Causes and Consequences of Globally Warm Climates in the Early Paleogene: Boulder, GSA, p. 49-63.

Kraus, M. J., and Riggins, S., 2007, Transient drying during the Paleocene–Eocene Thermal Maximum (PETM): Analysis of paleosols in the bighorn basin, Wyoming: Palaeogeography, Palaeoclimatology, Palaeoecology, v. 245, p. 444-461.

Lourens, L. J., Sluijs, A., Kroon, D., Zachos, J. C., Thomas, E., Röhl, U., Bowles, J., and Raffi, I., 2005, Astronomical pacing of late Palaeocene to early Eocene global warming events: Nature, v. 435, p. 1083-1087.

Maestro, E., 2008, Sedimentary evolution of the Late Eocene Vernet lacustrine system (South-Central Pyrenees). Tectono-climatic control in an alluvial-lacustrine piggyback basin: Journal of Paleolimnology, v. 40, p. 1053-1078.

Martin, J., Paola, C., Abreu, V., Neal, J., and Sheets, B., 2009, Sequence stratigraphy of experimental strata under known conditions of differential subsidence and variable base level: AAPG bulletin, v. 93, p. 503-533.

Miall, A. D., and Arush, M., 2001, The Castlegate Sandstone of the Book Cliffs, Utah: Sequence Stratigraphy, Paleogeography, and Tectonic Controls: Journal of sedimentary research, v. 71, p. 537-548.

Moore, J., Taylor, A., Johnson, C., Ritts, B. D., and Archer, R., 2012, Facies Analysis, Reservoir Characterization, and LIDAR Modeling of an Eocene Lacustrine Delta, Green River Formation, Southwest Uinta Basin, Utah: Lacustrine sandstone reservoirs and hydrocarbon systems: AAPG Memoir, v. 95, p. 183-208.

Morgan, C. D., 2003, Geologic Guide and Road Logs of the Willow Creek, Indian, Soldier Creek, Nine Mile, Gate, and Desolation Canyons, Uinta Basin, Utah (OFR-407).

Nicolo, M. J., Dickens, G. R., Hollis, C. J., and Zachos, J. C., 2007, Multiple early Eocene hyperthermals: Their sedimentary expression on the New Zealand continental margin and in the deep sea: Geology, v. 35, p. 699-702.

Olariu, C., and Bhattacharya, J. P., 2006, Terminal Distributary Channels and Delta Front Architecture of River-Dominated Delta Systems: Journal of Sedimentary Research, v. 76, p. 212-233.

Osleger, D. A., Heyvaert, A. C., Stoner, J. S., and Verosub, K. L., 2009, Lacustrine turbidites as indicators of Holocene storminess and climate: Lake Tahoe, California and Nevada: Journal of Paleolimnology, v. 42, p. 103-122.

Osmond, J. C., 1965, Geologic history of site of Uinta Basin, Utah: AAPG Bulletin, v. 49, p. 1957-1973.

Picard, M. D., 1955, Subsurface stratigraphy and lithology of Green River Formation in Uinta Basin, Utah: AAPG Bulletin, v. 39, p. 75-102.

Picard, M. D., 1957, Green shale facies, Lower Green River Formation, Utah: AAPG bulletin.

Picard, M. D., and High, L. R., 1972, Paleoenvironmental Reconstructions in an Area of Rapid Facies Change, Parachute Creek Member of Green River Formation (Eocene), Uinta Basin, Utah: Geological Society of America bulletin, v. 83, p. 2689-2708.

Pietras, J. T., and Carroll, A. R., 2006, High-Resolution Stratigraphy of an Underfilled Lake Basin: Wilkins Peak Member, Eocene Green River Formation, Wyoming, U.S.A: Journal of sedimentary research, v. 76, p. 1197-1214.

Pilskaln, C. H., and Johnson, T. C., 1991, Seasonal signals in Lake Malawi sediments: Limnology and Oceanography, v. 36, p. 544-557.

Plink-Bjorklund, P., and Birgenheier, L. P., in review, Facies model for the seasonal to ephemeral river systems: Effect of extreme precipitation on river systems form and function: Geology.

Plummer, P. S., and Gostin, V. A., 1981, Shrinkage cracks; desiccation or synaeresis?: Journal of Sedimentary Research, v. 51, p. 1147-1156.

Pratt, B. R., 1998, Syneresis cracks: subaqueous shrinkage in argillaceous sediments caused by earthquake-induced dewatering: Sedimentary Geology, v. 117, p. 1-10.

Pusca, V. A., 2003, Wet/dry, Terminal Fan-dominated Sequence Architecture: A New, Outcrop-based Model for the Lower Green River Formation, Utah, University of Wyoming.

Remy, R. R., 1989, Deltaic and lacustrine facies of the Green River Formation, southern Uinta Basin, Utah: Cretaceous Shelf Sandstones and Shelf Depositional Sequences, Western Interior Basin, Utah, Colorado and New Mexico: Salt Lake City, Utah to Albuquerque, New Mexico June 30-July 7, 1989, p. 1-11.

Remy, R. R., 1992, Stratigraphy of the Eocene part of the Green River Formation in the south-central part of the Uinta Basin, Utah: U.S. Geological Survey Bulletin, BB1-BB79.

Renaut, R. W., 1994, Lake Bogoria, Kenya rift valley—a sedimentological overview: Special publication - Society for Sedimentary Geology, v. 50, p. 101-123.

Renaut, R. W., and Gierlowski-Kordesch, E. H., 2010, Lakes, *in* N. P. James, and R. W. Dalrymple, eds., Facies Models 4, Geological Association of Canada, St. John's, p. 541-575.

Renaut, R. W., Tiercelin, J., and Owen, R. B., 2000, Lake Baringo, Kenya Rift Valley, and its Pleistocene precursors: AAPG Studies in Geology, v. 46, p. 561-568.

Rosenberg, M. J., 2013, Facies, stratigraphic architecture, and lake evolution of the oil shale bearing Green River Formation, Eastern Uinta Basin, Utah, University of Utah, Salt Lake City, Utah.

Rosenberg, M. J., Birgenheier, L. P., and Vanden Berg, M. D., in press, Facies, stratigraphic architecture, and lake evolution of the oil shale bearing Green River Formation, eastern Uinta Basin: Stratigraphy and Limnogeology of the Eocene Green River Formation, Springer.

Rowe, H., Hughes, N., and Robinson, K., 2012, The quantification and application of handheld energy-dispersive x-ray fluorescence (ED-XRF) in mudrock chemostratigraphy and geochemistry: Chemical Geology, v. 324–325, p. 122-131.

Ryder, R. T., Fouch, T. D., and Elison, J. H., 1976, Early Tertiary sedimentation in the western Uinta Basin, Utah: Geological Society of America bulletin, v. 87, p. 496-512.

Scholle, P. A., and Ulmer-Scholle, D. S., 2003, A Color Guide to the Petrography of Carbonate Rocks: Grains, Textures, Porosity, Diagenesis: AAPG Memoir, v. 77.

Scholz, C. A., 1995, Deltas of the Lake Malawi Rift, East Africa: seismic expression and exploration implications: AAPG bulletin, v. 79, p. 1679-1697.

Schomacker, E. R., Kjemperud, A. V., Nystuen, J. P., and Jahren, J. S., 2010, Recognition and significance of sharp-based mouth-bar deposits in the Eocene Green River Formation, Uinta Basin, Utah: Sedimentology, v. 57, p. 1069-1087.

Schubel, K. A., and Lowenstein, T. K., 1997, Criteria for the recognition of shallow-perennial-saline-lake halites based on Recent sediments from the Qaidam Basin, western China: Journal of Sedimentary Research, v. 67, p. 74-87.

Sewall, J. O., and Sloan, L. C., 2006, Come a little bit closer: A high-resolution climate study of the early Paleogene Laramide foreland: Geology, v. 34, p. 81-84.

Sexton, P. F., Norris, R. D., Wilson, P. A., Pälike, H., Westerhold, T., Röhl, U., Bolton, C. T., and Gibbs, S., 2011, Eocene global warming events driven by ventilation of oceanic dissolved organic carbon: Nature, v. 471, p. 349-352.

Smith, J. J., Hasiotis, S. T., Kraus, M. J., and Woody, D. T., 2009, Transient dwarfism of soil fauna during the Paleocene–Eocene Thermal Maximum: Proceedings of the National Academy of Sciences, v. 106, p. 17655-17660.

Smith, M. E., Carroll, A. R., and Singer, B. S., 2008, Synoptic reconstruction of a major ancient lake system: Eocene Green River Formation, western United States: Geological Society of America bulletin, v. 120, p. 54-84.

Smith, M. E., Chamberlain, K., Singer, B., and Carroll, A., 2010, Eocene clocks agree: Coeval 40Ar/39Ar, U-Pb, and astronomical ages from the Green River Formation: Geology, v. 38, p. 527-530.

Sømme, T. O., Helland-Hansen, W., Martinsen, O. J., and Thurmond, J. B., 2009, Relationships between morphological and sedimentological parameters in source-to-sink systems: a basis for predicting semi-quantitative characteristics in subsurface systems: Basin Research, v. 21, p. 361-387.

Surdam, R. C., and Eugster, H. P., 1976, Mineral reactions in the sedimentary deposits of the Lake Magadi region, Kenya: Geological Society of America Bulletin, v. 87, p. 1739-1752.

Tanavsuu-Milkeviciene, K., and Sarg, J. F., 2012, Evolution of an organic-rich lake basin – stratigraphy, climate and tectonics: Piceance Creek basin, Eocene Green River Formation: Sedimentology, v. 59, p. 1735-1768.

Tucker, G. E., and Slingerland, R., 1997, Drainage basin responses to climate change: Water Resources Research, v. 33, p. 2031-2047.

Tucker, M. E., and Wright, V. P., 2009, Carbonate sedimentology, John Wiley & Sons.

Van Wagoner, J. C., 1995, Sequence stratigraphy and marine to nonmarine facies architecture of foreland basin strata, Book Cliffs, Utah, USA: AAPG Memoirs, v. 64, p. 137-223.

Vanden Berg, M. D., 2008, Basin-wide evaluation of the uppermost Green River Formation's oil-shale resource, Uinta Basin, Utah and Colorado. Abstracts: Annual Meeting - American Association of Petroleum Geologists.

Vanden Berg, M. D., and Birgenheier, L. P., 2014, Hypersaline Facies and the Termination of Eocene Lake Uinta, Upper Green River Formation, Uinta Basin, Utah, 2014 Rocky Mountain Section AAPG Annual Meeting, Denver, Colorado.

Weiss, M., Witkind, I., and Cashion, W., 1990, Geologic map of the Price 30'X 60'quadrangle: Carbon, Duchesne, Uintah, and Wasatch counties, Utah: US Geological Survey Miscellaneous Investigations Series Map, p. 1-1981.

Wilf, P., Wing, S. L., Greenwood, D. R., and Greenwood, C. L., 1998, Using fossil leaves as paleoprecipitation indicators: an Eocene example: Geology, v. 26, p. 203-206.

Williamson, C. R., 1972, Carbonate Petrology of the Green River Formation (Eocene), Uinta Basin, Utah and Colorado, University of Utah.

Williamson, C. R., and Picard, M. D., 1974, Petrology of carbonate rocks of the Green River Formation (Eocene): Journal of sedimentary research, v. 44, p. 738-759.

Wing, S. L., and Greenwood, D. R., 1993, Fossils and fossil climate: the case for equable continental interiors in the Eocene: Philosophical Transactions of the Royal Society of London. Series B: Biological Sciences, v. 341, p. 243-252.

Witherow, R. A., and Lyons, W. B., 2011, The fate of minor alkali elements in the chemical evolution of salt lakes: Saline systems, v. 7, p. 2.

Wright, L. D., 1977, Sediment transport and deposition at river mouths: A synthesis: Geological Society of America Bulletin, v. 88, p. 857-868.

Yang, W., Spencer, R. J., Krouse, H. R., Lowenstein, T. K., and Casas, E., 1995, Stable isotopes of lake and fluid inclusion brines, Dabusun Lake, Qaidam Basin, western China: Hydrology and paleoclimatology in arid environments: Palaeogeography, Palaeoclimatology, Palaeoecology, v. 117, p. 279-290.